Investigating the antimicrobial potential of

Thalassomonas actiniarum

UNIVERSITY *of the*
WESTERN CAPE

By Fazlin Pheiffer

A thesis submitted in partial fulfilment of the requirements for the degree of Doctor of Philosophy (PhD)

Department of Biotechnology, University of the Western Cape

Supervisor: Prof Marla Trindade

Co-supervisor: Dr Leonardo van Zyl

2020

Declaration

I, Fazlin Pheiffer, hereby declare that '***Investigating the antimicrobial potential of Thalassomonas actiniarum***' is my own work, that it has not been submitted for any degree or examination in any other university, and that all the sources I have used or quoted have been indicated and acknowledged by complete references.

Date**:** 16 March 2021

Signed: 

Abstract

The World Health Organisation predicts that by the year 2050, 10 million people could die annually as a result of infections caused by multidrug resistant bacteria. Individuals with compromised immune systems, caused by underlying disease such as HIV, MTB and COVID-19, are at a greater risk. Antibacterial resistance is a global concern that demands the discovery of novel drugs. Natural products, used since ancient times to treat diseases, are the most successful source of new drug candidates with bioactivities including antibiotic, antifungal, anticancer, antiviral, immunosuppressive, anti-inflammatory and biofilm inhibition. Marine bioprospecting has contributed significantly to the discovery of novel bioactive NPs with unique structures and biological activities, superior to that of compounds from terrestrial origin. Marine invertebrate symbionts are particularly promising sources of marine NPs as the competition between microorganisms associated with invertebrates for space and nutrients is the driving force behind the production of antibiotics, which also constitute pharmaceutically relevant natural products.

In this study, the sea anemone-associated marine bacterium *T. actiniarum* was investigated for antibacterial activity against 4 indicator strains. Antibacterial activity was observed from a compound in the molecular size range 50kDa-100kDa against all indicator strains. Notably, the bioactivity profile and estimated molecular size of the active compound was similar to TVP1, a putative prophage-encoded hypothetical protein with lytic activity produced by *T. viridans*, the closest relative of *T. actiniarum*. The *T. actiniarum* homologue, TAP1 showed 78.14% similarity to TVP1, leading to the hypothesis that the strains produce a similar antibacterial protein. Therefore, the initial aim of this study was to heterologously express the putative prophage-encoded hypothetical proteins TVP1 and TAP1 and assess their antibacterial activity. Following expression of the proteins and subsequent antibacterial assays, neither TVP1 nor TAP1 showed antibacterial activity suggesting that these proteins were likely mis-identified as being responsible for the observed bioactivity from these two strains. Furthermore, transmission electron microscopy revealed that *T. actiniarum* produces particles that resemble tailocins, observed in a fraction containing compounds in the molecular size range >100kDa. Although not the focus of this study, investigating the antibacterial activity of these particles may further demonstrate the expansive bioactive potential of this strain.

A bioassay guided isolation approach was then used to isolate the high molecular weight antibacterial compound (50kDa-100kDa) from *T. actiniarum* fermentations. With common protein isolation, purification and detection methods failing to provide insight into the nature of the antibacterial compound, we hypothesized that the active agent is not proteinaceous in nature and may be a high molecular weight exopolysaccharide. Extraction and antibacterial screening of the exopolysaccharide fraction from *T. actiniarum* showed antibacterial activity as well as lytic activity when subjected to a zymography assay using *Pseudomonas putida* whole cells as a substrate. Additionally, the biosynthetic pathways for the production of poly-β-1, 6-*N*-acetyl-glucosamine (PNAG), an exopolysaccharide involved in biofilm formation and chondroitin sulfate, a known and industrially important glycosaminoglycan with antibacterial and anti-inflammatory activity was identified and the mechanism may be novel.

Genome mining identified a variety of novel secondary metabolite gene clusters which could potentially encode other novel bioactivities. Therefore a bioassay guided isolation, focused on the small (<3kDa) molecules, was pursued. Secondary metabolites were extracted, fractionated and screened for biofilm inhibition, antibacterial and anticancer activity and activity was observed in all assays. Active fractions were dereplicated by UHPLC-QToF-MS and compounds of interest were isolated using mass guided preparative HPLC. The purity of the isolated compounds was assessed using UHPLC-QToF-MS and NMR and the structure of the target compounds elucidated. Structures that could be determined were the bile acids cholic acid and 3-oxo cholic acid and although not responsible for the observed activities, this is the first report of bile acid production for this genus.

This is the first study investigating the bioactive potential of the strain and the first demonstrating that *T. actiniarum* is a promising source of potentially novel pharmaceutically relevant natural products depicted through both culture-dependent and culture-independent approaches.

Keywords: *bioactive natural products, marine natural products, heterologous expression, genome mining, exopolysaccharides, bioassay-guided fractionation*

Acknowledgements

I would like to thank my supervisor, Professor Marla Trindade and my co- supervisor, Dr Lonnie van Zyl for this amazing opportunity and for their exceptional leadership, continuous support, motivation and encouragement.

A big thank you to the NRF for funding this research.

I would also like to thank everyone at IMBM, support staff and students, as completing this work would have been all the more difficult without all of you.

A special thanks to Shanice, for her continuous motivation and wonderful friendship from the start of this journey, until now.

I'd like to thank everyone at Marbio, UiT (The Arctic University of Norway) as well as Johan Isaksson for their assistance and input with regards to Chapter 4 of this work.

Lastly, I would like to thank my family for their patience, reassurance and support. This accomplishment is yours as much as it is mine.

Dedication

This work is dedicated to those who often asked me, 'So, when are you done?'

To my son, Seth. Unknowingly, you kept me going.

Abbreviations

µ	micro
µg	microgram
µg/ml	Microgram per milliliter
µl	microliter
µm	micrometer
A domain	adenylation domain
ACP	acyl carrier protein
antiSMASH	antibiotic and Secondary Metabolite Analysis Shell
APS	ammonium persulfate
AT	acyl transferase
ATCC	American Type Culture Collection
ATP	adenosine triphosphate
BCC	*Burkholderia cepacia* complex
BGC	biosynthetic gene cluster
BLAST	Basic Local Alignment Tool
bp	base pair
BPI	base peak intensity
C domain	condensation domain
CFU/ml	colony forming units per milliliter
CLB's	colicin-like bacteriocins
cm	centimeter

CoA	co-enzyme A
Contig	contiguous
COVID-19	Coronavirus Diseases 2019
Da	Dalton
DH	dehydratase
dH_2O	distilled water
DMSO	dimethyl sulfoxide
DNA	deoxyribonucleic acid
EDTA	ethylenediaminetetraacetic acid
EPS	exopolysaccharide
ER	enoyl reductase
ESKAPE	***E****nterococcus faecium*, ***S****taphylococcus aureus*, ***K****lebsiella pneumonia*, ***P****seudomonas aeruginosa* and ***E****nterobacter* sp.
FDA	Food and Drug Administration
FPLC	Fast Protein Liquid Chromatography
g	gram
g/L	grams per liter
g/ml	grams per milliliter
GAG	glycosaminoglycan
HIV	Human Immunodeficiency Virus
HMW	high molecular weight
HPLC	High Performance Liquid Chromatography
HR-MS	High Resolution Mass Spectrometry

IMBM	Institute for Microbial Biotechnology and Metagenomics
kDa	kilodalton
KR	ketoreductase
KS	ketosynthase
L	liter
LB	Luria Broth
LC-MS	Liquid Chromatography Mass Spectrometry
LC-NMR	Liquid Chromatography Nuclear Magnetic Resonance Spectroscopy
LPS	lipopolysaccharide
m/z	mass to charge
MDR	multidrug resistant
MERS-CoV	Middle East Respiratory Syndrome Coronavirus
mg/ml	milligrams per milliliter
MIC	Minimum Inhibitory Concentration
ML	Machine Learning
ml	milliliter
mm	millimeter
mM	millimolar
M	Molar
MS	Mass Spectrometry
MT	methyltransferase
MTS	3-(4,5-dimethylthiazol-2-yl)-5-(3-carboxymethoxyphenyl)-2-(4-sulfophenyl)-2H-tetrazolium)

NCBI	National Centre for Biotechnology Information
NMR	Nuclear Magnetic Resonance
NP	natural product
NRP	nonribosomal peptide
NRPS	nonribosomal peptide synthase
°C	Degrees Celcius
OD	Optical density
OSMAC	One Strain Many Compounds
PCP	peptidyl carrier protein
PG	peptidoglycan
PK	polyketide
PKS	polyketide synthase
ppm	parts per minute
PRISM	PRediction Informatics for Secondary Metabolomes
RNA	ribonucleic acid
RP	reversed-phase
rpm	rotations per minute
SDS	sodium dodecyl sulphate
SDS-PAGE	sodium dodecyl sulphate polyacrylamide gel electrophoresis
ST domain	sulfotransferase
TE	thioesterase
UHPLC	ultra-high performance liquid chromatography
UHPL-MS	ultra-high performance liquid chromatography mass spectrometry

xg	relative centrifugal force
α	alpha
β	beta
γ	gamma
λ	lambda
tRNA	transfer ribonucleic acid
PTM	post translational modification
HEPES	4-(2-hydroxyethyl)-1-piperazineethanesulfonic acid)
psi	pound-force per square inch
PHASTER	PHage Search Tool Enhanced Release
mg	milligram
TEM	transmission electron microscopy
ng	nanogram
kV	kilovolt
NEB	New England Biolabs
w/v	weight per volume
v/v	volume per volume
Ω	ohm
µF	microfarad
hr	hour
V	Volts
TAE	Tris-acetate-EDTA
UV	Ultraviolet

nm	nanometer
IPTG	isopropyl-β-d-1-thiogalactopyranoside
TEMED	Tetramethylethylenediamine
kB	kilobase
LC-MS/MS	liquid chromatography with tandem mass spectrometry
TFF	tangential flow filtration
NaCl	sodium chloride
Tris	Trisaminomethane
HCl	hydrochloric acid

Table of Contents

Declaration i

Abstract ii

Acknowledgements iv

Dedication v

Abbreviations vi

Table of Contents xii

List of figures xvii

List of tables xxiv

Chapter 1: Literature review 1

1.1 Introduction 1

1.2 Natural products as bioactive molecules 2

1.3 Classes of NPs 6

1.3.1 Polyketides (PKs) 6

1.3.2 Nonribosomal peptides (NRPs) 8

1.4 Alternative treatments to “classic” antibiotics 10

1.4.1 Bacteriocins 10

1.4.2 Phage therapy 12

1.4.3 Bacterial Exopolysaccharides 21

1.5 NPs from the marine environment 27

1.5.1 Marine invertebrates 27

1.6 Bacterial symbionts of marine invertebrates 29

1.7 Approaches in natural product discovery 31

1.7.1 Top-down approach to NP discovery 32

1.7.2 Bottom up approach to NP discovery 35

1.8 Conclusion 40

1.9 Research objectives 40

Chapter 2: Heterologous expression of a putative prophage-encoded hypothetical protein from *T. actiniarum* 41

2.1 Introduction 41

2.2 Methods and Materials 43

2.2.1 Buffers, stock solutions, bacterial strains and plasmids used in this study 43

2.2.2 BLAST analysis and identification of prophage regions 44

2.2.3 Preparation of *T. actiniarum* cell free culture supernatant 45

2.2.4 Antibacterial screening of *T. actiniarum* cell free culture supernatant 46

2.2.5 Size fractionation of *T. actiniarum* cell free culture supernatant 46

2.2.6 Analysis of the 50kDa-100kDa and >100kDa fractions using Transmission electron microscopy (TEM) 46

2.2.7 Heterologous expression of TAP1 and TVP1 in *E. coli* Rosetta pLysS 47

2.3 Results and Discussion 51

2.3.1 Identification of prophage regions in *T. actiniarum* 51

2.3.2 Analysis of fractions (50kDa-100kDa and >100kDa) for phage particles using TEM 52

2.3.3 Protein sequence alignment using BLASTp 53

2.3.4 Preliminary antibacterial screening of *T. actiniarum* 54

2.3.5 Size fractionation and bioactivity screening of *T. actiniarum* cell free supernatant 55

2.3.6 Heterologous expression of TAP1 and TVP1 57

2.3.7 Conclusion 63

Chapter 3: Extraction and semi-purification of a putative high molecular weight antibacterial exopolysaccharide from *T. actiniarum* 65

3.1 Introduction 65
3.2 Methods 66
3.2.1 Preparation of culture supernatant for semi-purification 66
3.2.2. Semi-purification of antibacterial compound using anion exchange chromatography 66
3.2.3 Antibacterial screening of cell free supernatant 67
3.2.4 SDS and native PAGE analysis 67
3.2.5 Phenol-Sulphuric acid test 69
3.2.6 Ammonium sulphate precipitation of the active compound 70
3.2.7 Exopolysaccharide isolation 70
3.2.8 Zymography assay 70
3.2.9 Genome annotation using Prokka 71
3.3 Results and Discussion 71
3.3.1 Semi-purification of antibacterial compound from *T. actiniarum* using FPLC 71
3.3.2 Antibacterial screening of Fraction 1 and Fraction 2 73
3.3.3 SDS-PAGE analysis of FPLC Fractions 1 and Fraction 2 74
3.3.4 Phenol-Sulphuric acid test of Fraction 1 and 2 75
3.3.5 Ammonium sulfate precipitation of the active compound from *T. actiniarum* culture supernatant 77
3.3.6 Exopolysaccharide isolation from *T. actiniarum* fermentation 79
3.3.7 In-gel staining of exopolysaccharide fraction with Stains-All 82
3.3.8 Zymography assay of exopolysaccharide fraction 85
3.3.9 Biosynthesis of exopolysaccharides in bacteria 88
3.3.10 Poly-β-1, 6-*N*-acetyl-glucosamine (PNAG) structure and synthesis 93
3.3.11 Synthesis and antibacterial activity of chondroitin and chondroitin sulfate 99
3.3.12 Conclusion 100

Chapter 4: Isolation of cholic acid and 3-oxo cholic acid, from *Thalassomonas actiniarum*. ... 102

4.1 Introduction ... 102

4.2 Methods and Material ... 104

4.2.1 Bacterial strains and cell lines used in this study ... 104

4.2.3 Strain cultivation ... 104

4.2.4 Extraction of secondary metabolites from cultures using Diaion® HP-20 ... 104

4.2.5 Fractionation of Diaion® HP-20 extracts using the Biotage® system ... 105

4.2.6 Bioactivity screening of FLASH fractions ... 106

4.2.7 Dereplication of bioactive fractions using UHPLC-QTof-MS ... 111

4.2.8 Mass Guided isolation of compounds using preparative HPLC-MS ... 112

4.2.9 Structural elucidation of isolated compounds by NMR ... 113

4.2.10 Genome annotation and secondary metabolite pathway detection ... 113

4.3 Results ... 114

4.3.1 Genome mining for secondary metabolite biosynthetic pathways using antiSMASH and PRISM ... 114

4.3.2 Extraction and prefractionation of secondary metabolites from *T. actiniarum* fermentation broth ... 120

4.3.3 Bioactivity screening of FLASH fractions ... 121

4.3.4 Dereplication of active fractions ... 123

4.3.5 Mass guided isolation of candidate compounds ... 129

4.3.6 Structural Elucidation and bioactivity of compounds 407 and 405 ... 133

4.4 Biosynthesis of bile acids in eukaryotes ... 144

4.5 Bile acid synthesis in prokaryotes ... 153

4.6 Bile acid production by *T. actiniarum* ... 159

4.6 Conclusion ... 161

Chapter 5: General Conclusion ... 162

Appendices 169
Appendix 2A 169
Appendix 2B 170
Appendix 2C 172
Appendix 2D 174
Appendix 3A 175
Appendix 3B 175
Appendix 4A 177
Appendix 4B 178
Appendix 4C 179
Appendix 4D 180
Appendix 4E 181
Appendix 4F 182
Appendix 4G 183
Appendix 4H 184
Appendix 4I 185
Appendix 4J 186
Appendix 4K 187
Appendix 4L 188
References 189

List of figures

Chapter 1

Figure 1.1: New drugs approved by the FDA between 1981 and 2014. B: Biological macromolecule, N: Unaltered NP, NB: Botanical drug (defined mixture), ND: NP derivative, S: Synthetic drug, S*: Synthetic drug (NP pharmacophore), V: Vaccine, S/NM or S*/NM: Synthetic drug mimicking NP or Synthetic drug (NP pharmacophore mimic of NP)

Figure 1.2: Main classes of natural products, adapted from Hanson, 2013

Figure 1.3: Modular structure of Erythromycin A, taken from Lagunin et al., 2010

Figure 1.4: Modular structure of Nocardicin A, taken from Gaudelli, 2015

Figure 1.5: Epothilone biosynthesis gene cluster and modular structure, taken from Chen et al., 2001

Figure 1.6: Representative structure of tailed phages Myoviridae and Siphoviridae, taken from Nobrega, 2018

Figure 1.7: *P. luteoviolacea* tailocin structure. A: tailocin aggregate (175nm), B: tailocin tubular elements (100nm) taken from Freckelton, 2017

Figure 1.8: Structure of chondroitin sulfate and the various positions at which sulfation can occur, taken from Volpi, 2019. CS-O/: not sulfated; CS-A/chondroitin-4-sulfate: R1=$SO3^-$ and R2=R3=H; CS-B/chondroitin-2,4-disulfate: R1=R3= $SO3^-$ and R2=H; CS=C/chondroitin-6-sulfate: R2= $SO3^-$ and R1=R3=H; CS-D/chondroitin-2,6-disulfate: R2=R3 =$SO3^-$ and R1=H; CS-E/chondroitin-4,6-disulfate: R1=R2 =$SO3^-$ and R3=H; trisulfated chondroitin R1=R2=R3= $SO3^-$

Figure 1.9: Monosulfated nonasaccharide repeating units of EPS GY785 produced by *Alteromonas infernus*, taken from Rederstorff et al., 2011

Figure 1.10: Distribution of compound chemical classes and compound activities in Cnidarians, adapted from Rocha et al., 2011

Figure 1.11(A, B, C): Structurally and functionally diverse bioactive compounds isolated from marine bacteria from 2012 to 2015, taken from Schinke et al., 2017

Figure 1.12: Natural product discovery approaches, taken from Luo et al., 2014

Chapter 2

Figure 2.1: Construct maps of pET21-dTa (left) containing 1400 bp insert and pET21-aTv (right) containing 1395 bp insert representing the expression vectors for TAP1 and TVP1 respectively

Figure 2.2: Prophage regions 2, 3 and 4 identified in *T. actiniarum* showing TAP1 located upstream of Region 3. The pink box shows phage tail related proteins encoded in region 3, downstream of TAP1.

Figure 2.3: Electron micrographs (A, B and C) of fraction >100kDa showing tailocins (indicated by the red arrows) at bar 200nm. Tailocins from *T. actiniarum* resemble contracted phage tails

Figure 2.4: Amino acid sequence alignment of TVP1 (query 1) and TAP1 (subject)

Figure 2.5: Antibacterial activity of concentrated cell-free culture supernatant of *T. actiniarum*. Zone of clearance indicates inhibition of test strain *P. putida*. Growth media (Marine Broth), dH_2O and 0.1M Tris-HCl pH 8 buffer was used as negative controls

Figure 2.6: Well diffusion assay showing zones of inhibition against *P. putida* from fractions 50kDa-100kDa (A) and >100kDa (B)

Figure 2.7: Agarose gel (1%) showing uncut and digested plasmid DNA isolated from the transformants harbouring PCTa-1 and PCTV-1. Plasmid DNA was digested with restriction enzymes NcoI and XhoI for TAP1 and XhoI and NdeI for TVP1. Lane 1: Lambda PstI DNA size marker, Lane 3: Uncut plasmid DNA from PCTa-1, Lane 4: Single digest of plasmid DNA with XhoI from PCTa-1, Lane 5: Double digest of plasmid DNA with NcoI and XhoI liberating the 1400 bp insert from PCTa-1. Lane 7: Uncut plasmid DNA from PCTv-1, Lane 8: Single digest of plasmid DNA with XhoI from PCTv-1, Lane 9: Double digest of plasmid DNA with NdeI and XhoI liberating the 1395 bp insert from PCTv-1

Figure 2.8: SDS-PAGE analysis of expression of TAP1 (left) and TVP1 (right) (indicated by the red squares). Lane 1: Prestained Protein Ladder, Lane 2: Induced-soluble (20µl), Lane 3: Uninduced-soluble, Lane 4: Prestained Protein Ladder, Lane 5: Uninduced-soluble (20µl), Lane 6: Induced-soluble

Figure 2.9: Semi-purified soluble fraction of TAP1 (left, 10µl) and TVP1 (right, 10µl) resolved on SDS-PAGE after dialysis and size fractionation

Figure 2.10: Well diffusion assay of semi purified TAP1 (left) and TVP1 (right) against *P. putida* showing no inhibition of the test strain (indicated by the red arrows). Concentrated cell free culture supernatant (50kDa-100kDa labelled crude/control) from *T. actiniarum* was used as a crude control

Chapter 3

Figure 3.1: Well diffusion assay of the concentrated TFF fraction (>30kDa) tested against *Pseudomonas putida*, with buffer (100mM Tris-HCl pH 8) and distilled water used as negative controls and concentrated culture supernatant used as a positive control

Figure 3.2: FPLC chromatogram of *T. actiniarum* concentrated cell free culture supernatant

Figure 3.3: Antibacterial activity of Fraction 1 and Fraction 2 (50-100kDa) against *P. putida*

Figure 3.4: SDS-PAGE of FPLC Fraction 1 and Fraction 2 (active) after dialysis and size fractionation. Lane 1: marker, Lane 2: fraction 2 (50kDa-100kDa), Lane 3: fraction 1 (50kDa-100kDa)

Figure 3.5: Phenol-sulphuric acid assay of Fraction 1 (F1) and Fraction 2 (F2) and the concentration of the carbohydrates present in each fraction in reference to the glucose standard curve

Figure 3.6: Well diffusion assay of ammonium sulfate precipitated proteins (1: 30% saturation and 2: 75% saturation) following dialysis and size fractionation. The activity was tested against *P. putida* and concentrated culture supernatant was used as a positive control

Figure 3.7: Antibacterial assay of the EPS fraction isolated from *T. actiniarum* culture supernatant. The red arrow shows zone of inhibition against *P. putida* conferred by the exopolysaccharide preparation using the Sevag method. The green arrow shows no zone of inhibition against *P. putida* of the exopolysaccharide fraction deproteinized with TCA

Figure 3.8A: SDS-PAGE and B: Native PAGE analysis of the EPS purification from *T. actiniarum* following the Sevag method. A: lane 1: Protein Marker, lane: 3 BSA, lane 5: EPS

fraction (50-100kDa). B: lane 1: Protein Marker, lane 2: BSA, lane 3: EPS fraction (50-100kDa). This fraction represents 2L of starting material that was concentrated to 200µl and 20µl was resolved.

Figure 3.9: Well diffusion assay of the EPS fraction after removal of precipitate. Zone of inhibition against *P. putida* is indicated by the red square. Concentrated culture supernatant was used as a positive control

Figure 3.10: EPS fraction resolved under denaturing conditions and stained with Coomassie staining solution (A) and Stains-All (B)

Figure 3.11: EPS fraction resolved under non-denaturing conditions and stained with Coomassie staining solution (A) and Stains-All (B)

Figure 3.12(A, B, C, D): In-gel zymography assay of EPS fraction conducted under non-denaturing (A) and denaturing (B) conditions. Protein profile of EPS fraction stained with silver nitrate (C) and Coomassie (D) under non-denaturing conditions

Figure 3.13: Heptose synthesis pathway, adapted from Gaudet and Owen, 2002

Figure 3.14: Biosynthetic pathway for the production of UDP-N-acetylglucosamine (Li et al., 2012; Rodriguez-Diaz, 2012); UDP-glucuronic acid (Broach et al., 2012), UDP-glucose (Broach et al., 2012) and UDP-N-acetylgalactosamine (Dong et al., 2009) from trehalose (Thammahong et al., 2017) and glycogen (Seibold and Eikanns, 2007)

Figure 3.15: Synthase dependent pathway for PNAG synthesis, adapted from Schmid et al., 2015 and Kwan and Withers, 2014

Chapter 4

Figure 4.1: The bioassay guided isolation pipeline as followed by Mabcent (Svenson, 2013)

Figure 4.2(A and B): Modular structure of a potentially sulfated PK/NRP hybrid (A) and modular structure of a potentially sulfated NRP (B) identified through PRISM in *T. actiniarum*. KS-ketosynthase, Mal-acyltransferase, DH-dehydratase, KR-ketoreductase, T-thiolation, C-condensation, Thr-adenylation, ST-sulfotransferase, Gly, Phe, Ser, Asp, Glu and Thr-adenylation,

TE-thioesterase, PAA and C10-acyl adenylating enzymes, PPTase-phosphopantetheinyltransferase

Figure 4.3: Minutoside A, a sulfated steroid that loses antifungal activity against *Aspergillus flavus* when desulfated, taken from Carvalhal et al., 2018

Figure 4.4: Biofilm inhibition assay results of Fractions 1 to 5. Each sample was tested in duplicate. The red rectangle shows inhibitory activity of Fraction 5 in wells F4 and F5. Fractions 1 to 4 are present in wells B4-5, C4-5, D4-5 and E4-5 respectively, exhibiting no activity

Figure 4.5: MTS cell proliferation assay of Fractions 1 to 5. Each sample tested in triplicate. The red rectangle indicates bioactivity exhibited from Fraction 5 in wells B-6, C-6 and D-6. Fraction 1: wells B-2, C-2, D-2; Fraction 2: wells B-3, C-3, D-3; Fraction 3: B-4, C-4, D-4 and Fraction 4: B-5, C-5, D-5 shows no activity against A2058

Figure 4.6: Comparison of BPI chromatograms ESI+ (*m/z* 50-2000) for inactive Fractions (4 and 6) and active Fractions (5). The arrow corresponds to compounds with retention time 5.62 minutes (*m/z* 355.2633)

Figure 4.7: Predicted elemental composition, structure and identity of compound 7 (*m/z* 355.26) analysed in ESI+ mode

Figure 4.8: Structure of Mooloolabene A (R1: H and R2: β-CHO) and B (R1: H and R2: α-CHO) taken from Prasad, 2017

Figure 4.9: Comparison of BPI chromatograms ESI- (*m/z* 50-2000) for inactive Fractions (4 and 6) and active Fractions (5). The arrow indicates compound with retention times 5.64 (*m/z* 407.2633)

Figure 4.10: Mass spectrum of 5β-tetrahydrocortisol showing loss of water molecules during ESI+, adapted from Saba et al., 2018

Figure 4.11: BPI chromatogram from the initial isolation of compounds 407 from Fraction 5 separated over an Xterra RP C18 column using mass as fraction triggers

Figure 4.12: BPI chromatogram from the second isolation of compound 407 (dimer 815.8) separated over a RP fluorophenyl HPLC column using mass as a fraction trigger.

Figure 4.13: Isotope pattern of compound 407

Figure 4.14: Isotope pattern for compound 405

Figure 4.14: Compound 407 with elemental composition $C_{24}H_{40}O_5$

Figure 4.15A and B: Compound 407 (A) with elemental composition $C_{24}H_{40}O_5$ and compound 405 (B) with elemental composition $C_{24}H_{38}O_5$.

Figure 4.16: Compound 1: 3, 3, 12-trihydroxy-7-ketocholanic acid and Compound 2: 3,3,12-trihydroxy-7-deoxycholanic acid

Figure 4.17: Antibacterial activity of 3-oxo cholic acid against 6 test strains

Figure 4.18: Antibacterial activity of cholic acid against 6 test strains

Figure 4.19: Anticancer activity of 3-oxo cholic acid against cancer cell lines HT29, A2058 and MRC5

Figure 4.20: Anticancer activity of cholic acid against cancer cell lines HT29, A2058 and MRC5

Figure 4.21: Bile acid derivatives isolated from the symbiont *Psychrobacter* sp

Figure 4.22: Structures of C27 bile alcohols with primary alcohol on the C-terminal carbon of the side chain, and C27 and C24 bile acids with carboxyl group at C terminal carbon on the side chain taken from Christie, 2019

Figure 4.23: Bile acid synthesis pathway, taken from Li and Chiang 2009

Figure 4.24: Detailed cholic acid synthesis pathway showing 3-oxo cholic acid (indicated by the red square) as an intermediate in cholic acid synthesis, taken from Mukhopadhyay and Maitra, 2004.

Figure 4.25: Schematic representation of bile acid synthesis in eukaryotes

Figure 4.26: MVA pathway for isoprenoid synthesis in prokaryotes, adapted from Heuston et al., 2012

Figure 4.27: Biosynthetic pathway of squalene from FPP in eukaryotes, taken from van der Donk, 2015.

Figure 4.28: Cholesterol production from squalene taken from Belter et al., 2011

Figure 4.29: Proposed representation of bile acid synthesis in prokaryotes

Figure 4.30: MEP pathway for isoprenoid synthesis in prokaryotes, adapted from Heuston et al., 2012.

Figure 4.31: Biosynthetic pathway of squalene from FPP in bacteria, taken from van der Donk, 2015

Figure 4.32: Structure of the hopanoid bacteriohopanetetrol taken from Doughty et al., 2014

Figure 4.33: Hopanoid biosynthesis operon in *Zymomonas mobilis*, adapted from Pan et al., 2015

List of tables

Chapter 1

Table 1.1: Biological activity of NPs derived from microorganisms, taken from Pham et al., 2019

Table 1.2: Bacteriocins from Gram-positive and Gram-negative bacteria and their applications, adapted from Pieters and Todorov, 2010

Table 1.3: Phage therapies to treat bacterial infections in human and animal models, taken from Lin et al., 2017

Table 1.4: Companies developing phage therapies, taken from Schmidt 2019

Table 1.5: Sources and applications of polysaccharides, taken from Li et al., 2018

Table 1.6: List of bioactive polysaccharide produced by marine organisms, taken from Bajpai et al., 2014

Table 1.7: General characteristics of biologics vs small molecules, adapted from Kovaleinen 2018

Table 1.8: Marine natural products isolated from marine invertebrate symbionts, adapted from Trindade et al., 2015 and Blockley et al., 2017

Table 1.9: Bioactive secondary metabolites discovered through genome mining, taken from Sekurova et al., 2019

Chapter 2

Table 2.1: Bacterial strains and plasmid used in this study

Table 2.2: SDS-PAGE gel components

Table 2.3: Prophage regions identified on the genome of *T. actiniarum*

Chapter 3

Table 3.1: SDS and native PAGE gel components

Table 3.2: Overview of the most relevant bacterial EPS including monomer composition, substituent decorations, industrial application and biosynthetic pathway routes, adapted from Schmid et al., 2015

Table 3.3: BLASTp hits of *ica* and *pga* genes encoded on the genome *T. actiniarum*

Chapter 4

Table 4.1: Test organisms and cell lines used in this study

Table 4.2: FLASH purification mobile phase gradients

Table 4.3: Test bacteria, their growth media and incubation periods to reach the desired 0.5 McFarland standard

Table 4.4: Absorbance (OD_{600}) values required to define activity of the flash fraction

Table 4.5: MIC of gentamycin on the bacterial strains used for antibacterial screening

Table 4.6: 96-well microtitre plate layout for the anti-biofilm assay

Table 4.7: Absorbance values required to define activity of the extract in the biofilm inhibition assay

Table 4.8: 96-well tissue culture plate layout for the anticancer assay

Table 4.9: Mobile phase gradient used for the UHPLC system that is coupled to the MS

Table 4.10: Vion IMS QToF parameters for dereplication process in ESI+/-

Table 4.11: Mobile phase gradient used for Xterra RP C18 column in the first round of purification

Table 4.12: Mobile phase gradient used for X-Select Fluoro-phenyl column in the second round of purification

Table 4.13: Secondary metabolite biosynthetic gene clusters encoded on the genome of *Thalassomonas actiniarum*, predicted by anti-SMASH 5.0

Table 4.14: Relevant BLASTp hits of ST domain of PK/NRP hybrid of *T. actiniarum*

Table 4.15: Relevant BLASTp hits of ST domain of NRP of *T. actiniarum*

Table 4.16: Weight of FLASH Fractions 1-6

Table 4.17: Retention time, *m/z* ratio, predicted elemental composition and predicted structure of related compounds detected in active Fraction 5 analysed in ESI+ mode

Table 4.18: Retention time, *m/z*, predicted elemental composition and predicted structure for target compound 407 in active Fraction 5 analysed in ESI- mode

Table 4.19: ^{1}H and ^{13}C-NMR data for cholic acid in acetonitrile-d3

Table 4.20: ^{1}H and ^{13}C-NMR data for 3-oxo cholic acid in acetonitrile-d_3

Table 4.21: Bile acid producing marine bacteria

Table 4.22: Terpene nomenclature and linear precursors, adapted from Christianson 2017

Table 4.23: Hopanoid synthesis genes in *Z. mobilis*, taken from Pan et al., 2015

Table 4.24: Enzymes involved in the MEP pathway that are present on the genome of *T. actiniarum* based on Prokka annotation.

Chapter 1: Literature review

1.1 Introduction

The need for new drugs for the treatment of infections and chronic disease is obvious (Whitworth, 2004). With the advent of multidrug resistant (MDR) pathogens and the emergence of new infectious diseases, the search for new drugs has become of utmost importance (Bertrand et al., 2014). The ESKAPE pathogens (***E****nterococcus faecium*, ***S****taphylococcus aureus*, ***K****lebsiella pneumonia*, ***P****seudomonas aeruginosa* and ***E****nterobacter* sp.) in particular are a major concern. These pathogens exhibit multidrug resistance and are the leading cause of hospital acquired infections (Santajit and Indrawattana, 2016; Mulani et al., 2019). One of the major reasons why bacteria acquire resistance to antibiotics is as a result of antibiotic misuse (Santajit and Indrawattana, 2016) and bacteria that live in biofilms also show increased levels of resistance to antibiotics causing significant problems in the public health sector (Donlan, 2011; Lu et al., 2019). Biofilms are aggregates of microorganisms encased in a self-produced extracellular matrix. Over the last 20 years biofilm studies have increased rapidly as the importance of these structures in the survival of bacteria under unfavorable conditions (e.g., changes in pH, nutrient scarcity and UV rays) as well as providing resistance to antimicrobials has become apparent (Armbuster and Parsek, 2018; Sharma et al., 2019; Tewari et al., 2018).

Staphylococcus aureus is a biofilm forming pathogen (Chung and Toh, 2014) and multidrug resistant strains have been isolated from hospitals and clinical environments, mostly from medical devices. Biofilms form on catheters, prosthetic heart valves and other implanted devices and these often need to be removed and replaced, possibly resulting in complications and can be very traumatic for patients. The need for biofilm inhibitory compounds becomes imperative with the advent of multidrug resistant *Staphylococcus* and other biofilm producing strains (Chung and Toh, 2014). Apart from the burden of infectious diseases, chronic diseases such as cancer are also a major concern. According to reports in 2019, cancer has topped heart disease as the leading cause of death in middle aged adults in several countries (Howard, 2019). The incidence and occurrence of the disease is expected to rise by 70% over the next 20 years (Rayan et al., 2017). Current treatment options include surgical removal of cancerous tumors, radiation and/or chemotherapy. The disadvantage of chemotherapy is that the cancer tends to reoccur and the side effects are severe, decreasing patient quality of life. Despite this, chemotherapy is still widely used. The

molecular mechanisms of cancer cell growth and progression has been well studied and as a result many drugs have been chemically synthesized (Rayan et al., 2017). These drugs are however detrimental to patients and in many cases suppress the immune system of the patients, making them vulnerable to other infections. There is thus a need for effective anticancer drugs with minimal or no effect on patient quality of life (Rayan et al., 2017).

In light of the abovementioned cases, there is an obvious need for new therapeutic agents.

1.2 Natural products as bioactive molecules

Natural products (NPs) represent a family of chemical entities with a variety of biotechnological applications (Katz and Baltz, 2016). NPs or secondary metabolites are synthesized in stress induced situations, are not required for organism growth and generally have an antagonistic effect (Clardy and Walsh, 2004). NPs include antibiotics, pigments, toxins, enzymatic inhibitors and many other bioactive and pharmaceutically relevant compounds (Demain, 1998).

Natural products have been used since ancient times to treat diseases and are the most successful source of new drug candidates (Dias et al., 2012) with the majority of new drug candidates being NPs or derivatives of NPs (Lahlou, 2013). An assessment of all FDA-approved new chemical entities revealed that natural products and their derivatives represent over one-third of all new molecular entities (Patridge et al., 2016). Figure 1.1 shows all new drugs approved between 1981 and 2014 (Newman and Cragg, 2016). It is clear that most of the new drug candidates are NPs or derivatives of NPs.

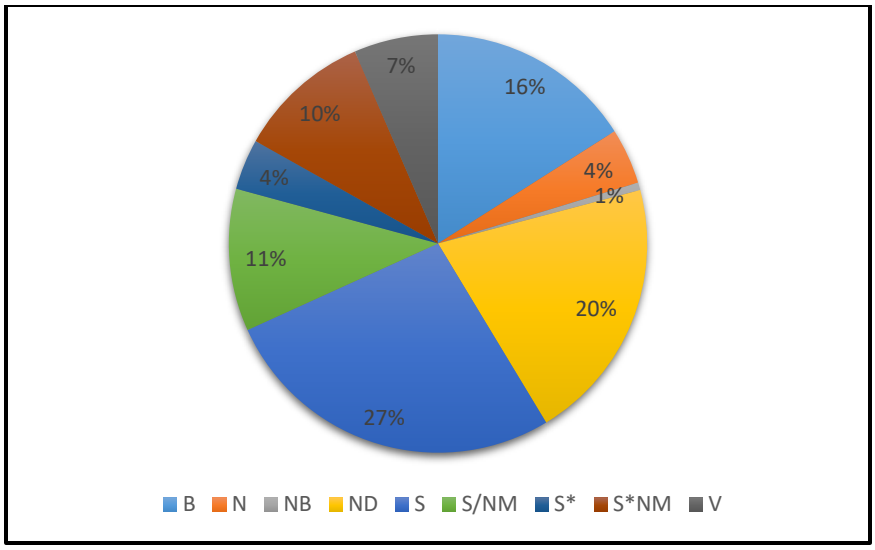

Figure 1.1: New drugs approved by the FDA between 1981 and 2014. B: Biological macromolecule, N: Unaltered NP, NB: Botanical drug (defined mixture), ND: NP derivative, S: Synthetic drug, S*: Synthetic drug (NP pharmacophore), V: Vaccine, S/NM or S*/NM: Synthetic drug mimicking NP or Synthetic drug (NP pharmacophore mimic of NP.

Natural products are diverse both chemically and structurally and show high specificity and a predilection for biological targets making them favorable over chemically synthesized compounds (Martins et al., 2014). NPs have diverse activities including antimicrobial, anticancer, anti-inflammatory, antibiofilm and antiviral activities (Sun et al., 2019; Pham et al., 2019). With the ongoing pandemic, natural products could also play an important role in the development of COVID-19 treatment as they have contributed to the treatment of other viral infections such as HIV, influenza and MERS-CoV (da Silva Antonio et al., 2020; Xian et al., 2020).

In the early 1900s approximately 80% of all pharmaceutically relevant NPs were obtained from plants. In 1928, upon the discovery of penicillin from *Penicillium notatum* by Alexander Fleming, microorganisms became an important source of NPs and examples of natural products isolated from microorganisms are depicted in Table 1.1. Notably, many of these bioactive NPs were isolated from *Streptomyces* species, the richest known source of antibiotics (Chater, 2016). Since the year 2000, 77% of FDA approved antibiotics were NPs derived from microbes (Pham et al., 2019).

Table 1.1: Biological activity of NPs derived from microorganisms, taken from Pham et al., 2019.

Name	Origin	Activity
Antibiotic		
Erythromycin	*Saccharopolyspora erythaea*	Antibacterial
Tetracycline	*Streptomyces rimosus*	Antibacterial
Vancomycin	*Amycolatopsis orientalis*	Antibacterial
Streptomycin	*Streptomyces griseus*	Antibacterial
Nisin A	*Lactococcus lactis*	Antimicrobial
Reuterin	*Lactobacillus reuteri*	Antimicrobial
Antifungal Agents		
Amphotericin B	*Streptomyces nodosus*	Antifungal
Ieodoglucomide	*Bacillus licheniformis*	Antifungal
Anticancer and Antitumor		
Bleomycin	*Streptoalloteichus hindustanus*, *Streptomyces verticillus*	Squamas cell carcinomas, Hodgkin's lymphomas and testis tumours
Ddaunorubicin	*Streptomyces peucetius* and various related strains	Acute lymphoblastic or myeloblastic lymphoma
Immunosuppressant/Anti-inflammatory Agents		
Rapamycin	*Streptomyces rapamycinicus*, *Streptomyces iranensis*, *Actinoplanes* sp. N902-109	Immunosuppressive, antifungal, antitumor, neuroprotective, neuroregenerative, lifespan extension activities
FK506	*Streptomyces tsukubaensis* and several *Streptomyces* species	Immunosuppressive, antifungal, anti-inflammatory, neuroprotective, neuroregenerative, rheumatoid arthritis treatment
Biofilm-Inhibitory Agents		
Cahuitamycins	*Streptomyces gandocaensis*	Inhibitors of *Acinetobacter baumannii* biofilms
Other		
Avermectins	*Streptomyces avermitillis*	Onchocerciasis and lymphatic filariasis
Mollemycin A 20	*Streptomyces* sp. (CMB-MO244)	Gram-positive and Gram-negative bacteria, antimalarial activity
Lipstatin	*Streptomyces toxytricini*	Pancreatic lipase inhibitor for obesity and diabetes

Using combinatorial chemistry, the synthesis of new antibiotics was attempted but has failed to produce anything as diverse as natural products (Zhang, 2005). Big Pharma companies have over the years abandoned natural product discovery operations due to the laborious and time consuming nature of this process. However, with new technologies such as automated screening, separation and structural elucidation techniques, drug discovery approaches are being revolutionised, giving rise to a 'new age of antibiotic discovery' (Wohlleben et al., 2016).

Natural product synthesis involves the repeated interaction with modulating enzymes and their activity is dependent on binding to other proteins (Lahlou, 2013). The efficacy of binding to and interacting with other molecules is an important feature of an effective drug (Lahlou, 2013). Natural products show better binding efficacy than synthetic molecules and this may be a result of their diverse and complex structures (Lahlou, 2013). The screening of NP/synthetic compound libraries is a laborious process and *in silico* techniques aimed at prioritizing attractive compounds are evolving. Machine learning (ML) is one of the most dynamic topics in computer-assisted drug discovery and involves the use of computer programs to analyze data and make predictions based on previously seen examples (Kirchweyer and Rollinger, 2013; Rupp, 2014). It does this by identifying patterns in datasets and generates mathematical relationships that can be used to predict the functional properties of candidate compounds (Kirchweyer and Rollinger, 2013). In 2019, Chen and co-workers devised a ML approach to identify NPs with high accuracy since commercial compound libraries often contain a mixture of NPs and synthetic molecules. The approach can be used to determine whether a compound is a NP or a synthetic molecule by determining its NP–likeness through identifying atoms that are characteristic of NPs or synthetic compounds.

ML has also shown to be an effective tool in describing the quantitative structure-activity relationships of compounds allowing the selection of attractive compounds during the initial phases of screening (Kirchweyer and Rollinger, 2013; Ivanenkov et al., 2019). In a study conducted by Egieyeh et al. (2018), the authors used a ML approach to identify potential antimalarial compounds from a compound library by comparing their chemical features and 2D structure to that of known antimalarial compounds. They found that the presence of an amine functional group on the compound is essential for antimalarial activity. These findings suggest that

in future, in vitro assays could be narrowed down to compounds that have the required chemical features, instead of screening entire compound libraries, saving time and reducing costs.

1.3 Classes of NPs

There is no rigid system in place for classifying NPs because their structural diversity, functions, and biosynthesis is too great to allow them to fit into a few simple categories. NP researchers however often speak of the NP classes presented in Figure 1.2.

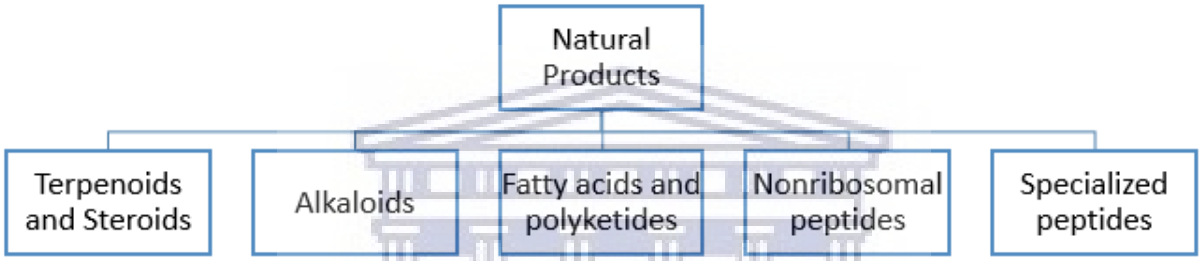

Figure 1.2: Main classes of natural products, adapted from Hanson, 2013.

For the purpose of this review, polyketides (PKs), nonribosomal peptides (NRP) and alternatives to classic antibiotics will be discussed. Polyketides and nonribosomal peptides constitute two of the largest classes of bacterially derived NPs that have found a use in the pharmaceutical space (Müller et al., 2015; Komaki et al., 2018; Walsh, 2008; Cane and Walsh, 1999; Pham et al., 2019). Encoded on the genome of *T. actiniarum*, several pathways of each type could be identified, which is why their synthesis and importance is discussed here.

1.3.1 Polyketides (PKs)

Polyketide synthases and nonribosomal peptide synthases are large multi-enzyme complexes with modular structures and the wide variety of arrangements in which these subunits can occur is key to the chemical diversity seen in polyketides and nonribosomal peptides (Machado et al., 2015; Woodhouse et al., 2013).

Polyketide biosynthesis occurs in the same modular manner in which nonribosomal peptide synthesis occurs but different protein domains and starting precursors are used (Keating and Walsh, 1999; Helfrich et al., 2010). Polyketide synthases (PKS) are multimodular enzymatic structures (Keating and Walsh, 1999; Helfrich et al., 2010). Generally polyketide synthesis is initiated with acetate that is derived from the precursors malonyl-CoA or acetyl-CoA. The acyl transferase (AT) domain selects and activates one of these acyl coenzyme A precursors prior to being transferred to the acyl carrier protein (ACP) that carries the growing chain (Keating and Walsh, 1999; Helfrich et al., 2010). The ketosynthase (KS) domain is responsible for elongation and extension of the peptide chain by means of a condensation reaction (Keating and Walsh, 1999). The thioesterase (TE) domain in turn cleaves the completed PK chain from the ACP domain and the polyketide is then modified by modifying domains (Keating and Walsh, 1999; Helfrich et al., 2010; Müller et al., 2015). These modifying domains include ketoreductase (KR), dehydratase (DH), methyltransferase (MT) and enoyl reductase (ER) (Skiba et al., 2016; Ma et al., 2019). Following condensation, a β-keto group is formed. The ketoreductase domain reduces this β-keto group to a secondary alcohol followed by the dehydration to form an α, β double bond. Enoyl reductase then reduces this double bond resulting in the conversion of the carbonyl unit to a methylene unit. Methylation of polyketides is also a common modification and involves the addition of a methyl group to the α-carbon. Figure 1.3 presents the modular structure of Erythromycin A, a polyketide based antibiotic.

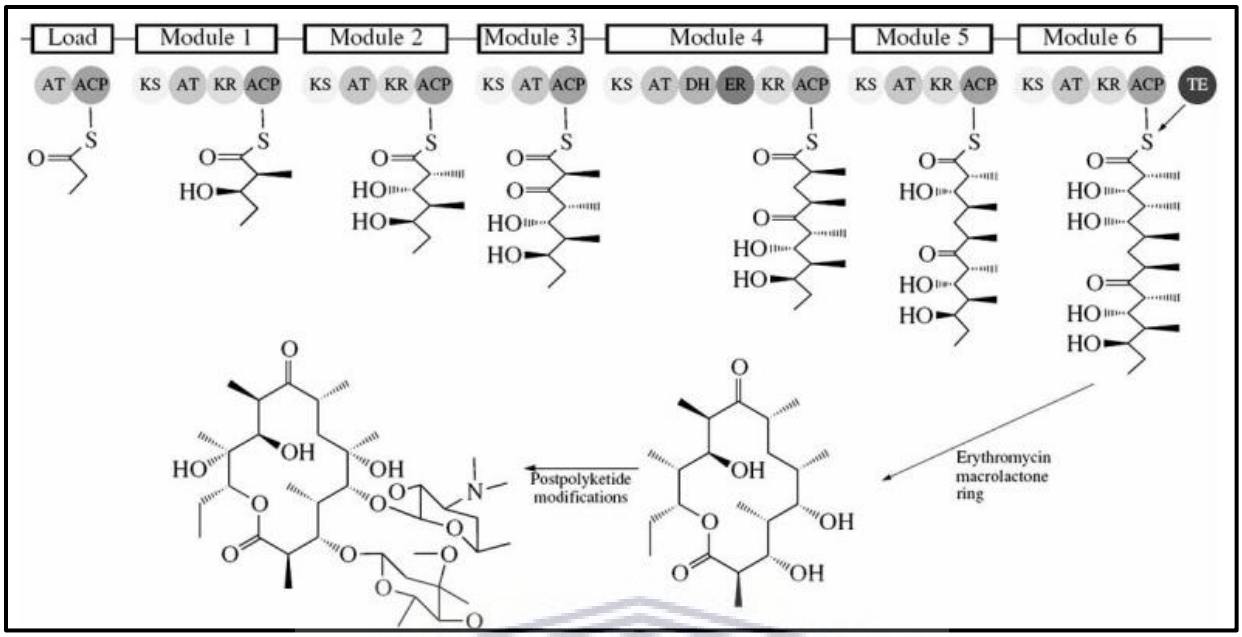

Figure 1.3: Modular structure of Erythromycin A, taken from Lagunin et al., 2010.

1.3.2 Nonribosomal peptides (NRPs)

Biosynthesis of NRPs is facilitated by multimodular enzymes known as nonribosomal peptide synthases (NRPS) (Keating and Walsh, 1999). Each module contains a number of domains which aid in the activation and condensation of a single amino acid (Keating and Walsh, 1999). The adenylation domain (A domain) is responsible for the activation of an amino acid and transfers it to the peptidyl carrier protein (PCP domain) that carries the growing peptide chain (Keating and Walsh, 1999). The condensation domain (C domain) is involved in the formation of a peptide bond between the next amino acyl and the growing peptide chain (Keating and Walsh, 1999). Thioesterase domains play the same role as for PKSs and release the mature NRP. Modification domains may be integrated for modification of the NRP (Keating and Walsh, 1999). Figure 1.4 illustrates the modular structure of Nocardicin A, a nonribosomal based antibiotic.

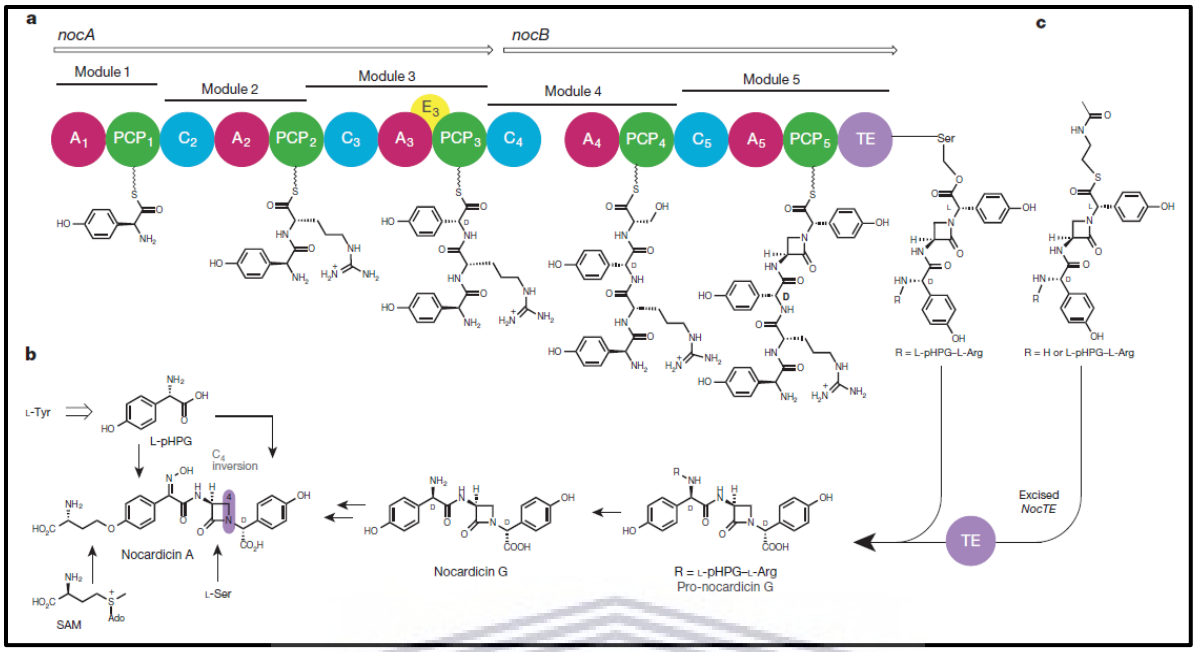

Figure 1.4: Modular structure of Nocardicin A, taken from Gaudelli, 2015.

Hybrids of these systems can also occur and are a fusion of the assembly of both PK and NRP modules to produce a single compound e.g. Epothilone D, an anticancer agent (Fisch, 2013; Chen et al., 2001) (Figure 1.5).

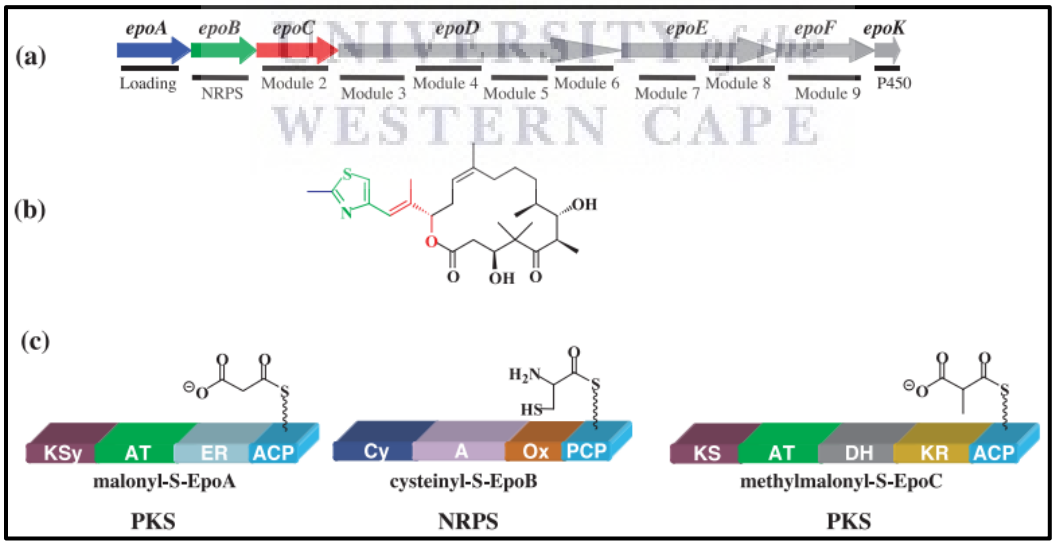

Figure 1.5: Epothilone biosynthesis gene cluster and modular structure, taken from Chen et al., 2001.

1.4 Alternative treatments to "classic" antibiotics

Antimicrobial molecules come in a wide gamut. Some of these are considered as alternatives to "classic" small molecule antibiotics. This section of the review will focus on the use of bacteriocins, phage therapy, endolysins, tailocins and exopolysaccharides as alternatives to traditional antibiotics.

1.4.1 Bacteriocins

Bacteriocins are antimicrobial peptides that are synthesized ribosomally and are considered narrow spectrum antibiotics as they act only on organisms who are closely related or belonging to the same species (Birri et al., 2010). These features set them apart from classic antibiotics that are synthesized through secondary metabolism and have a wide antibacterial spectrum (Giri and Singh, 2013). Some bacteriocins do however have a broader spectrum of activity that extends to fungi, viruses and yeasts. A few recorded bacteriocins have also shown antitumour activity (Giri and Singh, 2013). Both Gram-positive and Gram-negative organisms are capable of producing these peptides (Birri et al., 2010). Bacteriocins from Gram-negative bacteria can be classified into groups, namely colicin-like bacteriocins (CLB's), peptide bacteriocins and tailocins.

These can be further divided into two main groups: high molecular mass (30-80 kDa) colicins and low molecular mass (between 1-10 kDa) microcins. In response to DNA damage, the SOS regulon is activated and mediates colicin biosynthesis while microcins are produced by enteric bacteria under nutrient depleted conditions and are highly stable, protease resistant molecules (Blaszczyk and Moczarny, 2016). The genes necessary for bacteriocin production and immunity are usually arranged as operons on conjugative transposable elements, on the host and also on plasmids (Field, 2007).

Colicins, produced by *E. coli* are the most extensively studied bacteriocins from Gram-negative bacteria. These proteins consist of 3 domains responsible for killing, protein translocation and receptor recognition. To date, 25 different types of colicins have been identified from *E. coli* strains. These colicins differ in terms of their release mechanism from the producer, their translocation systems, killing mechanism and receptor specificity (Micenkova et al., 2019). The primary mode of action of colicins is the formation of ion permeable channels in the bacterial cytoplasmic membrane which affects nucleic acid synthesis, protein synthesis and causes cell

leakage which eventually leads to cell death (Allen et al., 2014; Konisky, 1982). Table 1.2 shows bacteriocins isolated from Gram-positive and Gram-negative bacteria as well their bioactivity.

Table 1.2: Bacteriocins from Gram-positive and Gram-negative bacteria and their applications, adapted from Pieters and Todorov, 2010.

Bacteriocin	**Producer**	**Potential use**
Gram-positive bacteria		
Nisin	*Lactococcus lactis* subsp. *lactis*	Treat peptic ulcer disease, Antimicrobial activity in medical devices such as catheters, Treat *S. pneumonia* infections, Treat mastitis in cattle, Vaginal contraceptive agent
Lacticin 3147	*L. lactis* subsp. *lactis*	Treat mastitis in cattle
Galliderm	*Staphylococcus gallinarum*	Treat skin infections such as acne
Epidermin	*S. epidermidis*	Treat skin infection such as acne
Mutacin B-Ny266	*Streptococcus mutans*	Bacterial infection caused by methicillin-resistant staphylococci
Tomicid	*Streptococcus* sp. Thom-1606	Streptococcal respiratory infections (Scarlet fever) in children
Gram-negative bacteria		
Microcins J25 and 24	*E. coli*	Treat *E. coli* and *Salmonella* infections in chickens
Colicins E1, E4 , E7, E8, K & S4	*E. coli*	Treat hemorrhagic colitis and hemolytic uremic syndrome caused by *E. coli* 0157:H7

Resistance to bacteriocins is very rare as seen with the widespread use of nisin A, a food preservative, with no reports of resistance to this bacteriocin. This may be due to the fact that these bacteriocins act on a small fraction of target bacteria in a community and in so doing fewer bacteria are under selective pressure to adapt (Allen et al., 2014). Resistance to bacteriocins has been observed however, in a study conducted on *E. coli* and *Listeria monocytogenes*, where long term exposure to increased concentrations of bacteriocins resulted in the strains acquiring resistance (Allen et al., 2014). The use of bacteriocins as alternative treatments, just as any other, must be carefully monitored and controlled to prevent resistance (Allen et al., 2014).

1.4.2 Phage therapy

Phages are biological entities made up of RNA and DNA enclosed in a protein capsid. They are bacterial parasites and depend on their bacterial host for survival. Additionally they are considered the most abundant biological entity on Earth and are responsible for regulating bacterial populations (Lin et al., 2017).

Phages attach to specific receptors on the bacterial cell wall and inject their genetic material into the cell. The genetic material integrates into the bacterial genome where it remains as a prophage that propagates with cell division. This process is referred to as the lysogenic cycle. Following environmental triggers the phages may convert to the lytic cycle. During the lytic cycle, the phage will hijack the hosts' genetic machinery and replicate to produce the next generation of phages. Once a critical phage titer is reached the phage progeny escape from the host cell by lysing it through the action of two proteins encoded by the virus (endolysin and holin) thereby killing the host. The virus can then go on to find a new host (Lin et al., 2017). Some phages however, are lytic phages and instead of integrating their genetic material into the host genome, will infect the host, propagate with cell division and lyse the host cell releasing progeny phages (Griffiths et al., 1999; Oliveira et al., 2012; Mirski et al., 2019).

The use of lytic phages to kill bacteria is referred to as phage therapy (Allen et al., 2014). This definition however is changing as bacteriophages can be genetically engineered and used as vehicles for the delivery of proteins, peptides and vaccines and not just as killing machines (Jafari and Abediankenari, 2015). For the most part phages are strain specific in their bactericidal activity compared to antibiotics that generally have a much broader effect. Therefore phage therapy can be much more target specific where it does not cause any undesired inhibition of non-target bacteria (Allen et al., 2014). Phage specificity can be advantageous when a specific bacterial species or genus is being targeted but can also be a drawback when phages targeting the infectious strain are unavailable.

For every bacterium there is a variety of phages able to infect it. Lytic phages have been cultured and administered to treat disease in both humans and animals. Currently phage therapy makes use of 'cocktails' of phages that infect the target pathogens, thus slowing down the rate of bacterial resistance to phage therapies (Allen et al., 2014). In May 2019, a group of researchers at the University of Pittsburg reported the successful treatment of a teenager infected with

Mycobacterium abscessus using a cocktail of genetically engineered phages. In 2016, phage therapy was also used to treat an individual infected with MDR *Acinetobacter baumanni*. By the time the treatment was admitted the individual had already suffered organ failure but made a full recovery. Interestingly, the researchers observed that the MDR bacteria that survived the phage therapy were now resensitized to antibiotics as well as immune cells suggesting that when used synergistically with antibiotics it can be very effective (Schmidt, 2019).

Most phages display no risks to human health but are however capable of mobilizing genes between bacteria by means of horizontal gene transfer and do elicit an immune response. As a result, bacterial pathogenicity and virulence can be promoted, negatively affecting human health.

Phage therapy was initially developed for the treatment of topical infection but evidence suggests that it is effective in treating systemic infections (Allen et al., 2014). In addition to treating human infections, in the US, phage therapy has been used to treat foodborne pathogens in animals and as a biocontrol agent for the treatment of plant pathogens. Table 1.3 shows cases in which phage therapy has been used to treat bacterial infections in both animal and human models (Lin et al., 2017).

Table 1.3: Phage therapies to treat bacterial infections in human and animal models, taken from Lin et al., 2017.

Causative agent	Model	Condition	Oral	Result summary
Shigella dysenteriae	Human	Dysentery	Oral	All four treated individuals recovered after 24hr
Vibrio cholerae	Human	Cholera	Oral	68 of 73 survived in treatment group and only 44 of 118 in control group
Pseudomonas aeruginosa	Murine	Sepsis	Oral	66.7% reduced mortality
Clostridium difficile	Hamster	Ileocecitis	Oral	Co-administration with *C. difficile* prevented infection
	Hamster	Ileocecitis	Oral dose every 8h for 72h	92% reduced mortality
Vancomycin-resistant *Enterococcus faecium*	Murine	Bacteremia	i.p	100% reduced mortality
β-lactamase producing *Escherichia coli*	Murine	Bacteremia	i.p	100% reduced mortality
Imipenem-resistant *P. aeruginosa*	Murine	Bacteremia	i.p	100% reduced mortality
Acinetobacter baumannii, *P. aeruginosa* and *Staphylococcus aureus*	Murine	Sepsis	i.p	Animals protected against fatal dose of *A. baumannii* and *P. aeruginosa* but not *S. aureus*
E. coli	Murine	Meningitis and Sepsis	i.p or s.c.	100% and 50% reduced mortality for meningitis and sepsis, respectively
Vibrio parahaemolyticus (MDR)	Murine	Sepsis	i.p. and oral	92% and 84% reduced mortality for i.p. and oral routes, respectively
S .aureus	Rabbit	Wound infection	s.c.	Co-administration with *S. aureus* prevented infection
MDR *S. aureus*	Human	Diabetic foot ulcer	Topical	All 6 treated patients recovered
Unclassified bacterial dysentery	Human	Dysentery	Oral	Phage cocktail improved symptoms of 74% of 219 patients
Salmonella typhi	Human	Typhoid	Oral	In cohort of 18577 children, phage treatment associated with 5-fold decrease in typhoid incidence compared to placebo
Antibiotic-resistant *P. aeruginosa*	Human	Chronic otitis	Oral	Phage treatment safe and symptoms improved in double-blind, placebo-controlled Phase I/II trial

- **(i.p.): intraperitoneal injection, (s.c.): subcutaneous injection**

Although phage therapy seems to be an avenue to explore in the search for new antibiotics or alternatives, much controversy surrounds its use (Nilsson, 2014). Phage therapy is considered complex in terms of pharmacokinetics and pharmacodynamics (Nilsson, 2014). This is because phages are very large compared to "classic'' antibiotics, and the effectiveness of treatment is

dependent on the number of phages which also vary in virulence. The time taken by a phage to attach to and inject its genetic material into the host can either be faster or slower and the speed with which progeny are produced and the number of progeny phages released also varies (Nilsson, 2014).

Because phages rely on host machinery for replication and particle synthesis, the rate at which progeny are generated does depend on the particular phage and the replication machinery encoded by it, however the rate is mostly determined by the host's metabolism (the faster the host grows, the faster the progeny can be produced) making phages an elegant way to regulate host growth. As mentioned previously, phages are often referred to as "promiscuous" because they can swop out genes between phages and their hosts related to virulence, bacterial toxins and resistance genes. In light of this, clinical trials involving human models are very rare due to the high regulatory load. However, with new sequence technologies phage therapies are better positioned due to faster and cheaper screening and key strides have been made in their understanding.

Although few cases have been reported, phage therapy has shown to be an effective alternative to antibiotics and many companies have invested in developing this therapy (Table 1.4) for a variety of targets and many are at preclinical levels (Schmidt, 2019).

Table 1.4: Companies developing phage therapies, taken from Schmidt 2019.

Company	Founded	Funding	Platform	Target	Status
Adaptive phage therapeutics	2016	$5 million seed	Individualized phage therapy, PhageBank, Host Range Quick Test	Infectious disease, urinary tract infections	Preclinical
AmpliPhi Biosciences	2002	$8.3 million market capitalization	Phage combinations for bacteria	Infectious disease	Phage 1 cocktail of three phages, skin safety test; individual access for *S. aureus* and *P. aeruginosa*
BiomX (Ness Ziona, Israel)	2015	$24 million	Customized phage cocktails	Irritable bowel disease	Preclinical
C3J Therapeutics	2005	$136 million	Antimicrobial peptides and engineered phages	Infectious disease, microbiome	Preclinical
Eligo Bioscience (Paris)	2014	$20.2 million series A (Khosla, Seventure)	CRISPR engineered phage	Infectious disease	Preclinical
EnBiotix	2012	Not disclosed	Engineered phage	Joint, skin, wound, cystic fibrosis, prosthetic joint infections	Preclinical
Intralytix	1998	$17.5 million	Phage cocktail against adherent, invasive *E. coli*	Crohn's disease	Phase 1/2
Locus Biosicences	2015	$26 million	CRISPR engineered phage	Infectious disease, microbiome	Preclinical
Nemesis Biosciences (Cambridge, UK)	2014	$2.3 million	Transmid	Extended spectrum β-lactamase-producing bacteria	Preclinical
Pherecydes Pharma (Romainville, France)	2006	$12.3 million	Individualized phage therapy	Infectious disease	Phase 2 (burns)

Phage based therapies can either make use of the entire phage structure as described above or employ single enzymes such as endolysins as discussed below.

1.4.2.1 Endolysins

Following holin mediated puncture of the cell's plasma membrane during cell lysis, endolysins (lytic enzymes encoded by phages) gain access to the cell wall where they cleave the bonds of the peptidoglycan (PG) layer of the bacterial host cell wall resulting in cell lysis during the phage lytic cycle (Allen et al., 2014). Cells treated externally with purified endolysin undergo "lysis from without" (Kashani et al., 2018).

Because of the diversity of cell wall structures, endolysins encompass a diverse array of targets and activities, targeting various bonds in the peptidoglycan matrix (Allen et al., 2014). One disadvantage of using endolysins as an antibiotic is that they are mostly effective against Gram-positive bacteria since the cell wall of Gram-positive bacteria is constructed in such a way that the peptidoglycan layer is exposed (Allen et al., 2014). Progress has however been made in developing and identifying endolysins active against Gram-negative pathogens, e.g. the lysin PlyE146, encoded by an *E. coli* prophage, is active against *E. coli*, *P. aeruginosa* and *A. baumanni* (Allen et al., 2014, Larpin et al., 2018; Yan et al., 2019; Zampara et al., 2018).

Phage endolysins are considered promising alternatives to antibiotics and have proven effective in various animal models of bacterial infection. Most phage endolysins are species specific, a very advantageous property considering the current prominence of broad-range antibiotic resistance. Just like phage therapy, development of resistance against endolysins is unlikely for several reasons. Since the phage and the host bacteria have co-evolved, endolysins too have evolved to bind to and cleave highly conserved structures in the cell wall that are essential for host survival. External application of endolysins, without having to enter the bacterial cell, allows the endolysins to avoid possible removal by bacterial efflux pumps (Kashani et al., 2018). Several endolysins also target different bonds in the peptidoglycan, further reducing the chances of bacteria developing resistance. Finally, to enhance their therapeutic activity and to avoid the development of resistance, multiple endolysins may be used in combination with "classic" antibiotics to treat bacterial infection (Kashani et al., 2018).

SAL200 is a phage endolysin based drug candidate for the treatment of staphylococcal infections. Jun and co-workers investigated the pharmacokinetics and tolerance of this endolysin on a group of healthy individuals. This is the first study in which an endolysin-based drug administered

intravenously was tested on human models. SAL200 shows potent bacteriolytic activity and is also active against MDR staphylococcal and biofilm producing strains (Jun et al., 2017).

1.4.2.2 Tailocins

Tailocins, also called high molecular mass bacteriocins, do not just resemble the tail structures of bacteriophages from the Myoviridae (R-type) and Siphoviridae (F-type) families (Figure 1.6) they are also morphologically and genetically similar to phage tails and do not contain a head or any genetic material. Francois Jacob discovered these bacteriocins in *P. aeruginosa* in 1954 and only in 2011, Gill and Young coined the term tailocins (Saha, 2016). Although they are thought to be derived from phages, they are not simply defective phages, but are adapted specifically to their function as bacteriocins. The best studied tailocins are the R- and F-type pyocins produced by *P. aeruginosa.* R-type pyocins, have a core sheath and resemble the contractile tail of P2-like phages while F-type pyocins resemble λ phage, have no sheath and are flexible (Nakayama, 2000).

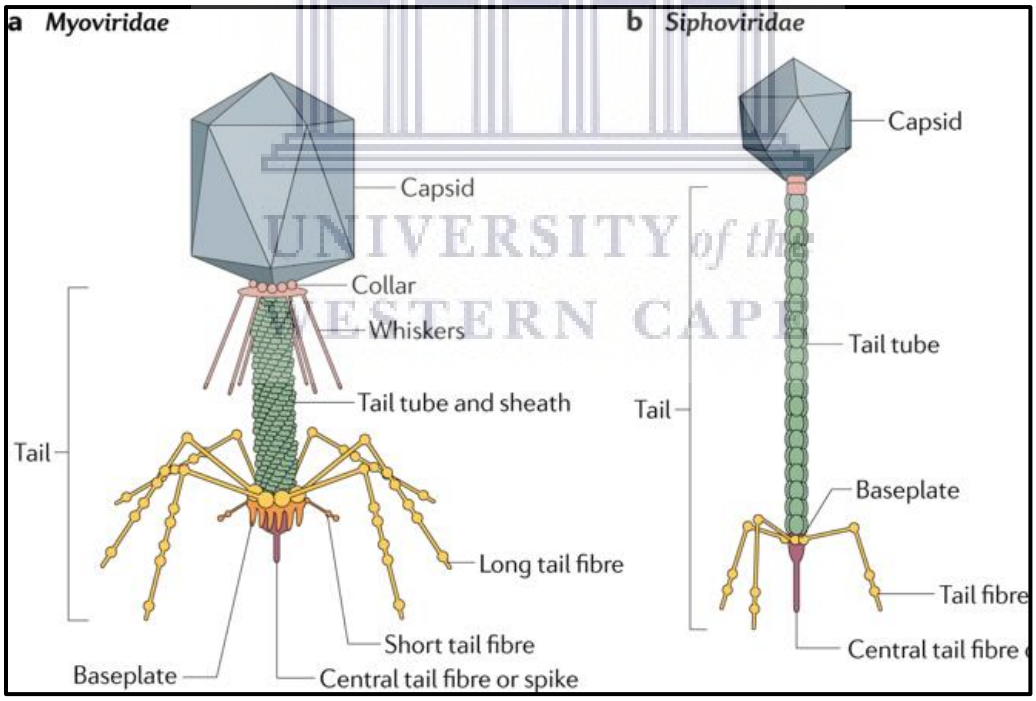

Figure 1.6: Representative structure of tailed phages Myoviridae and Siphoviridae, taken from Nobrega, 2018.

Both groups target bacterial cells only and generally have narrow specificity and are considered to cause minimal damage to non-target microbiota. Some also have broader spectrum of activity as seen by the tailocin Bcep0435 from *Burkholderia* sp. Members of the *Burkholderia cepacia*

complex (BCC) are plant and human opportunistic pathogens with broad spectrum antibiotic resistance. In a dissertation by Duarte, 2012, the author investigated the antibacterial activity of tailocin Bcep0425 produced by *B. cenocepacia* strain BC0425 against other members of the BCC group as well as *E. coli* and *Pseudomonas*. The tailocin was active against members of the BCC group as well as *E. coli* and *Pseudomonas* indicating its broad spectrum activity.

Only a handful of studies have investigated F-type pyocins and very little is known about their biochemical properties, abundance, mode of action and therapeutic potential (Saha, 2016). However, like R-type pyocins, F-type pyocins are also thought to kill cells by puncturing the cell membrane and causing membrane depolarization (Ohnishi et al., 1971) an example of 'lysis from without' (Saha, 2016).

Tailocin specificity is modulated by tail fibers, which have been demonstrated to bind to lipopolysaccharides, with different residues involved depending on the tailocin. Bacterial membrane damage occurs when conformational changes of the tailocin are induced upon contact with the lipopolysaccharide (LPS) receptor. Not much is known about the acquisition of resistance to tailocins but it is proposed that the alteration of LPS receptors may assist as it prevents the tailocin from recognizing specific receptors (Behrens et al., 2017). With that being said, tailocins also have the potential to be genetically engineered to target strains that were previously resistant to them. In a publication by Williams et al. (2008), the authors show that by replacing the tail fibers of a R2 pyocin from *P. aeruginosa* PAO1 with tail fibers from *Pseudomonas* phage PS17, the bactericidal specificity was altered.

Furthermore, in a study conducted by Príncipe et al. (2018), the authors investigated the inhibitory activity of tailocins produced by *Pseudomonas fluorescens* strain SF4c against the phytopathogenic strain *Xanthomonas vesicatoria* Xcv Bv5-49 that causes bacterial spot disease in tomatoes. Treatment with the tailocins revealed a decrease in *X. vesicatora* cell viability and reduction in bacterial spot disease symptoms in infected tomatoes 12 hrs after treatment. Significantly these tailocins showed no cytotoxicity. Currently copper containing bactericides are used for the treatment of bacterial spot disease in tomatoes. With consumers demanding chemical free products and the need for the use of environmentally friendly alternatives to bactericides, these tailocins are promising candidates (Príncipe et al., 2018).

Many marine organisms require external cues from surface bound bacteria to metamorphose from larval to adult stage. In 2014, Shikuma et al. showed that *Pseudoalteromonas luteoviolacea* HI1 produced tailocins (Figure 1.7) that trigger metamorphosis of the tubeworm *Hydroides elegans*. Upon deletion of the genes encoding sheath, tube and base plate proteins of the tailocin, no metamorphosis was observed from the larvae of *H. elegans*. Once the functional genes were replaced, metamorphosis of *H. elegans* larvae was observed. *P. luteoviolacea* is known to also induce metamorphosis of corals and sea urchins indicating its significance in aquaculture ecology, but also raising the question as to a wider role of tailocins in the metamorphosis of other invertebrates.

Figure 1.7: *P. luteoviolacea* tailocin structure. A: tailocin aggregate (175nm), B: tailocin tubular elements (100nm) taken from Freckelton, 2017.

In light of the abovementioned cases, tailocins are promising candidates that can be used in pharmaceutical, agricultural and aquaculture industries.

1.4.3 Bacterial Exopolysaccharides

Polysaccharides from plants, animals and microorganisms have been widely used as food additives, viscosifiers, gelling agents and drug adjuvants in various application fields (Table 1.5). In recent years the increased demand for natural polymers for pharmaceutical, food and other industrial applications has led to a remarkable interest in polysaccharides produced by microorganisms (Li et al., 2018). These biopolymers have emerged as new polymeric materials with novel and unique physical characteristics and therefore they have found extensive applications (Poli and Nicolaus, 2010).

Table 1.5: Sources and applications of polysaccharides, taken from Li et al., 2018.

Polysaccharide	**Source**	**Function**
Starch	Plants	Storage, drug adjuvant
Cellulose	Plants	Cell structure, food additives
Pectin	Plants	Food additives
Alginate	Microorganisms	Drug adjuvant
Carrageenan	Microorganisms	Food additive
Heparin	Animals	Animal tissue structure, therapeutic agent
Hyaluronan	Animals	Animal tissue structure, therapeutic agent
Chondroitin sulfate	Animals	Animal tissue structure
Heparin sulfate	Animals	Animal tissue structure
Chitin and Chitosan	Animals	Tissue scaffolds

Polysaccharides are high molecular weight macromolecules ranging from 50 Da to several thousand kDa (Casillo et al., 2018). They are long chain biopolymers composed of repeating monosaccharide units linked through glycosidic bonds and can be categorized as either homopolysaccharides or heteropolysaccharides (de Carvalho and Fernandes, 2010). The common linkages between monosaccharides occur at position β-1,4 and β-1,3 giving the polysaccharide a rigid backbone. If linkages occur at α-1,3 and α-1,6 positions, polysaccharides will have a more flexible backbone. The repeating units can be branched or unbranched and can be modified with salts like phosphate, sulfate and acids like lactic acid, succinic acid, acetic acid and pyruvic acid (de Carvalho and Fernandes, 2010).

Bacterial polysaccharides include capsular polysaccharides and exopolysaccharides and are categorized based on their linkage to the cell surface (Cescutti, 2010). Several pathogens produce capsular polysaccharides that are often composed of glycosaminoglycan's (GAGs) (Schiraldi et al., 2010). GAGs are linear heteropolysaccharides consisting of amino sugars (glucosamine and galactosamine) as well as acid sugars (glucuronic and iduronic acid) and are of value to the pharmaceutical, medical and cosmetic industries (Badri et al., 2018). The main commercial GAGs are hyaluronic acid (moisturizer, wrinkle filler), heparin sulfate (anticoagulant) and chondroitin sulfate (treat osteoarthritis) (Badri et al., 2018; Delbarre-Ladrat et al., 2014). Most GAGs are currently isolated from animal sources with the exception of hyaluronic acid which is the only GAG produced at large scale by *Streptococci* sp. (Badri et al., 2018). The main application of chondroitin sulfate, isolated from shark cartilage and/or bovine trachea, is in the treatment of osteoarthritis but it has also been shown to assist in tissue regeneration, drug delivery, has antibacterial activity and the potential to be used as a cancer biomarker (Karakurt et al., 2019; Schiraldi et al., 2010; Badri et al., 2018). Chondroitin sulfate is composed of repeating disaccharide units of glucuronic acid and N-acetylgalactosamine and undergoes sulfation at various positions through the activity of sulfotransferases (Figure 1.8) (Schiraldi et al., 2010; Volpi, 2019).

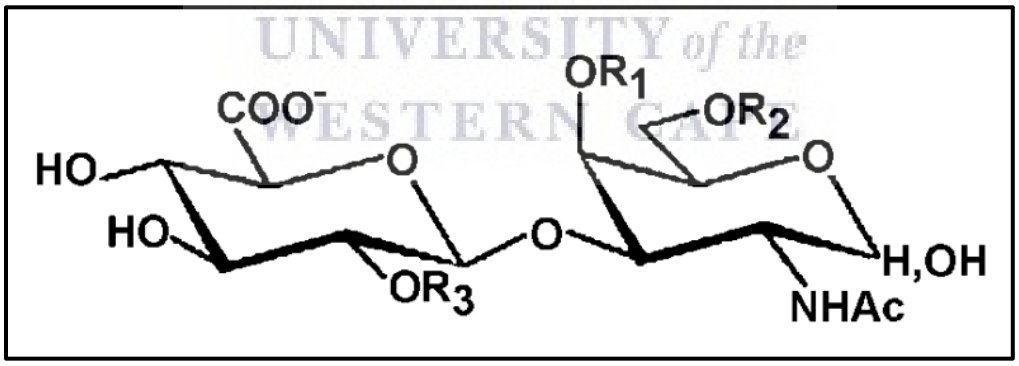

Figure 1.8: Structure of chondroitin sulfate and the various positions at which sulfation can occur, taken from Volpi, 2019. CS-O/: not sulfated; CS-A/chondroitin-4-sulfate: R1=SO_3^- and R2=R3=H; CS-B/chondroitin-2,4-disulfate: R1=R3= SO_3^- and R2=H; CS=C/chondroitin-6-sulfate: R2= SO_3^- and R1=R3=H; CS-D/chondroitin-2,6-disulfate: R2=R3 =SO_3^- and R1=H; CS-E/chondroitin-4,6-disulfate: R1=R2 =SO_3^- and R3=H; trisulfated chondroitin R1=R2=R3= SO_3^-.

Given that by the year 2021, the expected market for chondroitin sulfate is said to increase to 3 million kg per year, there is a need for the large scale sustainable production of chondroitin sulfate

(Badri et al., 2018). The production of unsulfated chondroitin has been recorded in *E. coli* K4 and *Pasteurella multicoda* Type D and F (Green and DeAngelis, 2017; Schiraldi et al., 2010) and currently enzymatic modifications are used to add the necessary sulfate groups to the molecule given that these bacteria do not produce chondroitin sulfotransferases (Badri et al., 2018). Although this approach seems feasible, the use of animal derived biopolymers in human therapies and the exploitation of sharks and bovine is a public concern, which further emphasizes the need for new sources of chondroitin sulfate and other GAG-like molecules (Schiraldi et al., 2010).

Marine bacterial polysaccharides and their application as GAG-like molecules have been investigated and have shown to be an attractive and renewable source of alternatives to current commercial GAGs. The bacterial polysaccharide producers can be cultivated in bioreactors that allows for the optimization of the growth conditions and the production yield through genetic engineering. Furthermore, extraction from bacterial fermentations is easier and less expensive compared to other sources, making them a more economically feasible source (Delbarre-Ladrat et al., 2014; Badri et al., 2018).

In the marine environment, bacterial exopolysaccharides are ubiquitous where they are essential for microbial survival and make up a large portion of the reduced carbon found in oceans (Nichols et al., 2005). Bacteria colonize other invertebrates as a survival strategy by producing EPSs and forming biofilms on their host surfaces. This attachment gives them access to nutrients and protects them from potential predators and other environmental stressors (Elsakhawy et al., 2017; Poli and Nicolaus, 2010). Most of the functions ascribed to EPSs are of a protective nature and their precise roles are dependent on the ecological niches in which the microorganisms live (Poli and Nicolaus, 2010; Dave et al., 2020). Some exopolysaccharides are involved in pathogenicity as in *Pseudomonas aeruginosa* which produces alginate that blocks the respiratory tract and exacerbates the bacterial infection (Morris and Harding, 2009). Several types of EPSs produced by marine macro- and microorganisms show biotechnological promise (Table 1.6). Although the majority of these polysaccharides listed were isolated from macro organisms, many reports investigating the bioactivity of marine bacterial exopolysaccharides exist (Orsod and Huyop, 2012; Mohamed, 2018; Wu et al., 2016; Aullybux et al., 2019; Jiang et al., 2011; Hassan and Ibrahim, 2017; Ruocco et al., 2016).

Table 1.6: List of bioactive polysaccharide produced by marine organisms, taken from Bajpai et al., 2014.

Compound	Source	Biological activity
Polysaccharide AJP	*Apostichopus japonicas*	Antioxidant & anti-hyperlipidemic
Fucoidan	*Ascophyllum nodosum*	Anti-proliferative, antitumor, anticancer, antimetastastic and fibrinolytic
Sulfated polysaccharide	*Sargassum wightii*	Anticoagulant activity
Rosacelose	*Mixylla rosacea*	Anti-HIV
Spirulan	*Anthrospira platensis*	Antiviral
Fucan	*Cladosiphono kamuranus*	Inhibit the infection of BHK-21 cells with dengue virus type 2 (DENV-2)
Chitinase	*Streptomyces* sp.	Antifungal against *A. niger* & *C. albicans*
Chitinase	*Craniella australiensis*	Antifungal against *A. niger* & *C. albicans*
Polysaccharide YCP	*Phomaherbarum*	Antitumor
Polysaccharide (PS1-1, PS1-2 & PS2-1	*Penicillus* sp.	Antioxidant
Sulfated polysaccharide	*Sargassum swartzii*	Antioxidant
Sulfated polysaccharide	*Sargassum tenerrimum*	Antioxidant
Sulfated polysaccharide PK-G03	*Gyrodinium impudium*	Anti-influenza virus
GY785	*Alteromonas infernus*	Bone healing

EPSs from extremophiles are particularly interesting because they have unique properties that make them stable in environments where desiccation, temperature, pressure, salinity and acidity are extreme. EPSs from moderately halophilic organisms such as *Halomonas* sp., *Alteromonas* sp. and *Idiomarina* sp. have shown potential in industrial and pharmaceutical application where biopolymers with emulsifying, jellying and metal binding capabilities is in demand. Sulfated EPSs are particularly interesting and find their application in the pharmaceutical industry as antitumor or antiviral agents (Elsakhawy et al., 2017). Figure 1.9 illustrates the structure of the repeating unit of the EPS GY785, an anionic, branched, sulfated heteropolysaccharide with bone regeneration activity produced by the marine bacterium *Alteromonas infernus* (Roger et al., 2004).

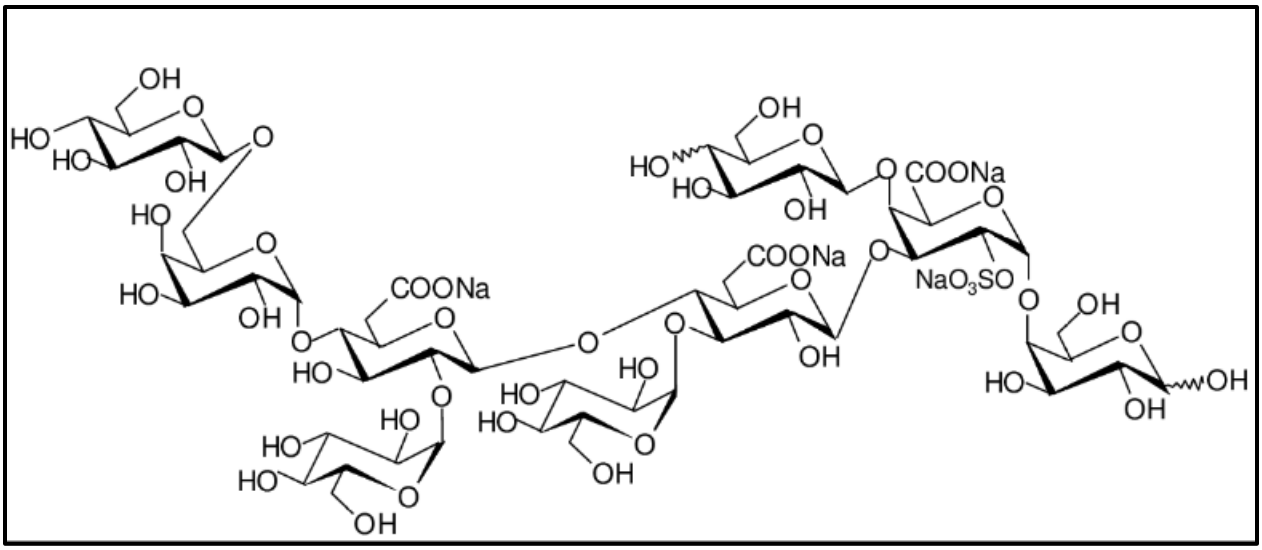

Figure 1.9: Monosulfated nonasaccharide repeating units of EPS GY785 produced by *Alteromonas infernus*, taken from Rederstorff et al., 2011

Most exopolysaccharides from the marine environment are heteropolysaccharides consisting of hexoses, pentose, amino sugars and up to 50% uronic acids (Nichols et al., 2005). Uronic acids are carboxylated sugars that afford the polysaccharide with a net negative charge and acidic properties at pH 8, the pH of seawater. The type of modification as well as its frequency of occurrence in the polymer, affects the tertiary structure and overall properties of the polysaccharide. These polysaccharides are also highly hydrated and may contain hydroxyl and carboxylic groups making them hydrophilic. The monosaccharide composition, sequence of repeating units and added modifications are dependent on the physiological state of the producing organism as well as culturing conditions (de Carvalho and Fernandes, 2010).

Many reviews on marine derived EPS have been published, discussing the bioactivity, properties and application of these EPSs. However, very few published papers discuss the chemical structure of these EPSs and the relationship between structure and properties. This may be due to the fact that these EPSs are very complex and it is difficult to ascertain EPS purity. As drugs, these high molecular weight, often hydrophilic macromolecules, have many advantages over small molecules such as target specificity and reduced side effects (Table 1.7). The structural characterization of these and other high molecular weight (HMW) biologics however is more complicated than the structural elucidation of small molecules and is considered one of the bottlenecks since structural

elucidation is important in development and quality control (Kovaleinen, 2018). HMW biologics do not fall into the criteria devised by the Lipinski rule of 5 and oral route availability is practically impossible due to poor membrane permeability. According to Lipinski's rule of 5, drug candidates should possess 4 chemical and physical properties that makes them drug-likely. One of these properties is that it should not exceed a molecular weight of more than 500 Da (Lipinski et al., 1997). The low oral bioavailability of macromolecules is due primarily to their large molecular weight and variable solubility (Sing et al., 2008). Oral drug administration is however the preferred drug delivery system due to patient compliance (Shaji and Patole, 2008). A number of approaches have been devised and proved successful in delivering macromolecules as drugs and include using drug conjugates that assist in improving the bioavailability, development of formulations with permeation and absorption enhancers, co-administration with delivery agents and/or digestive enzyme inhibitors, nanoparticle encapsulation and altering the physiochemical properties of the drug (Singh et al., 2008). These approaches, along with new advancements in biotechnology facilitates the development of HMW biologics as drugs (Gomez-Orellana, 2005; Bajracharya et al., 2019; Muheem et al., 2016; Kovaleinen, 2018).

Table 1.7: General characteristics of biologics vs small molecules, adapted from Kovaleinen 2018.

Property	**Small molecules**	**Biologics**
Size	<1kDa	1>200kDa
Stability	stable	unstable
Structure	simple	complex
Specificity	non-specific	specific
Administration	oral	parenteral, invasive
Permeability	high	low
Immunogenicity	non-specific	yes

1.5 NPs from the marine environment

Marine bioprospecting has contributed significantly in the discovery of novel therapeutic agents (Urbarova et al., 2012). With the constant rediscovery of known compounds from terrestrial environments, natural product discovery has shifted to the marine environment (Gerwick & Fenner, 2013; Gulder & Moore, 2009). The oceans cover more than 70% of the Earth's surface and have become an important resource in bioprospecting for pharmaceutically relevant compounds (Felczykowska et al., 2012). The extreme conditions associated with this ecological niche such as high salinity, low temperatures, high pressures and its oligotrophic nature supports a variety of living organisms, all well adapted to these extremes (Felczykowska et al., 2012; Banik & Brady, 2010). These conditions force the evolution of novel biochemical pathways, producing natural products with anticancer, anti-inflammatory, antibacterial and antiviral activities and is also a source for enzymes, molecular tools and agrichemicals (Gerwick & Fenner, 2013; Villa and Gerwick, 2010).

The marine environment with its rich biodiversity has provided natural product researchers with a wealth of novel pharmaceutically relevant bioactive compounds (Molinski et al., 2009). Well known examples of drugs from the sea include ziconotide, isolated from a cone snail and used for the treatment of chronic pain as well as Yondelis®, used for treatment of soft tissue sarcoma and isolated from a sea squirt (Molinski et al., 2009).

Many of the compounds from the ocean have unique structures and biological activities superior to that of compounds from terrestrial origin, making them particularly interesting candidates (Jaspars et al., 2016). The next section discusses the significance of sea anemones and their associated symbionts as potential sources of NPs.

1.5.1 Marine invertebrates

Marine invertebrates are rich sources of bioactive natural products and the majority of marine natural products in clinical trial have been isolated from marine invertebrates. These normally soft bodied, sessile or slow moving organisms lack morphological defense mechanisms such as shells or spines, but harbour a wealth of bioactive metabolites presumably for defense (Rohde et al., 2015).

Sea sponges of the phylum Porifera have long been the chief providers of bioactive natural products (Rocha et al., 2011) and early investigations of natural products from the marine environment found that the most potent and structurally diverse compounds came from sponges (Clardy and Walsh, 2004). Although sponges have been recorded as the leading producers of marine bioactive compounds, Cnidarians have also been investigated and have shown to produce bioactive proteins, polypeptides, cytolytic toxins, protease inhibitors (Urbarova et al., 2012).

1.5.1.1 Sea anemones

Sea anemones of the class Anthozoa, Phylum Cnidaria are sessile marine invertebrates with an interesting evolutionary history. Due to their sessile nature, they need to defend themselves against predators, pathogens, the constant changing environment of the sea and catch prey, much like sea sponges. This makes them a good candidate for bioprospecting (Urbarov et al., 2012). A number of antitumor, anti-inflammatory, anti-HIV and antimicrobial agents have been isolated from these organisms over the past decade (Rocha et al., 2011). Just like marine sponges, these sessile holobionts harbour complex communities of bacteria and it would not be surprising that the compounds isolated from sea anemones are mostly of bacterial origin. A large proportion of the compounds investigated from Cnidarians are terpenoids and display a range of activities (Figure 1.10).

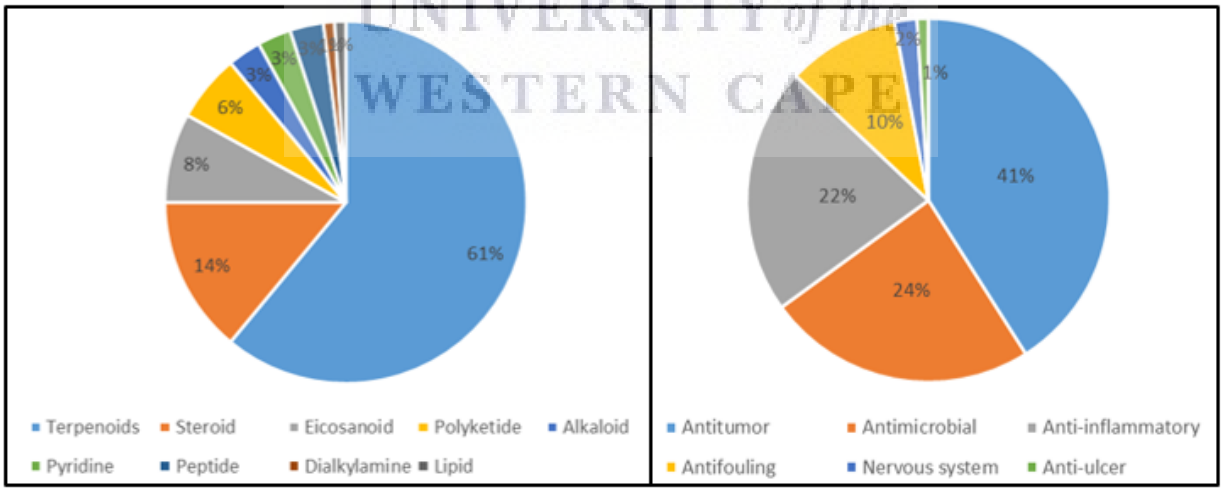

Figure 1.10: Distribution of compound chemical classes and compound activities in Cnidarians, adapted from Rocha et al., 2011.

Apart from the examples given above, sea anemones are capable of producing various other bioactive compounds such as cycloaplysinopsin C, an alkaloid active against *Plasmodium falciparum*, Cladocorans A and B, sesterpenoids (possessing a γ-hydroxybutenolide thought be responsible for the activity of these compounds) with anti-inflammatory activity as well as antifungal and biofilm inhibitory compounds (Rocha et al., 2011; Hamaleyi, 2019, Borbon, 2016). Methanol extracts of sea anemones *Paracondactylis indicus*, *Heteractis magnifica* and *Stichodacyla haddoni* have also shown activity against *Salmonella typhi* and *Klebsiella pneumonia* (Nalini et al., 2018).

These findings suggest that sea anemones, just like sponges, are promising sources of a number of different classes of NPs with pharmaceutical relevance.

1.6 Bacterial symbionts of marine invertebrates

Many compounds that were initially thought to be produced by marine invertebrates were noticed to have a striking similarity to compounds produced by microorganisms upon structural elucidation (Li, 2009). It is now acknowledged that microbial symbionts of marine invertebrates are the true producers of many of these bioactive compounds. A non-exhaustive list of bioactive marine natural products produced by marine invertebrate symbionts previously thought to be produced by invertebrates is shown in Table 1.8.

Table 1.8: Marine natural products isolated from marine invertebrate symbionts, adapted from Trindade et al., 2015 and Blockley et al., 2017.

Compound	Class	Activity	Isolation source	Bacterial Producer
Bryostatin 1	polyketide	cytotoxic	*Bugula neritina*	*Candidatus* Endobugula sertula
Calyculin A	nonribosomal peptide/polyketide hybrid	cytotoxic	*Discodermia calyx*	*Candidatus* Entotheonella factor
Ecteinascidin-743	nonribosomal peptide	anticancer	*Ecteinascidia turbinata*	*Candidatus* Endoecteinascidia frumentensis
Pettazoles	polyketide	anticancer, antifungal	*Lissoclinum patella*	*Candidatus* Endolissoclinum faulkneri
Polytheonamides	ribosomal peptide	cytotoxic	*Theonella swinhoei*	*Entotheonella* spp.
Norharman	β-carboline alkaloid	antimicrobial	*Hymeniacidon perleve*	*Pseudoalteromonas piscicida*

All invertebrates harbour microorganisms such as bacteria, cyanobacteria and fungi either within their tissue or on their surfaces. The competition between microorganisms associated with invertebrates for space and nutrients is the driving force behind the production of these antibiotics which consequently also constitute pharmaceutically relevant natural products (Gerwick & Fenner, 2013).

Additionally, microbes play an essential role in animal phenotype, fitness and other important traits of their hosts (Bosch, 2013). Since the epithelia of animals appear to be colonized by bacterial communities, any multicellular organism can be considered as a metaorganism with a synergistic interdependence with bacteria. In a study conducted on the *Hydra*, in a sterile environment with no bacteria, no morphological changes were observed but fungal infections were prominent, suggesting that bacteria associated with the *Hydra* that produce antimycotics may prevent fungal infections and induce metamorphosis (Bosch, 2013).

In a review by Schinke et al. (2017), the authors summarize reports on the discovery of new antibacterial compounds from marine bacteria over a 5 year period (2012-2015). Over 50 antibacterial compounds were isolated and 69% were from the family of Actinomycetes. Known compounds were also isolated but new assays gave access to activities not previously described for these known compounds. New broad-spectrum antibiotics were also isolated with activity against MDR Gram-negative and Gram-positive strains. Of the isolated compounds, 28 different chemical classes were identified and of these, 10 represented an entirely new class of compound. Figure 1.11 presents some of the compounds isolated from marine bacteria from 2012-2015. Anthracimycin (Figure 1.11A) shows Gram-positive specific activity with a potentially new mechanism of action, gageomacrolactin (Figure 1.11B) shows broad spectrum activity against both Gram-positive and Gram-negative bacterial strains and piercidin A1 (Figure 1.11C) belongs to a new class of antibiotics involved in virulence blocking (Schinke et al., 2017).

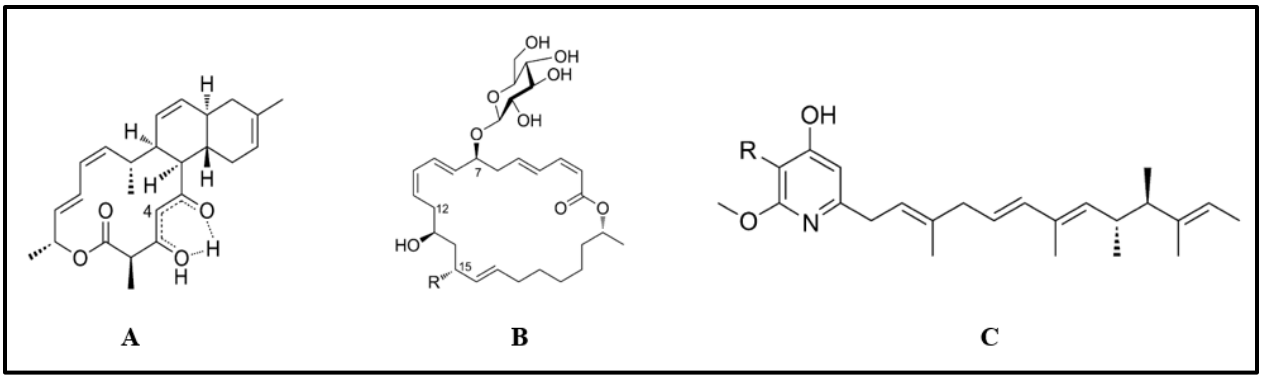

Figure 1.11: Structurally and functionally diverse bioactive compounds isolated from marine bacteria from 2012 to 2015, taken from Schinke et al., 2017.

Marine invertebrate symbionts are therefore promising sources of NPs not only because they produce a wide gamut of compounds with diverse activities, but could also assist in overcoming the supply issue. Obtaining a renewable supply of active molecules from natural sources such as marine invertebrates can be problematic and represent one of the bottlenecks associated with natural product discovery (Proksch et al., 2003). These bioactive compounds are generally produced in minute amounts and large amounts of biomass is required to obtain industrially feasible amounts of compound, a practice that could lead to invertebrate species extinction (Proksch et al., 2003). It may be possible to chemically synthesize a compound but given the complexity of these compounds and the costs involved, this approach is not feasible. Aquaculture is another option however, a disease break out could wipe out the entire production. It is clear that bacteria are a reliable source for the production of bioactive compounds and are amenable to genetic engineering, allowing for improved production and yield (Santhi et al., 2017).

1.7 Approaches in natural product discovery

The methods used in the discovery of natural products can be classified into two categories, top-down approaches and bottom-up approaches (Figure 1.13). Top-down approaches aim to use the organism and elicit production of new natural products without prior knowledge of the genes and enzymes involved in their biosynthesis. In contrast, bottom-up approaches, use genome mining to

identify interesting gene clusters and then implement genetic engineering tools to drive natural product production (Luo et al., 2014).

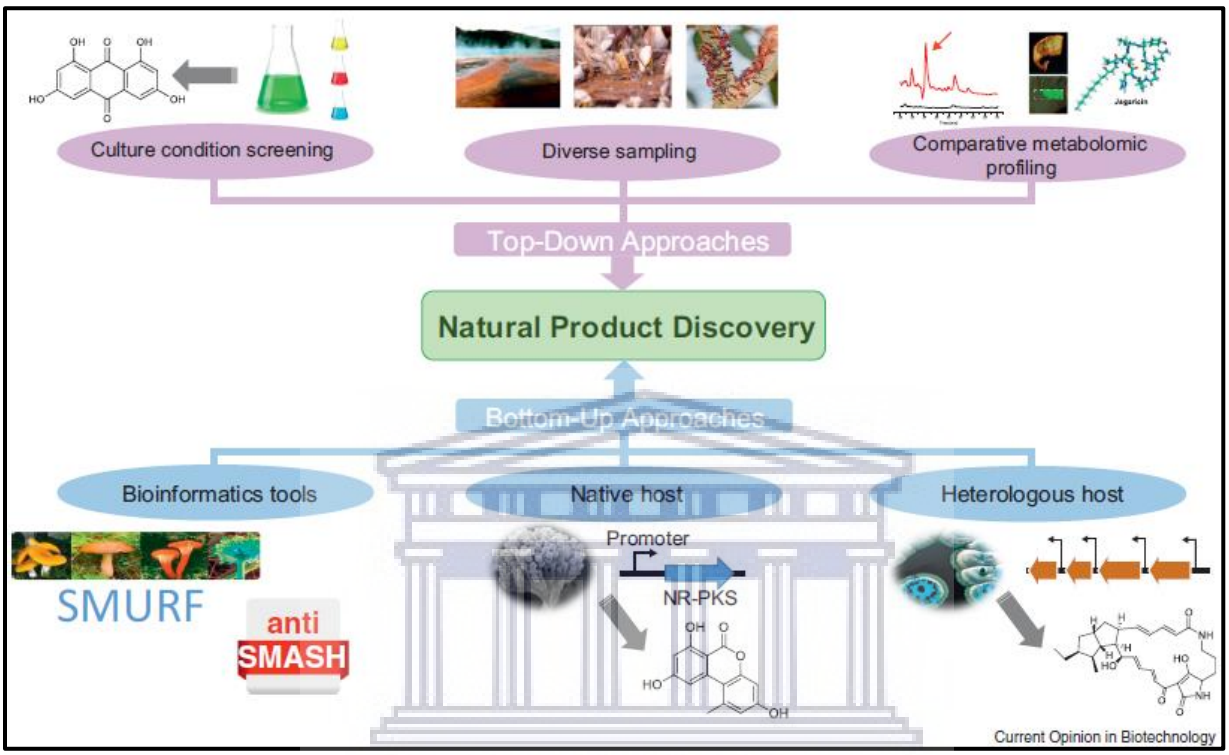

Figure 1.12: Natural product discovery approaches, taken from Luo et al., 2014.

1.7.1 Top-down approach to NP discovery

Top-down approaches have traditionally been the primary means of natural product discovery and to this day is still successful (He et al., 2017; Jassbi et al., 2016; Casertano et al., 2019; Teasdale et al., 2009; Siranjeevi, 2019). It involves collection of biological samples from diverse environments, cultivation or direct extraction, bioactivity screening, isolation of target compounds and structural elucidation (Luo et al., 2014).

Due to the frequent isolation of known compounds from terrestrial environments using this approach, natural product discovery efforts required diversification. Through investigating the underexplored marine environment and its associated microorganisms, novel natural products that are unique both structurally and functionally have been isolated (Luo et al., 2014; January, 2020). Furthermore, cultivation strategies such as OSMAC can be used to activate gene clusters that may

be silent under lab conditions (Li and Lou, 2017). OSMAC refers to a cultivation strategy based on the ability of microorganisms to activate expression of different secondary metabolite pathways when exposed to different environmental conditions (Chiang et al., 2011). It involves altering the environmental conditions of cultivation such as aeration, temperature, media composition, carbon sources, incubation periods and other factors in order to elicit a stress response in the microbe and in so doing, activate various secondary metabolite pathways (Chiang et al., 2011) and add to NP diversification. In studies conducted by Matobole et al. (2017) and January (2020), the authors demonstrate how using the OSMAC approach can be a valuable tool in activating silent BGCs allowing one to tap into otherwise undetected bioactivities.

Prefractionation of extracts is also required to reduce the overall complexity of the samples to be screened to remove components that may interfere or mask the activity of potentially active compounds. This greatly facilitates the isolation and dereplication process and makes samples more amenable to automated liquid sample handling in the microliter range used in high throughput screening (Wagenaar, 2008; Appleton et al., 2007).

Dereplication is an important process in natural product discovery and is used to quickly identify known substances in order to focus on new ones. The frequent rediscovery of known compounds after time consuming purification and identification processes can be trying (Hubert, 2015). Different strategies involving the dereplication of natural products have been reported and the 2 main strategies involves the preparation of crude extracts from either plants, microorganisms or invertebrates, fractionation of these crude extracts followed by purification using High Performance Liquid Chromatography (HPLC), dereplication by mass spectrometry (MS) and Nuclear Magnetic Resonance Spectroscopy (NMR) to elucidate the structure and identify the compounds using database searches. The other strategy involves preparation of crude extracts, functional screening that produces active factions followed by dereplication, purification and structural elucidation. The latter is the most widely used strategy as it is aimed at targeting compounds with activity. This method was identified to prevent the isolation of uninteresting compounds with no activity (Hubert, 2015). HPLC is the most commonly used technique for the separation of NPs at an analytical scale. Ultra High Performance Liquid Chromatography (UHPLC) has increased sensitivity, resolution and reproducibility compared to conventional HPLC. Coupled to MS, a sensitive, rapid and accurate high throughput detection technique

frequently used for dereplication, UHPLC-MS is the most powerful high throughput screening platform for the dereplication and identification of secondary metabolites. High Resolution Mass Spectrometry (HR-MS) acquired *m/z* ratios and isotopic patterns can be used to calculate the elemental composition of individual compounds. It characterizes compounds based on mass, elemental composition, fragmentation pattern and adducts. It can also detect trace levels of compounds. The high separation efficiency of UHPLC combined with the acquisition of high resolution mass data from the HR-MS permits characterization of individual components of samples with complex components, making this strategy ideal for the analysis of crude extracts. With commercial databases such as MARINLIT, Marine Natural Product Database, Chemspider and PubChem, bioactivity profiles and elemental composition of compounds can be determined using HR-mass data (Hanssen, 2014).

Database searching using molecular weight only often results in large answer sets and often cannot be used to identify a compound with a certain level of confidence and in most cases more information is required to identify the compound/s. NMR spectra produces a great deal of structural information of compounds and can discern structural differences between compounds with the same molecular weight and even molecular formula (Bobzin et al., 2000).

NMR is a powerful technique that can be used for the dereplication of NPs and is an efficient tool used to unambiguously elucidate the structure of individual small molecules and is so sensitive that it can elucidate the structure of minor compounds in a mixed sample. One of the major drawbacks of using this tool is that pH and solvents affect and induce significant chemical shift variations across samples that could hamper NP dereplication processes (Hubert et al., 2015).

Organic molecules are made up of a significant amount of carbon atoms. The use of ^{13}C NMR analysis of organic molecules is however underutilized due to the low abundance of the ^{13}C isotope which results in decreased sensitivity of detection. However, each ^{13}C position in a molecule corresponds to a single resonance broadband in a spectrum. In addition, the ^{13}C NMR spectral width (220ppm) is higher than that of ^{1}H (12ppm) and significantly reduces signal overlaps. With the emergence of new technologies such as dynamic nuclear polarization, the acquisition of ^{13}C spectra of mixed samples with high resolution, increased sensitivity and in shorter periods of time, is possible (Hubert et al., 2015). The complexity of ^{1}H spectra is also a major challenge in NMR and reporting chemical shifts from ^{1}H spectra for mixtures of NPs is not easy and requires adequate

precision. Advances in NMR have led to the combined use of HPLC and NMR (LC-NMR) as a dereplication technique. LC-NMR is a powerful tool that can be used especially when the information provided from LC-MS is incomplete or does not allow identification of the active compound/s in a sample. This strategy has been used successfully for the identification of the alkaloid aaptamine from the sponge *Aaptos* sp. (Bobzin et al., 2000).

With the continuous introduction of sophisticated software and hardware tools, NMR is progressively becoming one of the most powerful resources for NP dereplication (Hubert et al., 2015).

1.7.2 Bottom up approach to NP discovery

While top-down strategies have been successful, whole genome sequencing has introduced an alternative approach to NP discovery in that it allows investigation of the biosynthetic potential and metabolic capacity of microorganisms, rather than just what can be detected in assays. Genome sequencing of thousands of bacterial strains including well-known secondary metabolite producers has revealed that many bacteria encode secondary metabolite pathways. Moreover, those bacteria from which bioactive compounds had been characterized previously contained pathways that researchers had yet to characterize the compounds of. This demonstrated that there are many as yet undiscovered metabolites even in well-studied organisms. A combination of genomics and culture-based approaches should improve and speed up NP discovery.

Whole genome sequencing has provided natural product researchers with the tools to prioritize metabolically talented strains on their ability to produce diverse natural compounds and so doing also use genome mining as a dereplication tool (Gulder & Moore, 2009; Zerikly & Challis, 2009; Gaudencio and Pereira, 2015). It has revealed the full potential of microorganisms to produce more compounds than is normally observed under standard axenic conditions (Bertrand et al., 2014; Weber and Kim, 2016). Using computational methods, bacterial whole genome sequences can be assembled and uploaded to a variety of software databases in which secondary metabolite pathways can be predicted (Machado et al., 2015; Weber, 2014) and expressed in heterologous hosts (Sekurova et al., 2019). Popular examples of such databases are the antibiotic and secondary metabolite analysis shell (antiSMASH) that identifies gene clusters encoding these metabolites (Medema et al., 2011) as well as PRediction Informatics for Secondary Metabolites (PRISM)

(Skinnider et al., 2015). Using antiSMASH, a number of compound classes, including but not limited to, lantibiotics, bacteriocins, terpenes, nonribosomal peptide synthases, polyketide synthases and siderophores can be predicted (Medema et al., 2011) while PRISM, first used only for the detection of nonribosomal peptides, type I and type II polyketides has now been updated to extend predictions to antimetabolites, aminocoumarins, ribosomal peptides and others (Skinnider et al., 2015).

Genes encoding biosynthesis machinery for secondary metabolites are organized into clusters known as biosynthetic gene clusters. These BGCs provide information about the chemical classes the compounds belong to (Sekurova et al., 2019). Secondary metabolite biosynthetic pathways are very large and complete biosynthetic pathways may not be assembled on solitary contigs. The efficiency of the software used to assemble these sequencing reads into contigs and the depth and coverage of the sequencing may also affect pathway capturing. Flanking regions and genes with unknown end products associated with the secondary metabolite gene clusters leaves many uncertainties in terms of the regulatory network surrounding its expression (Jensen et al., 2014). However, with constantly developing sequencing technologies such as PacBio and MinIon, assembly algorithms, and annotation software, it is possible that in the near future, sequencing, assembling and annotating bacterial genomes will become a routine procedure in every microbial laboratory (Tyson et al., 2018). On the other hand, predictive bioinformatics tools deduce gene functions through homology based methods and align gene clusters to nearest relatives from databases containing known gene clusters (Medema et al., 2011). One of the drawbacks of using bioinformatics based tools is that novel discoveries are not readily extrapolated. Also, inconsistent nomenclature is often used to name and define genes and different databases may have different annotations for the same gene. To reconcile genome annotations and metabolic models, new methods are required (Cuevas et al., 2016). Many of the BGCs identified through bioinformatics tools are silent under standard laboratory culturing conditions or the compounds may be produced in small amounts that are not detected in assays or insufficient for further downstream processing. These cryptic pathways can be induced by using the OSMAC approach presented earlier in this chapter.

Alternatively, BGCs can be expressed in heterologous hosts. *E. coli* is the most commonly used expression host as it is easy to cultivate and the genetic tools are well established. Many molecular

tools are available for the expression of heterologous proteins / peptides in this host and include a variety of expression vectors and engineered strains (Rosano et al., 2014). However, it often lacks the necessary precursors, post translational modification machinery and often produces misfolded proteins and is affected by toxic nature of final products. Over the last 10 years, *Streptomyces* strains have shown to be successful expression hosts for the expression of a variety of NP classes (Table 1.9). These bacteria are capable of producing a variety of precursors, are equipped with post translational machinery and genes that render them resistant to a variety of toxic compounds such as antibiotics. However, one of the drawbacks of using *Streptomyces* is that these bacteria too produce many secondary metabolites and may use the precursors required for expression of the target compound, for the production of its own metabolites. Although genome mining is a promising tool for the discovery of new compounds and has been successful for the discovery of a range of compound classes, cryptic pathways and the need for new expression hosts capable of expressing functional products from these generally large BGCs is still a major bottleneck (Sekurova, 2019).

Table 1.9: Bioactive secondary metabolites discovered through genome mining, taken from Sekurova et al., 2019.

Compound	Class	Activity	BGC original host	Identification strategy
Scleric acid	(2(benzolyoxy)acetyl)-L-proline	*Mycobacterium tuberculosis*	*Streptomyces sclerotialus* NRRL ISP-5269	Heterologous expression in *Streptomyces albus* J1074
Enterocin	Polyketide	Cytotoxic	*Salinispora pacifica* CNT-150	Heterologous expression in *Streptomyces coelicolor* M1146
Borregomycin A	Indolotryptoline	CaMKIIδ kinase inhibition	Metagenomic DNA from Anza-Borrego Desert soil	Heterologous expression in *Streptomyces albus* J1074
Avermectins	Polyketides	Antihelminthic	*Streptomyces avermitillis* ATCC 31267	Heterologous expression in *Streptomyces lividans* 1326
Tetarimycin A	Polyketide	MRSA	Metagenomic DNA	Heterologous expression in *Streptomyces albus* J1074
Cosmomycins	Polyketides	Cytotoxic	*Streptomyces* sp. CNT-302	Heterologous expression in *Streptomyces coelicolor* M512
Alterochromide	Lipopeptide	Antibacterial, cytotoxic	*Pseudoalteromonas piscicida* JCM 20779	Heterologous expression in *Escherichia coli* BL21(DE3)
Taromycin A	NP peptide	Antibacterial	*Saccharomonaspora* sp. CNQ490	Heterologous expression in *Streptomyces coelicolor* M512
Streptoseomycin	Polyketide	*Helicobacter pylori*	*Streptomyces seoulensis* A01	Heterologous expression in *Streptomyces chartreusis* 1018
Actinoallolides	Polyketides	Anti-trypanosomal	*Actinoallomurus fulvus* MK10-037	Heterologous expression in *Streptomyes coelicolor* M1152
Thaxtomins	Nitrated diketopiperazines	Herbicide	*Streptomyces scabiei* 87.22	Heterologous expression in *Streptomyces albus* J1074
Syringolin	NR peptide	Cytotoxic	*Pseudomonas syringae* pv. *syringae* (Pss) B728a	Heterologous expression in *Streptomyces lividans* TK24
Pseudomycoicidin	Lantibiotic	Antibacterial	*Bacillus pseudomycoides* DSM 12442	Heterolgous expression in *Escherichia coli* BL21(DE3)
Amicoumacin	Dihydroisocoumarin	Antibacterial	*Bacillus subtilis* 1779	Heterologous expression in *Bacillus subtilis* JH642
Pyxidicyclines	Polyketides	Topoisomerase inhibitor	*Pyxidicoccus fallax* An d48	BGC activation an heterologous expression

Chattamycins	Polyketides	Cytotoxic	*Streptomyces chattanoogensis* L10	Overexpression of pathway-specific activator
Stambomycins	Polyketides	Cytotoxic	*Streptomyces ambofacien*s ATCC 23877	Overexpression of pathway-specific activator
Coelimycin P1	Polyketide	Antibacterial	*Streptomyces coelicolo*r A3(2)	Inactivation of pathway-specific repressor
Gacamide A	Lipopeptide	Antibacterial	*Pseudomonas fluorescens* Pf0-1	Repair of defective pathway-specific activator
Atolypenes	Sesterterpenes	Cytotoxic	*Amycolatopsis tolypomycina* NRRL B-24205	Cas9-TAR BGC refactoring

1.8 Conclusion

This review has demonstrated the significance of the marine environment as well as the invertebrates and their associated symbionts as potential sources for novel pharmaceuticals. Additionally it has demonstrated the effectiveness of natural products as drug candidates and explored the approaches involved in isolating new natural products.

1.9 Research objectives

The overarching aim of this project was to investigate the antimicrobial potential of the marine bacterium *Thalassomonas actiniarum* (*T. actiniarum*) using both culture-dependent and culture-independent approaches, leading to the assessment of bioactivity of both secondary metabolites and high molecular weight compounds. This included the following objectives:

- Assess the antibacterial activity of *T. actiniarum* HMW (>50kDa) compound
- Identify, heterologously express and assess the bioactivity of the putative antibacterial protein
- Extraction, semi-purification and antibacterial assessment of putative HMW exopolysaccharides from *T. actiniarum* fermentations
- Genome mining of *T. actiniarum* for exopolysaccharide and secondary metabolite biosynthesis pathways
- Screening *T. actiniarum* for antibacterial, anticancer and biofilm inhibitory activity
- Dereplication, purification and identification of the target compounds

Chapter 2: Heterologous expression of a putative prophage-encoded hypothetical protein from *T. actiniarum*

2.1 Introduction

Thalassomonas viridans (Accession: JYNJ00000000) is a Gram-negative bacillus that was isolated from an oyster harvested off the coast of Spain (Macian *et al.*, 2001). In a study conducted by a former member of the lab (Shanice Adams, MSc), the marine bacterium *T. viridans* was investigated for its antimicrobial potential using a bioassay guided approach, in search of novel antimicrobial compounds. It exhibited activity against *Escherichia coli* 1699 (genetically engineered to have resistance against over 50 antibiotics), *Staphylococcus epidermidis*, *Pseudomonas putida* and *Bacillus cereus*. Following semi-purification and identification of the antimicrobial agent produced by *T. viridans*, a 52kDa phage-encoded hypothetical protein (TVP1) was postulated to be responsible for the antibacterial activity (Adams, 2019).

Based on genomic comparison, *T. viridans* is the closest relative of *T. actiniarum*, with 85% average nucleotide identity (Olonade et al., 2015). *T. actiniarum* is a Gram-negative bacillus that was isolated from a sea anemone harvested off the coast of Japan (Hosoya *et al.*, 2009). When cultivated in Marine Broth (BD Difco™), it produces a brown pigment. Interestingly, a protein sequence alignment revealed that TVP1 shared 78.14% similarity at an amino acid level, to a protein (referred to here as TAP1) encoded on the genome of *T. actiniarum*. With this in mind, the antibacterial potential of *T. actiniarum* was explored by conducting the same bioactivity assays and it too exhibited the same bioactivity profile and within the same molecular size range as TVP1. We hypothesized that the activity observed from these two organisms was a consequence of a similar antibacterial protein produced by both strains.

To confirm this, heterologous expression of the prophage encoded hypothetical proteins from both strains was conducted to determine if these proteins are in fact responsible for the antibacterial activity. Bioinformatics analysis may be useful in predicting the function of some proteins but the real function of a protein can only be inferred with a certain level of confidence through biochemical characterization (Birkholtz et al., 2008). This process requires a large quantity of

target protein, rarely produced by the native organism, but can be acquired through the heterologous expression of the target protein in microbial systems (Rosano and Ceccarelli, 2014).

E. coli is the most commonly used heterologous host for the production of recombinant proteins and peptides because it is easy to cultivate and inexpensive (Saïda *et al.*, 2006; Gomes *et al.*, 2016). Although a variety of strains and expression vectors are available and are optimized for various applications, problems associated with heterologous production of proteins/peptides in *E. coli* do exist and often affect protein folding, yield and activity (Gomes et al., 2016). A need for the expression of toxic genes in *E. coli* has risen in the post genomic era and especially in natural product research. These toxic genes may affect host viability and in so doing, may result in decreased or no expression (Saïda et al., 2006). Additionally, due to codon bias, if a cloned gene contains a high proportion of rare codons, the host cell's tRNAs may have difficulty translating the gene of interest, affecting protein folding and yield (Novy et al., 2001; Gomes et al., 2016; Mignon et al., 2018; Cortazzo et al., 2002). Furthermore, insufficient availability of molecular chaperones is a major bottleneck for the proper folding of recombinant proteins. While the co-production of selected sets of cell chaperones along with recombinant proteins is a common approach to increase the yield of properly folded recombinant proteins in bacterial cells, unbalanced amounts of these chaperones might trigger undesired proteolytic activities, affecting target protein stability, quality and yield (Martinez-Alonso et al., 2010). Another factor that could affect recombinant protein production is the requirement for post translational modifications (PTMs) that not only tailor and fine tune protein properties but also significantly change the integral characteristics of proteins that affect their stability, solubility, charge, hydrophobicity and solvent accessibility. Hence, in addition to the physicochemical and structural features of amino acid sequences, PTMs should also be considered as major determinants of successful protein synthesis (Müller et al., 2018). Notably, bacterial expression systems have only a limited capacity for PTMs and the inability of heterologous protein synthesis to support all PTMs that a protein requires to fold is considered to be a major factor behind the decreased yield and solubility of many recombinant proteins (Tokmakov et al., 2012). In addition, tagging a protein to enhance its solubility and ease of purification (Zhao and Huang, 2016) could affect protein tertiary structure as well as activity (Rosano and Ceccarelli, 2014; Zhao and Huang, 2016). In a paper by Majorek et al. (2014) the authors show that both the protein extraction and purification buffer HEPES and the poly-histidine tag interacted with the active site of the *Pseudomonas aeruginosa* PA4794

Gcn5-related N-acetyltransferase. The activity of the acetyl transferase was not significantly affected in this case but it demonstrates how a purification tag and choice of buffer could possibly affect protein activity. Additionally, the position of the tag, whether placed at the C- or N-terminal of the protein, may affect protein activity (Aslantas and Surmeli, 2019). Considering all the factors mentioned above, the heterologous expression of proteins with unknown function and structure, like TAP1 and TVP1, is reasonably complex and this study therefore utilizes a specialized vector and expression host designed to circumvent some of the abovementioned issues.

2.2 Methods and Materials

2.2.1 Buffers, stock solutions, bacterial strains and plasmids used in this study

All buffers, stock solutions and growth media used throughout this study were autoclaved at 120^{o}C for 15 minutes at 15psi and buffers and stock solutions not pliable to autoclaving were filter sterilized using a 0.22µm filter.

Table 2.1: Bacterial strains and plasmids used in this study.

Bacterial Strains/Plasmid	Description/Genotype	Assay	Source
Thalassomonas actiniarum A5K-106^{T}	Strain under study		Hosoya et al., 2009
Escherichia coli (E. coli) 1699 – multidrug resistant strain, Appendix 2B	MG1655 *gyr*A *rps*L150 *rpoB*516 *met*E::*tet*A *latt*::*mini*Tn7*plus* D*csp*A::*aac* (3')-IV *cit*AB:(*neo ble*)	Antibacterial	Cubist, USA
Pseudomonas putida KT2440	Kan^{r}; φC31 *attB* site^{+}	Antibacterial	Martinez et al., 2004
Bacillus cereus ATCC 10702		Antibacterial	Abcam
Staphylococcus epidermidis ATCC 14990		Antibacterial	Abcam
E. coli Rosetta™ pLysS	F^{-} *ompT hsdS*$_{B}$ (r_{B}^{-} m_{B}^{-}) *gal dcm* (DE3) pLysSRARE (Cam^{R})	Expression host	Abcam
pET21-d	T7/*lac* promoter, amp^{R}, C-terminal His·Tag	Expression vector	Novagen
pET21-a	T7/*lac* promoter, amp^{R}, C-terminal His·Tag	Expression vector	Novagen
pET21-dTa	T7/*lac* promoter, amp^{R}, C-terminal His·Tag, harbours TAP1 gene	Construct	Biomatik
pET21-aTv	T7/*lac* promoter, amp^{R}, C-terminal His·Tag, harbours TVP1 gene	Construct	Biomatik

2.2.2 BLAST analysis and identification of prophage regions

The draft genome of *T. actiniarum* which is available on NCBI (accession: JYNI00000000) was assessed for the presence of prophage genes encoded on the genome using the PHASTER server available at https://phaster.ca/ (Arndt et al., 2017). Protein sequences were aligned using the NCBI protein collection database (BLASTp) (https://blast.ncbi.nlm.nih.gov/Blast.cgi?PAGE=Proteins) with default parameters.

2.2.3 Preparation of *T. actiniarum* cell free culture supernatant

Seed cultures of *T. actiniarum* were prepared by inoculating 100µl of bacterial suspension from a 50% glycerol stock stored at -80ºC into a 14ml McCartney bottle containing 10ml Marine Broth (BD Difco™). The seed culture was incubated at 28ºC overnight in a shaking incubator with shaking at 180 rpm. Of the overnight seed cultures, 10ml was inoculated into 100ml Erlenmeyer flasks containing 50ml of Marine Broth (BD Difco™) and incubated at 28ºC with shaking at 150 rpm for 14 days. Following the 14 day incubation period, bacterial cells were removed by centrifugation at 3214 xg for 30 minutes. The culture supernatant was then filtered using a 0.22µm particle size filter. Filtered culture supernatant was dried at 40ºC, resuspended in 0.1M Tris-HCl pH 8 (Appendix 2A) to a final concentration of 1g/ml and stored at room temperature (20ºC-22ºC) until further testing.

2.2.4 Antibacterial screening of *T. actiniarum* cell free culture supernatant

For primary antibacterial screening the well diffusion assay was used. Briefly, the indicator strains used for the antibacterial assay (Table 2.1) were prepared by culturing in 10ml of Luria Broth at 37°C with shaking at 150 rpm to an OD_{600} of 0.4. Subsequently, 100µl of the cell suspension was spread onto LB agar (Appendix 2A) and wells were cut into the agar using a yellow pipette tip. To the well, 50µl (50mg) of the cell free culture supernatant (section 2.2.4) was loaded and the plates were incubated at 37°C for 24 hours. A zone of clearance around the wells indicated inhibition of the indicator strain. Distilled water, 0.1M Tris-HCl pH 8 and Marine Broth was used as a negative control for the assay.

2.2.5 Size fractionation of *T. actiniarum* cell free culture supernatant

Cell free culture supernatant was dialyzed and size fractionated using 3kDa, 50kDa and 100kDa molecular weight cut off centrifugal Amicon filters (Merck, USA) according to the manufacturers' instructions. This process resulted in 4 size-selected fractions: <3kDa, ii) 3kDa-50kDa, iii) 50kDa-100kDa and iv) >100kDa. Starting volumes were reduced to 200µl and the exchange buffer used was 0.1M Tris-HCl at pH 8. Fractions were stored at room temperature (20°C-22°C).

2.2.6 Analysis of the 50kDa-100kDa and >100kDa fractions using Transmission electron microscopy (TEM)

Fractions ranging in sizes 50kDa-100kDa and >100kDa (section 2.2.5) were subjected to electron microscopy to determine if phage particles were present. Briefly, carbon coated copper grids (Agar Scientific, UK) were glow discharged using a EMS100 Glow Discharge Unit (Electron Microscopy Sciences, USA) to render the carbon surface hydrophilic. A sample volume of 3µl was placed on the grids. After 30 seconds the grids were blotted with filter paper and negatively stained with 2% uranyl acetate (SPI Supplies, USA) followed by washing with distilled water for 5 minutes. Samples were resolved and analysed using a FEI Tecnai F20 transmission electron microscope (FEI, Eindhoven, Netherlands) operating at 200kV (Lab6 emitter) and fitted with a Tridiem energy filter and Gatan CCD camera (Gatan, UK).

2.2.7 Heterologous expression of TAP1 and TVP1 in *E. coli* Rosetta pLysS

2.2.7.1 Construct synthesis

The DNA constructs pET21-dTa (for expression of TAP1) and pET21-aTv (for expression of TVP1) were synthesized by Biomatik (US) at yields of 5µg respectively and resuspended in 1X TE buffer pH 8 (Appendix 2A) to a final concentration of 100ng/µl. These constructs were designed using the expression vectors pET21-d and pET21-a as the vector backbones, containing the TAP1/TVP1 gene with restriction sites XhoI (NEB) and NcoI (NEB) for TAP1, and XhoI and NdeI (NEB) for TVP1, engineered for assisting with the cloning. The genes were also fused to a C-terminal histidine tag (Appendix 2C). The construct maps can be seen in Figure 2.1.

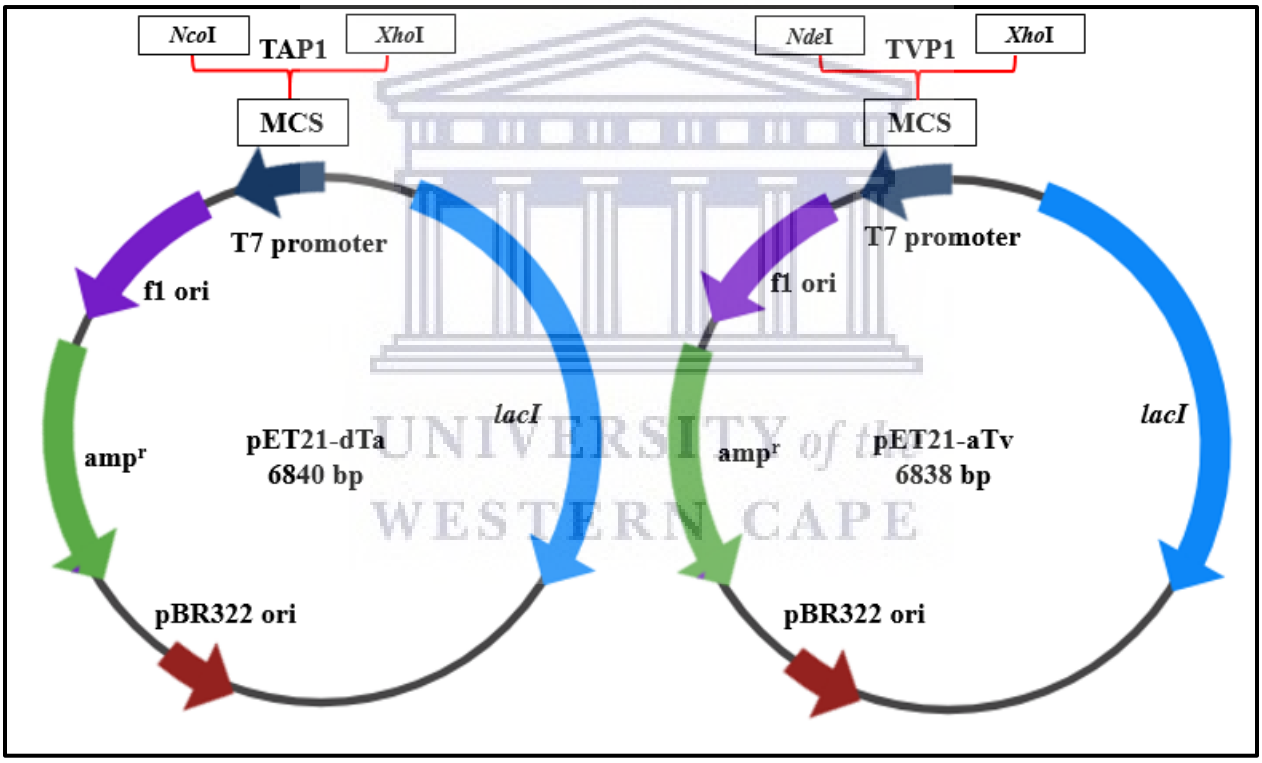

Figure 2.1: Construct maps of pET21-dTa (left) containing 1400 bp insert and pET21-aTv (right) containing 1395 bp insert, representing the expression vectors for TAP1 and TVP1 respectively.

2.2.7.2 Preparation of competent cells

From a glycerol stock, 100µl of *E. coli* Rosetta pLysS cells were inoculated into 10ml Luria Broth (LB) and incubated overnight at 37°C with shaking at 150 rpm. Electrocompetent *E. coli* Rosetta

pLysS cells were prepared by inoculating 200ml of LB with 2ml of the overnight culture and incubated at 37°C while shaking at 150 rpm to an OD_{600} of 0.4 and immediately placed on ice for 30 minutes. All subsequent steps were performed on ice. Once cooled, cells were harvested at 3214 xg for 20 minutes at 4°C and the supernatant discarded. The cell pellet was re-suspended in 100ml of ice-cold MilliQ water and harvested at 4°C for 10 minutes at 3214 xg. The supernatant was discarded and the cell pellet re-suspended in 20ml ice-cold MilliQ water and harvested at 3214 xg for 5 minutes at 4°C. This was repeated 3 times. Once thoroughly washed, the cell pellet was re-suspended in 20ml of ice-cold sterile 10% (v/v) glycerol (Merck, USA) and harvested at 3214 xg for 30 minutes at 4°C. The supernatant was discarded and the cell pellet re-suspended in 1ml of ice-cold 10% (v/v) glycerol. Aliquots (50µl) were transferred to chilled sterile 1.5ml micro-centrifuge tubes on ice and electrocompetent cells were snap frozen in liquid nitrogen and stored at -80°C until further use.

2.2.7.3 Transformation of competent cells

The constructs pET21-dTa and pET21-aTv, respectively, were used to transform electrocompetent *E. coli* Rosetta pLysS cells. Briefly, 50µl of frozen competent cells were thawed on ice for approximately 3 minutes and 100ng (1ul) of construct DNA was added to the thawed cells. The mixture was kept on ice for 1 minute prior to transferring to a pre-cooled 1ml electroporation cuvette (Bio-Rad). Electroporation was conducted using a Bio-Rad MicroPulser™ (USA) with the following parameters: 2 pulses at 1.8 kV, 25µF and 200 Ohms (Ω). Immediately after electroporation, 1ml of pre-warmed (to 37°C) LB was added to the cells and transferred to a 2ml micro-centrifuge tube. Cells were incubated at 37°C for 1 hr. Following incubation, 100µl of transformed cells were spread plated onto LB agar containing ampicillin (Sigma-Aldrich, USA) and chloramphenicol (Sigma-Aldrich, USA) at concentrations of 100mg/ml and 34µg/ml respectively. Thereafter, plates were incubated at 37°C overnight. Following incubation, 6 ampicillin and chloramphenicol resistant TAP1 transformants (PCTa-1, PCTa-2, PCTa-3, PCTa-4, PCTa-5, PCTa-6) and 5 ampicillin and chloramphenicol resistant TVP1 transformants (PCTv-1, PCTv-2, PCTv-3, PCTv-4, PCTv-5) were observed, picked and cultured in 10ml LB overnight at 37°C and stored in 80% glycerol at -80°C until further use.

2.2.7.4 Plasmid DNA isolation, quantification and digestion

For plasmid DNA isolation, 100µl of each transformant (PCTa-1 to PCTa-6 and PCTv-1 to PCTv-5) was cultured in 10ml LB containing ampicillin (100mg/ml) and chloramphenicol (34µg/ml) overnight at 37ºC with shaking at 150 rpm. Following incubation, plasmid DNA was isolated from each transformant using the Qiaprep® mini-prep kit (Qiagen) according to the manufacturer's instructions. After plasmid isolation, plasmid DNA was quantified using a NanoDrop® ND-1000 (NanoDrop technologies, Inc., USA) and the purity of the plasmid DNA determined based on 260/280 and 260/230 ratios. Plasmid DNA (10µl) was resolved on a 1% agarose gel at 90 Volts (V) for 1 hr. Plasmid DNA (1µg) was digested in 50µl volumes using restriction enzymes XhoI and NcoI (for pET21-dTa) and XhoI and NdeI (for pET21-aTv). Single and double digests were conducted at 37ºC for 1.5 hrs and digested plasmid DNA (50µl) was resolved on a 1% agarose gel at 90 V for 1 hr.

2.2.7.5 Agarose gel electrophoresis

Plasmid DNA (uncut and digested) was resolved using agarose gel electrophoresis. Agarose gels were prepared in 1X TAE buffer (Appendix 2A) at a concentration of 1% (w/v) agarose. The agarose gel was stained with ethidium bromide (Sigma-Aldrich, USA) at a final concentration of 0.5µg/ml. Prior to loading, the DNA samples were prepared by the addition of 6X DNA sample buffer (Appendix 2A) (1µl per 5µl of DNA). Electrophoresis was performed in 1X TAE buffer at 90 V for 1 hr. DNA size was estimated using lambda DNA molecular weight marker (NEB). DNA was visualized under ultraviolet (UV) light (302 nm) and images obtained using the digital imaging system Alpha Imager® HP 2000 (Alpha Innotech, USA). Only the transformants PCTa-1 and PCTv-1 was used for further analysis.

2.2.7.6 Recombinant protein expression and isolation

To determine expression of TAP1 and TVP1, 50µl of glycerol stocks of *E. coli* Rosetta pLysS harbouring either pET21-dTa (PCTa-1) or pET21-aTv (PCTv-1) were inoculated into 10ml LB containing ampicillin (100mg/ml) and chloramphenicol (34µg/ml) and incubated at 37ºC overnight, with shaking at 150 rpm. After incubation, 5ml of cell culture was inoculated into 50ml of LB and incubated at 28ºC with shaking at 150 rpm until the OD_{600} reached 0.4. Thereafter,

expression was induced by the addition of 0.5mM IPTG (Sigma-Aldrich, USA) and the induced cultures incubated overnight at 28ºC with shaking at 150 rpm. Uninduced cultures were used as controls. Following overnight incubation of induced and uninduced cultures, cells were harvested (3214 xg for 30 minutes at 4ºC) and the recombinant proteins isolated using B-PER reagent (Pierce™) according to the manufacturer's instructions. Soluble and insoluble fractions of both induced and uninduced cultures were resuspended in 500µl of 0.1M Tris-HCl pH 8 and stored at 4ºC until further analysis.

2.2.7.7 Bradford protein quantification assay

The Bradford (Pierce™) protein quantification assay was performed in accordance with the manufacturer's instructions to determine protein concentration. A standard curve was constructed using bovine serum albumin with concentrations 0 to 1.75 mg/ml. Absorbance readings were taken at 595 nm using a SpectroStar® nano (BMG Labtech) multiplate reader and the results analysed using a standard curve.

2.2.7.8 SDS-PAGE analysis of recombinant proteins

Electrophoretic separation of proteins was carried out under denaturing conditions in a Hoefer™ discontinuous vertical gel electrophoresis system. The composition of separating and stacking gels are indicated in Table 2.2. First, the separating gel was poured and layered with isopropanol. It was allowed to polymerize for 30 minutes at room temperature. The isopropanol was decanted, and the stacking gel was poured on top of the separating gel. A comb was inserted into the layer of stacking gel solution. Again, it was left to polymerize for 30 minutes. Afterwards, the gel was placed in the electrophoresis apparatus, filled with 1X SDS-PAGE running buffer (Appendix 2A), and the comb was removed. Samples (20µl) were mixed with 1/5 volume of 4X sample buffer (Appendix 2A) and heated at 95°C for 5 minutes using a heating block prior to electrophoresis. The electrophoresis was performed at 180 V for 1h. A prestained protein ladder (NEB) was used to determine the size of the resolved proteins. SDS polyacrylamide gels were stained with Coomassie staining solution (Appendix 2A) for 24 hrs with gentle shaking at 80 rpm following electrophoresis. Destaining was carried out using destaining solution (Appendix 2A) until the gel background was cleared of Coomassie stain. Gels were visualized using a light box.

Table 2.2: SDS-PAGE gel components.

SDS-PAGE gel (12%)			
10ml stacking gel (4%)	**Volume (ml)**	**15ml separating gel (12%)**	**Volume (ml)**
Distilled water	6.3	Distilled water	6.9
0.5M Tris-HCl, pH6.8	2.5	1.5M Tris-HCl, pH8.8	4
10% (wt/vol) SDS	0.1	10% (wt/vol) SDS	0.16
Acrylamide/ Bis-acrylamide (40%)	1	Acrylamide/ Bis-acrylamide (40%)	4.8
10% (wt/vol) Ammoniumpersulfate (APS)	0.1	10% (wt/vol) Ammoniumpersulfate (APS)	0.16
TEMED	0.01	TEMED	0.016

2.3 Results and Discussion

2.3.1 Identification of prophage regions in *T. actiniarum*

Considering that TAP1 was hypothesized to be a phage encoded protein with lytic activity, the presence of prophage genomes/genes on the genome of *T. actiniarum* was investigated using PHage Search Tool Enhanced Release (PHASTER), a web server designed to identify and annotate phage genes and genomes within bacterial genomes (Arndt et al., 2016). Following annotation of the draft genome, 4 putative prophage regions of which one is considered questionable and the rest considered incomplete, based on the completeness scoring system, were identified (Table 2.3). No intact prophage genomes were identified and the genes identified were related to phage base plate and phage tail proteins.

Table 2.3: Prophage regions identified on the genome of *T. actiniarum*.

Region	Length (kB)	Completeness	Score	Total proteins	Closest related phage
1	6.4	incomplete	50	7	PHAGE_*Bacill*_BCD7_NC_019515(4)
2	10	incomplete	50	10	PHAGE_*Vibrio*_vB_VpaM_MAR_NC_019722(3)
3	10.6	questionable	90	10	PHAGE_*Vibrio*_vB_VpaM_MAR_NC_019722(4)
4	3.5	incomplete	40	6	PHAGE_*Vibrio*_vB_VpaM_MAR_NC_019722(4)

Upon investigation of the prophage regions, we observed that TAP1 was located upstream of prophage region 3 (Figure 2.2), a region encoding a variety of phage tail proteins, suggesting that TAP1, like TVP1, may also be phage encoded as phage tail proteins tend to be clustered on phage

genomes (Veesler and Cambillau, 2011; Paul et al., 2005; Farlow et al., 2018) and lytic proteins are typically associated with the phage tail (Mirski et al., 2019).

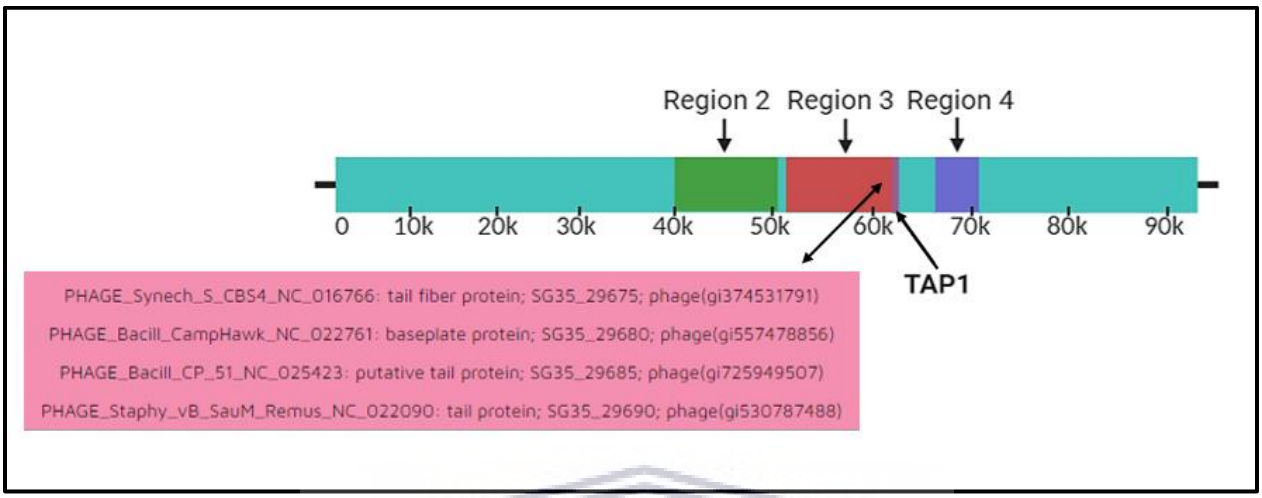

Figure 2.2: Prophage regions 2, 3 and 4 identified in *T. actiniarum* (contig_86 (92 554 bp) showing TAP1 located upstream of Region 3. The pink box shows phage tail related proteins encoded in region 3, downstream of TAP1.

2.3.2 Analysis of fractions (50kDa-100kDa and >100kDa) for phage particles using TEM

Transmission Electron Microscopy (TEM) as described in section 2.2.6 was conducted on the active fractions to see if any phage particles were present. Although PHASTER did not predict any intact phage genomes, factors such as the sensitivity of the algorithms used to predict these genomes as well as the genome sequence assembly could affect whether a phage genome is correctly predicted (Arndt et al., 2017). Furthermore, the similarity between phage proteins encoded on the genome of *T. actiniarum* compared to those present in the databases used by PHASTER also influence predictions since homology-based methods are used and novel phage protein sequences may go undetected. Following TEM, in the fraction containing compounds within the molecular size range 50kDa-100kDa, no phage particles were observed implying that the activity observed was not a consequence of the action of an intact phage. In the fraction >100kDa, structures proposed to be tailocins (discussed in Chapter 1) were observed (Figure 2.3 A, B and C).

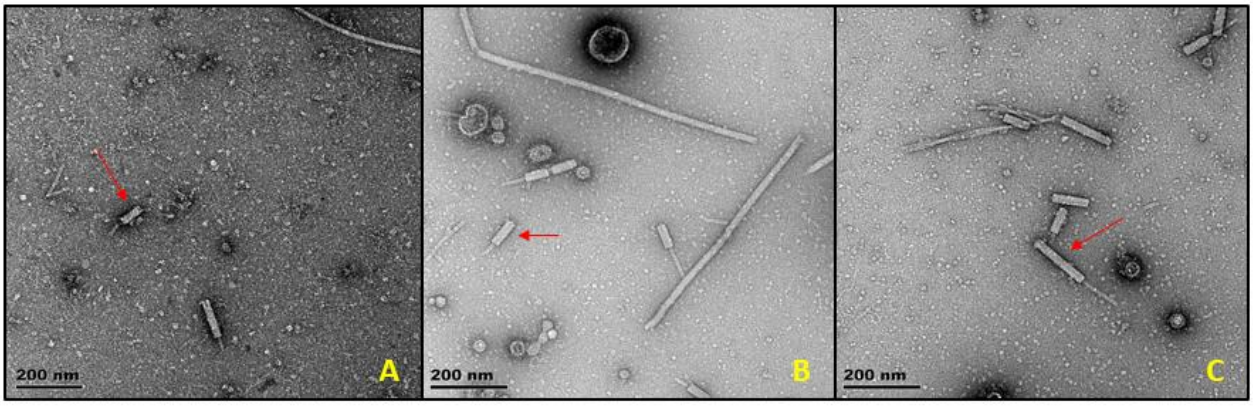

Figure 2.3: Electron micrographs (A, B and C) of fraction >100kDa showing tailocins (indicated by the red arrows) at bar 200nm. Tailocins from *T. actiniarum* resemble contracted phage tails.

For the purpose of this study, only the prophage encoded hypothetical protein (TAP1) will be investigated. However, this is the first report on the production of tailocins by *T. actiniarum* and these results form the foundation for future studies investigating the antibacterial activity of these particles.

2.3.3 Protein sequence alignment using BLASTp

A sequence alignment of the phage derived protein produced by *T. viridans* (TVP1) was conducted using the BLASTp tool from NCBI and revealed that *T. actiniarum* encodes a hypothetical protein of approximately 52kDa in molecular size that is 78.14% similar to TVP1 at an amino acid level, suggesting that these strains may be producing a similar putatively antibacterial protein (Figure 2.4).

```
Query  1    MSTISNAAQIMVDKLVADLNSDTPLSAEDQLLVAKALDTMKNSTTFETALIAVVEEHFNT  60
            MSTISNAAQIMVDKLVADLNS+TPLSAEDQLLVAKALDTMKNSTTFETALIAVVEEHFNT
Sbjct  1    MSTISNAAQIMVDKLVADLNSETPLSAEDQLLVAKALDTMKNSTTFETALIAVVEEHFNT  60

Query  61   ADAALTAAKDDINAAKNSIETQATNLDLIPGLQTSIDTSLSGMTSSLDTSLATIAPTVRN  120
            ADAALTAAK+DINAAK SIETQ+TNLDLIPG+QTSIDTSLS M +SLDTSLATIAP+VR+
Sbjct  61   ADAALTAAKNDINAAKTSIETQSTNLDLIPGIQTSIDTSLSDMNTSLDTSLATIAPSVRD  120

Query  121  NISGVFNKHQIGFYQTDHTLTGAVGQNGYQYAPANVTSLDNYATKEFYCFLDFGNQTTTY  180
            N+ GVFNKHQIG+YQ DH+LT  VGQNGYQYAPANV SLDNYAT EFY F+DFGNQTT+
Sbjct  121  NVRGVFNKHQIGYYQVDHSLTAYVGQNGYQYAPANVASLDNYATGEFYTFVDFGNQTTSV  180

Query  181  RRSCIVRVKADGSVSTATGTGQFFASGSYGFCPFSDDSCRLLRYDSGTLYVQKLGALSWE  240
            RR+ I+RVK+DGSVSTA+   QFF SG YGFCPF+D S RL RYD+GTL +QKLGA SWE
Sbjct  181  RRALIIRVKSDGSVSTASHAAQFFTSGIYGFCPFADGSSRLCRYDAGTLSIQKLGAFSWE  240

Query  241  FNKSVDYLSIYYDKSSKDLYCVSGGFLHTIDATDGFTTIGDTTFIDADAFAAWAEGEGHL  300
            F+K+VDY +IYYDK+SKDLYCVSGGFLHTIDATDGFTTIGD TFI+ +AF AWA   GHL
Sbjct  241  FSKAVDYQNIYYDKASKDLYCVSGGFLHTIDATDGFTTIGDVTFINVEAFEAWALENGHL  300

Query  301  RADSFIGYFNGQRGKSDVENQGSYFEKSWTAPYMGGYAAASTKRTGFDLDNGIMVADFPQ  360
            RADSF+ YFNG RGK+ V NQG+ F+      MGG++   TKR GFDL +GIM AD+P
Sbjct  301  RADSFVNYFNGSRGKNQVSNQGNRFDAPMIVSIMGGFSNTYTKRAGFDLTSGIMTADYPL  360

Query  361  ANNFAVYNTAVTPINTTTTRPVWISWKGQAMFRDVYGVMERQSIDLFSLANTYHYTNQRM  420
             N F+VYNTA+T  +TTT+R VW+SWKGQAMFRDVYGVMERQS++LFSLANT+   NQRM
Sbjct  361  TNYFSVYNTAITAYDTTTSRAVWLSWKGQAMFRDVYGVMERQSVELFSLANTHRDDNQRM  420

Query  421  YTPVMVAFSHIHKCLISDVSGYDYYSSSSAAFWQICGLSFGR  462
            YTPVMVAFSHIHKCLISDVSGYDYY+S+SAA+WQ CGLSFGR
Sbjct  421  YTPVMVAFSHIHKCLISDVSGYDYYTSTSAAYWQACGLSFGR  462
```

Figure 2.4: Amino acid sequence alignment of TVP1 (query 1) and TAP1 (subject)

2.3.4 Preliminary antibacterial screening of *T. actiniarum*

To determine whether *T. actiniarum* conferred the same activity profile as *T. viridans* (Adams, 2019), antibacterial screening of the cell free culture supernatant (50ml) of *T. actiniarum* fermentations was conducted using the well diffusion method described in section 2.2.4 and an illustration of the assay is depicted in Figure 2.5.

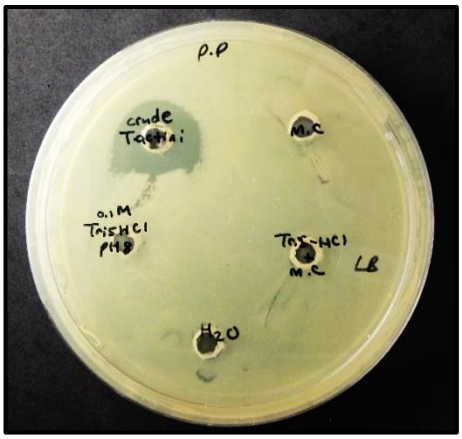

Figure 2.5: Antibacterial activity of concentrated cell-free culture supernatant of *T. actiniarum*. Zone of clearance indicates inhibition of test strain *P. putida*. Growth media (Marine Broth), dH_2O and 0.1M Tris-HCl pH 8 buffer was used as negative controls.

Bioactivity was observed against both Gram-positive *(S. epidermidis, S. aureus, B. cereus*) and Gram-negative (*P. putida, E. coli* 1699) test bacterial strains, similar to the bioactivity profile exhibited by TVP1. To determine the molecular size range of the active compound, size fractionation was conducted.

2.3.5 Size fractionation and bioactivity screening of *T. actiniarum* cell free supernatant

Cell free culture supernatant was concentrated and size fractionated using Amicon Ultra centrifugal size exclusion filters (3K, 50K and 100K) as described in section 2.2.5. In the event that the active compound is large (>3kDa) this also assists in removing salts and other medium components which may interfere with downstream processes. Four fractions were generated (<3kDa, 3kDa-50kDa, 50kDa-100kDa and >100kDa) and assayed for antibacterial activity against the four indicator strains (Table 2.1). Antibacterial activity was observed in the fraction 50kDa-100kDa (Figure 2.6A) against all the indicator strains used, with *P. putida* identified as the strain most sensitive to the active agent. The size range in which the active agent was retained confirms that it is likely not a secondary metabolite since secondary metabolites are considered low molecular weight compounds below 900 Da (Hadacek and Bachmann, 2015). This result also agreed with that observed for *T. viridans* in terms of both the size of the active compound produced as well as the antibacterial profile of the compound. Although the activity against the test strains could've resulted from other compounds produced by *T. actiniarum* that are >50kDa, it was

reasoned to be unlikely and as a result of its sensitivity to the compound, *P. putida* was used as the indicator for all subsequent antibacterial assays.

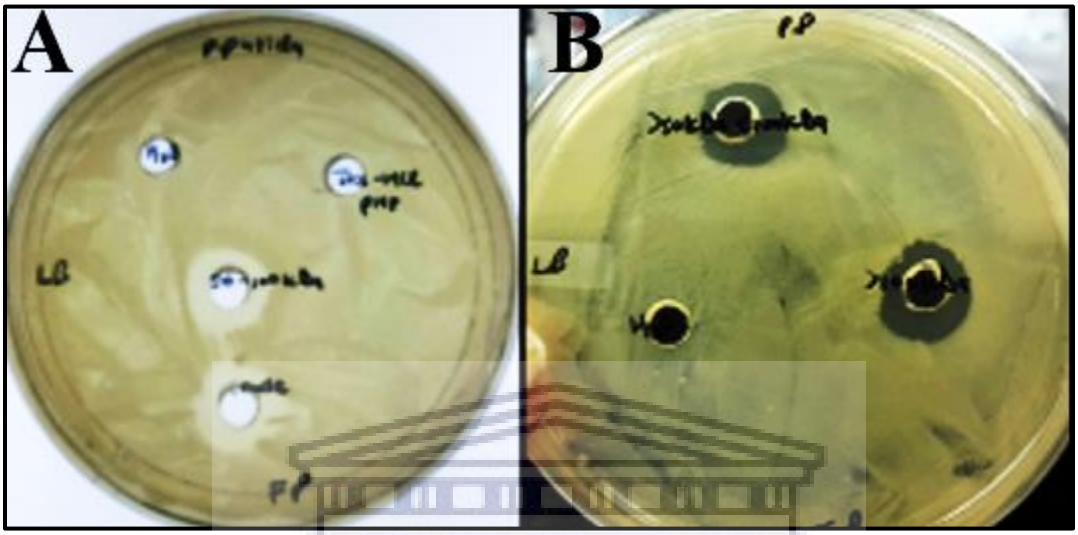

Figure 2.6: Well diffusion assay showing zones of inhibition against *P. putida* from fractions 50kDa-100kDa (A) and >100kDa (B).

Interestingly, antibacterial activity was also observed in the fraction >100kDa, (Figure 2.6B), which in section 2.3.2 was showed to contain tailocins. As mentioned previously, tailocins are antibacterial particles (Duarte, 2012; Príncipe et al., 2018) that may be responsible for the antibacterial activity observed in this fraction and future studies aiming to isolate and characterize the proposed tailocins could further elucidate the extensive bioactive potential of this strain. Also, investigating these tailocins as potential signals for the metamorphosis of invertebrate larva could provide insight into the ecological role of this strain and may be useful in aquaculture studies (Shikuma et al., 2014).

No antibacterial activity was observed from the fractions containing compounds with a molecular size less than 50kDa. This however does not mean that no active compounds with a molecular size below 50kDa are produced or encoded on the genome of *T. actiniarum*. For one, the well diffusion assay used for the antibacterial screening is a quick and inexpensive method used for primary antibacterial screening, but a number of factors such as thickness of the agar used for the assay, the concentration of the active compound/s, their solubility and rate of diffusion into the agar as

well as the optical density (OD) of the test strain should be considered (Furuno et al., 2014). This method may be useful in the early stages of screening to assess whether there are any active compounds but as a result of the factors mentioned above, activities could go undetected. With these factors in mind Chapter 4 describes how an alternative method of secondary metabolite extraction, fractionation, isolation, purification and screening allows for the detection of otherwise undetected bioactivity.

2.3.6 Heterologous expression of TAP1 and TVP1

2.3.6.1 Transformation of constructs into E. coli Rosetta™ *pLysS*

Assuming that TVP1 was correctly identified as being responsible for inhibiting the growth of all the strains tested by Adams (2019), (including *E. coli*), and assuming that due to the high similarity between TAP1 and TVP1, heterologous expression of these proteins in *E. coli* would be particularly challenging owing to the toxicity to the expression host. For this reason, the heterologous host strain *E. coli* Rosetta™ pLysS was selected for expression of these proteins as it has been designed for the expression of proteins that may affect host cell viability (Saïda et al., 2006). It bears the pLysS plasmid (Novy et al., 2001) which harbours the gene encoding T7 lysozyme. T7 lysozyme suppresses basal level expression of T7 RNA polymerase prior to induction, thus regulating gene expression. The strain also supplies tRNAs for rare codons that may be required for expression of non-native proteins. Following transformation of *E. coli* Rosetta™ pLysS with the respective constructs pET21-dTa and pET21-aTv, positive transformants were selected using antibiotic selection. To determine whether the transformation was successful and that the plasmids contained the correct size insert, plasmid DNA was isolated, quantified and digested as described in section 2.2.7.4. Figure 2.7 shows the plasmid DNA isolated from transformant PCTa-1 and PCTv-1, the linearized plasmid DNA (single digest with XhoI) and liberation of the 1.4 kB DNA insert following double digestion of the plasmid DNA.

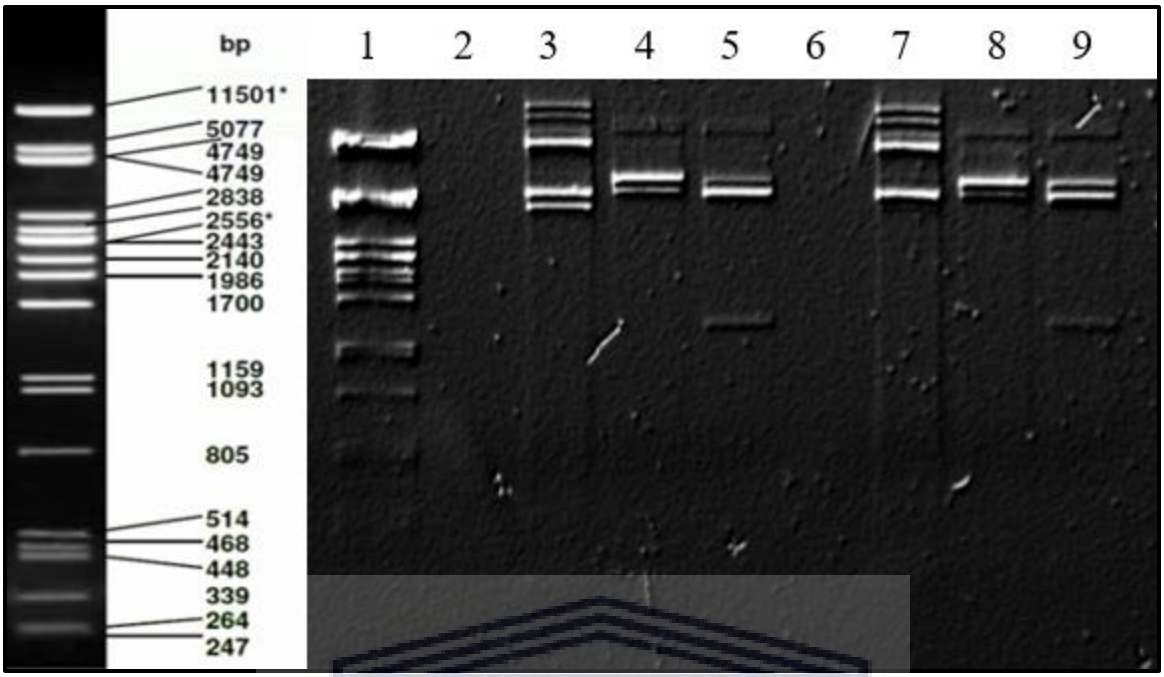

Figure 2.7: Agarose gel (1%) showing uncut and digested plasmid DNA isolated from the transformants harbouring PCTa-1 and PCTV-1. Plasmid DNA was digested with restriction enzymes NcoI and XhoI for TAP1 and XhoI and NdeI for TVP1. Lane 1: Lambda PstI DNA size marker, Lane 3: Uncut plasmid DNA from PCTa-1, Lane 4: Single digest of plasmid DNA with XhoI from PCTa-1, Lane 5: Double digest of plasmid DNA with NcoI and XhoI liberating the 1400 bp insert from PCTa-1. Lane 7: Uncut plasmid DNA from PCTv-1, Lane 8: Single digest of plasmid DNA with XhoI from PCTv-1, Lane 9: Double digest of plasmid DNA with NdeI and XhoI liberating the 1395 bp insert from PCTv-1.

2.3.6.2 Expression and antibacterial activity of TVP1 and TAP1

Considering that the target protein may be toxic to *E. coli*, it was highly likely that when expressed, it would aggregate in inclusion bodies. To prevent this from occurring, low temperature expression was conducted (Sørensen and Mortensen, 2005) and the IPTG concentration was decreased to 0.5mM since temperature and IPTG concentration has shown to affect the rate of expression as well as the formation of inclusion bodies (Rizkia *et al* , 2015). Prior to induction, the PCTa-1 and PCTv-1 clones were cultivated at 37ºC to an OD_{600} of 0.4 and following induction with 0.5mM IPTG, expression was conducted overnight at 28ºC, the temperature at which *T. actiniarum* the native organism is cultivated. Following SDS-PAGE analysis, the results showed that TAP1 and TVP1 were expressed in the soluble fraction, (Figure 2.8; lane 2 and lane 6) under these conditions.

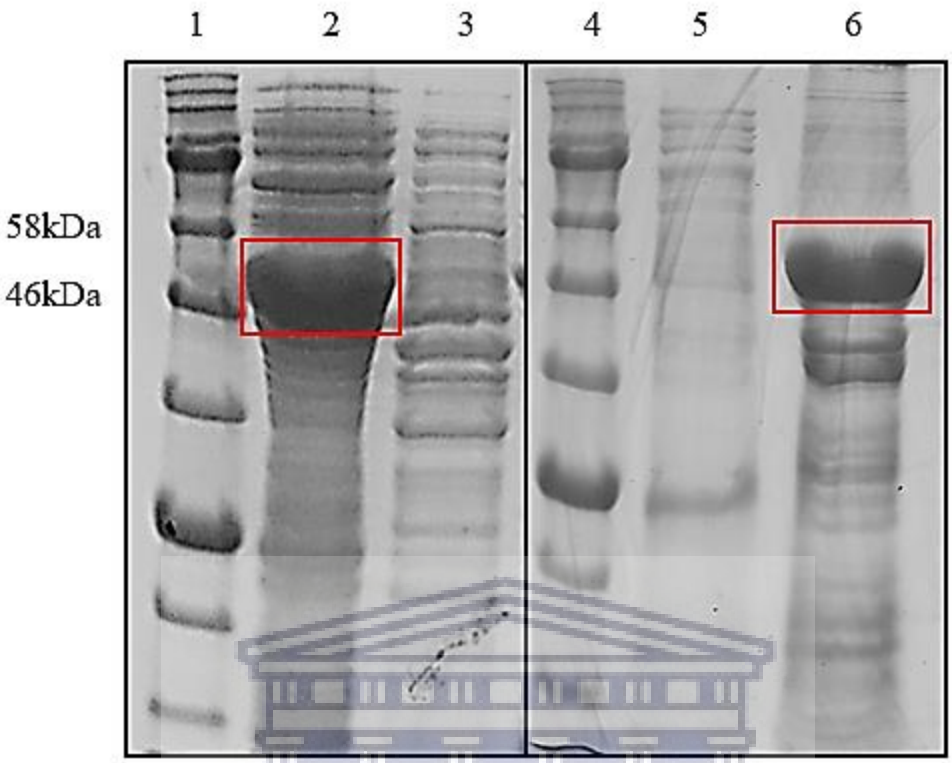

Figure 2.8: SDS-PAGE analysis of expression of TAP1 (left) and TVP1 (right) (indicated by the red squares). Lane 1: Prestained Protein Ladder, Lane 2: Induced-soluble (15ul), Lane 3: Uninduced-soluble, Lane 4: Prestained Protein Ladder, Lane 5: Uninduced-soluble (15ul), Lane 6: Induced-soluble

Despite the widespread use of metal affinity chromatography for the purification of recombinant proteins that are his-tagged, many proteins native to *E. coli* have an affinity for metals such as nickel and cobalt that may interfere with the binding of the target protein to the chromatography column (Bolanos-Garcia and Davies, 2006; Samuelsen, 2016). This would require multiple chromatography steps. Given that these contaminants are less than 25kDa in size, and the target proteins in this study are between 50Da and 100kDa in size, the induced soluble fractions of TAP1 and TVP1 were size fractionated and dialyzed against 0.1M Tris-HCl pH 8 as described in section 2.2.5 which resulted in fractions of 200ul each. This size fractionation step is important for improving the purity of the target protein. The resultant 50kDa-100kDa fractions were resolved using SDS-PAGE (Figure 2.9) to determine the integrity and extent of semi-purification of the proteins of interest.

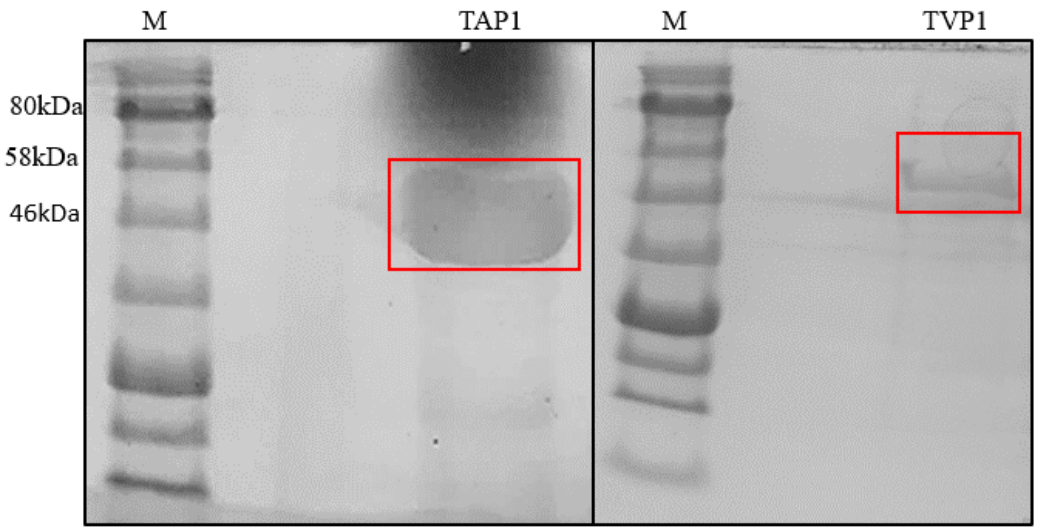

Figure 2.9: Semi-purified soluble fraction of TAP1 (left, 5ul) and TVP1 (right, 5ul) resolved on SDS-PAGE after dialysis and size fractionation. M: Protein size marker.

Following semi-purification of TAP1 and TVP1, it appeared that much of TVP1 was lost during dialysis and size fractionation resulting in a poor yield. This may have been due to the presence of proteases as no protease inhibitor was used; or due to a defective size fractionation column. In order to standardize the bioactivity screening process, a Bradford assay was conducted to determine the concentration (Appendix 2D) and each protein was subjected to the well diffusion assay at a concentration of 50µg. No inhibitory action against *P. putida* (Figure 2.10) was observed from either protein as indicated by the red arrows.

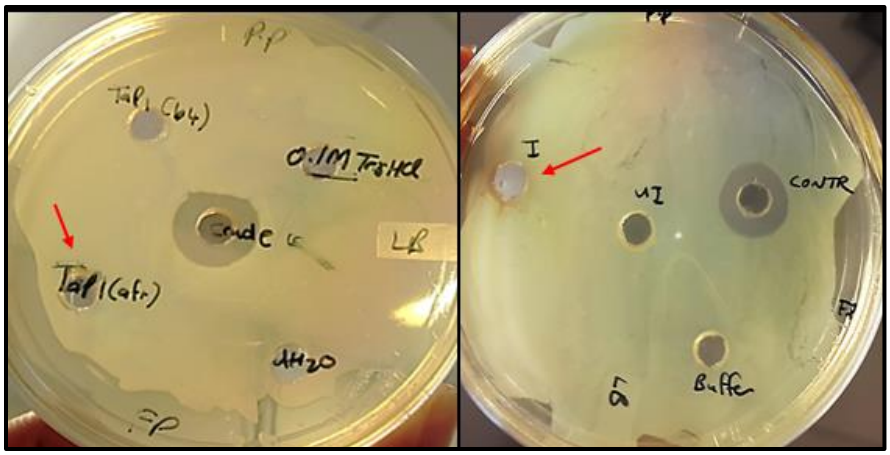

Figure 2.10: Well diffusion assay of semi purified TAP1 (left) and TVP1 (right) against *P. putida* showing no inhibition of the test strain (indicated by the red arrows). Concentrated cell free culture supernatant (50kDa-100kDa, labelled crude/control) from *T. actiniarum* was used as a positive control.

These results would suggest that, if correctly expressed, neither TAP1 nor TVP1 are responsible for the observed activity detected by the two *Thalassomonas* species. It could also imply that *E. coli* Rosetta™ pLysS may not be a suitable host for the expression of these proteins in their active form. Although the proteins may have adopted a soluble conformation, the architecture of their active sites may be unsuitable due to improper folding, which may have been effected by the presence of the purification tag and its position, the buffer used and the requirements for PTMs. Considering all the factors that may influence active recombinant protein production, it is even more challenging to express a protein with no conserved domains and without any knowledge of the protein structure, properties, required post translational modifications, co-factors, chaperones, etc. Heterologous expression of recombinant proteins is usually a trial and error process and can it can take time to identify the parameters leading to the expression of soluble, active proteins, making direct isolation from the producer sometimes a more feasible approach.

However, if the proteins were correctly folded into their biological confirmations, these results would imply that TVP1 was erroneously identified as the protein responsible for the observed antibacterial activity in *T. viridans*. In the study conducted by Adams (2019), the size of the active compound produced by *T. viridans* was first determined through size fractionation as being >50kDa and later confirmed through zymography, as being between 46kDa and 58kDa, where a zone of clearance in the zymogram at approximately this molecular size was observed. Notably,

using zymography to determine the molecular weight of an active enzyme is often hindered by the fact that some enzymes migrate anomalously, often slower, in acrylamide gels containing a substrate (Pan et al., 2011). This was also reported by Hummel et al. (1996) who observed that migration distance in substrate-embedded acrylamide gels was reduced by up to 20% suggesting that simply aligning a zymogram (with substrate) and a SDS-PAGE (without substrate) is not a failsafe approach to determine the molecular size of an active protein. Ideally, determining the relative molecular weight is done by using standards of enzymes with known molecular weights (Vandooren et al., 2013). Additionally, since the zymogram was conducted under denaturing conditions, it is possible that the zone of clearance is a consequence of the peptidoglycan lytic activity of a subunit of a multimeric protein.

Furthermore, Adams (2019) used an OSMAC approach to identify conditions under which the active protein is produced or not, and found that when using sucrose as a carbon source, no activity was observed whereas in the presence of yeast extract, maltose, cellibiose, starch and glucose, activity was observed. Total protein extracted from the culture supernatant of *T. viridans* when cultured under each condition as well as a semi-purified fraction (prepared from cultivation in yeast extract) was subjected to LC-MS/MS and showed that a protein, in the expected size range (approximately 52kDa), later termed TVP1, was present in all active fractions and absent in the inactive fraction where sucrose was used as a carbon source, pointing towards this protein likely being the active agent. Adams then undertook additional studies to confirm the result using LC-MS/MS where the target band at approximately 52kDa was excised and later identified as a putative prophage encoded protein. Considering all the above, it is possible that the size of the active protein was misidentified in the zymogram, resulting in the incorrect band being excised from the SDS-PAGE gel (without substrate). Additionally, the presence of this particular protein in all active fractions and absent in the inactive fraction may have been misinterpreted since the inactive fraction cannot be used as a negative control due to the strain not reaching a desirable biomass in the presence of sucrose. This implies that the active protein may be present in low abundance, and therefore not detected.

Furthermore, although LC-MS/MS is a widely used proteomic strategy for the identification of proteins present in biological samples (Pang et al., 2016) it is not recommended for studies

requiring high-throughput analysis (Masselon et al., 2008). One of the drawbacks of using bottom-up proteomics approaches is that exactly what is present in a sample is seldom established and complete coverage necessitates repeat analysis of the sample (Duncan et al., 2010). Often not all peptides are observed in MS scans (Karpievitch et al., 2010; Xie, 2011; Mirzaei and Regnier, 2006) and even if detected, the identity of the parent protein may be incorrectly assigned by the predictive software since correct matches can only be accomplished if the genome sequence of the organism is of high quality and efficiently assembled (Hird et al., 2011; Karpievitch et al., 2010).

Notably, in Adams's study, LC-MS/MS data generated from the total protein extract, specifically when cultured in yeast extract, and the semi pure fraction (also prepared from yeast extract), revealed that there were proteins present in the semi-pure fraction, that were absent in the total protein fraction. This is unexpected since in theory, the proteins observed in the semi-pure fraction should correlate to that found in the total protein fraction. This is likely a result of using different sample preparation methods for both the total protein fraction (acetone precipitation) and semi-pure fraction (ion exchange and gel permeation chromatography). All steps involved in preparing a sample for MS contribute to the variation observed in proteomic data and subtle variations in sample preparation could compromise precision, emphasizing the importance of normalizing the data as well as repeat analysis (Karpievitch 2010; Xie; Duncan; Callister).
Additionally, the Adams's study focused only on the putative phage encoded protein, not considering that other compounds not detected with Coomassie stain may be co-migrating in the gel and be responsible for the observed activity.

With all that being said, LC-MS/MS is still widely used and acceptable for protein identification studies as long as the limitations of the technique are understood in order to utilize it effectively (Karpievitch et al, 2010).

2.3.7 Conclusion

Since it appeared that TVP1 (and consequently TAP1) was erroneously identified as being responsible for the observed antibacterial activity, we decided to pursue purification of the high molecular weight antibacterial compound directly from the fermentation broth of *T. actiniarum*

using a bioassay guided isolation approach. This approach was devised also to rule out the possibility that the active protein did not adapt a biologically active conformation.

In this chapter we have showed that *T. actiniarum* displays antibacterial activity against *E. coli* 1699, *Bacillus cereus*, *Staphylococcus epidermidis* and *Pseudomonas putida* and that the compound responsible is an extracellular high molecular weight (50kDa-100kDa) compound. Antibacterial activity against *E. coli* 1699, resistant to 52 antibiotics, is also suggestive of the compound being novel. In addition, we report that the strain is capable of producing tailocins and future studies could investigate the antibacterial activity of these particles

Chapter 3: Extraction and semi-purification of a putative high molecular weight antibacterial exopolysaccharide from *T. actiniarum*

3.1 Introduction

High molecular weight polymers, comprising proteins and polysaccharides, have attracted attention as drugs and drug delivery systems (Singh et al., 2008), and are promising drug candidates as they exhibit bioactivity with increased specificity and reduced toxicity (Cao et al., 2019; Efthimiadou et al., 2014). Since the approval of Humulin in 1982, the FDA has approved many more protein drugs that are currently in pre-clinical screening (Bajracharya et al., 2019). The use of polysaccharides such as dextran, chitosan, chondroitin sulfate, hyaluronic acid and cellulose have also received much attention in biomedical applications, (Efthimiadou et al., 2014; Shelke et al., 2014) with many of these polymers chemically modified to achieve the desired physicochemical properties required for pharmaceutical application (Aminabhavi, 2015; Shelke et al., 2014).

Although promising drug candidates, the inherent properties of polysaccharides and proteins such as large molecular size and subsequent low permeability as well as the chemical/enzymatic instability is a great challenge in developing oral drug delivery systems (Gomez-Orellana, 2005; Bajracharya et al., 2019). However, approaches to enhance the bioavailability of these molecules and overcome the barriers associated with oral route administration (Gomez-Orellana, 2005; Bajracharya et al., 2019; Muheem et al., 2016) are constantly developed and have showed promising results. Although the Lipinski rule of 5 dictates that the active compound in this study, with an average molecular size between 50kDa-100kDa is not drug-likely, these rules are only applicable to drugs that will be administered orally and also that will be absorbed into the system *via* passive transport, not considering alternative administration routes and the current advances in enhancing oral route availability. Additionally, in an experiment by Veber et al. (2002) in which the oral availability of drug candidates was tested in rats, the authors observed that other parameters should be considered when classifying a drug. They noticed that the number of rotational bonds in a compound (which affects its molecular flexibility) affected its bioavailability and not only the molecular size.

Owing to the increased specificity and reduced toxicity of HMW biologics and their application as pharmaceuticals, the antibacterial profile of the HMW compound in this study and the potential for chemical modification to enhance oral availability, the isolation and characterization of the high molecular weight antibacterial compound/s produced by *T. actiniarum* was pursued.

Given that the putative prophage encoded hypothetical protein TAP1 was likely not responsible for the observed antibacterial activity as discussed in Chapter 2, in this Chapter, a bioassay guided approach toward identification and isolation of the HMW antibacterial compound from *T. actiniarum* is used.

3.2 Methods

3.2.1 Preparation of culture supernatant for semi-purification

Seed cultures were prepared as described in Chapter 2 section 2.2.3 in a final culture volume of 100ml. A 3L fermentation of *T. actiniarum* was prepared by inoculating 15ml of the overnight seed culture into in 1L narrow mouth Erlenmeyer flasks containing 500ml of Marine Broth (BD Difco™). Following a two-week incubation of the culture at 28°C with shaking at 150 rpm, cell free supernatant was prepared. Briefly, bacterial cells were removed by centrifugation at 7727 xg for 30 minutes. The culture supernatant was then filtered using a 0.22µm particle size filter. A 10ml volume was dried in an oven at 40°C, resuspended in distilled water at a final concentration of 1g/ml and stored for later use as a control. To the rest of the filtered culture supernatant, an equal volume of 0.1M Tris-HCl buffer pH 8 (Appendix 2A) was added. This was concentrated, desalted and compounds <30kDa removed using the tangential flow filtration system (TFF) (Merck) with a 30kDa molecular weight cutoff filter to a final volume of 200ml (TFF fraction). Of this concentrated TFF fraction, 50µl was stored at 4°C for antibacterial testing at a later stage.

3.2.2. Semi-purification of antibacterial compound using anion exchange chromatography

The remaining TFF fraction was further fractionated by FPLC using an Äkta Purifier system with FRAC 900 collector. Sample volumes of 50ml were injected onto a HiPrep QFF 16/10 column (Merck) using 100 mM Tris-HCl buffer pH 8 at a flow rate of 2ml/min. The column was pre-equilibrated with 4 column volumes of 100 mM Tris-HCl pH8 at 5ml/min. Protein was eluted with

a linear gradient 0.1 M NaCl to 1 M NaCl in 100 mM Tris-HCl pH 8 at 2ml/min. Fractions eluted during the wash step were pooled to make Fraction 1 and fractions eluting from the column with increasing NaCl concentration were pooled to make Fraction 2. These fractions were dried to completion at 40^{o}C and resuspended in 5ml of distilled water prior to dialysis and size fractionation using Amicon Ultra-centrifugal filters against 0.1M Tris-HCl pH 8 to obtain compounds between 50kDa- and 100kDa. Starting volumes (5ml) were reduced to 200µl and the buffer exchanged using 0.1M Tris-HCl at pH 8.

3.2.3 Antibacterial screening of cell free supernatant

For antibacterial screening of the semi pure Fractions 1 and Fraction 2 (50kDa-100kDa) and the TFF fraction, the well diffusion assay was used. Briefly, *P. putida* was prepared by culturing in 10ml of Luria Broth at 37^{o}C to an OD_{600} of 0.4. Subsequently, 100µl of the cell suspension was spread onto LB agar and wells were cut into the agar using the back of a 200µl pipette tip. To the well, 50µl of each fraction was loaded into the respective wells and the plates were incubated at 37^{o}C for 24 hours. A zone of clearance around the wells indicated inhibition of the indicator strain. Distilled water and buffers (100mM Tris-HCl pH 8 and 1M NaCl) were used as a negative control for the assays.

3.2.4 SDS and native PAGE analysis

Prior to electrophoretic separation of the proteins present in the FPLC fractions, the concentration of each fraction was determined using the Bradford assay as described in section 2.2.7.7. Electrophoresis was conducted under denaturing and non-denaturing conditions in a Hoefer™ discontinuous vertical gel electrophoresis system. The composition of separating and stacking gels are indicated in Table 3.1. First, the separating gel was poured and layered with isopropanol. It was allowed to polymerize for 30 minutes at room temperature. The isopropanol was decanted after polymerization of the gel and the stacking gel was poured on top of the separating gel. A comb was inserted into the layer of stacking gel solution. Again, it was left to polymerize for 30 minutes. Afterwards, the gel was placed in the electrophoresis apparatus, filled with 1X SDS-PAGE running buffer and the comb was removed. FPLC Fraction 1 and Fraction 2 (50kDa-100kDa) (5µg) prepared in section 3.2.2 were mixed with 1/5 volume of sample buffer (Appendix 3A) and heated at 95°C for 5 minutes using a heating block prior to electrophoresis. For native

PAGE electrophoresis, the heating step was omitted and no SDS or β-mercaptoethanol was used when preparing the native PAGE running buffer or native PAGE sample buffer (Appendix 3A). The electrophoresis was performed at 180V for 1h.

Table 3.1: SDS and native PAGE gel components.

SDS-PAGE gel preparation (12%)		**Native PAGE gel preparation (12%)**	
10ml stacking gel (4%)	**Volume (ml)**	**10ml stacking gel (4%)**	**Volume (ml)**
Distilled water	6.3	Distilled water	7.4
0.5M Tris-HCl, pH 6.8	2.5	1M Tris-HCl, pH 6.8	1.25
10% (wt/vol) SDS	0.1	Acrylamide/Bis-acrylamide (40%)	1.25
Acrylamide/ Bis-acrylamide (40%)	1	10% (wt/vol) ammoniumpersulfate	0.1
10% (wt/vol) ammoniumpersulfate	0.1	TEMED	0.01
TEMED	0.01		
15ml separating gel (12%)	**Volume (ml)**	**15ml separating gel (12%)**	**Volume (ml)**
Distilled water	6.9	Distilled water	6.6
1.5M Tris-HCl, pH 8.8	4	1.5M Tris-HCl, pH 8.8	3.75
10% (wt/vol) SDS	0.16	Acrylamide/Bis-acrylamide (40)	4.5
Acrylamide/ Bis-acrylamide (40%)	4.8	10% (wt/vol) ammoniumpersulfate	0.015
10% (wt/vol) ammoniumpersulfate	0.16	TEMED	0.006
TEMED	0.016		

3.2.4.1 Staining of SDS and native PAGE gels

SDS and native polyacrylamide gels were stained with either Coomassie staining solution (Appendix 2A), Stains-All (Sigma-Aldrich, USA) or silver nitrate as follows:

i) Coomassie staining: SDS / native PAGE gels were stained with Coomassie stain for 24 hrs with gentle shaking at 80 rpm following electrophoresis. Destaining was carried out using destaining solution (Appendix 2A) until the gel background was cleared of Coomassie stain. Gels were visualized using a light box.

ii) Stains-All: SDS / native PAGE gels were equilibrated in a petri-dish with 30% (v/v) ethanol for 1 hr while shaking. The ethanol was decanted and replaced with Stains-All (Sigma-Aldrich, USA) solution prepared as described by the manufacturer. The dish was covered with foil and incubated in the dark for 48 hrs. To destain, the staining solution was decanted, replaced with water and exposed to light from a Phillips 60W GLS incandescent light bulb, positioned 15-20cm from the gel for 30-60 seconds. Bovine serum albumin was used as a negative control.

iii) Silver-nitrate staining: after electrophoresis, native PAGE gels were fixed in a sterile petri-dish containing fixing solution (Appendix 3A) for 1hour. After this, the gel was washed with distilled water for 30 minutes with 3 changes of water. The water was then decanted, and the gel sensitized in 0.02% sodium thiosulfate (Appendix 3A) for 1 minute followed by washing in distilled water for 3 x 20 seconds. After washing, the water was decanted, and the gel incubated for 20 minutes in ice cold 0.1% (w/v) silver nitrate solution. The gel was washed again for 3 x 20 seconds and placed into a new sterile petri dish prior to washing for 1 minute with distilled water. The water was then decanted, and the gel developed in 3% sodium carbonate developer (Appendix 3A) until staining was sufficient. Once sufficiently stained, the gel was washed in water for 20 seconds and the staining terminated in 5% (v/v) acetic acid for 5 minutes. The gel was stored at 4^{o}C in 1% (v/v) acetic acid.

3.2.5 Phenol-Sulphuric acid test

The phenol-sulphuric acid assay was carried out in 1.5ml centrifuge tubes and the absorbance measured in a 96-well microtitre plate. Briefly, to 25µg of sample (Fraction 1 and Fraction 2), 100µl of sulphuric acid and 30µl of 5% (w/v) phenol solution was added and heated at 60^{o}C for 10 minutes until colour changes from colourless to yellow-orange was observed. This step was conducted in a 1.5ml eppendorf tube and heated in a dry block. Hereafter, the samples were transferred to a 96-well microtitre plate and the absorbance was determined using a SpectroStar® nano (BMG Labtech) multiplate reader at 490nm. A standard curve was generated using glucose as a standard with concentrations 0 to 1mg/ml.

3.2.6 Ammonium sulphate precipitation of the active compound

Salting out of proteins was conducted using ammonium sulphate precipitation at 30% (1.2M) and at 75% (2.92M) saturation. Briefly, 20ml of filtered cell free culture supernatant was prepared as described in section 3.2.1. The 20ml was split into two 10ml volumes and to the one, 1.64g ammonium sulphate was slowly added with continuous stirring at 4^{o}C for 1 hr to bring the cell free supernatant to 30% saturation. To the other 10ml of cell free culture supernatant, 4.76g ammonium sulphate was added in the same way, to bring the cell free supernatant to 75% saturation. Following precipitation, the proteins were centrifuged at 7727 xg for 20 minutes at 4^{o}C. The precipitated protein was resuspended in 0.1M Tris-HCl pH 8 prior to desalting and size exclusion using the Amicon Ultra centrifugal filters. The fractions containing compounds 50kDa-100kDa was tested for antibacterial activity as described in section 3.2.3.

3.2.7 Exopolysaccharide isolation

For isolation of polysaccharides, *T. actiniarum* was cultured in Marine Broth for two weeks at 28^{o}C in a culture volume of 2L. The culture was centrifuged at 7727 xg for 30 minutes and the supernatant deproteinized using the Sevag method (Su et al., 2013). Briefly, a chloroform: butanol (4:1) solution was prepared and added to the supernatant to a final concentration of 10%. The latter was incubated overnight with stirring. Following deproteinization, the mixture was centrifuged at 7727 xg and the aqueous phase isolated. To the aqueous phase, 4 volumes of ice-cold absolute ethanol was added and incubated at 4^{o}C overnight. The resultant precipitant was centrifuged at 7727 xg and the pellet, which now contains the exopolysaccharides, was dried at 40^{o}C. The pellet was resuspended in 10ml distilled water, dialyzed against 100ml of distilled water and size fractionated to obtain an exopolysaccharide fraction of 50kD-100kDa. This EPS fraction was resolved using SDS and native PAGE and stained with either Coomassie, silver stain and/or Stains-All as described in section 3.2.4.1. The fraction was also subjected to zymography under non-denaturing conditions.

3.2.8 Zymography assay

The bacterium, *P. putida* was cultured in 5 ml of LB medium and incubated at 37˚C overnight. Following incubation, cells were harvested by centrifugation at 7727 xg for 20 minutes at room

temperature and the supernatant was discarded. As described in section 3.2.4, Table 3.1, a 12% separating acrylamide native PAGE was prepared, and 4mg wet weight *P. putida* cells was added which served as the substrate. A 4% stacking gel, without cells was placed on top of the resolving gels. The exopolysaccharide fraction (20µl) (prepared in section 3.2.7) was resolved under native PAGE conditions (section 3.2.4). Following electrophoresis, the gel was incubated in a renaturation/incubation buffer (100 mM Tris-HCl, pH 8) overnight at 37˚C without shaking. Following incubation, the gel was rinsed with MilliQ water and stained with Coomassie Brilliant Blue G-250 for 24 hrs at room temperature. After staining, the gel was placed in a destaining solution for 24 hrs at room temperature. The appearance of white zones against a dark blue background was indicative of lytic activity (Valence and Lortal, 1995; Métayer et al., 2002).

3.2.9 Genome annotation using Prokka

The complete genome sequence of *T. actiniarum* (chromosome Accession: CP059735 and chromid Accession: CP059736) was assessed for polysaccharide biosynthetic pathways using the Prokka genome annotation server with default parameters (Seemann, 2014).

3.3 Results and Discussion

3.3.1 Semi-purification of an antibacterial compound from *T. actiniarum* using FPLC

To isolate the high molecular weight antibacterial compound from *T. actiniarum* fermentations, a bioassay guided isolation approach using anion exchange on a FPLC system was employed. Briefly, a 3L fermentation of *T. actiniarum* was cultivated and prepared as described in section 3.2.1. Antibacterial screening of the TFF fraction containing compounds greater than 30kDa was first conducted prior to FPLC purification, and was confirmed to confer antibacterial activity, Figure 3.1, indicated by the red arrow.

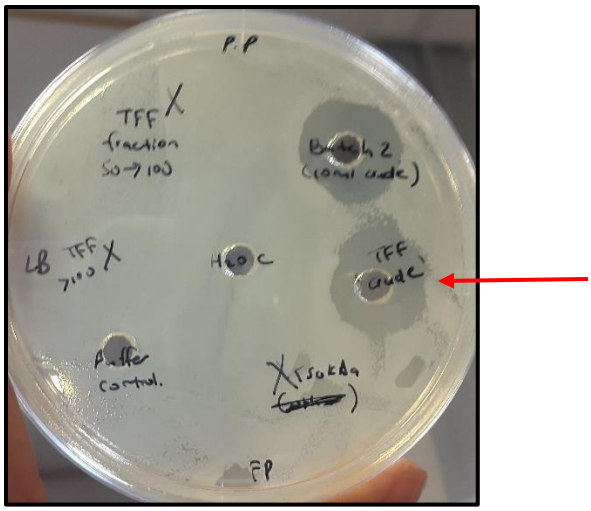

Figure 3.1: Well diffusion assay of the concentrated TFF fraction (>30kDa) tested against *Pseudomonas putida*, with buffer (100mM Tris-HCl pH 8) and distilled water used as negative controls and concentrated culture supernatant used as a positive control.

The remaining sample (approximately 200ml) was subjected to anion exchange chromatography as described in section 3.2.2. Following separation, fractions were collected and pooled as indicated on the chromatogram (Figure 3.2), resulting in two fractions. Briefly, 5ml fractions were collected and pooled to make Fraction 1 (fraction 0ml to 25ml) and fraction 2 (85ml-110ml) resulting in final volumes of 25ml for each fraction. Fraction 1 had a peak absorbance of approximately 250mAU and fraction 2 had a peak absorbance of approximately 1300mAU. Since there is a linear relationship between absorbance and concentration (Schmid, 2001) the protein concentration in peak 2 (Fraction 2) is approximately 5 times higher than that in peak 1 (Fraction 1) suggesting that in 0.1M Tris-HCl pH 8, most of the extracellular substances greater than 30kDa are anionic, with a strong binding affinity to the positively charged resin. Important to note is that many other compounds that absorb UV at 280nm might also be present in these fractions and these peaks do not necessarily represent protein only. Furthermore, compounds that do not absorb UV at 280nm, and are therefore not represented by a peak (Figure 3.2 between 25ml and 85ml), may have been missed.

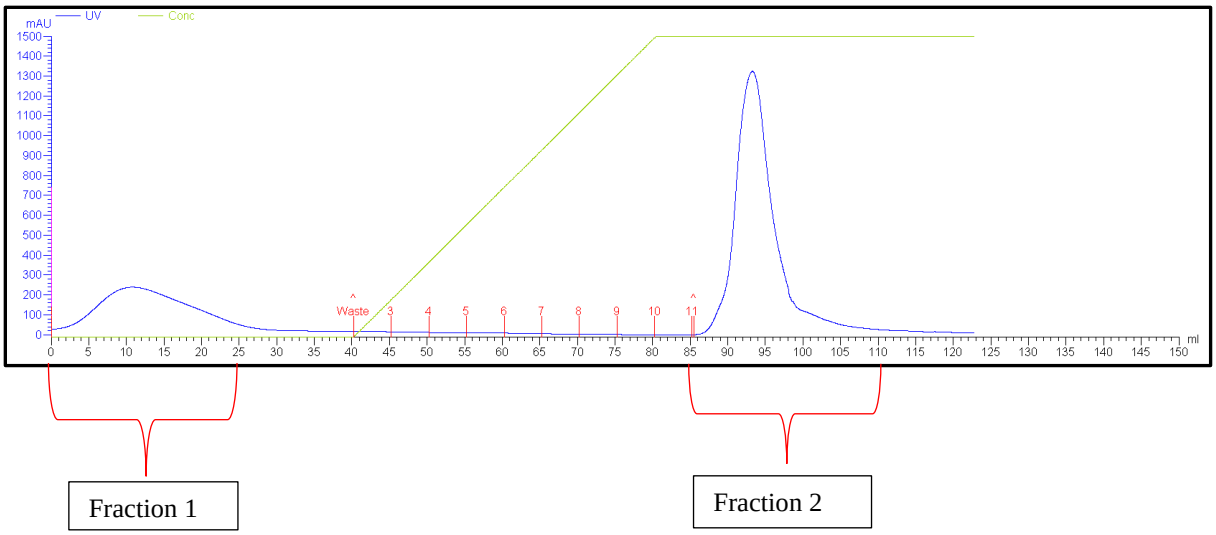

Figure 3.2: FPLC chromatogram of *T. actiniarum* concentrated cell free culture supernatant.

3.3.2 Antibacterial screening of Fraction 1 and Fraction 2

To determine whether the active compound was retained in Fraction 1 or Fraction 2, an antibacterial assay was conducted on each fraction as described in section 3.2.3. Briefly, both fractions were concentrated by dialysis and size fractionation as described in section 2.2.5. The protein concentration of the resultant 50kDa-100kDa fractions (200ul each) were determined using the Bradford assay (Appendix 3A) and 25ug of each fraction was screened for activity since the activity was observed in this size range (section 2.3.5) as well as in the Adams study.

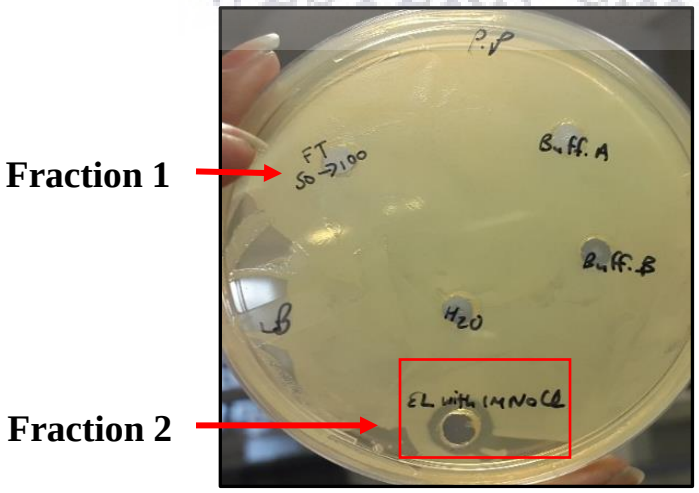

Figure 3.3: Antibacterial activity of Fraction 1 and Fraction 2 (50-100kDa) against *P. putida*.

Activity was observed only from Fraction 2 (Figure 3.3) which contains compounds that bound to the column, indicating that the active compound had a strong binding affinity to the positively charged resin likely owing to its net negative charge at pH 8. Although activity was observed, the zone of inhibition was greatly reduced compared to that of the TFF fraction (Figure 3.1) screened prior to FPLC. This suggests that the conditions and/or FPLC may not be a suitable method for the semi-purification of the active compound.

3.3.3 SDS-PAGE analysis of FPLC Fractions 1 and Fraction 2

To help ascertain the nature of the compound and to see whether any proteins are resolved in the expected size range (50kDa-100kDa), SDS-PAGE analysis of Fraction 1 and 2 was performed. Figure 3.4 below depicts the protein profiles of FPLC Fraction 1 and Fraction 2.

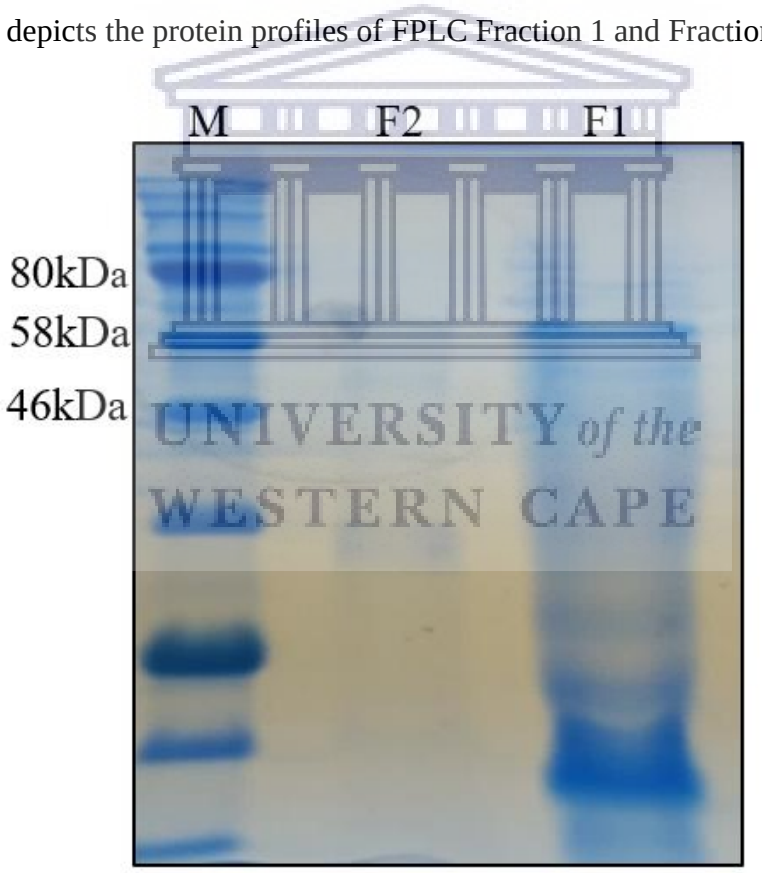

Figure 3.4: SDS-PAGE of FPLC Fraction 1 and Fraction 2 (active) after dialysis and size fractionation. Lane 1: marker, Lane 2: fraction 2 (50kDa-100kDa), Lane 3: fraction 1 (50kDa-100kDa).

Given that 5µg of protein was resolved for each fraction, the protein content visualized after Coomassie staining did not correlate with the amount of protein resolved or depicted by the FPLC chromatogram. It appears that the protein concentration was overestimated by the Bradford assay since the peak area of Fraction 2 (Figure 3.2), which corresponds to the amount of protein/compounds absorbing at A280, is according to the FPLC detector, larger than the peak area of Fraction 1, yet this is not depicted in the gel. Although the principal behind the Bradford assay and Coomassie staining are the same, and these results should correlate, it is important to consider that some compounds/proteins present in these FPLC fractions may not have entered the gel matrix, resulting in a decreased signal compared to that observed in the Bradford assay. In addition, the estimation of proteins in crude extracts by the Bradford method is often not an accurate representation due to a mixture of sugars, proteins and other metabolites, which can cause deviations in the absorbance of proteins in the Bradford assay, and is especially true for carbohydrates (Banik et al., 2009). Given that other high molecular weight compounds, such as carbohydrates, may be present in these fractions, which are well known as conferring antibacterial activity, including for a range of marine bacteria (Aullybux et al., 2019; He et al., 2010), the phenol-sulphuric acid test was employed to determine whether carbohydrates are in fact present and may be affecting the Coomassie staining and Bradford's quantification, or whether the bioactive compound was in fact a polysaccharide.

On the other hand, the concentration of the active compound may have been reduced after FPLC to a concentration that is now below the detection limit of Coomassie, which would also explain the reduced activity observed in the antibacterial assay after FPLC (Figure 3.3). Since activity was observed and depending on the MIC and diffusibility of the antibacterial compound in the agar medium used in the well diffusion assay, it is possible that low amounts of compound are required to display antibacterial activity.

3.3.4 Phenol-Sulphuric acid test of Fraction 1 and 2

The phenol-sulphuric acid test was conducted on each fraction to see whether carbohydrates were present in the fractions and may have been contributing to poor staining with Coomassie. The phenol-sulphuric acid assay is a colorimetric technique used to determine the carbohydrate content within a sample detecting sugars, their methyl derivatives, oligosaccharides and polysaccharides.

It is widely used as it is inexpensive, sensitive and simple (Masuko et al., 2005). In the presence of heat and acid, oligosaccharides are hydrolyzed to glucose, galactose and fructose which are further dehydrated to form hydroxymethyl furfural (Jain et al., 2017; Chow and Ländhausser, 2004). The latter reacts with phenol and changes to a yellow-brown colour with an absorbance maxima of 490nm that can be measured using a spectrophotometer (Jain et al., 2017). Figure 3.5 below depicts the phenol-sulphuric assay conducted on Fraction 1 and Fraction 2.

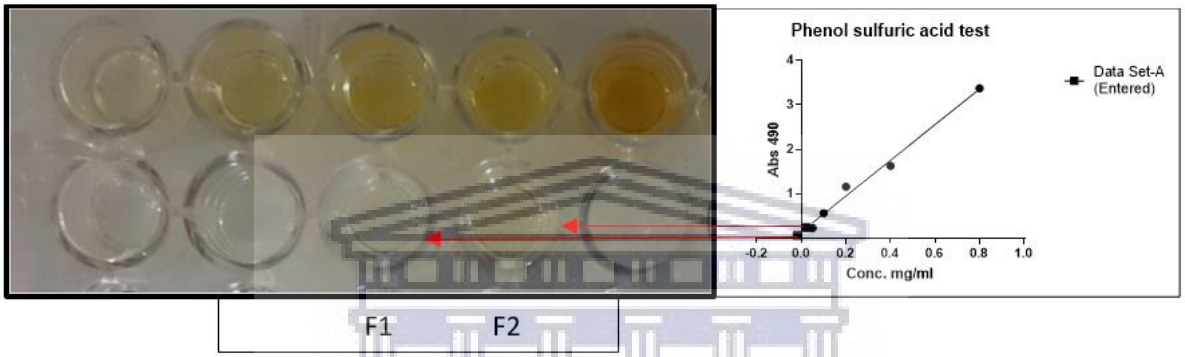

Figure 3.5: Phenol-sulphuric acid assay of undiluted Fraction 1 (F1) and Fraction 2 (F2) and the concentration of the carbohydrates present in each fraction in reference to the glucose standard curve.

Low concentration of carbohydrates was detected in both the active Fraction 2 (F2) and inactive Fraction 1 (F1), notably with a slightly higher concentration in the active fraction, while the concentration of carbohydrates present in inactive Fraction 1 falls below the constructed glucose standard curve. Unfortunately, just as protein concentration can be over - or underestimated using the Bradford assay in the presence of carbohydrates, carbohydrate concentration too can be over- or underestimated in the phenol-sulphuric acid assay when proteins are present (Hall, 2013). The characterization of proteins and polysaccharides from culture supernatant has been mostly limited to the use of these colorimetric assays that have a relatively low specificity that cannot accurately estimate individual components (Boleij et al., 2018). Also, one of the main disadvantages of using these methods is that it allows the characterization of separate classes, providing no insight into the macromolecular structure of these components. Given that proteins and polysaccharides present in the extracellular space are not only present as individual components but also as glycol-conjugates, colorimetric assays such as the Bradford and Phenol-Sulphuric assays are not always

accurate (Boleij et al., 2018), implying that the abovementioned results are inconclusive, in terms of identifying the molecular nature of the bioactive compound (i.e. either a protein, glycoprotein or polysaccharide).

Since the protein concentration and activity was reduced after FPLC purification and the approach devised to isolate and characterize the antibacterial compound from *T. actiniarum* is based on bioactivity-guided methods, ammonium sulfate precipitation was attempted as an alternative technique to isolate and semi-purify the active compound from the culture supernatant should it be proteinaceous in nature.

3.3.5 Ammonium sulfate precipitation of the active compound from *T. actiniarum* culture supernatant

Ammonium sulfate is the most common salt used to precipitate proteins out of solution in a process called salting out. Ions affect the solubility of proteins and as ionic strength increases, protein solubility decreases. Salting out can thus be used to separate proteins based on their solubility in the presence of high concentrations of salt. Generally, enzyme functionality and structure are not adversely affected and resolubilization of precipitated protein can be done in an appropriate buffer. Ammonium sulfate has also been shown to stabilize protein structure (Righetti et al., 2013; Wingfield, 2001). Ammonium sulfate is used not only to separate non-proteinacious compounds from proteins but also to fractionate proteins based on ionic strength and hydrophobicity. If the active protein was in fact a protein, using ammonium sulfate precipitation could be a suitable fractionation method. Ammonium sulfate precipitation was used to precipitate protein from 10ml of the culture supernatant at a saturation of 30% and 75% respectively. Following protein precipitation, dialysis against 0.1M Tris-HCl pH8 and size fractionation as described in section 3.2.6, no antibacterial activity was observed in the fraction 50kDa-100kDa, Figure 3.6.

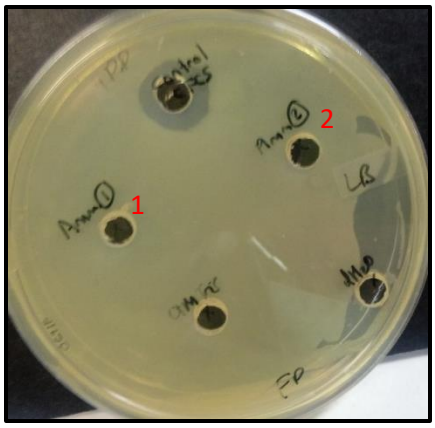

Figure 3.6: Well diffusion assay of ammonium sulfate precipitated proteins (1: 30% saturation and 2: 75% saturation) following dialysis and size fractionation. The activity was tested against *P. putida* and concentrated culture supernatant was used as a positive control.

Since no activity was observed from the ammonium sulfate precipitated fractions, the results suggest that the activity of the protein may have been adversely affected by ammonium sulfate or that the active agent may not be a protein and was thus not precipitated with ammonium sulfate. Although it is widely used for protein precipitation and generally has little adverse effects on protein properties and function, ammonium sulfate has been shown to affect protein activity and yield indicating that ammonium sulfate precipitation of proteins in their active form depends on the properties of the target protein (Purwanto, 2016). Given that ammonium sulfate precipitation was not conducted at 100% saturation, it is also possible that the active compound precipitates at a higher ammonium sulfate concentration. However, the collective results made us consider that the active compound may not be a protein. The size range in which the active agent is retained after size fractionation, its presence in the extracellular environment and its inability to stain with Coomassie, introduced the possibility that the active agent may be an exopolysaccharide whose activity is affected by the NaCl used during anion exchange chromatography (as seen by the reduction in activity) and the ammonium sulfate used for precipitation. Just as protein activity can be affected by salts, the activity of charged polysaccharides can also be affected by salts (BeMiller, 2019). In 2015, Burg and Oshrat investigated the effects of salt on the antioxidant activity of 2 sulfated polysaccharides from red microalgae. The authors found that in the presence of both monovalent and divalent cations, the antioxidant activity of the polysaccharides were enhanced. The authors hypothesize that the salt ions interfere with the polysaccharide chain interactions and

alter the structure in such a way that in their case the active site is better exposed. In 1996 Eteshola et al. also demonstrated that the viscosity of the exopolysaccharide isolated from red microalgae was also decreased in the presence of salts. In this study, where activity was not enhanced, Na^+ and $NH4^+$ ions could bind to the negatively charged compound, neutralizing its charge and leading to inactivation especially if antibacterial activity was charge related (Mohamed et al., 2018). Given that up to this point, the most common methods used for protein isolation, purification and detection failed to provide any insight into the nature of the antibacterial compound, we hypothesized that the active agent may be an exopolysaccharide not conforming to the standard methods used for protein isolation, purification and detection.

To confirm this, we next attempted to use methods specific to the isolation of exopolysaccharides to purify these from *T. actiniarum* fermentations to determine whether the antibacterial activity observed was a result of an exopolysaccharide. This method also included a deproteinization step to clarify whether the active compound was in fact proteinaceous.

3.3.6 Exopolysaccharide isolation from *T. actiniarum* fermentation

Most marine bacteria produce exopolymeric substances that have wide application in food, pharmaceutical, medical and textile industries (Zhang et al., 2015; Dave at al., 2020). Exopolymeric substances are high molecular weight polymers consisting mainly of exopolysaccharides (EPSs) but also proteins, nucleic acids and lipids secreted by microorganisms or released as a result of bacterial lysis into their surrounding environments (Orsod and Huyop, 2012). Although non-sugar components are present, they are present in small amounts and generally attached to sugar residues (Bhaskar and Bhosle, 2005). The production of EPSs from various marine bacterial strains has been investigated and include *Bacillus*, *Halomonas*, *Pseudoalteromonas*, *Planococcus*, *Enterobacter*, *Rhodococcus* and *Vibrio* species (Parkar et al., 2017). Exopolysaccharides, the major component of marine bacterial extracellular polymeric substances, exhibit significant structural diversity with novel biological properties (Mohamed et al., 2018) and are known to have antibacterial activity against both Gram-positive and Gram-negative test strains (Orsod and Huyop, 2012; Viju et al., 2018; Hassan and Ibrahim, 2017; Mohamed et al., 2018).

Exopolysaccharides were isolated as described in section 3.2.7. The Sevag method used for deproteinization of the exopolysaccharide fraction has been used widely for the deproteinization of exopolysaccharide fractions isolated from mushrooms (Su et al., 2013), succulents (Zhang et al., 2017) and bacteria (Liang and Wang, 2015; Chen et al., 2013; Shukla and Dave, 2018) and the pre-treatment of exopolysaccharide fractions with this method ensures the removal of both free proteins and lipids (Su et al., 2013). Following deproteinization and exopolysaccharide precipitation from *T. actiniarum*, the resulting precipitate was dialysed against distilled water and size fractionated using Amicon ultra-centrifugal filters to remove any small molecules that remained after the Sevag treatment. The exopolysaccharide fraction was tested for antibacterial activity and activity was observed in the 50kDa-100kDa EPS fraction (Figure 3.7) indicated by the red arrow.

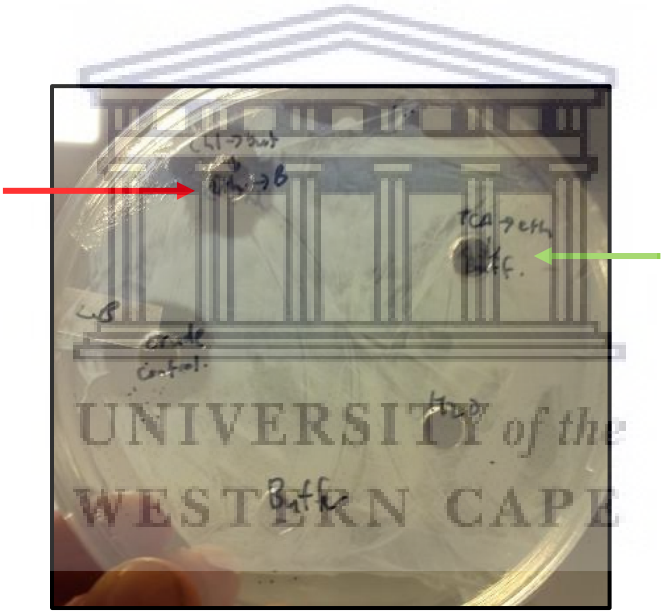

Figure 3.7: Antibacterial assay of the EPS fraction isolated from *T. actiniarum* culture supernatant. The red arrow shows zone of inhibition against *P. putida* conferred by the exopolysaccharide preparation using the Sevag method. The green arrow shows no zone of inhibition against *P. putida* of the exopolysaccharide fraction deproteinized with TCA.

The TCA (trichloro-acetic acid) method (Zhang et al., 2013) was also used for deproteinization but the activity was lost (green arrow), suggesting that the activity may have been affected by the decrease in pH (Isobe et al., 1992; Hosseini et al., 2017; da Silva et al., 2012). Also, the addition of TCA to the culture supernatant resulted in a brownish-orange co-precipitate that was difficult

to remove by centrifugation and filtration. As a result, the Sevag method was used for subsequent EPS extractions. Following antibacterial screening, the active exopolysaccharide fraction was resolved using SDS and native PAGE, and stained with Coomassie. Based on the ladder-like banding pattern observed in the EPS-containing lanes (Figure 3.8) it appears that many proteins were precipitated with the exopolysaccharide fraction indicating that the Sevag method used for deproteinization was not sufficient for removal of contaminating protein. BSA used as a control appears as multiple bands since it has a tendency to form non-covalent and covalent soluble aggregates (Li and Arakawa, 2019).

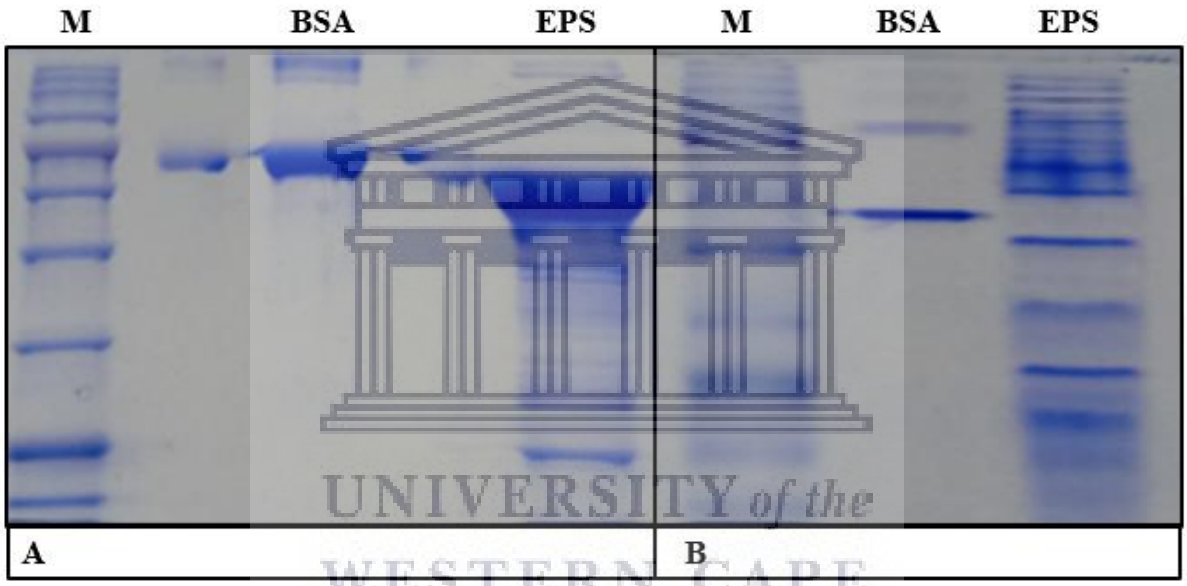

Figure 3.8 A: SDS-PAGE and B: Native PAGE analysis of the EPS purification from *T. actiniarum* following the Sevag method. A: lane 1: Protein Marker, lane: 3 BSA, lane 5: EPS fraction (50-100kDa). B: lane 1: Protein Marker, lane 2: BSA, lane 3: EPS fraction (50-100kDa). This fraction represents 2L of starting material that was concentrated to 200µl and 20µl was resolved.

Figure 3.8A represents a SDS-PAGE / denaturing gel used to resolve the proteins present in the EPS fraction. A prominent Coomassie-stained band between 46kDa and 58kDa was observed. Since size-fractionation has previously shown that the active compound was between 50-100kDa in size (Figure 2.6), therefore we were once again led to speculate that the prominent band represented the active compound and that it was of a proteinaceous nature. Since this sample underwent deproteinization, this result wasn't expected. The sample was also analysed under native PAGE / non-denaturing conditions (Figure 3.8B). The banding pattern was greatly different

compared to that resolved under denaturing conditions. The prominent band between 46kDa and 58kDa that was observed when the exopolysaccharide fraction was resolved under denaturing conditions was now no longer visible. Taken all together, none of the techniques used up to this point clarified the nature of the active compound. Given that colorimetric assays are typically used to determine the components of exopolymeric substances yet do not provide reliable qualitative and quantitative information about individual components in a mixed sample, Stains-All, a cationic dye was used to stain the components of the exopolysaccharide fraction in the gel after separation to provide better insight into the composition of the EPS fraction.

3.3.7 In-gel staining of exopolysaccharide fraction with Stains-All

Stains-All is a cationic multipurpose dye that stains proteins, DNA, RNA and exopolysaccharides. According to the manufacturer's description, proteins stain red, glycoproteins blue, lipids yellow to orange and calcium binding proteins blue to violet. SDS-PAGE and native PAGE was used to resolve the EPS fraction followed by staining with Stains-All. Prior to conducting the PAGE analyses, precipitation of the sample was observed suggesting that the storage conditions (MilliQ water at room temperature) were not conducive. The precipitate was removed by centrifugation at 1000 xg and an antibacterial test was conducted on the remaining supernatant to determine whether precipitation had affected the activity. Following the well diffusion assay the results indicated that the activity was not reduced (Figure 3.9) suggesting that the precipitated component that had been removed was not responsible for the activity.

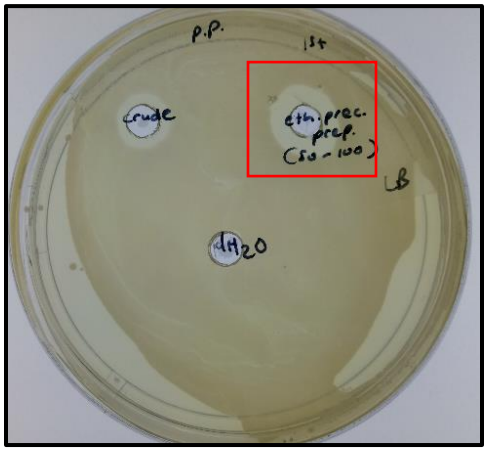

Figure 3.9: Well diffusion assay of the EPS fraction after removal of precipitate. Zone of inhibition against *P. putida* is indicated by the red square. Concentrated culture supernatant was used as a positive control.

Following confirmation of activity, the sample was resolved using SDS and native PAGE with one half of the gel stained with Coomassie and the other half with Stains-All. Interestingly, the prominent band between 46kDa and 58kDa that was resolved under denaturing conditions in Figure 3.8A, lane 5 had now disappeared (Figure 3.10A, EPS) and was likely the precipitate that was removed by centrifugation. Since antibacterial activity was not affected, we concluded that the protein present between 46kDa-58kDa in Figure 3.8A, thought to be the active protein, was not responsible for the antibacterial activity observed. In Figure 3.10B the other half of the denaturing gel was stained with Stains-All. A single distinct band at approximately 190kDa was resolved clearly and based on the blue colour suggests it was a glycoprotein or DNA. A smear of purple bands spanning from 32Da-58kDa were also observed.

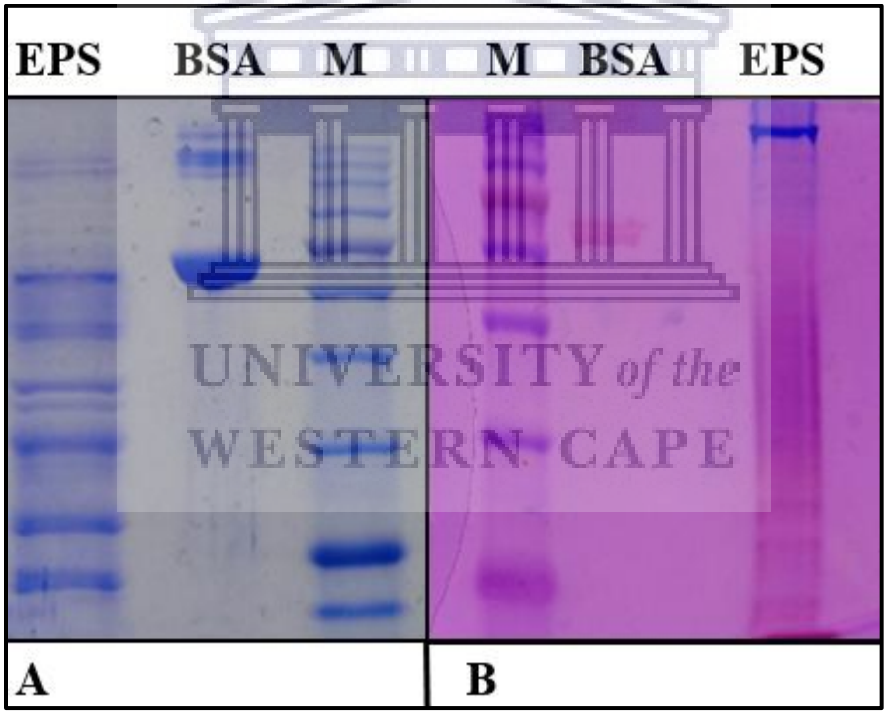

Figure 3.10: EPS fraction resolved under denaturing conditions and stained with Coomassie staining solution (A) and Stains-All (B).

After resolving the EPS fraction on native PAGE (Figure 3.11A) a decrease in the number of protein bands after Coomassie staining was also observed. In Figure 3.11B, following staining

with Stains-All, a blue band at approximately 190 kDa is also observed in the EPS fraction similar to Figure 3.10B when resolved under denaturing conditions.

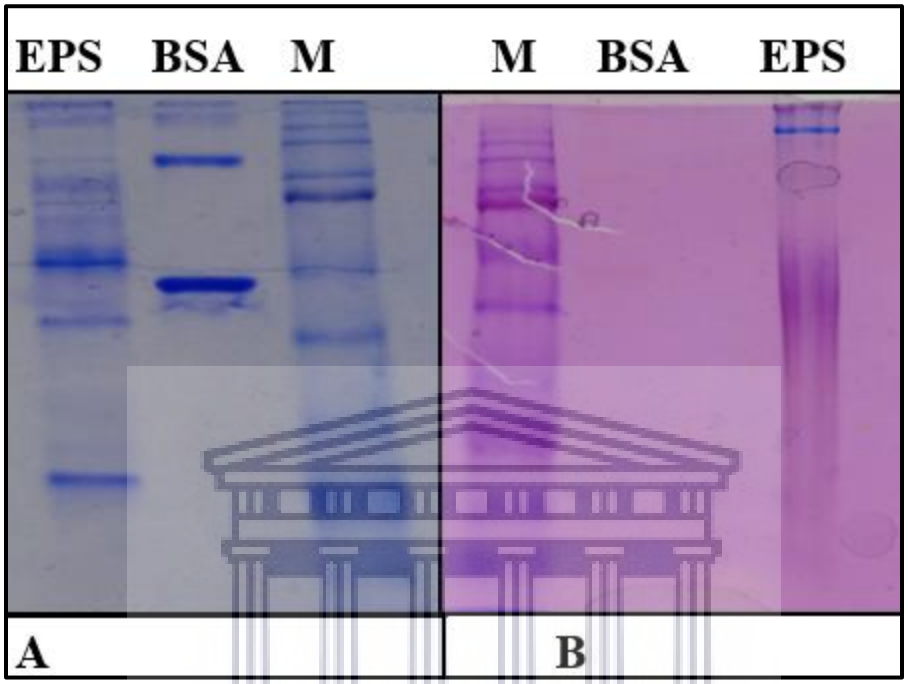

Figure 3.11: EPS fraction resolved under non-denaturing conditions and stained with Coomassie staining solution (A) and Stains-All (B).

Apart from the distinct blue bands at approximately 190kDa resolved under both denaturing and non-denaturing conditions, the results were inconclusive due to the appearance of smears. Given that the sample contained a mixture of proteins and polysaccharides, the binding of Stains-All to the various components may have been affected by the interference of the other components, similar to what is encountered when using colorimetric assays. Also, a single band may represent a compound with more than 1 chemical feature, which after staining with Stains-All, produces a composite colour.

BSA was used as a protein control for staining and the staining of BSA as red suggested that the method used was effective for staining proteins. However, literature suggests that the staining protocol used dictates the result and many methods used to prepare the staining solution are available in literature. According to Campbell et al. (1983) who were investigating calcium binding proteins, the staining solution used by King et al. (1976) stained calcium binding proteins red

instead of blue as specified by the manufacturer. The authors then modified the staining solution to ensure blue staining of the calcium binding proteins suggesting that the staining procedure can be manipulated to produce the desired result. In a paper by Catanzaro et al. (2017), the authors also stated that carbohydrate containing samples stained blue whereas Goldberg and Warner, 1997 indicated that highly acidic proteins stain blue. These contradicting statements suggest that the Stains-All procedure requires standardization. Notably, in literature, Stains-All was used mostly when the chemical features of target compounds were known (Campbell et al., 1983, Kawashima et al., 2009), it was pure and especially for the investigation of calcium binding and glycosylated proteins.

It is clear that in this study, where a mixture of compounds are present in the active fraction, Stains-All was not ideal and gave no clear indications as to what the composition of the EPS fraction could be. A zymography assay was next employed to determine whether any of the proteins or other compounds resolved in the gel show lytic activity against the Gram-negative test strain *P. putida*.

3.3.8 Zymography assay of exopolysaccharide fraction

Zymography is an electrophoretic technique designed to indicate either antimicrobial or enzymatic activity around protein bands of interest resolved on a polyacrylamide gel. An SDS-PAGE gel is impregnated with a substrate that should be degraded by the compound/protein being resolved in the gel. Zones of clearing in the location of the target compound are then observed following Coomassie staining. These zones appear as clear zones against a dark background (Leber and Balkwill, 1997). A zymogram can be used on any enzyme that acts on a biological substrate (Rodriguez-Rubio et al., 2019; Vandooren et al., 2013). In this study, whole cells of *P. putida* were used as a substrate and the EPS fraction was resolved under non-denaturing and denaturing conditions.

Under denaturing conditions, no activity was observed in the zymography assay (Figure 3.12B). The absence of activity observed in the zymogram conducted under denaturing conditions may suggest that the presence of SDS or other PAGE gel components along with heating of the sample affected the activity of the active agent as SDS has been shown to interact with both exopolysaccharides and proteins (Isobe et al., 1992; Bao et al., 2008; Nowakovsky et al., 2014).

Under non-denaturing conditions (without SDS and heat), the zymography assay revealed multiple clear bands against a uniform dark background, Figure 3.12A, suggestive of lytic activity. Interestingly, the white bands that represent lytic activity were not detected with silver staining (Figure 3.12C) or Coomassie staining (Figure 3.12D) of the EPS fraction. Silver staining is a staining technique used to stain proteins that are present at low concentrations. This method is 100 times more sensitive than Coomassie staining and is not exclusive to proteins since other macromolecules such as DNA and lipopolysaccharides can also be stained with silver stain (Farrell, 2010; Czarnik and Mei, 2007). This staining technique was employed to determine whether the white bands observed in the zymography assay following Coomassie staining appeared white due to proteins present in low concentrations. If so, silver staining may stain these bands due to its increased sensitivity compared to Coomassie. In a study conducted by Kropinski et al. (1986) the authors were investigating the basis of staining of *S. typhimurium* lipopolysaccharides with silver stain. After acid hydrolysis of the LPS, the polysaccharide portion did not stain with Silver stain, suggesting that the polysaccharides do not stain with silver stain and it is the lipid portion that stains. The use of silver stain for the detection of polysaccharides has been recorded however, and it is only effective when the polysaccharides are pre-stained with a cationic dye such as Alcian Blue as showed by Kachlani et al. (2001) and Corzo, (1991). Given that no bands were stained in the clear areas (representing lytic activity) with either Coomassie or silver stain, the results suggest that the active agent is not proteinacious or lipidaceous in nature and likely may be a polysaccharide of some description.

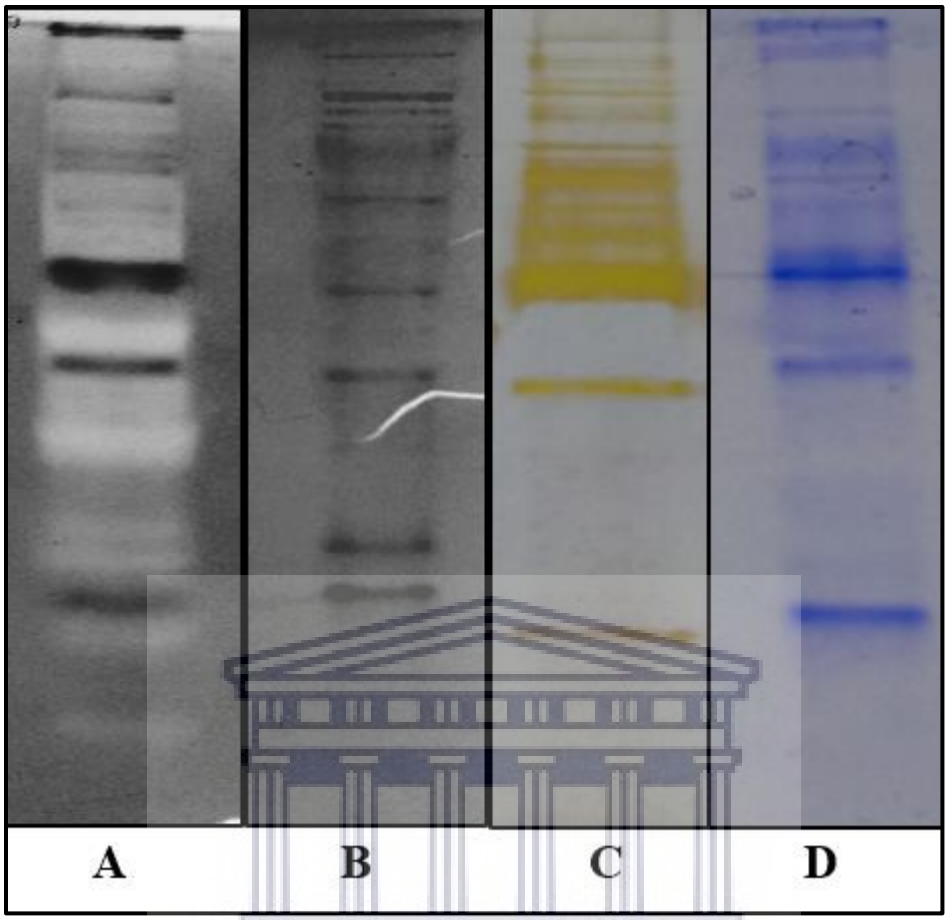

Figure 3.12: In-gel zymography assay of EPS fraction conducted under non-denaturing (A) and denaturing (B) conditions. Protein profile of EPS fraction stained with silver nitrate (C) and Coomassie (D) under non-denaturing conditions.

The appearance of multiple white bands in a ladder pattern (Figure 3.12A) in the zymogram is suggestive of the different chain lengths of heteropolymeric polysaccharides (Patrick, 2014). Given that whole cells were used as a substrate in the zymogram, these results also suggest that peptidoglycan hydrolase activity is observed (Rodriguez Rubio et al., 2019). Although known to show antibacterial activity, the mechanism of action of polysaccharides has not been fully characterized. Many have proposed that the mechanism of action involves damaging bacterial cell membranes resulting in leakage of the intracellular components and eventually cell death. This occurs through the electrostatic interaction of positively charged groups on the polysaccharides with negatively charged groups on the bacterial cell wall, leading to disruption of the cell membrane (Tachaboonyakiat, 2017). Polysaccharides with DNA damaging, and transcription

inhibition activities have also been identified (He et al., 2010; Shannon and Abu-Ghannam, 2016; Xing et al., 2009, Tachaboonyakiat, 2017). Additionally, anionic polysaccharides are proposed to show antibacterial activity through the chelation of metal ions and trace elements essential to the growth of microorganisms, resulting in growth inhibition (Mohamed et al., 2018).

Although not conclusive, our investigation of the composition of the active compound produced and secreted by *T. actiniarum* indicated that it was likely not proteinacious or lipidaceous in nature and that it could possibly be a polysaccharide. Using genome mining, putative biosynthetic pathways for the production of exopolysaccharides by *T. actiniarum* was investigated.

3.3.9 Biosynthesis of exopolysaccharides in bacteria

Bacteria produce a variety of exopolysaccharides composed of various monosaccharide subunits and substituents and are synthesized through different biosynthetic pathways. The most well-known bacterial EPS and the biosynthetic pathways responsible for the production are listed in Table 3.2 (Schmid et al., 2015). There are 4 general mechanisms known for the production of exopolysaccharides in bacteria; the Wzx/Wzy dependent pathway, the ATP-binding cassette (ABC-transporter dependent pathway), the synthase dependent pathway and the extracellular synthesis pathway which is facilitated by a single sucrase (Schmid et al., 2015).

Table 3.2: Overview of the most relevant bacterial EPS including monomer composition, substituent decorations, industrial application and biosynthetic pathway routes (adpated from Schmid et al., 2015).

EPS	Components	Substituents	Application	Biosynthetic pathway
Alginate	GulA, ManA	Ace	Food, feed, medicine, research	Synthase dependent
Cellulose	Glc	Ace, Pyr	Food, medicine, acoustics	Synthase dependent
Colanic acid	Glc, Fuc, GlcA, Gal		N.a	Wzx/Wzy dependent
Curdlan	Glc		Food, cosmetics, medicine, construction chemistry	Synthase dependent
Dextran	Glc		Medicine, chromatography	Extracellular dextran sucrase
Diutan	Glc, Rha, GlcA	Ace	Construction chemistry	Wzx/Wzy dependent
Gellan	Glc, Rha, GlcA	Ace, Gly	Construction chemistry, food, feed	Wzx/Wzy dependent
Hyaluronic acid	GlcA, GlcNAc		Medicine, cosmetics	Synthase dependent
Levan	Fru, Glc		Food (prebiotic), feed, medicine, cosmetics, industry, glue	Extracellular levan sucrase
Succinoglycan	Glc, Gal	Ace, Pyr, Suc	Oil industry, cosmetics	Wzx/Wzy dependent
Welan	Glc, Rha, GlcA, Man	Ace	Construction chemistry	Wzx/Wzy dependent
Xanthan	Glc, Man, GlcA	Ace, Pyr	Food, feed, technical applications, oil drilling	Wzx/Wzy dependent

- **Glc: glucose, Rha: rhamnose, Fuc: fucose, Fru: Fructose, Gal: galactose, Man: mannose, GlcA: glucuronic acid, ManA: mannuronic acid, GulA: guluronic acid, GalA: galacturonic acid, GlcNAc: N-acetylglucosamine, Pyr: pyruvate, Ace: acetate, Gly: glycerate, Suc: succinate, N.a: not announced (no commercial application but used in pathogenicity studies).**

Exopolysaccharide synthesis is a multistep process and the first step involves the synthesis of nucleotide sugars followed by the synthesis, assembly and export of the polysaccharide (Becker, 2015).

Nucleotide sugars are the precursors involved in the glycosylation of glycoconjugates and the biosynthesis of polysaccharides. Nucleotide sugars are sugar 1 phosphates activated by nucleotidyltransferases through the addition of a nucleoside monophosphate (UDP-, ADP-, CMP-, and GDP) to the sugar 1 phosphate *via* a phosphodiester linkage (Handford 2006). These nucleotide sugars then act as sugar donors that are transferred to glycans, proteins, lipids and other glycosylated metabolites by glycosyltransferases (Mäki and Renkonen, 2004). The most commonly occurring nucleotide sugars are UDP-glucose, UDP-N-acetylglucosamine, UDP-

galactosamine, UDP-galactose, UDP-N-acetylgalactosamine, UDP-xylose, GDP-fucose and GDP-mannose (Whitman et al., 2010). Upon investigating the genome of *T. actiniarum* for biosynthetic genes involved in polysaccharide and nucleotide sugar synthesis, unsurprisingly, a complete biosynthetic pathway for the production of heptose was identified.

Heptoses are highly characteristic of the Gram-negative cell wall and form part of the lipopolysaccharide layer of the outer membrane (Wang and Quinn, 2010; Maldonado et al., 2016). The LPS consists of lipid A, an inner core oligosaccharide and an O-specific polysaccharide (Figure 3.13) (Kneidinger et al., 2002). Well conserved in Gram-negative bacteria, a 5-step pathway responsible for the synthesis of ADP-heptose exists and is initiated by the conversion of sedoheptulose-7-phosphate, an intermediate in the pentose phosphate pathway (Gaudet and Owen, 2016). Figure 3.13 illustrates the biosynthetic pathway of ADP-heptose, the nucleotide sugar precursor for heptose synthesis. Encoded on the genome of *T. actiniarum* is the complete pathway for the synthesis of ADP-heptose and includes the genes *gmhA* (D-glycero-D-mannose-heptose 1, 7 bisphosphate phosphatase), *gmhB* (phosphoheptose isomerase), *hIdE* (D-glycero-β-D-manno-heptose-7-phosphate kinase) and *Waac/rfaQ* (ADP-heptose-LPS-heptosyltransferase) (Gaudet and Owen 2016, Kneidinger et al., 2002).

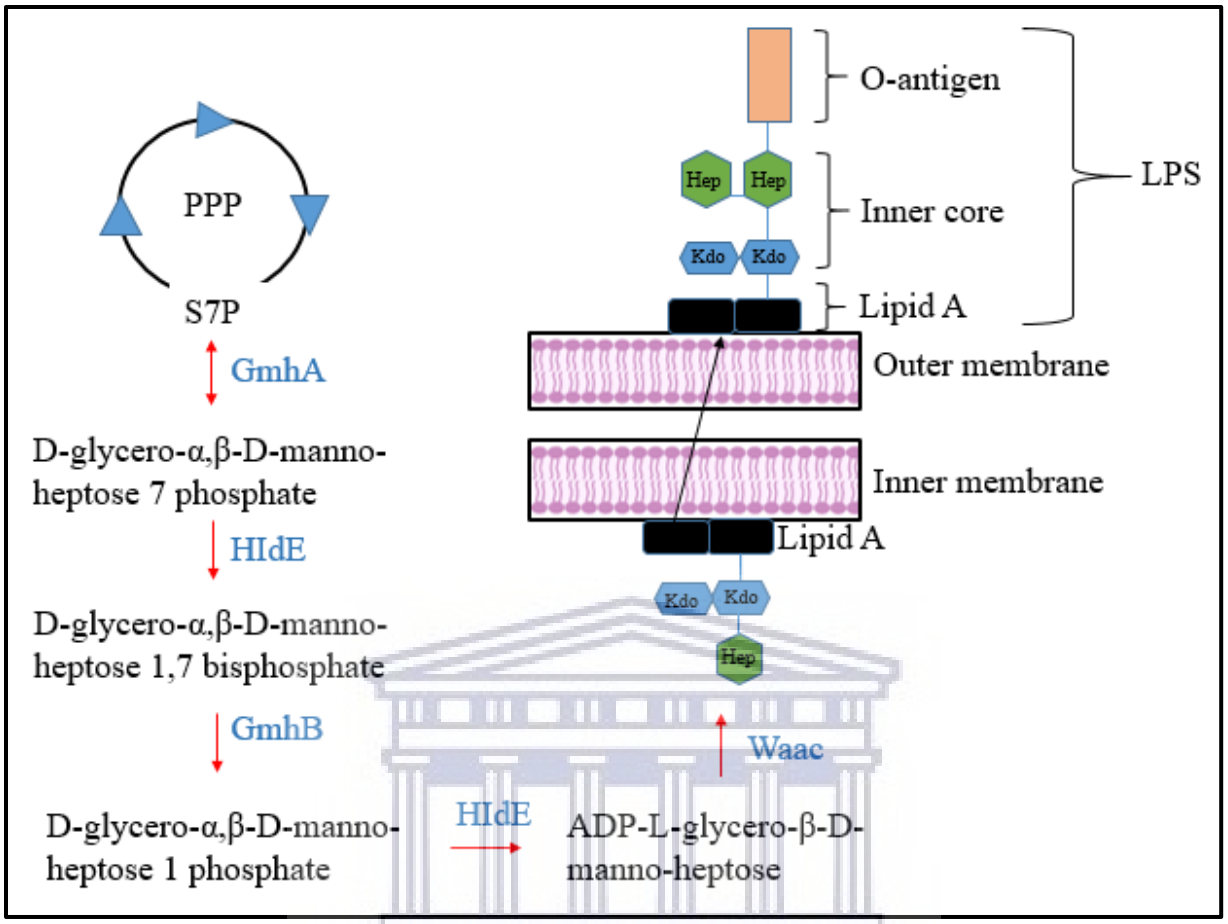

Figure 3.13: Heptose synthesis pathway, adapted from Gaudet and Owen, 2002

Although heptose sugars form part of the LPS portion of the outer membrane (Wang and Quinn, al, 2010; Maldonado et al., 2016) these sugars can also be incorporated into bacterial biofilms (Jiao et al., 2010) and possibly other polysaccharides and glycoconjugates as depicted in Table 3.2, which showcases the diverse combinations of sugars that occur within polysaccharide structures.

Apart from the ADP-heptose synthesis pathway, pathways responsible for the synthesis of nucleotide sugars UDP-N-acetylglucosamine, UDP-N-acetylgalactosamine, UDP-glucuronic acid and UDP-glucose from trehalose and glycogen as the predicted carbon sources are also present on the genome.

Trehalose is a non-reducing sugar comprising of 2 glucose units with an α-1,1- glycosidic linkage. It is found in plants, fungi, lichens, algae, bacteria, insects and invertebrates. Trehalose is similar to sucrose but less widely distributed and its conversion to glucose-1-phosphate does not require

energy (Davidson, 2020). In this study, the carbon sources present in the Marine Broth used for the cultivation of *T. actiniarum* were yeast extract and peptone. Yeast extract is composed of the soluble components of yeast cells and is commonly used in bacterial culture as a nutrient source. It is prepared through the disruption of yeast cells and the intracellular material is used as yeast extract (Zarei, 2016). Although the exact carbohydrate components present in yeast extract have not been elucidated, literature reports that the main carbohydrates present in the soluble fraction of the yeast is trehalose and glycogen (Plata et al., 2013; Paalman et al., 2003; François and Parrou, 2001). It has been established that *T. actiniarum* is capable of utilizing both trehalose and glycogen as carbon sources (Hosoya et al., 2009). Encoded on the genome of *T. actiniarum*, an α,α trehalose phosphorylase gene was identified that catalyzes the reversible conversion of trehalose to glucose and glucose-1-phosphate *via* the TreP pathway (Thammahong et al., 2017; Avonce et al., 2006; Zilli et al., 2015). No glycogen phosphorylase genes, involved in glycogen metabolism (Cifuente et al., 2019) were identified yet glycogen assimilation was observed by Hosoya et al. (2009) suggesting that the bacterium may be utilizing novel enzymes/pathways for the metabolism of glycogen that are therefore not predicted using homology based gene annotation methods. Assuming that *T. actiniarum* used trehalose and/or glycogen as a carbon source, the biosynthetic pathway for the production of the abovementioned nucleotide sugars is proposed (Figure 3.14). Notably, glucose-supplemented growth media could also facilitate the production of the abovementioned nucleotide sugars (Zilli et al., 2015), eliminating the requirement for the bacterium to first catabolize trehalose and glycogen to glucose subunits.

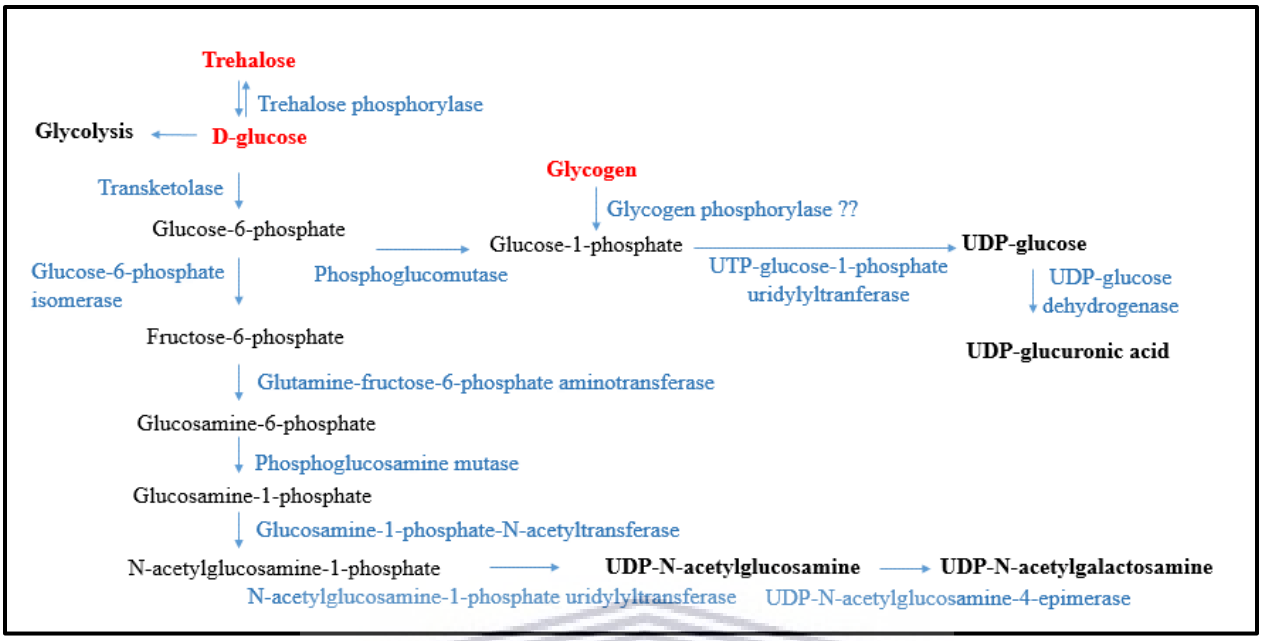

Figure 3.14: The biosynthetic pathway for the production of UDP-N-acetylglucosamine (Li et al., 2012; Rodriguez-Diaz, 2012); UDP-glucuronic acid (Broach et al., 2012), UDP-glucose (Broach et al., 2012) and UDP-N-acetylgalactosamine (Dong et al., 2009) from trehalose (Thammahong et al., 2017) and glycogen (Seibold and Eikanns, 2007).

EPS production is a complex process requiring a variety of regulatory components and networks and is relatively poorly understood. No studies aiming to investigate EPS production in *Thalassomonas actiniarum* have been conducted and we therefore have limited understanding of the EPS synthetic pathways and export mechanisms in this bacterium. When analyzing the genome for polysaccharide biosynthetic pathways, it became apparent that *T. actiniarum* has the genetic capacity required to synthesize the biofilm associated exopolysaccharide poly-β-1, 6-*N*-acetyl-glucosamine (PNAG) and the glycosaminoglycan, chondroitin.

3.3.10 Poly-β-1, 6-*N*-acetyl-glucosamine (PNAG) structure and synthesis

As a survival strategy, bacteria produce biofilms composed of polysaccharides, DNA and proteins that assist bacteria in adhering to surfaces and also act as a protective barrier against antibacterial compounds and other environmental stresses (Wang et al., 2016). Although the polysaccharides present in these biofilms are different between strains of bacteria, partially de-*N*-acetylated PNAG (dPNAG) is common to both Gram-negative and Gram-positive bacterial biofilms (Kwan and

Withers, 2014). The synthase dependent pathway for the synthesis of PNAG, which is a polymer of N-acetylglucosamine, is the best studied synthase dependent system in *E. coli* (Atkin et al., 2014).

The common components of a synthase dependent pathway is a polysaccharide synthase spanning the bacterial inner membrane, a bis-(3'-5')-cyclic dimeric guanosine monophosphate (ci-di-GMP) receptor protein, a tetratricopeptide repeat (TPR) containing protein, a β-barrel porin and in some cases, polysaccharide tailoring enzymes (Kwan and Withers, 2014). Polysaccharides produced through this mechanism may remain attached to the exterior of the cells but are frequently released into the extracellular environment (Yates et al., 2017).

In *E. coli*, the *pgaABCD* operon encodes the proteins required for the synthesis and translocation of deacetylated PNAG (dPNAG) across the bacterial double-layer membrane (Wang et al., 2016). The bifunctional enzyme PNAG synthase (*pgaC*) belonging to the glycosyltransferase 2 family synthesizes and translocates PNAG across the inner membrane to the periplasm (Figure 3.15) and the activity of this enzyme is regulated by the binding of the bacterial second messenger ci-di-GMP to pgaD, a c-di-GMP receptor protein. In the periplasm, pgaB, a metal-dependent *N*-deacetylase, partially de-*N*-acetylates (3-5%) PNAG to form dPNAG and also cleaves the polymer with its C-terminal glycoside hydrolase (Bundalovic-Torma et al., 2020). The enzyme pgaA, unique to the Gram-negative cell envelope, (Bundalovic-Toram et al., 2020) has a predicted C-terminal β-barrel domain and an N-terminal TPR domain and is responsible for the export of dPNAG to the extracellular space (Kwan and Withers, 2014). The presence of TPR-repeat containing proteins and the allosteric activator c-di-GMP are hallmarks of the synthase dependent pathway (Whitney and Howell, 2013). Partial deacetylation is essential for polymer export as *pgaB* deletion mutants resulted in the polymer localised in the periplasm and the mutant not able to produce a biofilm (Little, 2015). Additionally, *pgaA* deletion mutants also resulted in dPNAG remaining in the periplasm, showcasing the importance of pgaA, in addition to pgaB, in dPNAG transport to the extracellular space (Choi et al., 2009).

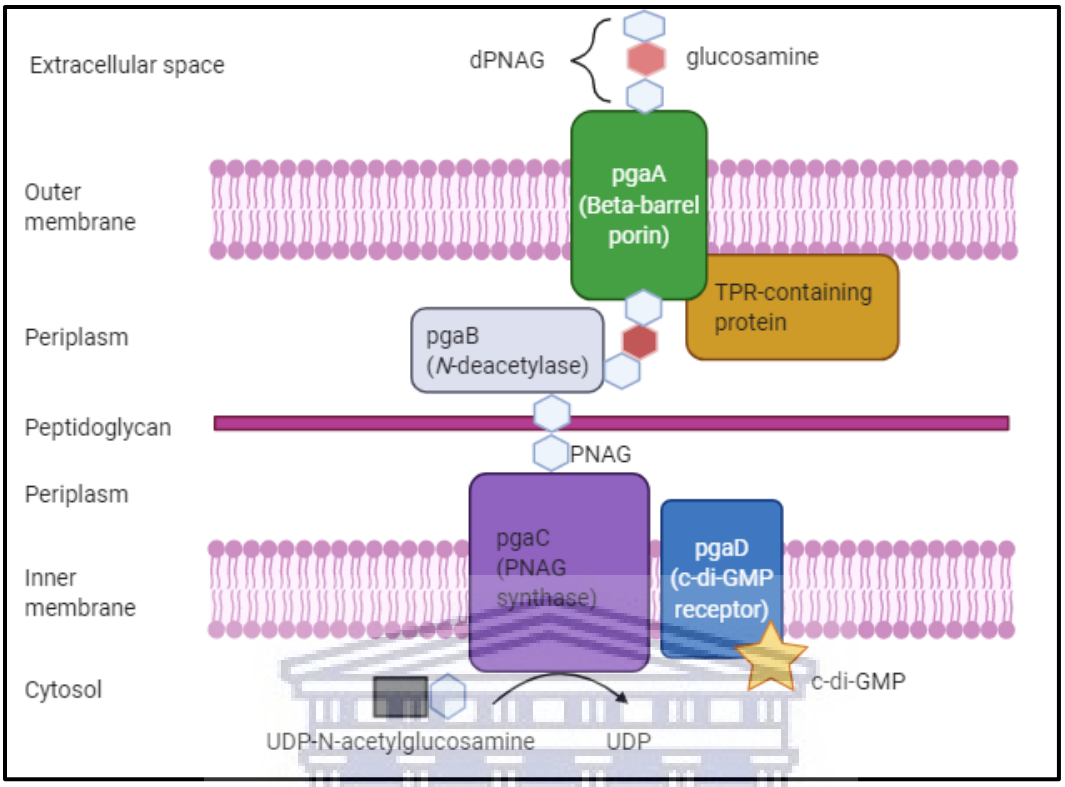

Figure 3.15: Synthase dependent pathway for PNAG synthesis, adapted from Schmid *et al.*, 2015 and Kwan and Withers, 2014.

Gram-positive bacterial strains such as *Staphylococcus aureus* and *Staphylococcus epidermidis* also produce biofilm associated PNAG but instead of using the *pgaABCD* operon for PNAG synthesis, Gram-positive bacteria use the *icaADBC* operon (Atkin et al., 2014; Bundalovic-Torma et al., 2020). The *ica* locus was first discovered in 1996 by Heilmann et al. through transposon mutagenesis. A library of *S. epidermidis* transposon insertion mutants were screened for isolates with defective biofilms and a mutant with an insertion in the *ica* locus exhibited the desired phenotype. The names of the proteins encoded in the *pga* operon may be different to the proteins encoded in the *ica* operon but both operons share a number of key proteins with the same function. The *pgaB* gene is equivalent to the *icaB* gene as both encode a PNAG deacetylase. The *pgaC* gene is equivalent to *icaA* with both belonging to glycosyltransferase family 2 proteins (Bundalovic-Torma et al., 2020). The genes *pgaD* and *icaD* (*icaD* being unique to Gram-positive organisms) share no sequence homology but are both essential to the function of *pgaC* and *icaA* respectively yet the precise function of *icaD* is still unclear. The only gene with no *pga* homolog is *icaC* which is not conserved and is proposed to be involved in PNAG O-succinylation which occurs in Gram-

positive bacteria. With that said, only *icaA, icaD* and *icaB* are required for the synthesis of PNAG (without O-succinylation) in Gram-positive bacteria (Atkin et al., 2014). Additionally, an *icaR* gene transcribed divergently from other *ica* genes has also been identified in staphylococcal strains and is the negative regulator of PNAG synthesis (Cue et al., 2012; Atkin et al., 2014).

Based on the Prokka annotated genome (with default parameters), the genes *pgaB* (PNAG deacetylase), *icaA* (PNAG synthase), *icaB* (PNAG deacetylase) are encoded on the genome of *Thalassomonas actiniarum;* with *icaA* and *icaB* located adjacent to one another while *pgaB* is located elsewhere on the genome. A BLASTp alignment of the genes upstream and downstream of *pgaB* did not give any positive hits for proteins involved in PNAG synthesis. Additionally, a diguanylate cyclase, involved in the synthesis of c-di-GMP was also identified, suggesting that PNAG synthesis may be regulated by c-di-GMP (Whitfield et al., 2020). Notably c-di-GMP is also a regulator of a variety of other pathways and not only PNAG synthesis (Vallentini and Filloux, 2016). Although not found on an operon, these genes, together with homologous genes located elsewhere on the genome may facilitate PNAG synthesis (Cywes-Bentley et al., 2013).

A BLASTp analysis of the core PNAG biosynthetic genes identified showed no homology to the *pga* or *ica* genes from *E. coli* and *Staphylococcus* respectively (Table 3.3). Although the description of the hits were functionally accurate, low sequence homology was observed.

Table 3.3: BLASTp hits of *ica* and *pga* genes encoded on the genome *T. actiniarum*.

Gene	BLASTp hit	Organism	E value	% Identity
icaA	Glycosyltransferase family 2 protein	*Gammaproteobacteria bacterium*	8e-^{113}	45.77%
icaB	Polysaccharide deacetylase family protein	*Lysobacter panacisoli*	1e-^{57}	38.40%
pgaB	Polysaccharide deacetylase family protein	*Colwellia* sp. PAMC 20917	6e-^{166}	61.32%

The presence of genes involved in PNAG production from both the *ica* operon (specific to Gram-positive bacteria) and the *pga* operon (specific to Gram-negative bacteria) is unexpected since the *ica* operon, to the best of our knowledge, has been found only in Gram-positive bacteria. Although these operons share similarities (and may be why Prokka detects both loci) certain features distinguish the *ica* from the *pga* operon such as protein domain composition and protein sequence lengths (Bundalovic-Torma et al., 2020).

PNAG production in *T. actiniarum* has not been elucidated however if it is produced by the strain, it may be synthesized by a novel PNAG synthase or mechanism and use an alternative mode of export. On the other hand, since the *icaA* and *icaB* genes are present, although known to be exclusive to Gram-positive organisms, this opens the possibility that *T. actiniarum*, if a producer of PNAG, may be using the *ica* operon for PNAG production and potentially a novel mechanism of regulation (*via* c-di-GMP) and export of dPNAG.

To the best of our knowledge, the *ica* operon has not been observed in Gram-negative bacteria however, this occurrence may not be unlikely since a study by Whitfield et al. (2020) showed that the Pel polysaccharide biosynthetic genes, thought to be present only in Gram-negative bacteria and involved in biofilm formation, are also present in the Gram-positive Pel polysaccharide producing bacterium, *Bacillus cereus* and is regulated by c-di-GMP, a novel c-di-GMP regulatory circuit (Whitfield et al., 2020) as Gram-positive PNAG production operons are generally not dependent on c-di-GMP (Bundalovic-Torma et al., 2020).

With the low sequence homology of the PNAG biosynthesis genes identified in *T. actiniarum* and the presence of genes from both *ica* and *pga* operons, it is possible that if produced, the PNAG synthesis pathway in *T. actiniarum* could be novel. Notably, it has been reported that bacteria who do not have established genetic loci for PNAG synthesis still produced surface associated PNAG including *Streptococcus pneumoniae*, *Streptococcus pyogenes* and *Mycobacterium tuberculosis* suggesting that orthologous systems can display differences that require experimental validation (Little, 2015).

Synthase dependent pathways are often used for the synthesis of homopolymers (like PNAG) requiring only a single type of sugar precursor. However, hyaluronan, a glycosaminoglycan (GAG) consisting of D-glucuronic acid and N-acetylglucosamine (Olczyk et al., 2008) is synthesized by a single enzyme (hyaluronan synthase), a bifunctional enzyme which performs the polymerization and secretion (Schmid et al., 2015).The hyaluronic acid operon of *Streptococci* consists of three genes encoding HasA (hyaluronan synthase), HasB and HasC. The enzymes HasC (UTP-glucose-1-phosphate uridylyltransferase) and HasB (UDP-glucose dehydrogenase) are involved in the synthesis of the nucleotide sugar UDP-glucuronic acid while UDP-N-acetylglucosamine is produced through global cell metabolism (Schmidt et al., 2015; Chong et al., 2005). Although HasC and HasB are encoded on the genome of *T. actiniarum* (Figure 3.14) the key enzyme, hyaluronan synthase was not identified, suggesting that the strain does not synthesize hyaluronan.

If however this GAG is produced, this strain may be producing GAG via a novel hyaluronan synthase.

3.3.10.1 Antibacterial activity of PNAG

Chitin is a β 1,4-linked polymer of N-acetylglucosamine and is a structural component of fungal cell walls as well the exoskeleton of crustaceans and has shown to have antibacterial activity (Tachaboonyakiat et al., 2017, Benhabiles et al., 2012). Chitosan, the deacylated form of chitin, has shown antitumor, antibacterial, antifungal and neuroprotective activities (Benhabiles et al., 2012). These polymers have received a lot of attention in recent years due to their bioactive potential. However, the high molecular weight and consequent poor solubility of these polymers has led researchers to investigate the bioactive potential of the oligomers that make up these polymers. In a study conducted by Raut et al. (2016), the authors investigated the antibacterial activity of low molecular weight N-acetylglucosamine obtained through the depolymerization of chitin using physical and chemical methods and found that N-acetylglucosamine showed bactericidal activity against both *E. coli* and *S. aureus*. Similarly, Benhabiles et al., (2012) showed that N-acetylglucosamine and glucosamine obtained from the chemical depolymerization of chitin and chitosan respectively exhibited antibacterial activity against *S. aureus*, *B. cereus*, *B. subtilis*, *E. coli*, *P. aeruginosa*, *S. typhimurium*, *Vibrio cholerae*, *Shigella dysenteriae*, *Prevotella melaninogenica* and *Bacteriodes fragilis*. The polymers chitin and chitosan also showed bacteriostatic activity against most, but not all, of the strains tested. These findings suggest that N-acetylglucosamine and glucosamine are potential antimicrobial candidates. Moreover, it suggests that exopolysaccharides containing N-acetylglucosamine and/or glucosamine, like PNAG and dPNAG, could display antibacterial activity as a result of the presence of these amino sugars.

Although the antibacterial activity of PNAG has not been extensively investigated, a study conducted by Lindner et al. (2011) showed that PNAG nanofibers enhanced diabetic wound healing and showed indirect antibacterial activity against *S. aureus* by upregulating defensin production. Defensins are positively charged small molecules that possess antimicrobial activity and are found in mammals, plants and insects, playing an important role in innate and adaptive immunity (Machado and Ottolini, 2015).

3.3.11 Synthesis and antibacterial activity of chondroitin and chondroitin sulfate

The application of chondroitin sulfate (CS), a polymer of repeating units of glucuronic acid and N-acetylgalactosamine as a treatment for arthritis demands its large-scale production but the lack of sustainable and steady production of CS is a problem for industry (Badri et al., 2018). The K4 capsular gene cluster of *E. coli* is a 14 Kb operon encoding genes *kfoA-G* responsible for the synthesis of the cell capsule made up of fructosylated chondroitin (Ninomiya et al., 2002; Schiraldi et al., 2010). The amount of fructosylated chondroitin produced naturally by *E. coli* K4 is not enough for industrial application and a study using a random mutagenesis approach showed that a missense mutation in codon 313 of chondroitin synthase resulted in an 80% increase in chondroitin production compared to the wild type strain (Ninomiya et al., 2004; Zanfardino et al., 2010). Since *E. coli* K4 does not have the genetic capacity to produce the sulfotransferase required for post polymer modification, fructosylated chondroitin must be enzymatically modified by first removing the β-fructose monosaccharide at position 3 of glucuronic acid (Ninomiya et al., 2002; Badri et al., 2018) followed by enzymatic sulfation at the desired position/s. Identified on the genome of *T. actiniarum* is the gene *kfoC*, which encodes chondroitin synthase responsible for the synthesis of the chondroitin backbone of the capsule of *E. coli* K4 (Cimini et al., 2018; Ninomiya et al., 2002). A BLASTp analysis of CS identified on *T. actiniarum* showed that it is 41.29% (E value 2e-38) similar to a glycosyltransferase family 2 protein from *Bathymodiolus puteoserpentis* and showed no homology to chondroitin synthases from *E. coli* (KfoC), *Pasteurella multicoda* (PmCS) or *Chromobacterium phaeobacteriodes* (CpCS). Additionally, the sequence length (275 base pairs) of the predicted *T. actiniarum kfoC* gene was also much shorter compared to the chondroitin synthases from the other bacteria that are approximately 700 base pairs. Chondroitin synthases have 2 glycosyl transferase domains, with N-acetylgalactosamine transferase found around residues 156-270 and glucuronic acid transferase found at 438-550 residues when CpCS is used as a reference in a multiple protein sequence alignment of KfoC, PmCA and CpCS (Green and DeAngelis, 2017). This suggests that the putative chondroitin synthase gene identified in *T. actiniarum* only has one glycosyltransferase domain. Should experimental validation show that chondroitin is produced by this strain and is facilitated by this enzyme, it may point towards a novel chondroitin synthase which has a single glycosyltransferase domain that alternatively transfers both glucuronic acid and N-acetylglucosamine to the polysaccharide chain (Weigel and DeAngelis, 2007).

No chondroitin sulfotransferase genes were identified suggesting that if produced, chondroitin is likely unsulfated. However, given that such a large portion of the genome is unannotated (47%), suggesting many unique genes and pathways yet to be discovered, a novel sulfotransferase may be present. Knowing whether chondroitin is sulfated is important since the structure-activity relationships of polysaccharides has been investigated and polysaccharides with sulfate or acetyl groups commonly show antioxidant activity while phosphate containing polysaccharides show antitumor activity. The presence of sulfates has also shown to enhance anti-HIV and antibacterial activity (Li et al., 2015). Additionally, studies have showed that the degree and pattern of sulfation, differences in chain elongation or molecular weight can also affect biological action (Neves et al., 2020). CS has been used as an antibacterial agent immobilized on the surface of polylactic acid (PLA), a bioplastic used in biomedical application that is vulnerable to contamination by bacteria and showed antibacterial activity against *E. coli*. The antibacterial activity of unsulfated chondroitin has not been investigated, but unsulfated chondroitin isolated from *E. coli* showed anti-inflammatory activity as well as increased cell proliferation (Stellavato et al., 2016). These studies suggest that even without sulfation, the anti-inflammatory activity of chondroitin is still achieved, suggesting that sulfate groups of chondroitin are not responsible for anti-inflammatory activity. Future studies aiming to investigate and compare the antibacterial activity of unsulfated and sulfated chondroitin could further elucidate the effect of sulfate groups in chondroitin on antibacterial activity.

These findings suggest that if produced, N-acetylglucosamine, glucosamine, chondroitin, PNAG and dPNAG are potential antimicrobial agents that may be responsible for the observed antibacterial activity or be incorporated into the structure of the putative antibacterial EPS and in this way contribute to its antibacterial activity.

3.3.12 Conclusion

To the best of our knowledge, this is the first report demonstrating that *T. actiniarum* produces a putative anionic exopolysaccharide with antibacterial activity against *P. putida*. To the best of our knowledge this is also the first study in which the zymography technique is applied to investigate the lytic activity of exopolysaccharides. Since the putative antibacterial polysaccharide was not structurally characterized, the exact synthesis pathway for its production in *T. actiniarum* could

not be deduced. However, genome mining with a focus on polysaccharide synthesis revealed that the strain has some of the genetic elements required to produce the polysaccharide PNAG and the glycosaminoglycan chondroitin. However, since complete operons were not identified for the respective pathways, it points strongly to *T. actiniarum* employing potentially novel pathways. Additionally, a number of nucleotide sugar biosynthetic pathways were identified, and these sugars, if incorporated into the structure of the putative antibacterial exopolysaccharide, may contribute to the antibacterial activity. Future studies aiming to structurally characterize the putative antibacterial EPSs produced by *T. actiniarum* should provide more insight into the biosynthetic pathway responsible for its production. Using a gene knockout approach to determine whether the putative EPSs are responsible for the antibacterial activity could assist in confirming its activity as well its biosynthetic pathway (Pérez-Burgos et al., 2020). This may however be challenging since the sugar phosphate precursors required for EPS production are more often than not required for other processes such as cell wall synthesis, so inactivating any of the genes involved in the synthesis of these sugars may prove lethal to the organism. Also, future studies aiming to structurally characterize the putative antibacterial polysaccharide could employ methods used by Castellane et al., 2015 and Zhang et al., 2017 and use genetic engineering/mutagenesis as an approach to increase EPS yields/alter EPS properties (Dave et al., 2020). It is important to note that polysaccharide characterization is not a trivial exercise and unlike proteins, polysaccharides are difficult to characterize for an exact structure as they have diverse chemical, structural composition, molecular weights and linkages all which contribute to their biological activity (Li et al., 2018).

Chapter 4: Isolation of cholic acid and 3-oxo cholic acid, from *Thalassomonas actiniarum*.

4.1 Introduction

T. actiniarum is an interesting candidate for the production of bioactive compounds as seen by the number and complexity of novel secondary metabolite biosynthetic gene clusters encoded on its genome. Whole genome sequencing has provided natural product researchers with the tools to prioritize metabolically talented strains on their ability to produce diverse natural compounds (Gulder & Moore, 2009; Zerikly & Challis, 2009). Based on antiSMASH and PRISM analysis, it is clear that a single bacterial genome could encode a number of pathways that remain undetected under standard laboratory culturing conditions. These tools have been used successfully not only for the prediction of secondary metabolite gene clusters producing novel compounds but have also been useful in detecting novel pathways (Johnston et al., 2016; Alberti et al., 2019; Larson et al., 2017; Panter et al., 2018; Park et al., 2017). Since activity of small molecules were not detected using the functional screening methods described in Chapter 2: section 2.2.4, but many potentially novel secondary metabolite gene clusters are encoded on its genome, Chapter 4 explores the production of small bioactive molecules by using alternative extraction, fractionation and screening approaches compared to that used in Chapter 2.

Bioactive natural products from marine bacteria are an important source of pharmaceutically relevant compounds (Debbab et al., 2010). Using bacteria, the sustainable production of bioactive natural products at reasonably low costs can be accomplished and may also overcome the supply issue associated with the isolation of natural products from marine invertebrates. Furthermore, owing to the challenging and competitive conditions associated with living in complex communities within invertebrates, marine bacteria produce unique compounds compared to terrestrial microorganisms and these compounds enable the bacteria and their hosts to withstand the adaptive pressures imposed by the marine environment (Debabb et al., 2010). Now with the advent of multidrug resistant pathogens and increased mortality due to chronic diseases such as cancer, there is a need for novel small-molecule chemical entities with novel mechanisms of action. To investigate the bioactivities of small molecules produced by *T. actiniarum* a bioassay and mass

spectrometry guided approach toward identification of potential bioactive compounds was used. This work was conducted at Marbio (UiT) where I conducted a 3 month secondment as part of the Horizon 2020 RISE Ocean Medicines project. The Ocean Medicines project is an initiative encompassing a network of international collaborators from both academia and industry with the aim to discover and develop novel drugs isolated form marine microorganisms and promotes the sharing of knowledge through secondments of research. The experimental outline is illustrated in the diagram below and was adapted from the MabCent pipeline, an initiative based in Tromsø, Norway, which aims to investigate the bioactive potential of marine organisms inhabiting the Arctic waters (Svenson, 2013).

Two compounds, cholic acid and 3-oxo cholic acid were identified in this study. Cholic acid is a primary bile acid and 3-oxo cholic acid is an intermediate in cholic acid production (Mukhopadhyay and Maitra 2004). Bile acids are the products of cholesterol catabolism in mammals and regulate cholesterol levels. In the gut, the bile acids also regulate the gut microflora due to their concentration dependent antibacterial activity. Although not responsible for the bioactivities observed in this study, the compounds are not commonly produced by bacteria and their biosynthetic pathway in prokaryotes is unknown. In this study, the partial biosynthetic pathway for the production of cholic acid in bacteria is proposed.

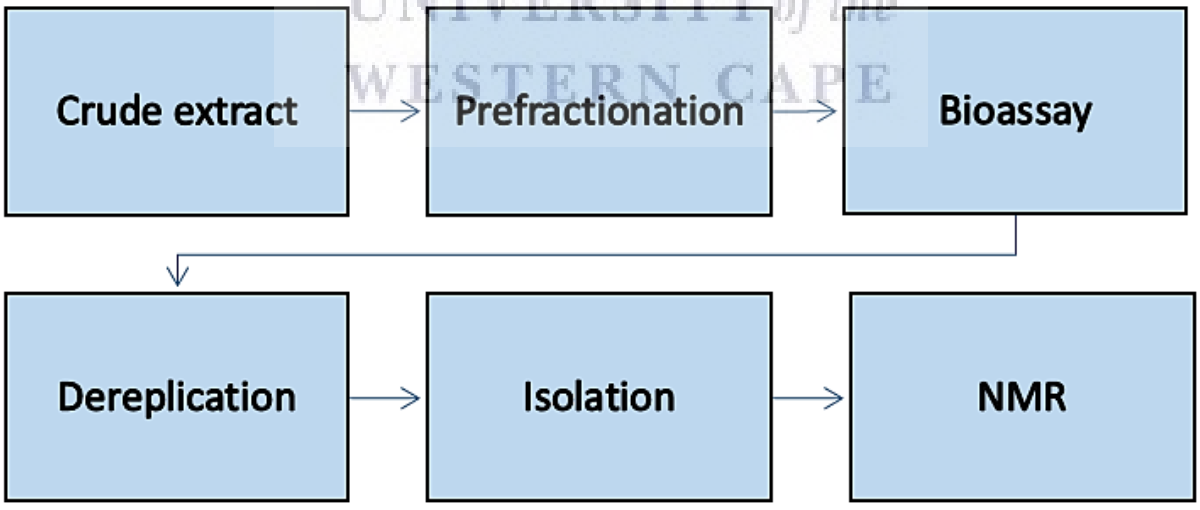

Figure 4.1: The bioassay guided isolation pipeline as followed by Mabcent (Svenson, 2013)

4.2 Methods and Material

4.2.1 Bacterial strains and cell lines used in this study

Table 4.1: Test organisms and cell lines used in this study.

Bacterial Strains	Description	Assay	Source
Thalassomonas actiniarum A5K-106^T	Strain under study		DSMZ (German Collection of Microorganisms and Cell cultures)
Enterococcus faecalis ATCC 29122		antibacterial	LGC standards (UK)
Streptococcus agalactiae ATCC 12386		antibacterial	LGC standards (UK)
E. coli ATCC 25922		antibacterial	LGC standards (UK)
Pseudomonas aeruginosa ATCC 27853		antibacterial	LGC standards (UK)
Staphylococcus aureus ATCC 25923		antibacterial	LGC standards (UK)
Multi-drug resistant Staphylococcus aureus (MRSA) ATCC 33591		antibacterial	LGC standards (UK)
Staphylococcus epidermidis ATCC (RP62A 42-77) 35984		biofilm inhibition	University hospital (UNN), Tromsø, NO
Staphylococcus haemolyticus Clinical isolate 8-7A		biofilm inhibition	University hospital (UNN), Tromsø, NO
Cell lines			
A2058 ATCC-CRL-11147	Human melanoma	anticancer	LGC standards (UK)
MRC-5 ATCC-CCL-171	Lung fibroblast	anticancer	LGC standards (UK)
HT-29 ATCC HTB-38	Human colon	anticancer	LGC standards (UK)

4.2.3 Strain cultivation

Seed cultures of *T. actiniarum* were prepared by inoculating 100µl of bacterial suspension from a 50% glycerol stock stored at -80^{o}C into a 100ml Erlenmeyer conical flask containing 50ml Marine Broth (BD Difco™) and incubated at 28^{o}C overnight with shaking at 150 rpm. Briefly, 5ml of overnight seed culture was inoculated into a 1L narrow mouth Erlenmeyer conical flask containing 500ml of media. For this study, a 3L fermentation volume was used. *T. actiniarum* was cultivated in Marine Broth (BD Difco™) at 28^{o}C with shaking at 150 rpm for a period of 14 days. Following fermentation, secondary metabolites were extracted from the cultures.

4.2.4 Extraction of secondary metabolites from cultures using Diaion® HP-20

Diaion® HP-20 beads were used at a concentration of 40g/L for the extraction of secondary metabolites from the cultures. The resin was first activated in 100% methanol for 30 minutes and then washed twice with MilliQ water. Cultures (3L) were incubated with resin (40g/L) for 3 days

at room temperature with shaking at 150 rpm prior to extraction. Following the 3-day incubation period the culture media was removed by vacuum filtration using a cheesecloth filter and the beads collected. The beads were then washed with 200ml of MilliQ water and filtered again. To extract secondary metabolites from the beads, 100ml of 100% methanol was added to the beads and incubated for 1 hour with shaking at 100 rpm. Following incubation with methanol, the extract was filtered using a Whatman filter and a second round of extraction was conducted on the beads. For the second round, 100ml of methanol was added to the resin and incubated for 15 minutes with shaking at 100 rpm. This was also filtered and added to the first extract. The methanol extract was dried at 40^{o}C using a rotary evaporator. Dried extract was stored at -20^{o}C until further use.

4.2.5 Fractionation of Diaion® HP-20 extracts using the Biotage® system

The Biotage® HPFC SP4 Flash Purification system was used for prefractionation of methanol extracts. Dried methanol extract was dissolved in 10ml of 90% methanol and combined with 1.5g of Diaion® HPSS-20 column material. This mix of column material and extract was dried in a rotary evaporator and prefractionated using a prepacked Biotage® SNAP cartridge as described below.

The column material used for SNAP columns was Diaion HP-20SS. To activate column material it was soaked in methanol for 20 minutes and washed twice with MilliQ water. The activated material was added to a 10g SNAP cartridge with the aid of a vacuum manifold and stored in MilliQ water at 4^{o}C until further use.

The flash column was connected to the Biotage system and equilibrated with MeOH: MilliQ water (1:1) prior to adding the extract. Following column equilibration, the extract was added to the SNAP column and a 2-step flash chromatography program was used resulting in 27 fractions (Table 4.2). These fractions were pooled as indicated resulting in 6 FLASH fractions.

Table 4.2: FLASH purification mobile phase gradients.

	MeOH	MilliQ water	Acetone	Fraction	Pooled fraction
Step 1	5	95	0	1-3	1
	25	75	0	4-6	2
	50	50	0	7-9	3
	75	25	0	10-12	4
	100	0	0	13-15	5
				16-18	6
Step 2	0	50	50	19-20	
	0	0	100	21-27	

After prefractionation and pooling of fractions, fractions were dried using a Syncor® Polyvap. Depending on the amount of material for each fraction, it was dissolved in 100% DMSO with concentrations varying between 10mg/ml and 80mg/ml. These were stored at -20ºC in cryotubes until later use in both bioassays and the dereplication process. Where the concentration of a fraction was too low to get an accurate weight measurement, the residue present after drying was resuspended in 200µl of 100% DMSO and stored at -20ºC for inclusion in the dereplication process.

4.2.6 Bioactivity screening of FLASH fractions

Working stocks of 1mg/ml of flash fractions were prepared with MilliQ water. Fractions were screened for antibacterial, biofilm inhibition and anticancer activity.

4.2.6.1 Antibacterial activity assay

For antibacterial screening five test strains were used (Table 4.1). All strains were maintained on blood agar (BD Difco™). For screening, a loopful of bacteria was inoculated into 8ml of media and incubated at 37ºC overnight with shaking at 150 rpm. Following overnight incubation, 2ml of cell suspension was inoculated into 25ml of fresh media and incubated at 37ºC with shaking at 150 rpm. The time period for incubation and growth media for each strain is illustrated in Table 4.3. Following incubation, cultures were diluted 1: 1000 in the appropriate culture media.

Table 4.3: Test bacteria, their growth media and incubation periods to reach the desired 0.5 McFarland standard.

Bacterial strain	Growth media	Incubation period (h)	Desired bacterial density
S. aureus	Mueller Hinton (BD Difco™)	2.5	0.5-3 x 10^5 CFU/ml
E. coli	Mueller Hinton	1.5	0.5-3 x 10^5 CFU/ml
E. faecalis	Brain heart Infusion (Sigma-Aldrich)	1.5	0.5-3 x 10^5 CFU/ml
P. aeruginosa	Mueller Hinton	2.5	3-7 x 10^4 CFU/ml
S. agalactiae	Brain Heart Infusion	1.5	0.5-3 x 10^5 CFU/ml
MRSA	Mueller Hinton	2.5	0.5-3 x 10^5 CFU/ml

One 96-well microtitre plate was used per bacterium to be tested. Diluted culture samples were added to a 96-well microtitre plate to a total volume of 50µl/well. FLASH fractions were screened at 250µg/ml for antibacterial activity and each flash fraction was tested in triplicate. For pure compounds, antibacterial screening was conducted at concentrations of 5µg/ml, 10µg/ml, 25µg/ml, 50µg/ml and 100µg/ml and was also screened for activity against MRSA (Table 4.1).

Plates were incubated overnight at 37°C before measuring growth at an absorbance of 600nm. Bacterial suspension diluted with water was used as a growth control. A dilution series of gentamycin (Merck) from 32µg/ml to 0.01µg/ml was used as a positive control in assays, the growth medium with no inoculum was used as a negative growth control.

Following overnight incubation, the absorbance of the microtitre plate was measured at 600nm. The software used was WorkOut2.5 (Dazdaq, England). The absorbance values were used to define whether fractions were active, inactive or questionable.

Table 4.4: Absorbance (OD_{600}) values required to define activity of the flash fraction

Description	Abs_{600nm}
Active	<0.05
Inactive	>0.09
Questionable	0.05-0.09

Routine gentamycin controls were performed to ensure that the test bacteria were not contaminated and served as a positive control. In a 96-well microtitre plate, 50µl of gentamycin was added to 50µl of bacterial suspension. The plates were incubated at 37°C overnight. The absorbance was

determined and the reference MIC values for a 0.5 McFarland standard are indicated in Table 4.5. If the measured absorbance did not correspond with the reference MIC, the result was rejected.

Table 4.5: MIC of gentamycin on the bacterial strains used for antibacterial screening

Bacterial Strain	Reference MIC of gentamycin (µg/µl)
S. aureus	0.25
E. coli	0.50
E. faecalis	10.0
P. aeruginosa	0.50
S. agalactiae	4.00

4.2.6.2 Biofilm inhibition assay

Fractions were screened for biofilm inhibition using test bacteria *S. epidermidis* and *S. haemolyticus* (Table 4.1). Both bacterial strains were kept on blood agar and re-streaked every other week. For screening, a loopful of bacteria was inoculated into 5ml of TSB (Merck) and incubated overnight at 37^{o}C with shaking at 150 rpm. Following overnight incubation, cultures were diluted 1:100 in TSB with 1% glucose (Sigma-Aldrich, USA) which induces biofilm formation.

Table 4.6: 96-well microtitre plate layout for the anti-biofilm assay

	1	2	3	4	5	6	7	8	9	10	11	12
A	N	N	N	N	N	N	N	N	N	N	M	P
B	N	N	N	1	1	N	N	N	N	N	M	P
C	N	N	N	2	2	N	N	N	N	N	M	P
D	N	N	N	3	3	N	N	N	N	N	M	P
E	N	N	N	4	4	N	N	N	N	N	M	P
F	N	N	N	5	5	N	N	N	N	N	M	P
G	N	N	N	N	N	N	N	N	N	N	M	P
H	N	N	N	N	N	N	N	N	N	N	M	P

*** N represents the negative control containing 50µl of *S. haemolyticus* and 50µl autoclaved MilliQ water, P represents the positive control containing 50µl autoclaved MilliQ water and 50µl *S. epidermidis* bacterial suspension. M represents media control containing 50µl MilliQ water and 50µl TSB+1% glucose. Values 1 to 5 indicate flash fractions 1 to 5 and each sample was tested in duplicate.**

Following overnight incubation, cells were removed from the plate by inverting the plate on paper towel. The wells were washed with MilliQ water and the biofilm fixed at 65ºC for 1 hour. Following fixation, 70µl of 0.1% crystal violet was added to each well and incubated for 10 minutes at room temperature. After incubation the crystal violet (Merck) was removed by inverting on paper towel and the wells rinsed again with MilliQ water until all crystal violet that was not attached to biofilm was removed. The plate was dried at 65ºC for 1 hr. After drying, 70µl of 70% ethanol was added to each well and placed on a shaker for 10 minutes at 70 rpm. The absorbance of the microtitre plate was measured at 600nm. The software used was WorkOut 2.5 (Dazdaq, England). The absorbance values were used to define whether fractions were active, inactive or questionable as shown in Table 4.7.

Table 4.7: Absorbance values required to define activity of the extract in the biofilm inhibition assay

Description	**Abs_{600nm}**
Active	<0.25
Inactive	>0.35
Questionable	0.25-0.35

4.2.6.3 Anti-cancer activity screening

The cancer cell lines A2058 and HT-29 were cultivated in Dulbecco's Modified Eagle's Medium (D-MEM) media with 10% Fetal Bovine Serum (FBS, Biochrom, UK), 0.01 mg/ml gentamycin and 1% L-alanyl-L-glutamine (Biochrom, UK) and Roswell Park Memorial Institute medium (RPMI-1640, Biochrom, UK) respectively at 37°C with 5% CO_2 for 24 hours in a Sanyo CO_2 incubator. The non-malignant MRC-5 cells used as toxicity controls were cultivated in Minimum Essential Medium with Earle's salts (E-MEM, Biochrom, UK) media with 10% FBS, 0.01ug/ml gentamycin, 1% L-alanyl-L-glutamine, 1% Non-essential amino acids (NEAA, Biochrom, UK), 1% sodium pyruvate (Biochrom, UK) and 1% sodium bicarbonate (Biochrom, UK) and incubated under the same conditions as the cancer cell lines. Cells were split to keep them in monolayer. To split the cells, the culture media was discarded, and the cells washed with Dulbecco's PBS (Sigma-Aldrich, USA) for 1 minute. After washing the cells, 0.25% trypsin (in PBS) was added to the cells and swirled gently for 10 seconds. The trypsin solution was discarded, and the flask incubated at 37°C for 5 minutes. Once detached from the culture flask, the cells were resuspended in 10ml of fresh growth media. Of this suspension, an appropriate volume (depending on cell density) was added to 15ml fresh media and incubated at 37°C with 5% CO_2 for 24-48 hours. Following incubation, cells were counted using a haemocytometer and cell morphology and density assessed using a microscope. For the A2058 cell line, a density of 2000 cells per well is required for the assay while the HT-29 and MRC-5 (toxicity control) cell lines are required at a cell density of 2000 and 4000 cells/well respectively. For screening, 100µl of cell suspension (at the desired cell density) was seeded into 96-well tissue culture plates (Table 4.8). The seeded plates were incubated for 24 hours at 37°C with 5% CO_2. Following 24-hour incubation and prior to adding the flash fractions to the wells, the media was removed from the wells and replaced with fresh RPMI-1640, the assay media. Flash fractions (prepared in section 4.2.5) were added to the wells at a final concentration of 100µg/ml and tested in triplicate while pure compounds were screened at concentrations of 5µg/ml, 25µg/ml, 50µg/ml and 100µg/ml. The plates incubated for 72 hours at 37°C with 5% CO_2.

Table 4.8: 96-well tissue culture plate layout for the anticancer assay

	1	2	3	4	5	6	7	8	9	10	11	12
A	N	N	N	N	N	N	N	N	N	N	N	P
B	N	1	2	3	4	5	N	N	N	N	N	P
C	N	1	2	3	4	5	N	N	N	N	N	P
D	N	1	2	3	4	5	N	N	N	N	N	P
E	N	N	N	N	N	N	N	N	N	N	N	P
F	N	N	N	N	N	N	N	N	N	N	N	P
G	N	N	N	N	N	N	N	N	N	N	N	P
H	N	N	N	N	N	N	N	N	N	N	N	P

*** N represents the negative control with 100µl of RPMI-1640 media containing 10% FBS, 0.01 mg/ml gentamycin and 1% L-alanyl-L-glutamine. P represents the positive control RPMI-1640 media containing 10% FBS, 0.01 mg/ml gentamycin, 1% L-alanyl-L-glutamine and 10%. Values 1 to 5 indicate flash fractions 1 to 5 and each sample was tested in triplicate.**

After incubation, 10µl of Aqueous One solution (Promega) was added to each well and the plates were incubated again for 1 hour at 37ºC with 5% CO_2. After incubation the absorbance was measured at 485 nm using a DTX 880 multimode detector and the multimode analysis software (Beckman Coulter). Cell survival was calculated using the equation below. Fractions inhibiting cell survival by 50% were considered active.

Equation: Survival % = (AbsF-AbsP) x 100 / (AbsN – AbsP)

To calculate cell survival in the MTS proliferation assay, AbsF is the average absorbance at 485nm of wells with fractions; AbsP is the average absorbance at 485nm of wells with positive control; AbsN is the average absorbance at 485nm of wells with negative control.

4.2.7 Dereplication of bioactive fractions using UHPLC-QTof-MS

Fractions were dereplicated using UHPLC-QToF-MS and were run in both positive and negative ionization mode. Prior to injection the flash samples (taken from DMSO stock) were diluted (1:20) in 80% methanol and transferred to a glass HPLC vial. The injection volume was 5µl and the samples run on a C18 column in an Acquity UHPLC class system. This was followed by mass analysis using the Vion IMS QToF package. The mobile phases used were A: MilliQ water + 0.1%

formic acid and B: acetonitrile + 0.1% formic acid. Table 4.9 shows the UHPLC gradient and mobile phases used and Table 4.10 shows the parameters used for ESI+/- on the Vion IMS QToF.

Table 4.9: Mobile phase gradient used for the UHPLC system that is coupled to the MS.

Time(minutes)	Flow rate(ml/minute)	Mobile phase A (%)	Mobile phase B (%)
0.00	0.450	90	10
12.00	0.450	0	100
13.50	0.450	0	100

Table 4.10: Vion IMS QToF parameters for dereplication process in ESI+/-

Parameters	ESI+/-
Capillary Voltage	0.80 kV
Cone Voltage	30 V
Source Temperature	120°C
Desolvation Temperature	450°C
Cone Gas Flow	50 L/h
Desolvation Gas Flow	800 L/h
Low Collision Energy	6.0 eV
High Collision Energy	15-45 eV
Scan Time	0.2s

Compounds present in the active fraction were compared to compounds present in the inactive fractions eluting before and after the active fraction. This was done to determine whether there were any compounds present in the active fraction and absent in the inactive fraction and also to see whether the concentration was higher in active fractions compared to inactive fractions. Possible candidates were identified, and the Waters UNIFI software was used to calculate elemental composition as well as isotopic pattern. The predicted elemental composition was used to search databases such as Marinlit.

4.2.8 Mass Guided isolation of compounds using preparative HPLC-MS

The active fraction was further purified by preparative high-performance liquid chromatography consisting of a 600 Pump, a 2996 PDA UV detector, 3100 Mass detector (in negative mode with an ESI source) and a 2767 sample manager. The system was controlled by Waters Masslynx version 4.1 and Waters FractionLynx software. An aliquot of 500µL was injected onto a Waters Xterra RP C18 HPLC column (10mm x 250 mm, 10µm particle size) with mobile phase gradient

as shown in Table 4.11. Mobile phases A and B was as described in section 4.2.7. A total of 40 fractions were collected. Fractions containing compounds with the targeted masses were concentrated under vacuum in a Speedy Vac and re-injected to further purify the compounds. This second round of purification was conducted using the same mobile phase as above but with an X-Select Fluoro-phenyl column (5µm particle size, 10mm x 250mm) with a mobile phase gradient as shown in Table 4.12.

Table 4.11: Mobile phase gradient used for Xterra RP C18 column in the first round of purification

Time (minutes)	Flowrate (ml/minutes)	Mobile phase A %	Mobile phase B %
0	6	80	20
2	6	80	20
30	6	0	100
40	6	0	100

Table 4.12: Mobile phase gradient used for X-Select Fluoro-phenyl column in the second round of purification

Time (minutes)	Flowrate (ml/minutes)	Mobile phase A %	Mobile phase B %
0	6	75	25
10	6	0	100
25	6	0	100

4.2.9 Structural elucidation of isolated compounds by NMR

Optical rotations were measured on an AA-10R automatic polarimeter (Optical Activity LTD) in methanol. NMR spectra were acquired in methanol-$_{d4}$ on a Bruker Avance III HD spectrometer (BioSpin, Fallanden, Switzerland) at 600MHz for protons equipped with an inverse detected TCI probe with cryogenic enhancement on ^{1}H, ^{2}H and ^{13}C operating at 600 MHz.

All NMR spectra were acquired at 298 K in 3mm solvent matched Shigemi tubes using standard pulse programs for Proton, Carbon, HSQC (bip), HMBC (bip) and H2BC (bip) experiments with gradient selection where applicable and processed in Mnova 12.0 in Topspin 3.5p17. $^{1}H/^{13}C$ chemical shifts were referenced to the residual solvent peak (acetonitrile-$_{d3}$: δH=1.94, δC=118.69).

4.2.10 Genome annotation and secondary metabolite pathway detection

The complete genome of *T. actiniarum* was assessed for secondary metabolite biosynthetic pathways using antiSMASH2.0 and PRISM available at https://antismash.secondarymetabolites.org/#!/start (Medema et al., 2011) and

http://magarveylab.ca/prism/ (Skinnider et al., 2015) respectively. antiSMASH and PRISM analysis parameters were set with all optional features turned on.

4.3 Results

4.3.1 Genome mining for secondary metabolite biosynthetic pathways using antiSMASH and PRISM

Using antiSMASH to assess the bioactive potential of *T. actiniarum,* 10 biosynthetic gene clusters were detected in the complete genome and are listed in Table 4.13. These 10 BGCs belong to 4 different classes of natural products, which included: 2 nonribosomal peptides, 1 siderophore biosynthesis pathway and 4 hybrid pathways. Of the gene clusters predicted, only 2 of them, 1 and 7, shared sequence identity to genes from other known clusters (encoding staphylobactin and nostophycin). However, the similarity was not between the core biosynthetic genes and therefore it is unlikely that they encode for these compounds. Given that no similarity to known BGCs was observed, if produced, these are potentially novel secondary metabolites.

Chromids are secondary replicons encoding essential genes required for cell survival. Chromids resemble chromosomes and plasmids, owing to its plasmid-like origin of replication and the presence of core essential genes. These replicons can be divided into two categories, primary and secondary chromids. Primary chromids encode genes that are essential for cell viability while secondary chromids harbour genes/pathways that may be expressed only under unfavourable conditions (Fournes et al., 2018; diCenzo and Finan, 2017). Interestingly, the secondary metabolite biosynthetic gene clusters 6-10 are encoded on the chromid of *T. actiniarum*. Furthermore strains that have lost the chromid were obtained in the laboratory by colleagues through routine culturing (data not shown), suggesting that this may be a secondary chromid that is required when the strain is exposed to unfavourable conditions e.g., nutrient depletion, during which these secondary metabolite pathways are expressed to inhibit the growth of competitors (Fournes et al., 2018).

Table 4.13: Secondary metabolite biosynthetic gene clusters encoded on the genome of *Thalassomonas actiniarum*, predicted by antiSMASH 5.0

Cluster	Class	Most similar cluster	% of similar genes
1	Siderophore	staphylobactin	18%
2	Bacteriocin	NA	0
3	Thiopeptide	NA	0
4	NRPS-lanthipeptide	NA	0
5	NRPS-butyrolactone-hserlactone	NA	0
6	Bacteriocin	NA	0
7	NRPS-T1PKS	nostophycin	18%
8	NRPS	NA	0
9	Bacteriocin-lanthipeptide	NA	0
10	NRPS	NA	0

*NA indicates not available

The PRISM tool was used to predict NRP and PK biosynthesis pathways encoded on the genome of *T. actiniarum*. Interestingly, cluster 7, the NRP/PK hybrid identified by antiSMASH and cluster 10, the NRPS (Figure 4.2 A and B), was predicted to be potentially sulfated owing to the presence of a sulfotransferase domain. These clusters are also present on the chromid.

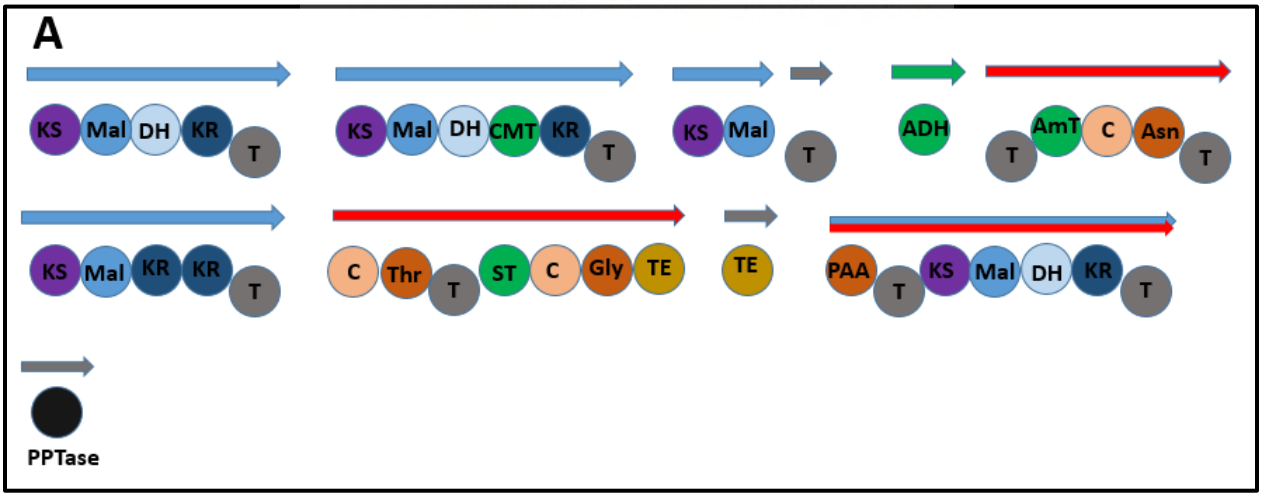

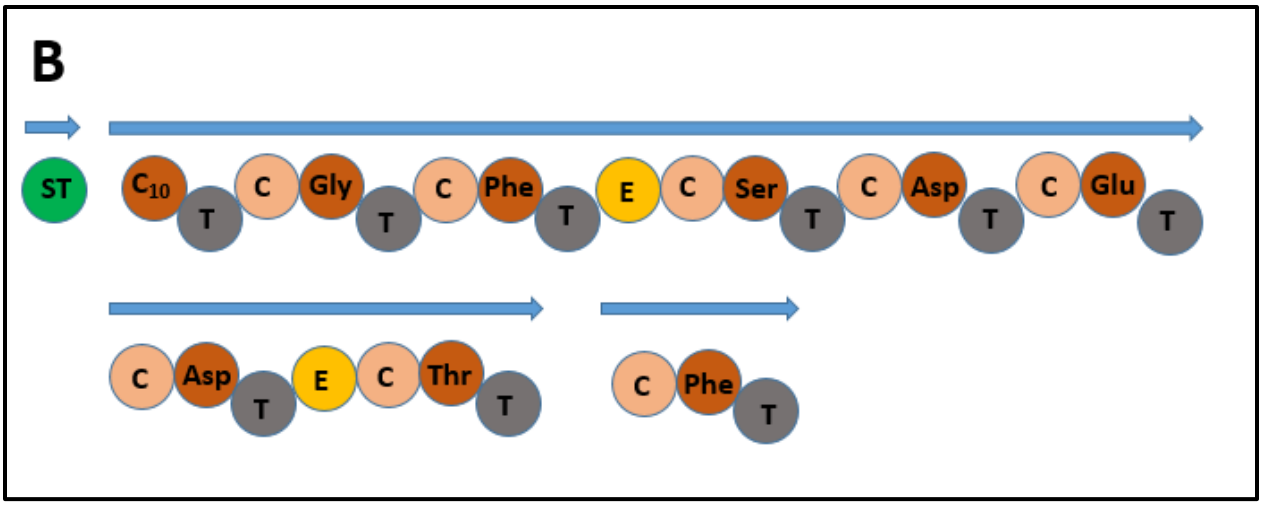

Figure 4.2 A and Figure 4.2 B: A: Modular structure of a potentially sulfated PK/NRP hybrid (A) and modular structure of a potentially sulfated NRP (B) identified through PRISM in *T. actiniarum*. KS-ketosynthase, Mal-acyltransferase, DH-dehydratase, KR-ketoreductase, T-thiolation, C-condensation, Thr-adenylation, ST-sulfotransferase, Gly, Phe, Ser, Asp, Glu and Thr-adenylation, TE-thioesterase, PAA and C_{10}-acyl adenylating enzymes, PPTase-phosphopantetheinyltransferase

The modification or tailoring of NRPs by sulfotransferases is rare and only 6 glycopeptide sulfotransferases were discovered between 2006 and 2016 (Zwahlen, 2018 and Winn et al., 2006). Among the many modifications these compounds can undergo, which include glycosylation, acylation and halogenation, sulfation is the least common (Winn et al, 2006; Zwahlen, 2018; Rounge et al., 2007). Cyanopeptolin 1138, a protease inhibitor produced by the cyanobacterial *Planktothrix* strain NIVA CYA 116, is a sulfated cyclic NRP encoded by the 30 kb *oci* gene cluster. The gene cluster contains 4 ORFs of which one, *ociA* (10.4kB) encodes 2 tailoring domains. One of these is a sulfotransferase domain that according to the authors, prior to their study conducted in 2007, had not been detected in NRP biosynthetic gene clusters (Rounge et al., 2007). BLASTp alignment of the sulfotransferase domain identified in the NRP/PK hybrid biosynthesis pathway (Figure 4.2 A) aligned to *ociA* from *Planktothrix* strain NIVA CA116 with 46.84% identity (E value 1e-41) (Table 4.14). Given that the ST domain encoded on the *ociA* ORF is responsible for the sulfation of cyanopeptolin 1138, the ST domain present in *T. actiniarum* may be involved in sulfation of the predicted hybrid NRP/PK. The BLASTp hits obtained also show that the sulfotransferase domain identified in *T. actiniarum* shows low homology to known sulfotransferases.

Table 4.14: Relevant BLASTp hits of ST domain of NRP/PK hybrid of *T. actiniarum*.

Description	E value	Identity	Accession number
amino acid adenylation domain-containing protein [*Catenovulum* sp. RQJ05]	2E-80	74.84%	WP_111977559.1
non-ribosomal peptide synthetase [*Desulfamplus magnetovallimortis*]	8E-64	61.49%	WP_080798675.1
amino acid adenylation domain-containing protein [*Ectothiorhodospiraceae* bacterium BW-2]	4E-61	61.25%	WP_149684709.1
sulfotransferase [*Moorea* sp. SIO2I5]	1E-45	47.50%	NEQ87400.1
OciA [*Planktothrix agardhii* NIES-205]	1E-42	47.47%	ABW84363.1
OciA [*Planktothrix agardhii* NIVA-CYA 126/8]	1E-42	47.47%	AQY60506.1
sulfotransferase [*Okeania* sp. SIO2H7]	1E-45	47.17%	NEP41453.1
OciA [*Planktothrix agardhii* NIVA-CYA 116]	1E-41	46.84%	ABI26077.1

Additionally, the ST domain identified in the NRP biosynthesis pathway (Figure 4.2 B) was analysed using BLASTp (Table 4.15), also showing low homology to known sulfotransferases, and no homology to the sulfotransferase domain identified in the hybrid NRP/PK.

Table 4.15: Relevant BLASTp hits of ST domain of NRP of *T. actiniarum*.

Description	E value	Identitiy	Accession number
hypothetical protein BFC16_18165 [*Pseudoalteromonas* sp. JW3]	2E-119	71.24%	OHU85819.1
MULTISPECIES: hypothetical protein [*Pseudoalteromonas*]	3E-119	71.24%	WP_083330610.1
hypothetical protein [*Pseudoalteromonas luteoviolacea*]	1E-95	58.95%	WP_063373279.1
sulfotransferase domain-containing protein [*Methylomonas* sp. Kb3]	1E-62	45.98%	WP_165786322.1
Sulfotransferase domain-containing protein [*Micromonospora pattaloongensis*]	1E-15	28.05%	SDY66118.1
sulfotransferase domain-containing protein [*Methylomonas* sp. GJ1]	1E-58	40.35%	WP_150048088.1
sulfotransferase family protein [*Methylomicrobium album* BG8]	3E-60	43.10%	EIC29087.1
sulfotransferase [*Methylocystis* sp. B8]	1E-19	28.57%	WP_138167505.1
sulfotransferase [*Verrucosispora* sp. FIM060022]	5E-16	29.36%	WP_126712540.1
sulfotransferase [*Verrucosispora* sp. LHW63014]	7E-16	29.41%	WP_117229189.1
sulfotransferase [*Micromonospora pattaloongensis*]	9E-16	28.05%	WP_091555694.1
Sulfotransferase [*Oscillatoriales cyanobacterium* USR001]	1E-15	28.39%	OCR00877.1
sulfotransferase [*Pseudosporangium ferrugineum*]	2E-15	28.95%	WP_106129776.1
sulfotransferase [*Verrucosispora maris*]	2E-15	28.94%	WP_013732760.1
sulfotransferase [*Nitrospinae* bacterium RIFCSPLOWO2_12_FULL_45_22]	3E-15	29.60%	OGW14291.1
sulfotransferase family protein [*Oscillatoria acuminata*]	3E-15	29.66%	WP_015163246.1
sulfotransferase [*Verrucosispora* sp. ts21]	5E-15	28.94%	WP_102658466.1
sulfotransferase family protein [filamentous cyanobacterium Phorm 46]	6E-15	26.36%	WP_106146612.1
sulfotransferase [*Actinobacteria* bacterium]	8E-15	29.11%	PZM97189.1
sulfotransferase [*Micromonospora* sp. S4605]	9E-15	28.51%	WP_109901198.1
sulfotransferase [*Micromonospora* sp. CV4]	1E-14	28.51%	WP_121652652.1
sulfotransferase [*Actinoplanes* sp. N902-109]	1E-14	27.00%	WP_015624538.1
TPA: sulfotransferase [*Deltaproteobacteria* bacterium]	1E-14	27.73%	HFZ29463.1
sulfotransferase family protein [*Planktothrix rubescens*]	2E-14	28.75%	WP_043938333.1
heparan sulfate-glucosamine 3-sulfotransferase 3 protein [Marine Group I thaumarchaeote SCGC AAA799-P11]	4E-16	29.52%	KFM18792.1

Sulfate salt is abundant in seawater and is unsurprisingly broadly distributed in marine organisms. In the marine environment, a variety of sulfated compounds belonging to different classes such as terpenoids, alkaloids, carotenoids and steroids have been identified with most of the sulfated compounds being steroids. Sulfated steroids show a variety of activities ranging from antifungal, antibacterial and antitumor activity. Interestingly, bioactivity studies of desulfated analogues of some sulfated steroids e.g., minutoside A (Figure 4.3) resulted in loss of activity (Chludil et al., 2005; Carvalhal et al., 2018, Almeida et al., 2017), indicating the significance of sulfate groups with regard to bioactivity. Given that no antibacterial activity was observed when small molecules produced by *T. actiniarum* were screened (section 2.3.5), these potentially sulfated natural products, if expressed, may have other activities or may be masked by the presence of interfering compounds/inhibitors. These findings also emphasize the possibility of isolating potentially novel compounds.

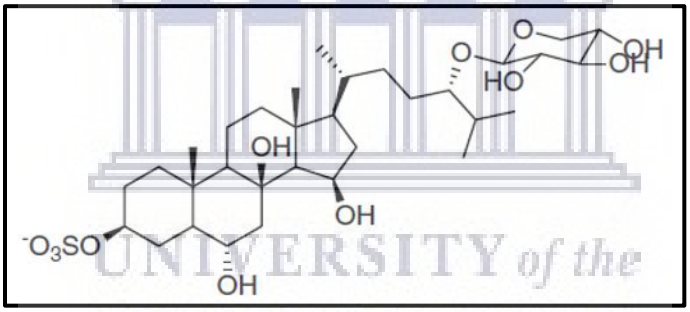

Figure 4.3: Minutoside A, a sulfated steroid that loses antifungal activity against *Aspergillus flavus* when desulfated, taken from Carvalhal et al., 2018.

antiSMASH predicted 10 potential bioactive secondary metabolite (small molecule) pathways encoded on the genome of *T. actiniarum*, which are expected to encode the production of small molecules. No antibacterial activity was observed in the <3kDa range using the well diffusion assay (section 2.3.5), suggesting that none of antiSMASH-predicted pathways, if expressed, produced antibacterial metabolites. Although many metabolites belonging to the classes of compounds predicted to be synthesized by *T. actiniarum* confer antibacterial activity (Chapter 1, section 1.3 and 1.4), there was no justifiable reason to expect that the metabolites should confer antibacterial activity. However, many studies have reported how prefractionation of crude cell free supernatant to a less complex extract assists in the removal of unwanted compounds, and in so

doing, concentrate potential bioactive compounds which are generally present in small amounts (Wagenaar, 2008; Appleton et al., 2007). Considering the genetic capacity of *T. actiniarum* to produce potentially novel secondary metabolites, we wanted to investigate whether chemically-dereplicated fractions would reveal any bioactivities that had been previously masked. Given the timing of the secondment to Marbio in Tromsø, we saw this as a perfect opportunity to assess this, due to the equipment and expertise available in their facility. This also provided the opportunity to subject the fractions to a range of other assays. This chapter investigates the antibacterial, anti-biofilm and anticancer potential of small molecules produced by *T. actiniarum* by employing an alternative isolation, fractionation and screening approach with the objective to structurally characterize active compound/s.

4.3.2 Extraction and prefractionation of secondary metabolites from *T. actiniarum* fermentation broth

Following strain cultivation, secondary metabolites were extracted with Diaion® HP-20 resin and the dry weight of the crude methanol extract was approximately 1500mg from a starting fermentation of 3L. The crude methanol extract was flash fractionated and resulted in 27 fractions that were pooled (Section 4.2.5, Table 4.2) to generate 6 working fractions. Table 4.16 shows the dry weight of Fractions 1 to 5. The concentration of Fraction 6 was too low to get an accurate weight measurement and was not considered for bioactivity assays but was included in the dereplication process.

Table 4.16: Weight of FLASH Fractions 1-6

Fraction	Weight (mg)
1	1189.6
2	208
3	143
4	95.93
5	9.98
6	-

4.3.3 Bioactivity screening of FLASH fractions

The sensitivity of the screening platform employed for bioactivity screening requires µg amounts of crude extract, thus even the lowest yield of 9.98 mg obtained for Fraction 5 (Table 4.16) was sufficient for the bioactivity screening process and all fractions 1-5 were subjected to bioassays. Following bioactivity screening, bioactivity was observed only from Fraction 5 in the anticancer, antibacterial and anti-biofilm assay. Therefore, only fraction 5 was used for further downstream processing. Antibacterial activity was observed from Fraction 5 against *S. aureus*, *E. faecalis* and *S. agalactiae* with an absorbance level of 0.04, just below the 0.05 cutoff value for active extracts. The sensitive strains are all Gram-positive suggesting that the active compound/s specifically target Gram-positive bacteria. Gram-positive bacterial cell walls are less complex than Gram-negative bacterial walls and are more permeable to antibiotics (Fischer and Braun, 1981) which may be why these bacteria are more sensitive. For biofilm inhibition, only Fraction 5 indicated activity based on an average optical density (OD) at 600nm of 0.08. Fractions that give an absorbance below 0.25 are considered active in this assay. Even though the assay is used to determine biofilm inhibition and the results appear positive (Figure 4.4, wells F4 and F5), the fraction inhibited bacterial growth altogether rather than biofilm formation. Since the test organism is *S. epidermidis*, a Gram-positive organism, this result is not unexpected due to the Gram-positive specific activity of the compound/s observed in the antibacterial assay. Due to the non-selectivity (biofilm inhibition as opposed to growth inhibition) of the result in the biofilm inhibition assay, this assay was not considered further.

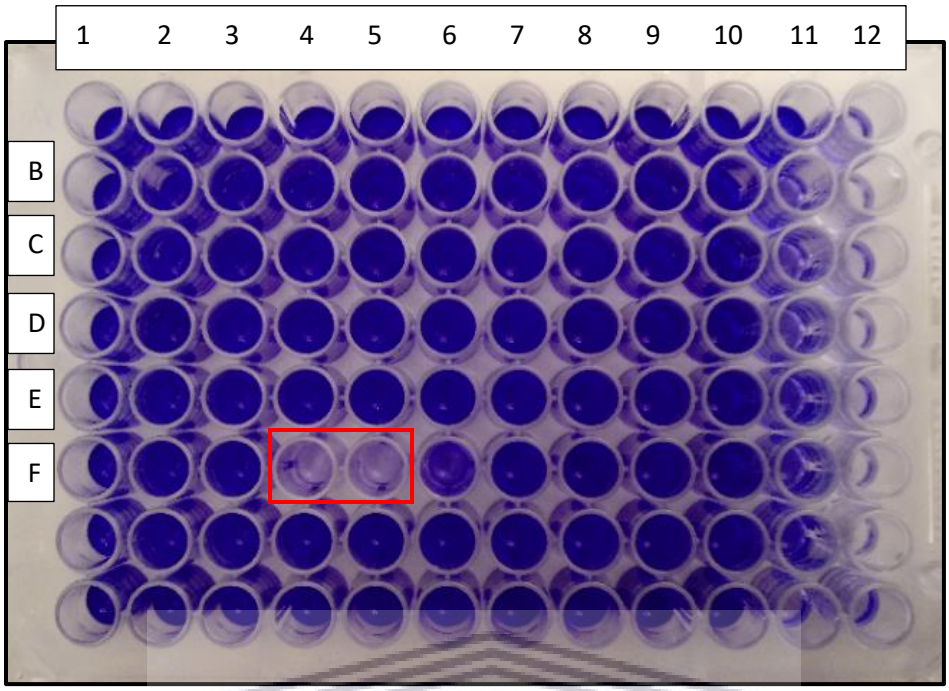

Figure 4.4: Biofilm inhibition assay results of Fractions 1 to 5. Each sample was tested in duplicate. The red rectangle shows inhibitory activity of Fraction 5 in wells F4 and F5. Fractions 1 to 4 are present in wells B4-5, C4-5, D4-5 and E4-5 respectively, exhibiting no activity.

All fractions were screened for anti-proliferative activity against the melanoma cell line A2058. Again, Fraction 5 showed activity against this cell line (Figure 4.5, wells B6, C6 and D6) with a cell survival lower than 50%.

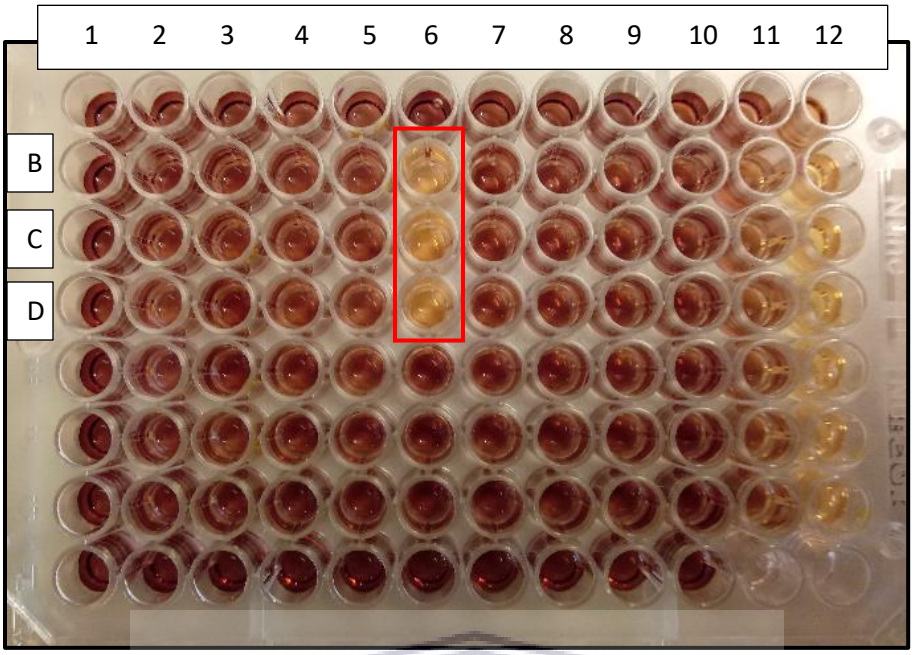

Figure 4.5: MTS cell proliferation assay of Fractions 1 to 5. Each sample tested in triplicate. The red rectangle indicates bioactivity exhibited from Fraction 5 in wells B-6, C-6 and D-6. Fraction 1: wells B-2, C-2, D-2; Fraction 2: wells B-3, C-3, D-3; Fraction 3: B-4, C-4, D-4 and Fraction 4: B-5, C-5, D-5 shows no activity against A2058.

Multiple activities from a single fraction could indicate that a single compound may be inhibiting growth in a non-specific fashion, or that the fraction contains more than 1 bioactive compound and these may or may not be acting synergistically.

This can however only be determined after compound isolation and purification. Prior to purification, the active fraction must be dereplicated primarily to ensure that known compounds are not being pursued. However, known compounds with new activities would also represent valuable discoveries for drug development, and is why a purely chemistry-based dereplication may result in the unnecessary discarding of valuable compounds for the treatment of new diseases or infections. A current example showcasing the significance of repurposing 'old drugs' through targeted screening is the use of hydroxychloroquine, an antimalarial drug with moderate antiviral activity against SARS-CoV-2, *in vitro* (White et al., 2020).

4.3.4 Dereplication of active fractions

Dereplication, especially when combined with screening data, is an important tool that aims to identify the compound(s) within the active fractions responsible for the observed bioactivity and

eliminate those that are known from the search. Isolation and structural elucidation can be very time and resource consuming, which is why effective and thorough dereplication is an important part of natural product drug discovery to avoid wasting time and resources on pursuing known compounds. In this study UHPLC-ESI-QToF-MS was used for dereplication.

Since activity was observed from Fraction 5 only in the antibacterial and anticancer assays, it was nominated for dereplication. For dereplication (Fraction 5) along with the inactive fractions eluted before (Fraction 4) and after (Fraction 6) the active fraction during the prefractionation step, were analysed. This was done to compare the compounds present in the active fraction and inactive fractions, and determine which compounds are present in the active fraction and absent in the inactive fraction. Alternatively, if compounds are present in both active and inactive fractions, to see if the concentration of these compounds are any higher in the active fraction compared to the inactive fraction. These compounds were then chosen as candidates responsible for bioactivity.

Figure 4.6 shows the Base Peak Intensity (BPI) chromatograms of inactive fractions (F4) and (F6) as well as active fraction (F5) analysed in ESI+ mode. In this chromatogram compound 7 (Table 4.17) with retention time 5.62 minutes and *m/z* of 355.2633 stood out as it is present in the active and inactive fractions but at much higher levels in the active fraction (Figure 4.6: Fraction 5). It was important to keep in mind that the concentration of Fraction 6 was too low to quantify and was not assessed in the bioactivity assays but was used in the dereplication process. Therefore, it was not possible to rule out that this fraction could contain an active compound and future studies aiming to investigate the bioactivity of this fraction will require larger scale fermentations. The peaks resolved in the active fraction 5 with retention times between 10.06 minutes and 12.11 minutes were not of interest since the compounds present here, predicted to be stearamides, erucamides and oleamides are common background contamination ions observed in mass spectrometry. These compounds are slip agents that are used in the production of polyethylene and polyethylene derivatives, commonly used laboratory plastics (Tran and Doucette, 2006; Guo et al., 2006).

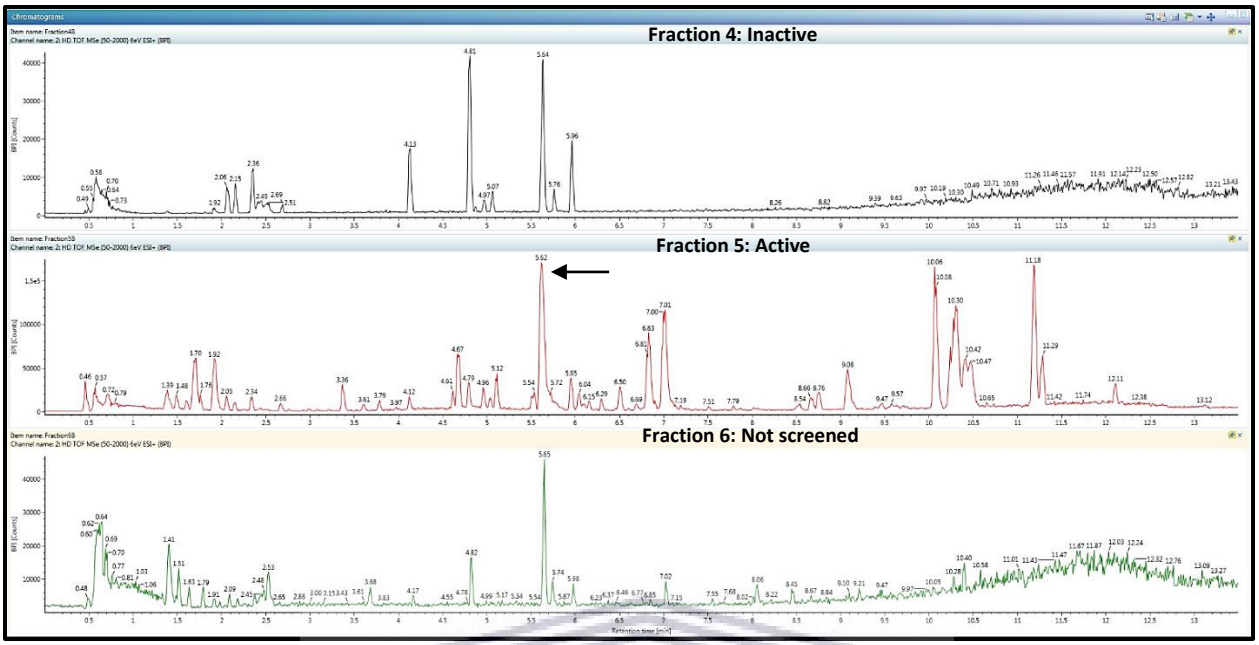

Figure 4.6: Comparison of BPI chromatograms ESI+ (*m/z* 50-2000) for inactive Fractions (4 and 6) and active Fractions (5). The arrow corresponds to compounds with retention time 5.62 minutes (*m/z* 355.2632).

While analyzing the peaks between retention times 4.37 minutes and 7.01 minutes of active Fraction 5, the elemental composition and *m/z* of these compounds appeared to be very similar indicating that these compounds may be related, Table 4.17. Compound 7 highlighted in blue in Table 4.17 was considered for isolation given that it was most abundant in the active fraction compared to the inactive fractions.

Table 4.17: Retention time, *m/z* ratio, predicted elemental composition and predicted structure of related compounds detected in active Fraction 5 analysed in ESI+ mode.

Compound	Retention time (minutes)	*m/z* $(M+H)^+$	Predicted elemental composition
1	4.3754	355.2628	C24H34O2
2	6.1580	355.2630	C24H34O2
3	6.5831	355.2631	C24H34O2
4	6.9593	355.2630	C24H34O2
5	6.6856	355.2631	C24H34O2
6	6.3023	355.2633	C24H34O2
7	5.6283	355.2633	C24H34O2
8	5.7238	357.2775	C24H36O2
9	7.0104	357.2787	C24H36O2
10	7.0065	357.2788	C24H36O2
11	6.8340	357.2791	C24H36O2
12	6.8292	357.2791	C24H36O2
13	6.0955	357.2797	C24H36O2

Notably, the fragment matches of compound 7, predicted through database searching revealed that this compound might be structurally similar to Mooloolabene A and B (Figure 4.7 and Figure 4.8).

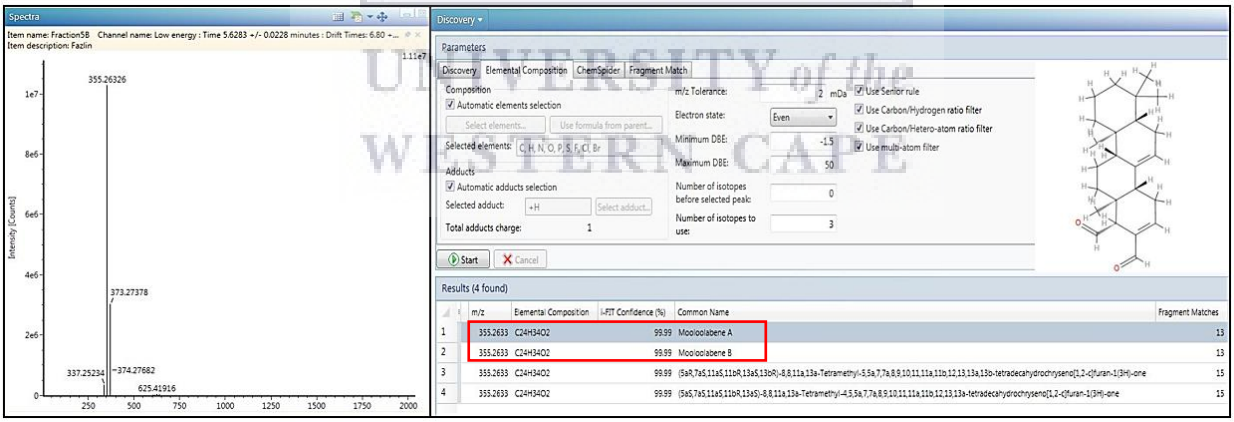

Figure 4.7: Predicted elemental composition, structure and identity of compound 7 (*m/z* 355.26) analysed in ESI+ mode.

Mooloolabene A and B (Figure 4.8) are scalarane norsesterpenes isolated from the sponge *Hyatella intesitinalis* with activity against the leukemia cell line p388 (Somerville et al., 2006). These compounds belong to the class scalarane sesterpenes and this compound class has been shown to

exhibit antibacterial and anticancer activities (Hassan et al., 2015; Evidente et al., 2015; González, 2010) and are not known to be produced by bacteria, making this a very interesting discovery.

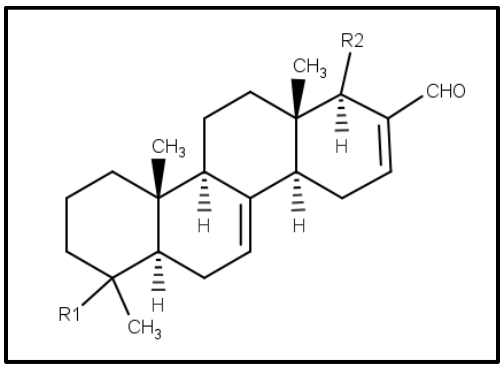

Figure 4.8: Structure of Mooloolabene A (R1: H and R2: β-CHO) and B (R1: H and R2: α-CHO) taken from Prasad, 2017.

To reduce the complexity of the spectrum, the sample was run in ESI- mode. ESI-LC-MS is almost always used in positive mode because most compounds are expected to ionize well in this mode. However, one of the major advantages of ESI- is a reduction in background noise. In a paper by Liigand et al. (2017) the authors showed that from analyzing 33 compounds in both ESI+ and ESI- modes, 46% of the compounds ionized better in ESI- mode, 18% ionized better in ESI+ mode and 36% of the compounds ionized well in both modes. Therefore due to different ionizations, compounds should be analysed in both modes in order to establish the best ionization mode for a specific analyte and so doing increase the ionization efficiency and resolution. Figure 4.9 shows the BPI chromatogram of Fractions 4, 5 and 6 analysed in ESI- mode with the arrow indicating the retention time of compound 7 in ESI- mode as well as the predicted elemental composition, *m/z* of the compound (Table 4.18). Using the elemental composition and *m/z*, a database search against the PubChem database revealed that the compound is likely cholic acid, and not a mooloolabene as initially proposed.

Figure 4.9: Comparison of BPI chromatograms ESI- (*m/z* 50-2000) for inactive Fractions (4 and 6) and active Fractions (5). The arrows indicate compounds with retention times 5.64 (*m/z* 407.2633)

Table 4.18: Retention time, *m/z*, predicted elemental composition and predicted structure for target compound *m/z* 407 in active Fraction 5 analysed in ESI- mode.

Retention time	*m/z* $(M-H)^-/(2M-H)^-$	Predicted elemental composition	Predicted compound
5.64	407.2727 / 815.56	$C_{24}H_{40}O_5$	Cholic acid

Interestingly, the *m/z* of compound 7 in ESI- mode represents a mass increase of 54 mass units from *m/z* 355 detected in ESI+ mode. This mass shift correlates to the loss of three water molecules. The detection of steroids even when using soft ionization techniques such as ESI is

difficult because these molecules tend to lose up to three water molecules, sometimes less, during positive ionization (Kuuranne and Vahermo, 2000; Li et al., 2006). This has been shown for the steroid 5 β-tetrahydrocortisol (*m/z* 366.5), losing up to three water molecules after ESI+ MS, (Figure 4.10).

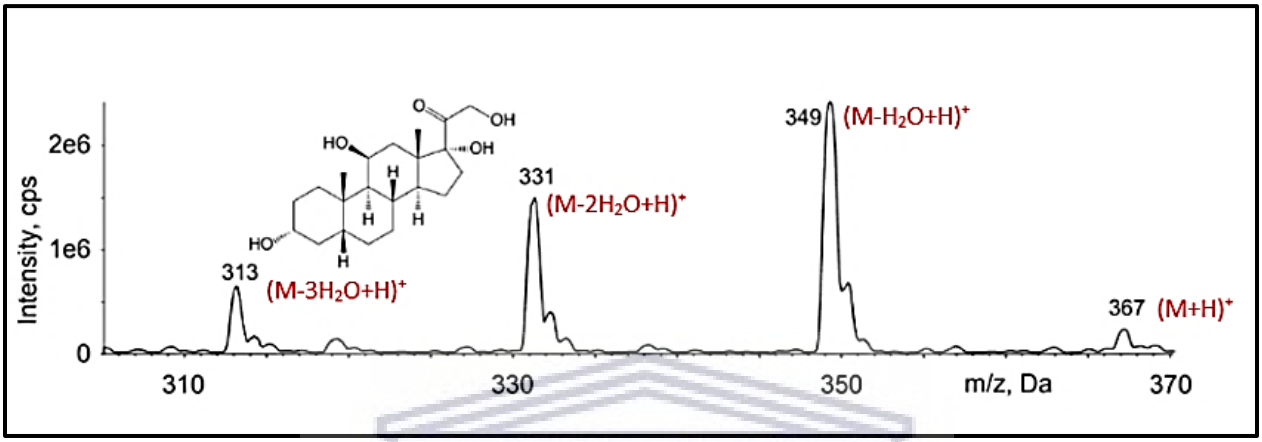

Figure 4.10: Mass spectrum of 5β-tetrahydrocortisol showing loss of water molecules during ESI+, adapted from Saba et al., 2018.

These results suggest that cholic acid, with *m/z* 407 lost three water molecules during ESI+, resulting in compound *m/z* 355. This compound was misidentified as Mooloolabene A and B due to the number of fragment matches between the two compounds and is not surprising given their similar structures. This result shows the importance of analyzing compounds in both positive and negative ionization modes, further proving that MS alone cannot be used to determine compound structures.

Although a known antibacterial compound, we proceeded to isolate cholic acid based on the predicted *m/z* generated from UHPLC-HR-QToF-MS analysed in ESI- mode, given that it has not been reported for this bacterium, and that it may demonstrate new activities.

4.3.5 Mass guided isolation of candidate compounds

In drug discovery, isolation of new chemical entities is an important step for further downstream processing such as characterization and confirmation of bioactivity. Typically, the target compounds are present in very low concentrations in a mixture of other unwanted components. Isolation of these pure compounds is not an easy task and is considered to be one of the bottlenecks

in drug discovery. In most cases the challenges are associated with low quantities of target compounds and loss of activity after isolation.

In this study, purification of target compounds by Preparative and Mass guided High-Performance Liquid Chromatography with an Xterra RP C18 column was used with elution gradients described in Table 4.11. Cholic acid was isolated by mass and the mass used was that identified following HR-ESI-MS. The initial purification of Fraction 5 resulted in 40 fractions collected based on time. Fraction 15 (*m/z* 815.56) (indicated in yellow in Figure 4.11) was collected for further processing since these fractions contained the target compound with *m/z* 815. Notably, compound 407 $(M-H)^-$ was not detected on the chromatogram but the dimer 815 $(2M-H)^-$ was observed and selected for isolation.

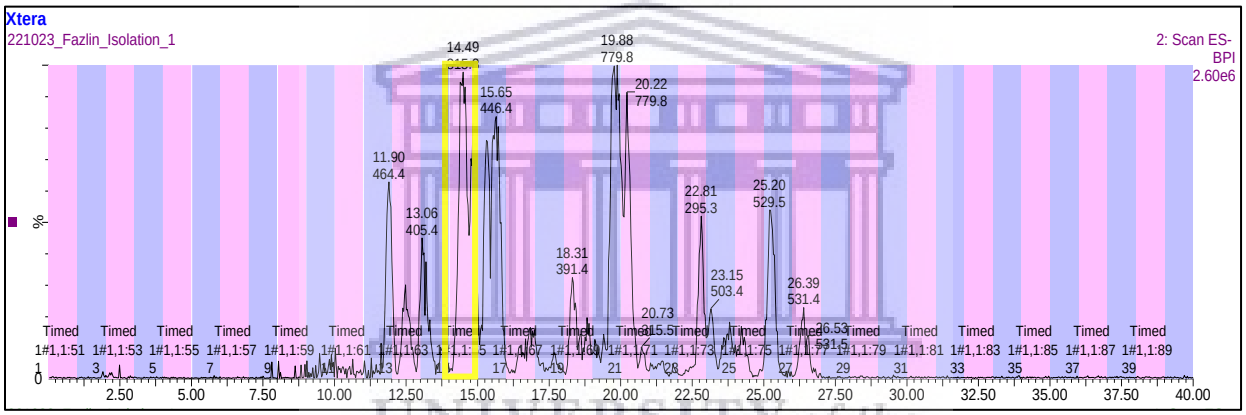

Figure 4.11: BPI chromatogram from the initial isolation of compounds 407 from Fraction 5 separated over a Xterra RP C18 column using mass as fraction triggers.

A single purification step is rarely sufficient for obtaining a pure active compound from a crude extract. Normally, when a compound of interest is subjected to a second HPLC purification step, columns with stationary phases different from the initial HPLC column are useful. In this study, the second purification step was done by using a fluorophenyl HPLC column.

Using mass spectrometry (MS) to trigger collection of the compounds eluting from an HPLC column, is known as mass guided fractionation. Mass guided prep-HPLC fractionation is a powerful tool, as it combines the high separation efficiency of the HPLC with the convenience of triggering the fraction collector at the presence of defined masses. Further purification of Fractions

15 was conducted using a fluorophenyl column, and the BPI chromatogram is depicted in Figure 4.12.

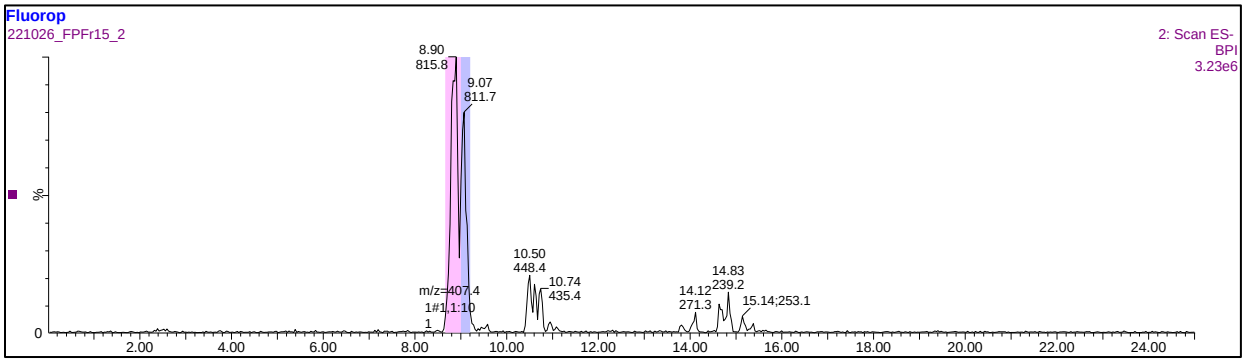

Figure 4.12: BPI chromatogram from the second isolation of compound 407 (dimer 815.8) and 405 (dimer 811.7) separated over a RP fluorophenyl HPLC column using mass as a fraction trigger.

The chromatogram above shows Fraction 15 separated on a fluorophenyl column. The pink peak represents compound *m/z* 407/815 and was isolated based on a set mass trigger. The blue peak next to it shows a compound with *m/z* of 405 and a similar retention time to that of compound 407. These compounds were difficult to separate as indicated by the formation of a split peak and both compounds were isolated. Following isolation, HR-MS was conducted to check compound purity and Figure 4.13 and Figure 4.14 show the isotope pattern for compounds 407 and 405 respectively, following isolation and HR-MS.

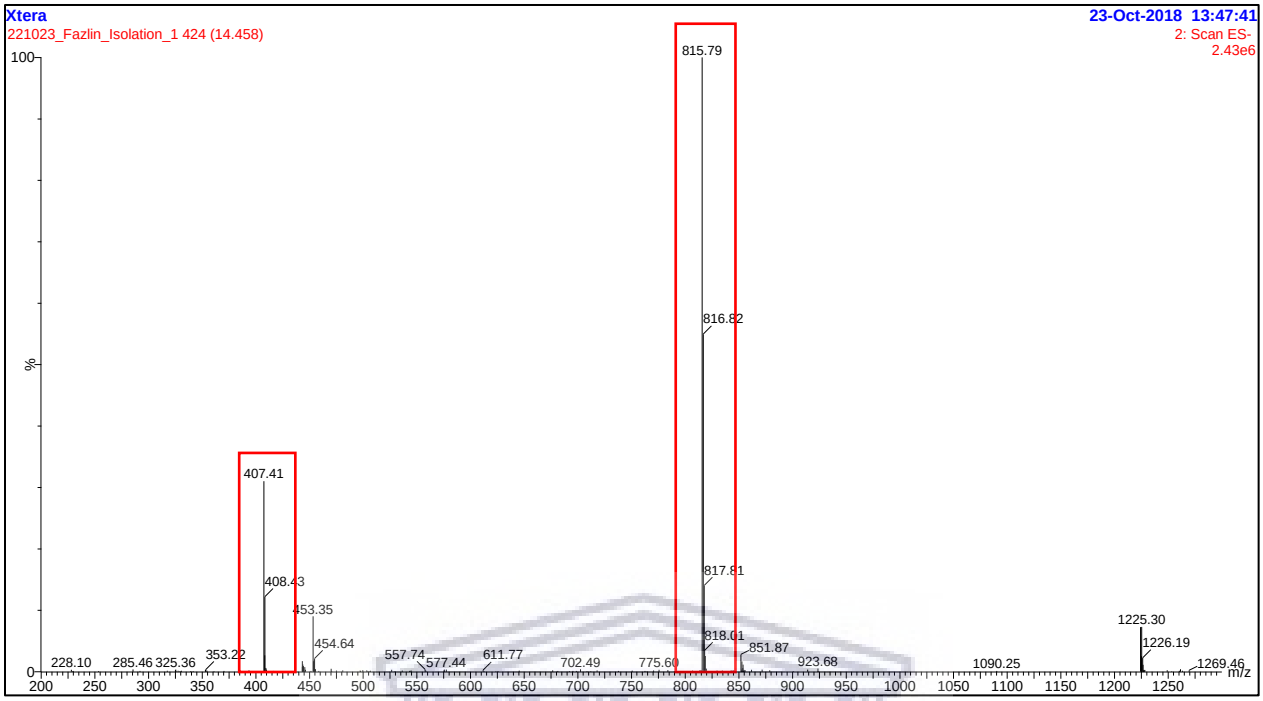

Figure 4.13: Isotope pattern of compound 407

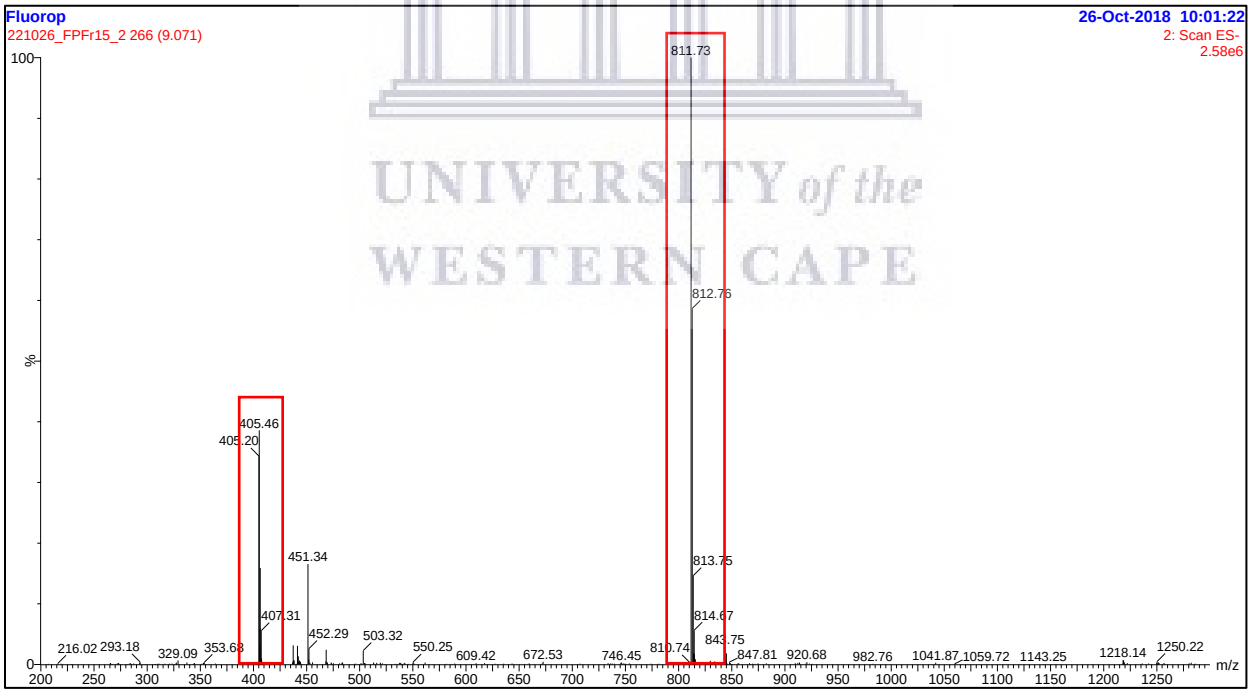

Figure 4.14: Isotope pattern of

The isotope pattern of compound 405 shows that compound 407 was present at very low abundance, confirming a mixture of the two compounds. The minor component which in this case was compound 407, shows up as smaller peaks in the spectrum with fewer molecules present and evidently less protons will be absorbed in the NMR spectrum. Given the relative purity of the compounds we proceeded with NMR based structural elucidation of both compounds 405 and 407.

For compounds 407 and 405 the isotope patterns indicate the presence of a main molecular ion $[M-H]^-$ as well as a dimer with molecular formula $[2M - H]^-$. The tendency for dimer formation is increased with analyte concentration and is a common occurrence in soft ionization techniques (De Vijlder et al., 2017, Kruve and Kaupmees, 2017). The compounds were relatively pure and structural elucidation of compound 407 (1mg) predicted to be cholic acid and compound 405 (0.3mg) was pursued using NMR.

4.3.6 Structural Elucidation and bioactivity of compounds 407 and 405

Structure elucidation represents another major bottleneck in natural product drug discovery. NMR spectrometry is an essential tool for the structural characterization of natural products (Urban and Dias, 2013). This spectroscopic technique provides the information necessary to elucidate the structure of a compound by identifying the number and position of carbon and hydrogen atoms in a molecule. One of the major challenges associated with structural elucidation of natural products is concentration and stability of the pure compound (Urban and Dias, 2013).

Compounds 407 and 405 were isolated as a white powder. Compound 407 had the molecular formula $C_{24}H_{40}O_5$ based on HR-QToF-MS analysis while compound 405 had a molecular formula of $C_{24}H_{38}O_5$. The ^1H and ^{13}C-NMR data for compound 407 (Table 4.19), and 405 (Table 4.20) confirmed that 24 carbons and 40 hydrogens are present in compound 407; and 24 carbons and 38 hydrogens are present in compound 405. Analysis of the 2D NMR data established that both compounds have a C-24 steroidal structure and that they are structurally similar. The ^1H-NMR spectrum for compound 407 showed a C3-OH signal recorded at 3.35ppm which is absent in compound 405. The remaining NMR data for compound 407 corresponded well to that of compound 405. Further evaluation of HSQC, HMBC and H2BC spectra of compound 407 were

consistent with that of compound 405, confirming their identical steroidal structures (Appendices 4A-4G (cholic acid) and 4H-4L (3-oxo cholic acid).

Table 4.19: ^{1}H and ^{13}C-NMR data for cholic acid in acetonitrile-d_3

Cholic acid (compound 407)			
Position	**δ_C, Type**	**δ_H, (J in Hz)**	**δ_{OH} (J in Hz)**
1	35.98, CH2	0.90 (d, *J* = 6.5 Hz, 3H),	
2	30.62, CH2	1.32 (ddd, *J* = 15.9, 9.8, 6.4 Hz, 1H)	
3	72.22, CH	3.32 (tt, *J* = 11.2, 4.4 Hz, 1H),	3.35
4	39.78, CH2	2.05 (td, *J* = 13.2, 11.6 Hz, 1H),	
5	42.34, CH	1.88 (ddd, *J* = 14.6, 5.6, 3.4 Hz, 1H),	
6	35.44, CH2	1.43 (dt, *J* = 14.8, 2.2 Hz, 1H),	
7	68.85, CH	3.74 (q, *J* = 3.0 Hz, 1H),	3.77
8	40.23, C		
9	27.26, CH	2.09 (ddt, *J* = 35.0, 17.8, 5.6 Hz, 1H),	
10	35.18, C		
11	28.81, CH2	1.52 (tdd, *J* = 12.4, 10.1, 2.9 Hz, 3H),	
12	73.58, CH	3.90 (t, *J* = 3.0 Hz, 1H),	3.92
13	47.05, C		
14	42.48, CH	1.25 (tdd, *J* = 14.6, 5.6, 3.4 Hz, 1H),	
15	23.87, CH2	1.03 (qd, *J* = 12.0, 6.1 Hz, 1H),	
16	28.19, CH2	1.23 (tdd, *J* = 12.4, 10.1, 2.9 Hz, 3H),	
17	47.52, CH	1.72 (q, *J* = 7.4 Hz)	
18	22.86,CH3	0.84 (s, 3H),	
19	12.81, CH3	0.63 (s, 3H),	
20	17.56, CH3	0.92 (d, *J* = 6.5 Hz, 3H),	
21	36.17, CH2	1.37 (q, *J* = 7.1 Hz)	
22	31.76, CH2	1.31 (tdd, *J* = 12.4, 9.8, 2.6 Hz, 3H),	
23	31.68, CH2	2.31 (ddd, *J* = 15.5, 10.2, 5.1 Hz, 1H),	
24	177.87, C		

Table 4.20: ^{1}H and ^{13}C-NMR data for 3-oxo cholic acid in acetonitrile-d_3

3-oxo cholic acid (compound 405)			
Position	**δ_C, Type**	**δ_H, (J in Hz)**	**δ_{OH} (J in Hz)**
1	36.51, CH2	1.37 (td, *J* = 13.2, 11.2 Hz, 3H),	
2	36.52, CH2	2.10 (ddd, *J* = 15.9, 9.8, 6.4 Hz, 1H)	
3	212.05, C		
4	45.36, CH2	2.07 (dt, *J* = 14.2, 5.6 , 3.4 Hz,1H),	
5	43.33, CH	1.75 (ddd, *J* = 14.2, 5.2, 3.0 Hz, 1H),	
6	33.70, CH2	1.52 (dt, *J* = 14.6, 2.2 Hz, 1H),	
7	67.46, CH	3.81 (t, *J* = 3.0 Hz, 1H),	3.77
8	39.55, C		
9	27.01, CH	2.33 (ddt, *J* = 35.0, 17.8, 5.6 Hz, 1H),	
10	34.73, C		
11	28.70, CH2	1.62 (tdd, *J* = 12.4, 10.1, 2.9 Hz, 3H)	
12	72.05, CH	3.97 (t, *J* = 3.0 Hz, 1H),	3.94
13	46.26, C		
14	41.71, CH	1.87 ((tdd, *J* = 14.6, 5.6, 3.4 Hz, 1H)	
15	22.83CH2	1.10 (qd, *J* = 12.0, 6.1 Hz, 1H),	
16	27.24, CH2	1.32 (tdd, *J* = 12.2, 10.2, 3.4 Hz, 3H),	
17	46.72, CH	1.78 (d, J=6.5)	
18	21.12, CH3	1.01 (s, 3H),	
19	11.92, CH3	0.54 (s, 3H),	
20	16.60,CH3	0.59 (d, *J* = 6.5 Hz, 3H),	
21	35.20, CH2	1.42 (tdd, *J* = 12.4, 9.8, 2.6 Hz, 3H),	
22	30.82, CH2	1.34 (ddd, *J* = 15.5, 10.2, 5.1 Hz, 1H),	
23	30.27, CH2	2.23 (ddd, *J* = 15.5, 10.2, 5.1 Hz, 1H),	
24	174.61, C		

Compounds 407 and 405 were identified based on molecular formula and structural homology as the bile acids cholic acid and 3-oxo cholic acid respectively, using PubChem (Figure 4.15A and Figure 4.15B)

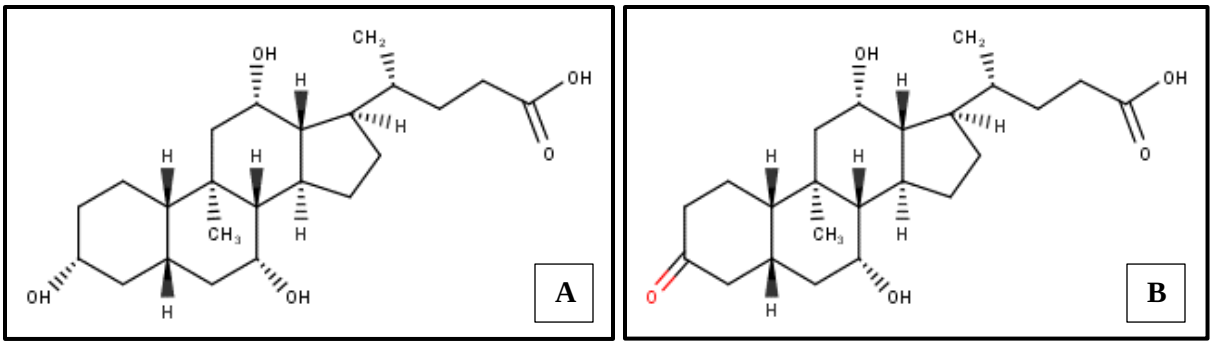

Figure 4.15A and B. Compound 407 (A) with elemental composition $C_{24}H_{40}O_5$ and compound 405 (B) with elemental composition $C_{24}H_{38}O_5$.

The first report on bile acid production from prokaryotes was published by Maneerat et al. (2005). The marine bacterial *Myroides* strain SMI isolated from seawater was investigated for its biosurfactant producing ability. When cultured in marine broth (BD Difco™), the organism produced surface active compounds that were identified as cholic acid, deoxycholic acid and their glycine-conjugated forms. A media control of marine broth was also screened through thin layer chromatography. No bile acids were detected in the media control confirming that the strain produced these bile acids *de novo* and that these bile acids are not part of the components present in marine broth (BD Difco™).

Two years later, Dockyu et al. (2007) reported the isolation of bile acids from several marine bacteria isolated from seawater in Dokdo, Korea. All strains were able to produce at least 3 bile acids including conjugated forms, Table 4.21. The authors make mention that the compounds were bioactive but no bioactivity data was reported in the paper.

Table 4.21: Bile acid producing marine bacteria

Strain	Cholic acid	Deoxycholic acid	Glycholic acid	Glyco-deoxycholic acid
***Dokdonia donghaensis* DSW-1**	✓	✓	✓	ND
***Polaribacter dokdonensis* DSW-5**	✓	✓	✓	✓
***Donghaeana dokdonensis* DSW-6**	✓	✓	✓	✓
***Maribacter dokdonensis* DSW-8**	✓	✓	✓	✓
***Hahella chejuensis* KCTC 2396**	✓	✓	✓	✓
***Rhodococcus marinonascens* sp. DSM 43752**	✓	ND	✓	✓
***Rhodococcus* sp. DK17**	ND	ND	ND	ND

'✓' indicates present and ND indicates not detected

In 2012, Kim and co-workers also isolated two new cholic acid derivatives, Figure 4.16, from the marine bacterium *Hasllibacter halocynthiae* strain KME 002[T] a symbiont of the marine ascidian *Halocynthia roretzi.*

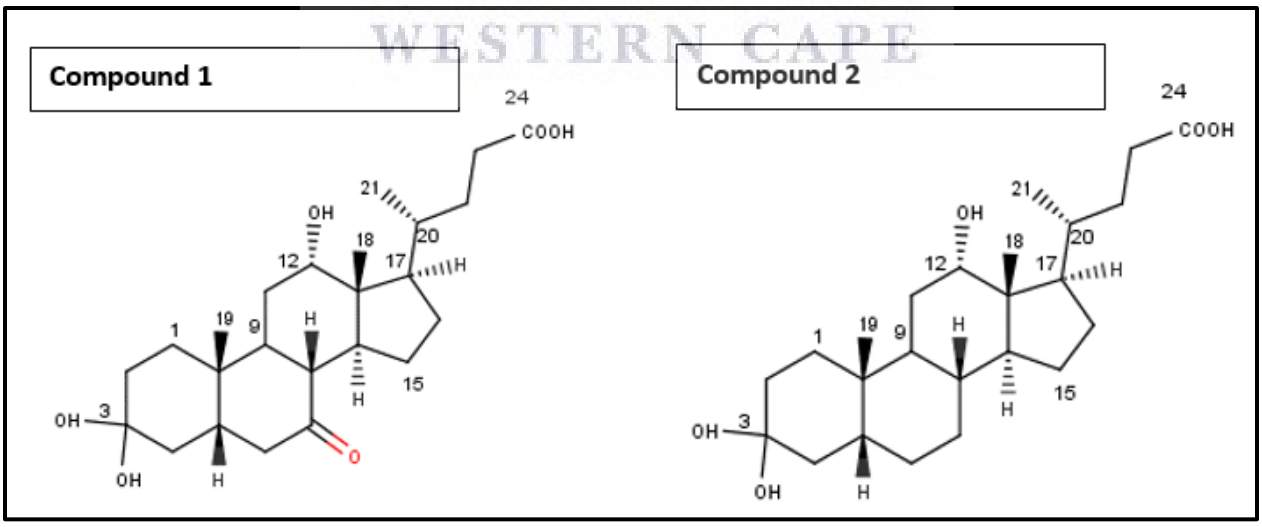

Figure 4.16: Compound 1: 3, 3, 12-trihydroxy-7-ketocholanic acid and Compound 2: 3,3,12-trihydroxy-7-deoxycholanic acid.

More and more bile acids and their derivatives are being isolated from bacteria that are not taxonomically related, indicating that the production of these compounds may be wider spread than expected.

To determine whether the isolated bile acids cholic acid and 3-oxo cholic acid were responsible for the observed antibacterial and anticancer activity in the initial screening process, bioassays were conducted as described in section 4.2.6 using concentrations between 5µg-100µg/ml. The antibacterial assay results are depicted in Figure 4.17 for 3-oxo cholic acid and Figure 4.18 for cholic acid.

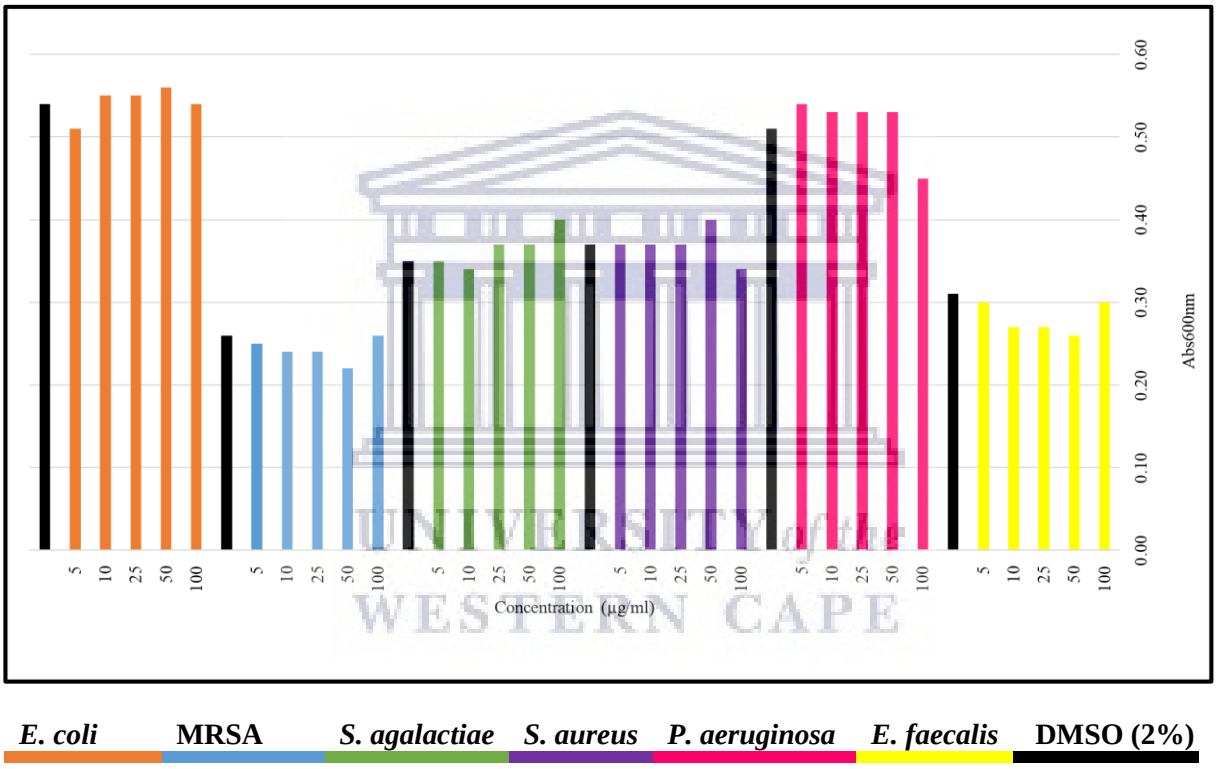

Figure 4.17: Antibacterial activity of 3-oxo cholic acid against 6 test strains. Coloured bars represent OD_{600} of the test strains following treatment with 3-oxo cholic acid at different concentrations. Black bars represent the DMSO control screened at a concentration of 2% (v/v).

Compared to the DMSO control, 3-oxo cholic acid did not show any significant inhibition of the test strains. Furthermore, as described previously, the antibacterial assay results are interpreted using cut off values that determine which compounds are active, inactive or questionable. Based on the bioassay data, the OD_{600} of the test organisms following treatment with 3-oxo cholic acid

was not less than 0.05 as desired by the platform to score a positive hit, suggesting that the compound was inactive and was not responsible for the observed antibacterial activity in Fraction 5 in the initial screening process (section 4.3.3).

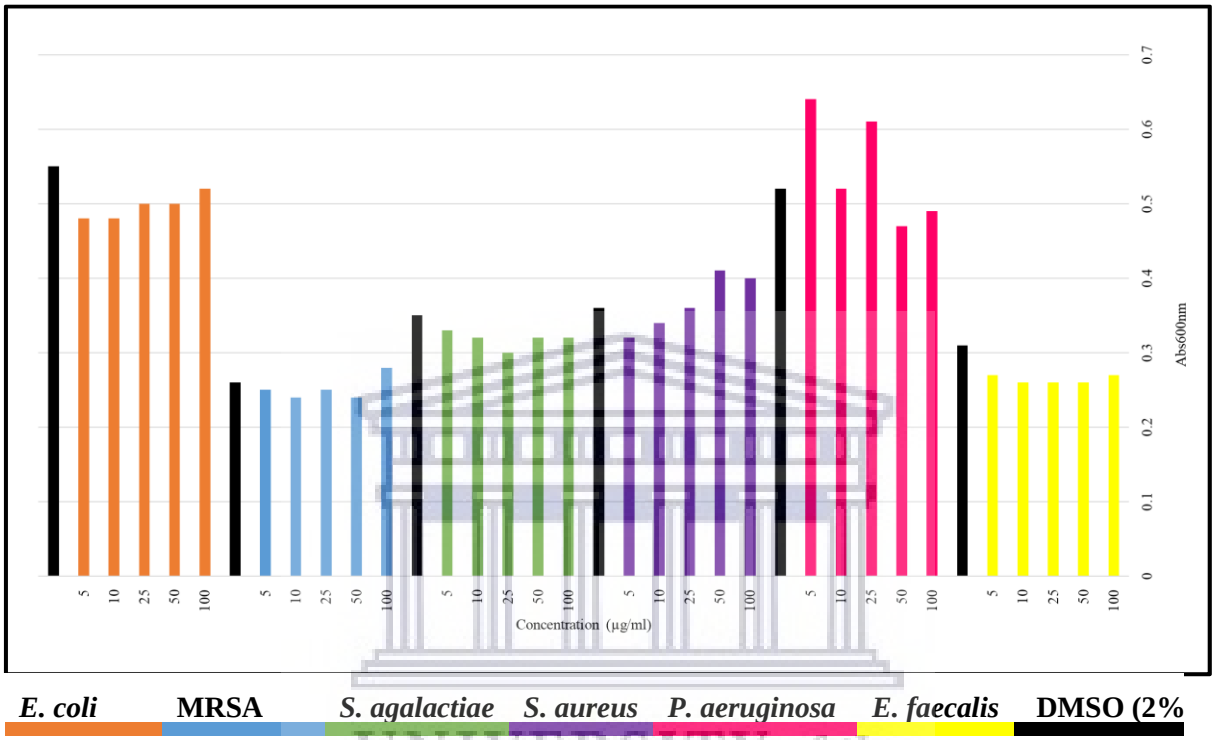

Figure 4.18: Antibacterial activity of cholic acid against 6 test strains.

Compared to the DMSO control, cholic acid did not show any significant inhibition of the test strain and again, an OD less than 0.05 as desired by the platform for active compounds was not observed. These results suggest that cholic acid was not responsible for the observed antibacterial activity in Fraction 5 in the initial screening stages.

Cholic acid and 3-oxo cholic acid was also screened for anticancer activity and the results are depicted in Figure 4.19 for 3-oxo cholic acid and Figure 4.20 for cholic acid.

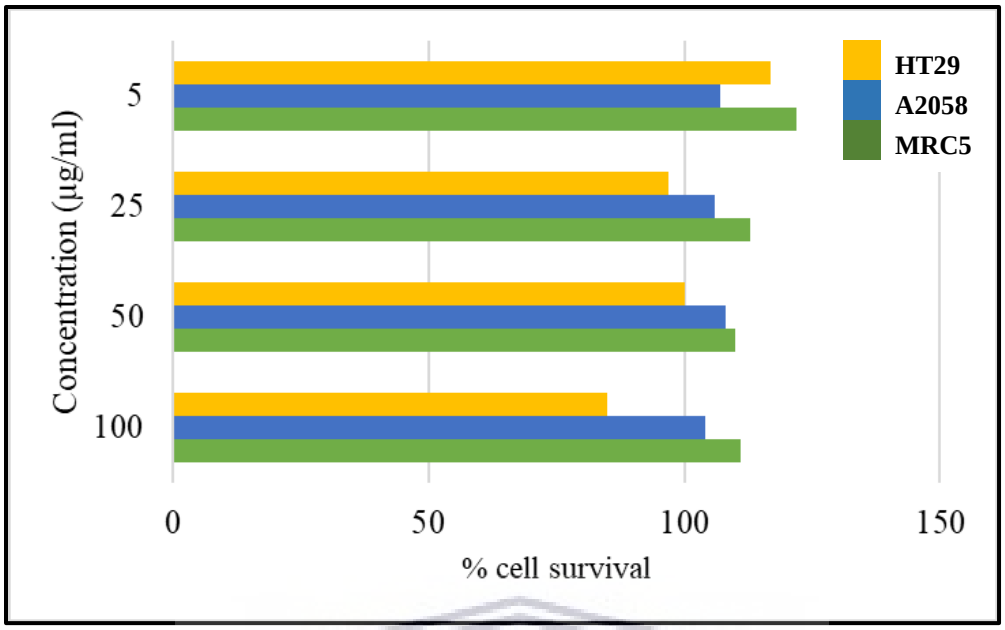

Figure 4.19: Anticancer activity of 3-oxo cholic acid against cancer cell lines HT29, A2058 and MRC5.

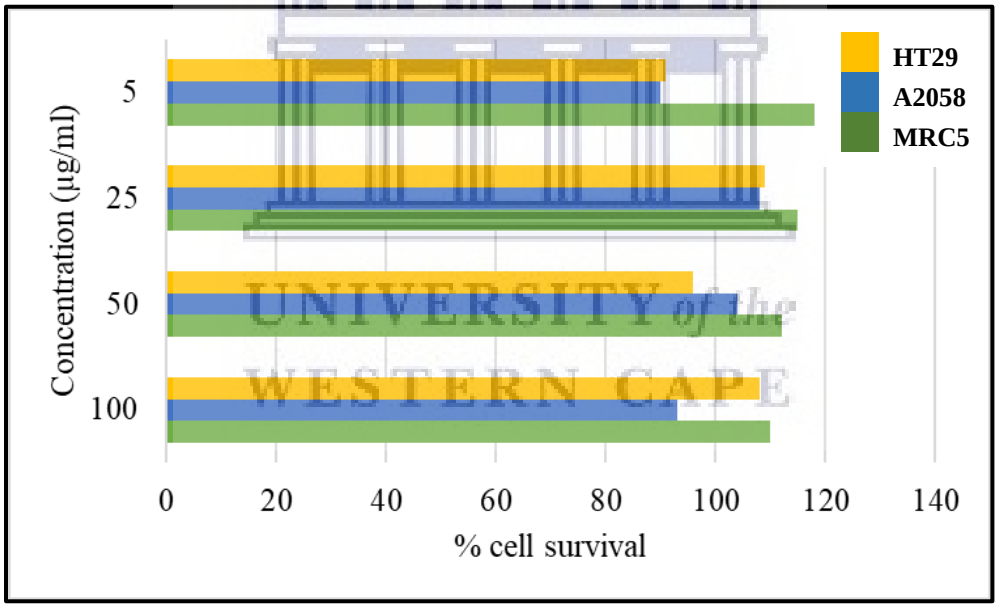

Figure 4.20: Anticancer activity of cholic acid against cancer cell lines HT29, A2058 and MRC5.

As depicted in Figure 4.19 and Figure 4.20, 3-oxo cholic acid and cholic did not show any anticancer activity as seen by the % cell survival greater than 50% for all cell lines screened against. This suggests that these compounds were not responsible for the observed anticancer activity in the initial stages of screening. Loss of or decreased bioactivity following purification is

a common phenomenon. This can be as a result of compound degradation, incorrect identification of the active compound or the separation of compounds that may be acting synergistically.

In humans, the antibacterial nature of bile acids play a role in intestinal homeostasis by controlling the intestinal microflora (Urdaneta and Casadesus, 2017). Gram-positive bacteria are inherently more sensitive to bile acids as a result of their membrane composition. Gram-positive bacteria have a membrane barrier that is relatively easy to penetrate, enabling many types of antibiotics to easily cross this membrane into the cell. Gram-negative bacteria on the other hand have a double membrane along with a variety of efflux pumps that expel drugs from the cell, making it difficult to design new antibiotics that target Gram-negative pathogens. The outer membrane of Gram-negative bacteria is also a potent barrier against bile acids. The lipopolysaccharide in the membrane plays a big role in conferring resistance to the bile acids (Begley et al., 2005; Kus et al., 2011; Prouty et al., 2002). The outer membrane of Gram- negative bacteria acts as a barrier through which permeability is slowed down or prevented. Molecules that pass through make use of porins to do so. Gram-negative bacteria are capable of altering these porins to prevent bile acids from entering (Begley et al., 2005). The Gram-positive bile resistant bacterium *Salmonella typhimurium* is able to remove bile acids by means of multidrug efflux pumps. A *tol* gene mutation in 3 bile sensitive *S. typhimurium* strains has been observed and these mutations affect membrane stability, allowing bile salts to access the cell (Prouty et al., 2002). Owing to the Gram-positive specific activity observed in the primary screening process and the increased sensitivity of Gram-positive bacteria to bile acids, the results showing that these bile acids were not responsible for the observed antibacterial activity was unexpected. However, factors such as concentration and whether the active compound may be working synergistically with another are to be considered.

In literature, the effect of bile acids on bacteria is typically determined by investigating cell membrane integrity (Watanabe et al., 2017; Sannassiddappa et al., 2017). One of the major factors affecting the action of bile acids on bacterial cell membranes is concentration. High concentrations of bile acids can swiftly dissolve membrane lipids (due to their detergent-like properties) and cause leakage of cell contents and eventually cell death. Low concentrations of bile acids may affect cell membranes in a more delicate way which does not necessarily cause cell lysis. At these sub-micellar concentrations, the chemical properties of the cell surface may be affected such as its hydrophobicity (Begley et al., 2005). In a paper by Sannasiddappa et al (2017), the bioactivity of

cholic acid and deoxycholic acid against *S. aureus*, a common intestinal commensal was assessed. The results indicated that cholic acid and deoxycholic at concentrations of 20mM and 1mM respectively, caused bacterial membrane disruption and leakage of cell contents. This suggests that an increased concentration of cholic acid in the antibacterial assay in this study may have been required to show activity given that the concentration used in this study was only 0.245mM compared to 1mM used by Sannasiddappa et al. (2017).

The antibacterial and anticancer activity of bile acids and their derivatives have been investigated and have shown promising results. In search of new bioactive compounds, Li et al. (2009), investigated the antimicrobial potential of a marine sponge symbiont *Psychrobacter* sp. A total of 7 bile acid derivatives were isolated (Figure 4.21). Compounds 2, 3, 4, 5 and 7 showed antibacterial activity and the same compounds also showed cytotoxic activity against solid tumor cell lines. Compound 6 showed no antibacterial or anticancer activity and happens to be identical to the 3-oxo cholic acid isolated in this study. In this study 3-oxo cholic did not show any bioactivity against the cancer lines A2058, MRC5 and HT29 nor did it show significant antibacterial activity confirming the results obtained by Li et al. (2009). In their study, the concentration used to screen 3-oxo cholic was 30µg/ml for antibacterial activity and >30µg/ml for anticancer activity. In this study, the highest concentration used to screen 3-oxo cholic acid was 100µg/ml for both antibacterial and anticancer activity, more than 3 times higher than the concentration used by Li et al., suggesting that concentration was likely not a factor affecting the activity.

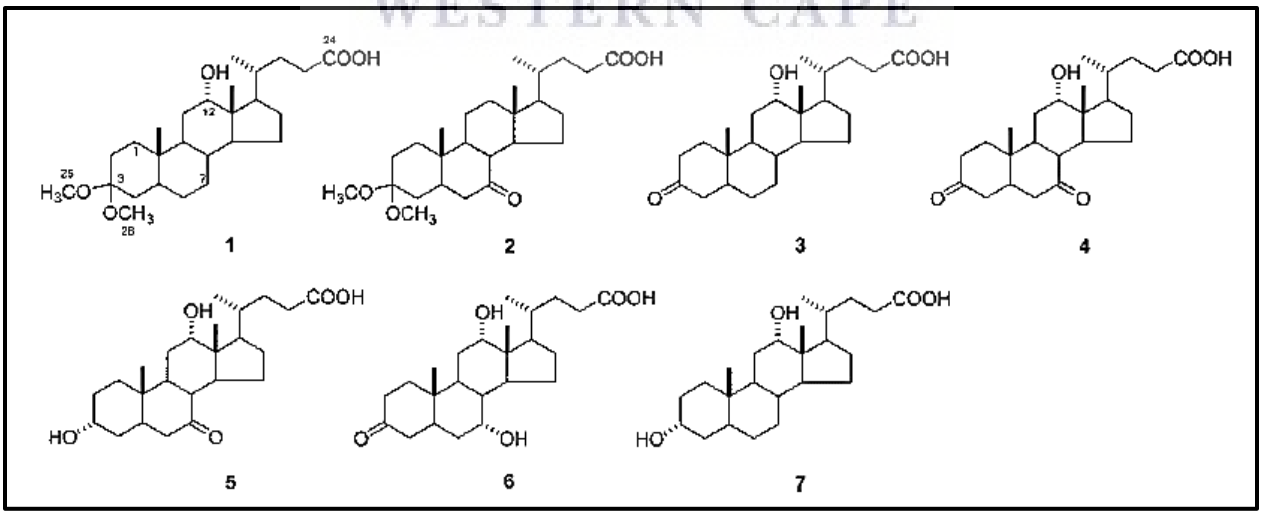

Figure 4.21: Bile acid derivatives isolated from the symbiont *Psychrobater* sp.

Furthermore, bile acids have been proven to be successful drug carriers aiding in the reduction of compound toxicity and improving selectivity. In a study conducted in 2010 by Darkoh et al., the antibacterial effect of the antibiotic rifamixin against Enterotoxigenic *E. coli* (ETEC) was improved in the presence of cholic acid. The authors conclude that the improved effect may be due to the bile acids increasing the solubility of the drug. They also do not exclude the possibility that the bile acids may be affecting the cell membranes directly, allowing the antibiotic to access the cell without difficulty. In 2014, Li et al. investigated the activity of camptothecin (CPT) by introducing bile acids (cholic acid, deoxycholic acid, ursodeoxycholic acid and chenodeoxycholic acid) to the CPT structure at C20 or C10 positions using different linker chains. CPT is a potent anticancer and antibacterial alkaloid that has been eliminated from clinical trials due to poor specificity and cytotoxicity. They generated 16 CPT-bile acid analogues and activity was tested *in vivo* and *in vitro*. *In vivo*, the CPT-bile acid analogue G4 (Camptothecin-20 (S)-O-acetate-[N-(3′α, 7′α-dihydroxy-24′-carbonyl-5′β-cholane)] showed the best antitumor activity. Compounds E2 (Camptothecin-20 (S)-O-glycine Ester-[N-(3′α,12′α-dihydroxy-24′-carbonyl-5′β-cholane)] and G4 showed better inhibition of the cancer cells than CPT alone. By introducing appropriate bile groups to the C20 position of CPT, enhanced selectivity and reduced cytotoxicity was observed, showcasing the ability of bile groups to act as drug carriers. This was also shown by Sreekanth et al. (2013) where the authors demonstrate that cholic acid-tamoxifen conjugates show superior anticancer activity compared to tamoxifen alone.

In this study, we cannot rule out the fact that the bile acids isolated may have acted as drug carriers or worked synergistically with other antibacterial or anticancer compounds and in so doing showed bioactivity in the initial screening stage. This hypothesis was further validated by the fact that the target compounds in this study were selected based on the *m/z* and database hits obtained from HR-QToF-MS and not necessarily by bioassay guided isolation. Since the HPLC fractions generated during the semi-purification process were not tested for activity, the active compound/s may have been present in one of the other fractions. As depicted in the BPI chromatogram of active fraction 5 between retention time 7.5 minutes and 12 minutes (Figure 4.6) and 7.5 minutes and 11minutes (Figure 4.9) many compounds present in this active fraction and absent in the inactive fractions were not investigated and we therefore cannot rule out the fact that the active compound may have been incorrectly identified.

Future studies could involve increasing the concentration of the compounds used in the bioassay to determine if activity is concentration dependent. Furthermore, the HPLC fractions not assayed could be screened to determine whether the active compound/s may be present in these fractions. Additionally, the isolated bile acids could be screened in combination to establish whether these compounds may have been working synergistically and their ability to act as drug carriers could also be investigated.

Bile acids are generally produced in eukaryotic cells and less than 15 bacterial strains are known to produce these metabolites (Kim et al., 2012). Given that the biosynthetic pathway for the production of these compounds in bacteria have not been elucidated, the following section aims to propose a partial biosynthetic pathway for the production of these bile acids isolated from *Thalassomonas actiniarum* using a genome mining approach and bile acid synthesis in eukaryotes as a guide.

4.4 Biosynthesis of bile acids in eukaryotes

Bile acids are water soluble, amphipathic, steroidal molecules and are the end products of the breakdown of cholesterol in the liver of mammals and fish (Li and Chiang, 2009; Christie, 2019). Bile acids are detergents and act as emulsifying agents that aid in the digestion and absorption of fatty acids. These molecules also regulate biochemical reactions and cholesterol levels.

Bile acids are divided into 3 subgroups (C27 bile alcohols, C27 bile acids and C24 bile acids) based on the number of carbon atoms and side chain substitutes present. The typical structure of these bile acids can be seen in Figure 4.22. These molecules consist of three 6 membered rings (A, B, C) attached to a pentacyclic ring (D). Hydroxyl groups occur at the C3 and C7 positions and a primary alcohol (in the case of bile alcohols) and carboxyl group (in the case of bile acids) at the C terminal carbon atom of the flexible, aliphatic, acidic sidechain. Bile acids have diverse structures resulting from stereochemical changes of the A/B ring, changes in orientation of the hydroxyl groups, the length of the side chain as well as the absence or presence of double bonds Šarenac and Mikov, 2018).

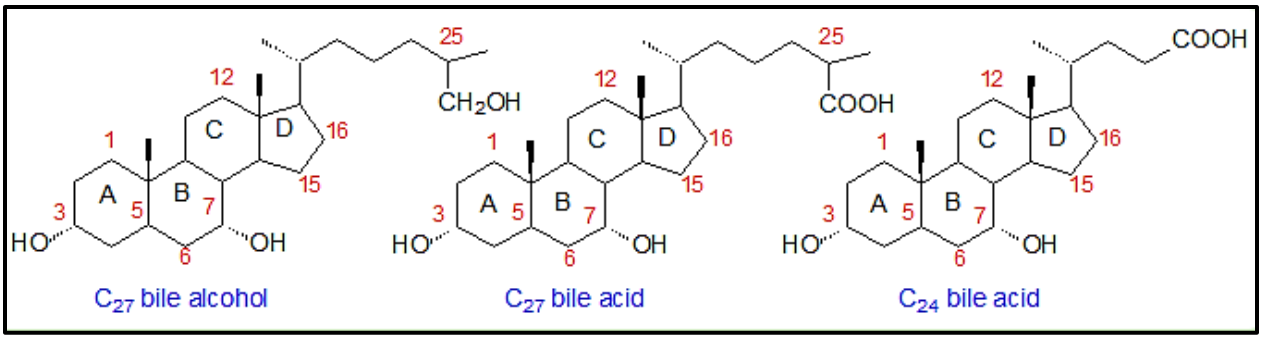

Figure 4.22: Structures of C27 bile alcohols with primary alcohol on the C-terminal carbon of the side chain, and C27 and C24 bile acids with carboxyl group at C terminal carbon on the side chain taken from Christie, 2019.

Two pathways exist for primary bile acid production from cholesterol in eukaryotes and are referred to as the classic pathway (producing cholic acid) and the alternative pathway (producing chenodeoxycholic acid) (Šarenac and Mikov, 2018) and only the classic pathway will be discussed here. Figure 4.23 (adapted from Li and Chiang, 2009) depicts a simplified illustration of the synthesis of cholic acid from cholesterol in humans. In the synthesis of primary bile acids, a number of structural modifications are made to the structure of cholesterol and most are hydroxylation reactions on the steroid nucleus. A total of 14 enzymes are involved in the synthesis of bile acids but only intermediate enzymes will be focused on in this mini review.

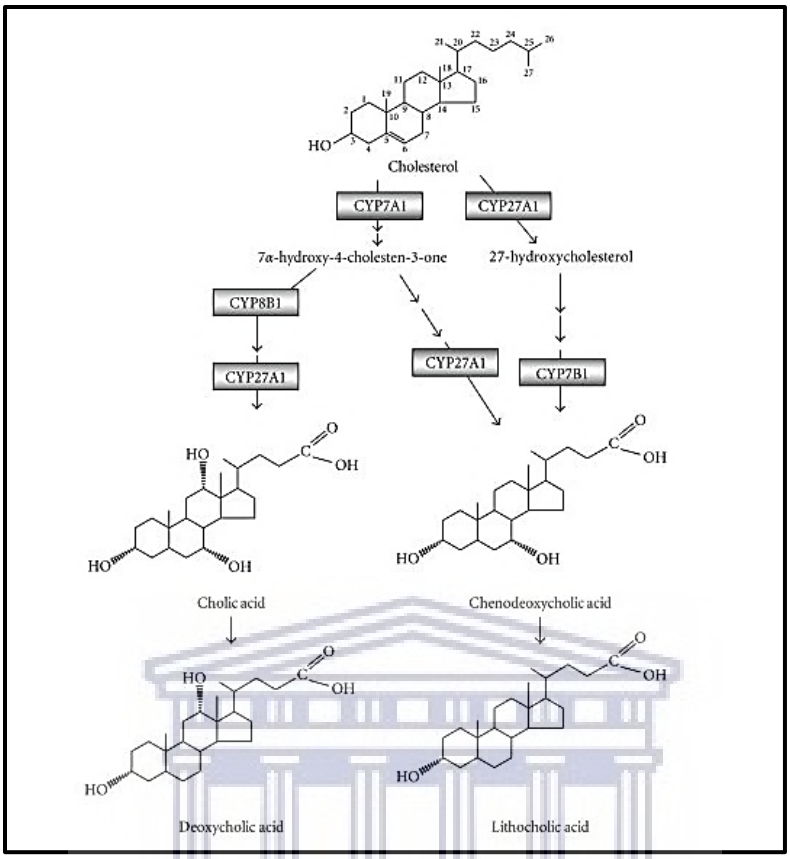

Figure 4.23: Bile acid synthesis pathway, taken from Li and Chiang 2009

In the classic pathway, the first reaction is catalyzed by CYP7A1 (cholesterol 7α hydroxylase) which converts cholesterol to 7α hydroxycholesterol, the rate limiting step of the classical pathway. In this step, a hydroxyl group is added to cholesterol in the α orientation at the C7 position. 7α hydroxycholesterol then undergoes several reactions to form cholic acid. Two enzymes, CYP8B1 (12 α hydroxylase) and CYP27A1 (sterol 27 hydroxylase), as well as other co-factors (O_2, NADPH, H^+, 2 Coenzyme A's (CoA) are required for the multistep process of converting 7α hydroxycholesterol to cholic acid (Šarenac and Mikov, 2018, Li and Chiang, 2009).

In a paper by Mukhopadhyay and Maitra 2004, the authors review the chemistry and biology of bile acids, providing a more detailed description of cholic acid synthesis in humans which revealed that 3-oxo cholic acid is an intermediate in the production of cholic acid. Following 7α hydroxycholesterol synthesis, this hydroxylated form of cholesterol is then reduced and isomerized to form the oxo derivative cholest-7α-hydroxy- Δ^4-3-one. Following 12α hydroxylation of this oxo

derivative, the side chain is oxidized to a C27 carboxylic acid. Hereafter, the double bond is saturated resulting in the formation of 3-oxo cholic acid as indicated by the red square in Figure 4.24. Lastly, 3-oxo cholic acid is reduced and the side chain cleaved to form cholic acid. It may be argued that compound 405, identified as 3-oxo cholic acid in this study is therefore a precursor to the production of compound 407, identified as cholic acid, during synthesis in *T. actiniarum*.

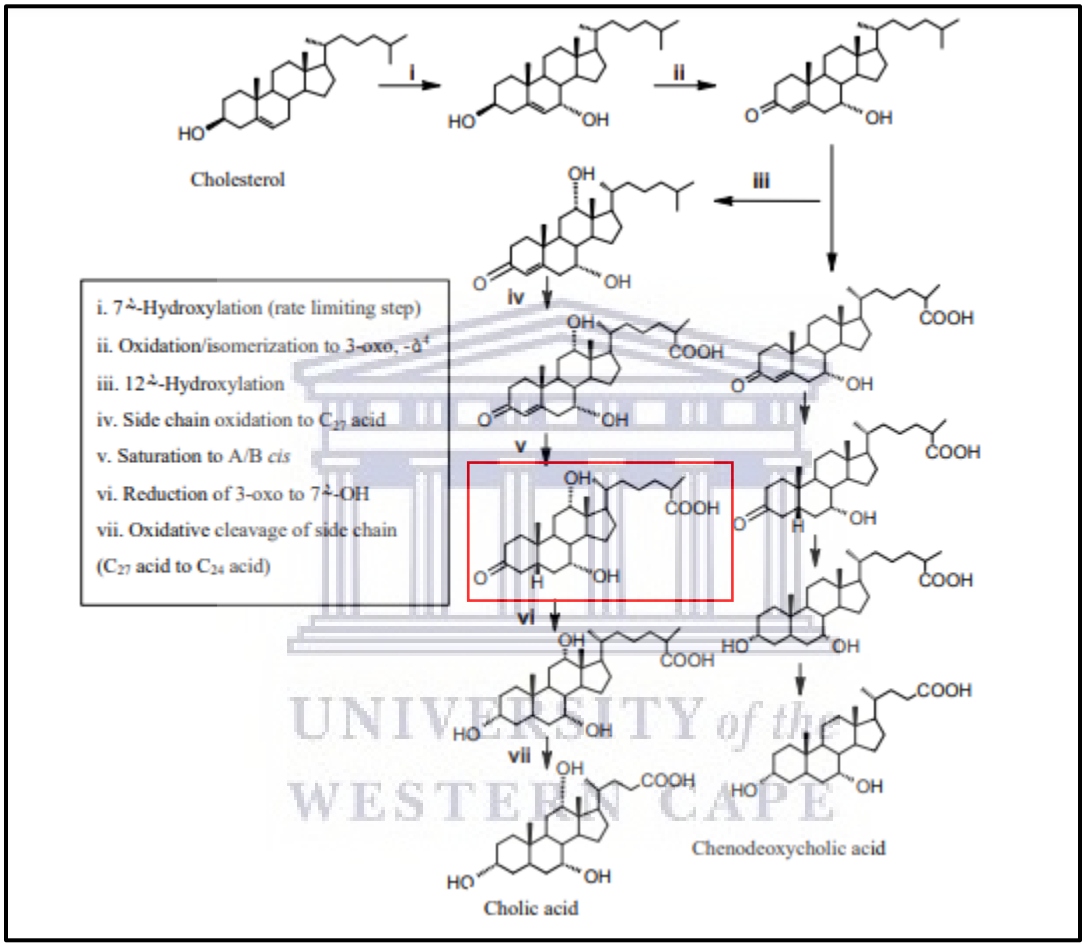

Figure 4.24: Detailed cholic acid synthesis pathway showing 3-oxo cholic acid (indicated by the red square) as an intermediate in cholic acid synthesis, taken from Mukhopadhyay and Maitra, 2004.

Figure 4.25 illustrates an overview of bile acid synthesis in eukaryotes. Briefly, isoprenoid precursor's dimethylallyl diphosphate (DMAPP) and isopentenyl pyrophosphate (IPP) are produced through the mevalonate (MVA) pathway. These precursors are further elongated to form the linear isoprenoid precursor squalene. Squalene then undergoes a series of 18 reactions to form

cholesterol (Kumari, 2018). Only intermediate steps crucial to cholesterol synthesis are mentioned here. Finally, bile acids are produced through the catabolism of cholesterol.

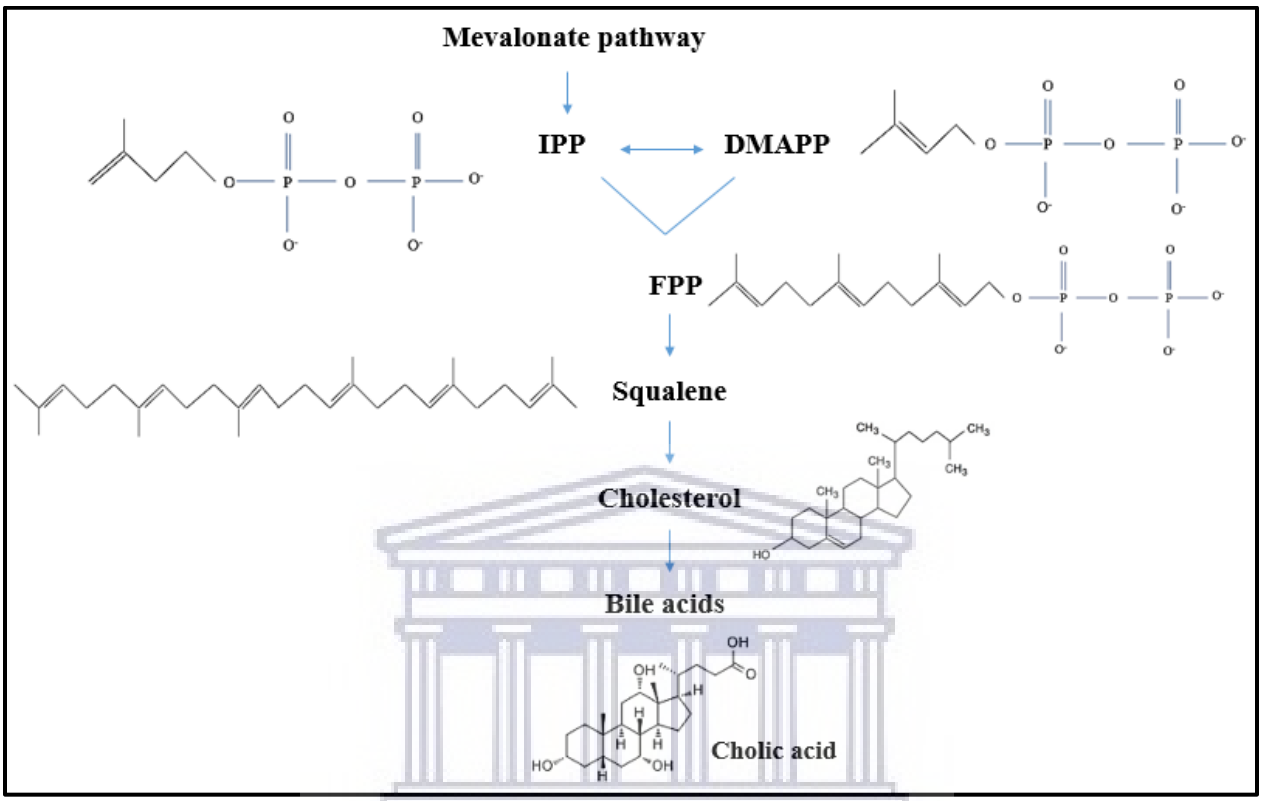

Figure 4.25: Schematic representation of bile acid synthesis in eukaryotes.

4.4.1 Synthesis of IPP and DMAPP in eukaryotes

Isoprenoids, also known as terpenoids (Odom, 2011) are synthesized *via* the condensation of isoprenoid precursor's IPP to DMAPP (Kuzuyama, 2002) and are produced by plants, microorganisms and animals. Table 4.18 shows the linear isoprenoid precursors generated through the condensation of DMAPP to one or more IPP molecules.

Table 4.22: Terpene nomenclature and linear precursors, adapted from Christianson 2017.

Carbon atoms	Terpene Prefix	Isoprenoid precursor	Linear isoprenoid precursor
5	hemi-	DMAPP (C5) ⟷ IPP (C5)	
10	mono-	DMAPP + IPP	geranyl diphosphate (GPP)
15	sesqui-	DMAPP + IPP + IPP	farnesyl diphosphate (FPP)
20	di-	DMAPP + IPP + IPP+ IPP	geranylgeranyl diphosphate (GGPP)
25	sester-	DMAPP + IPP + IPP + IPP + IPP	geranylfarnesyl diphosphate (GFPP)
30	tri-	FPP+ FPP	squalene

Isoprenoids are the largest known group of natural products, consisting of more than 35 000 known compounds including primary and secondary metabolites (Eoh and Crock, 2009). Although not structurally complex, the isoprenoid precursors DMAPP and IPP (Figure 4.25) may undergo a variety of modifications such as cyclization and oxidation of the carbon skeleton leading to diverse structures having diverse functions and activities (Odom, 2011). Isoprenoids such as cholesterol, play vital roles in maintaining eukaryotic cell membrane stability and is the precursor for the production of bile acids and other steroid hormones (Cerqueira, 2016).

In the cytosols of higher plants, in eukaryotes an in archaebacteria, the MVA pathway drives isoprenoid synthesis (Kuzuyama, 2002; Perez-Gil and Rodriguez-Concepcion, 2013). Figure 4.26 shows a detailed illustration of the MVA pathway for the synthesis of isoprenoid precursor's IPP and DMAPP in eukaryotes.

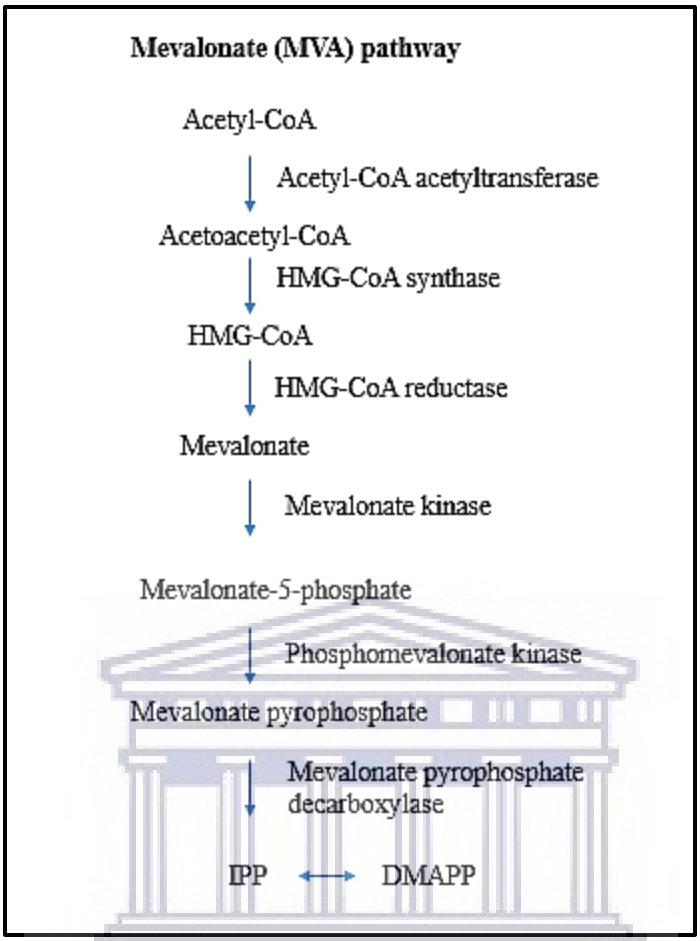

Figure 4.26: MVA pathway for isoprenoid synthesis in eukaryotes, adapted from Heuston et al., 2012

In the 1960s, Bloch and Lynen established the MVA pathway for cholesterol biosynthesis (Kuzuyama and Seto, 2012) from the precursors IPP and DMAPP. The MVA pathway starts with two acetyl CoA precursors which are converted to acetoacetyl CoA by acetyl-CoA acetyltransferase (ACAT). These precursors undergo a condensation reaction with the aid of HMG-CoA synthase to form 3-hydroxy-3-methyl-glutaryl-CoA (HMG-CoA). The enzyme HMG-CoA reductase converts HMG-CoA to mevalonate, the rate limiting step in this process. Mevalonate is then phosphorylated and the phosphorylated form of mevalonate is decarboxylated to form IPP and its isomer DMAPP.

4.4.2 Squalene synthesis in eukaryotes

The head-to-tail condensation of IPP to DMAPP is catalyzed by the prenyltransferase farnesyl diphosphate synthase (FPPS), resulting in the formation of geranyl diphosphate (GPP). Addition of another IPP molecule to GPP by FPPS leads to the formation of FPP (Table 4.22) (Christianson, 2017; Chhonker et al., 2018). Squalene, the precursor of cholesterol biosynthesis in eukaryotes is synthesized through the head-to-head condensation of two molecules of farnesyl diphosphate (FPP) to produce presqualene diphosphate (PSPP) which is subsequently reductively rearranged to form squalene (SQ) (Figure 4.27). These reactions are catalyzed by a single bifunctional squalene synthase (SQase) (Dhar et al., 2013; van der Donk 2015).

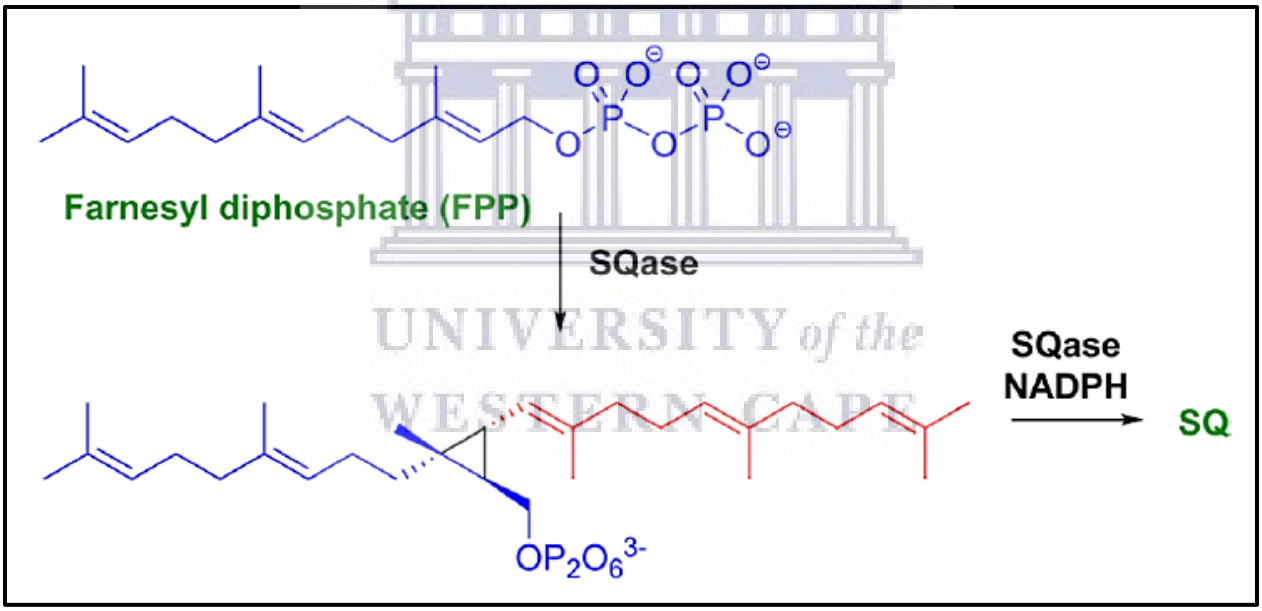

Figure 4.27: Biosynthetic pathway of squalene from FPP in eukaryotes, taken from van der Donk, 2015.

4.4.3 Cholesterol synthesis in eukaryotes

Cholesterol synthesis is initiated by the cyclization of squalene and Figure 4.28 shows a representation of the intermediates involved in this process.

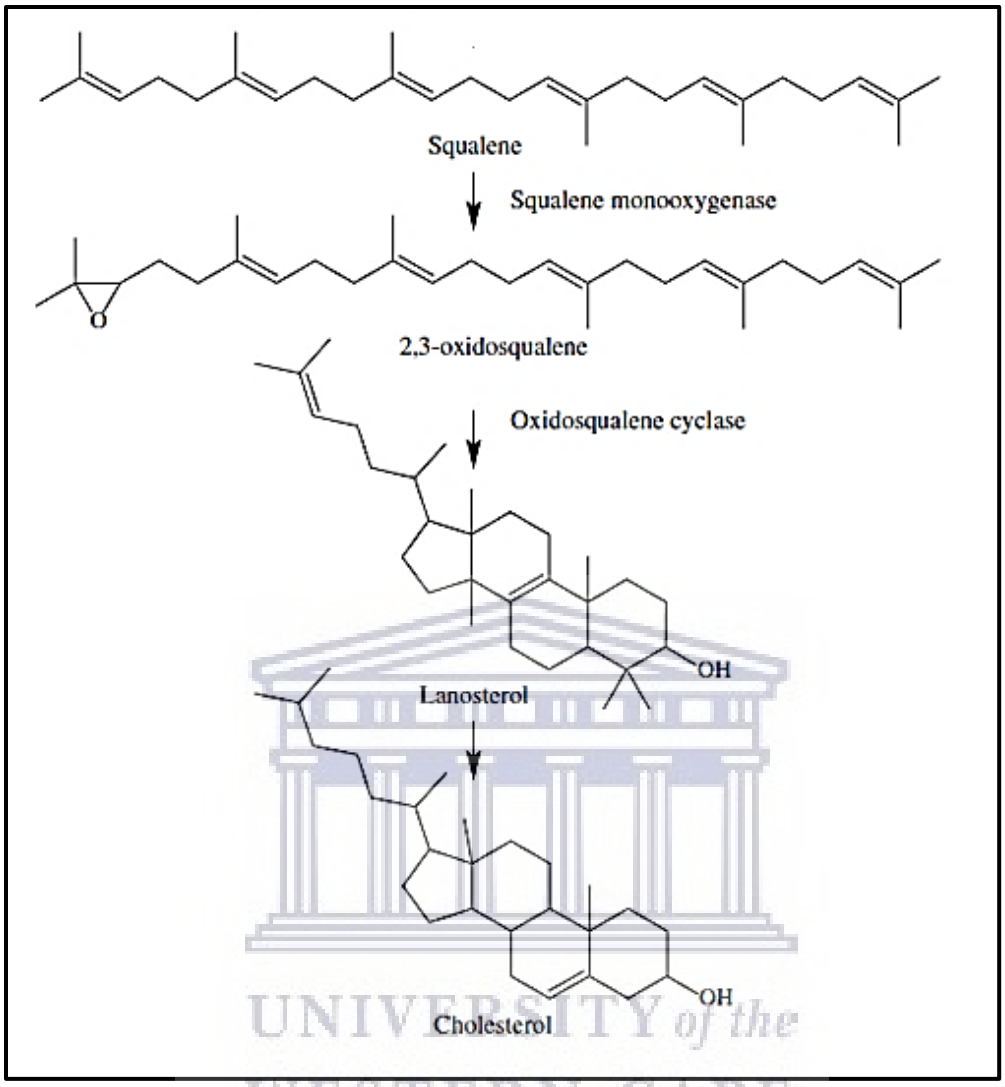

Figure 4.28: Cholesterol production from squalene taken from Belter et al., 2011.

Squalene is first converted to squalene epoxide (2, 3 – oxidosqualene) by the enzyme squalene monooxygenase in a reaction that requires O_2 and NADPH. Squalene epoxide is then cyclized to form lanosterol and this reaction is catalyzed by the enzyme oxidosqualene cyclase. Lanosterol is then converted to cholesterol through a multistep process (Belter et al., 2011) and as mentioned in section 4.4, cholesterol is the precursor for the production of bile acids. The next section will discuss the proposed biosynthetic pathway for bile acid synthesis in prokaryotes.

4.5 Bile acid synthesis in prokaryotes

Figure 4.29 illustrates a proposed overview of bile acid synthesis in prokaryotes. Briefly, isoprenoid precursors dimethylallyl diphosphate (DMAPP) and isopentenyl pyrophosphate (IPP) are produced through the mevalonate or non-mevalonate pathways in contrast to eukaryotes, which use only the MVA pathway. These precursors are further processed to form the linear isoprenoid precursor squalene. Squalene then undergoes a series of reactions to form hopanoids, the structural analogues of cholesterol in bacterial membranes. Hereafter, the production of bile acids from the catabolism of hopanoids/cholesterol is proposed.

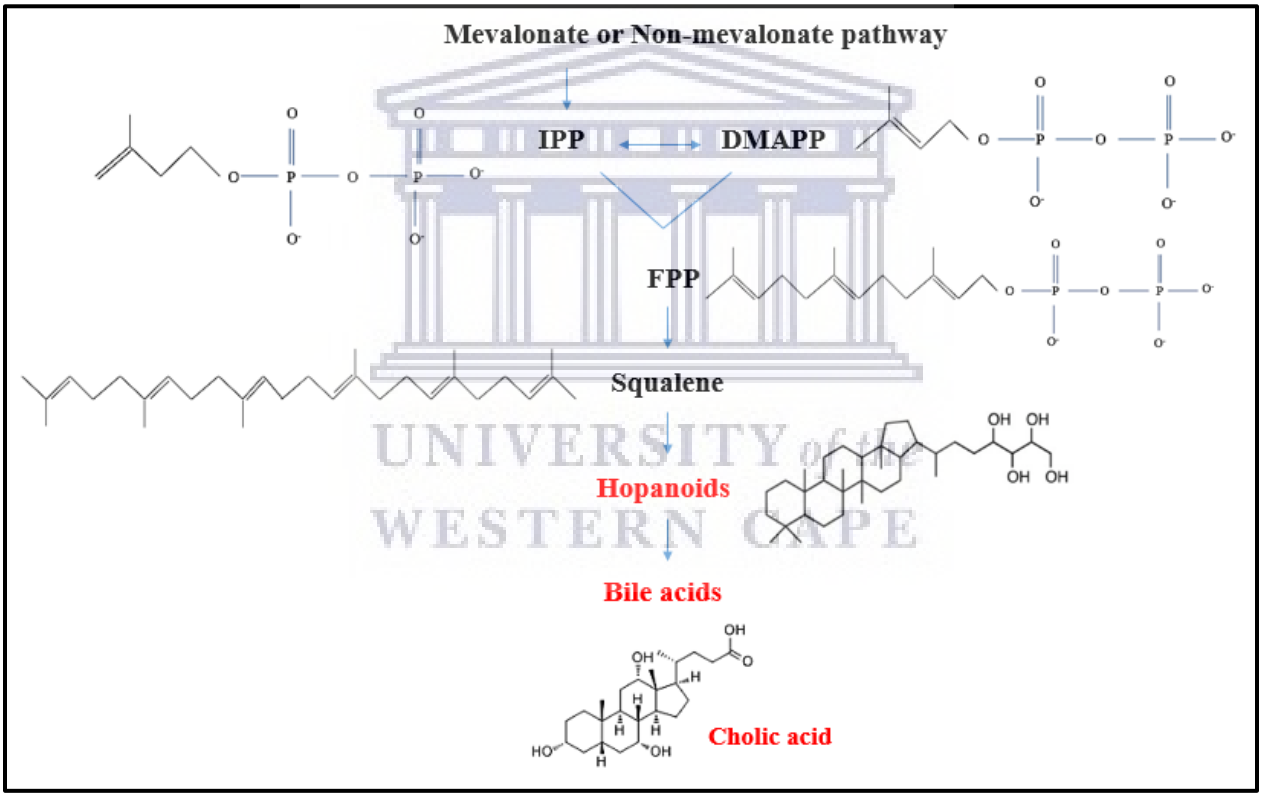

Figure 4.29: Proposed representation of bile acid synthesis in prokaryotes.

Most prokaryotes do not have the homologous genes involved in the MVA pathway yet still produce IPP and DMAPP. This led to the investigation of an alternative pathway for isoprenoid precursor synthesis and eventually the MEP pathway (Figure 4.30) was discovered (Kuzuyama and Seto, 2012).

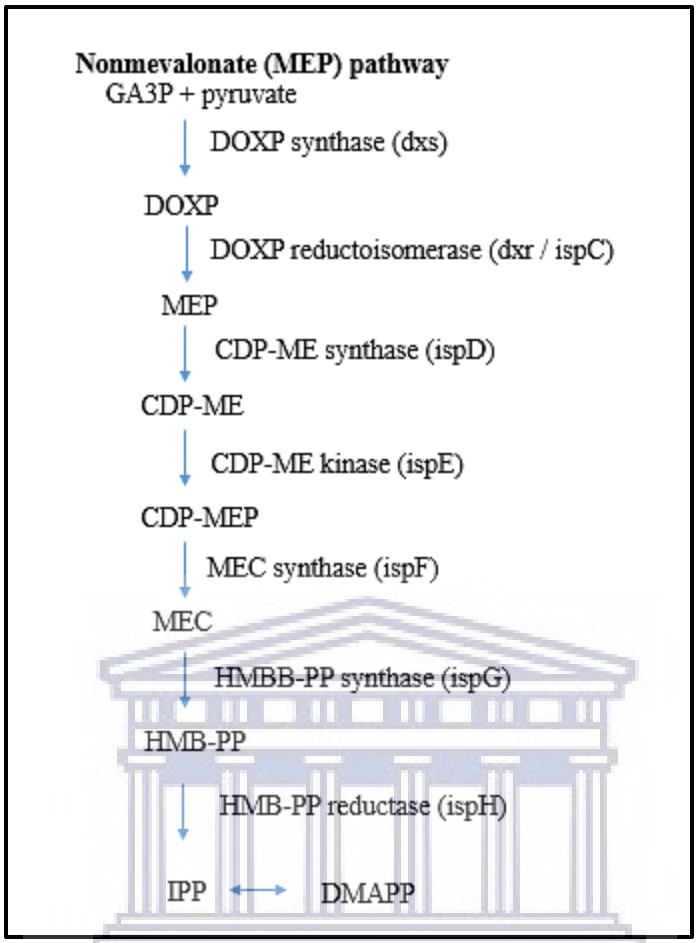

Figure 4.30: MEP pathway for isoprenoid synthesis in prokaryotes, adapted from Heuston et al., 2012.

The non-mevalonate pathway involves 8 biochemical reactions catalyzed by 6 main enzymes. *Mycobacterium tuberculosis* synthesizes IPP and DMAPP *via* the MEP pathway and this process has been well characterized in this organism. The enzymes involved in this pathway are termed IspC, IspD, IspE, IspF, IspG and IspH. The first step in the MEP pathway involves the condensation of D-glyceraldehyde-3- phosphate and pyruvate by *dxs* synthase to form DOXP (1-deoxy-D-xylulose-5-phosphate). DOXP is then reduced and rearranged to form MEP (2C-methyl-D-erythritol 4-phosphate) by the enzyme dxr/IspC, the first committed step in IPP and DMAPP synthesis. MEP is then cytidylylated by IspD to CDP-ME (4 – cytidine 5' diphospho-2-C-methyl-D-erythritol). CDP-ME is then converted to CDP-MEP (4-diphosphocytidyl-2C-methyl-D-erythritol 2-phosphate) in the presence of ATP by the enzyme IspE. CDP-MEP is then converted to MEC (2-C-methyl-D-erythritol 2,4-cyclodiphosphate) by the enzyme IspF. The enzyme IspG

then catalyzes the conversion of MEC to HMBPP (1-hydroxy-2-methyl-2(E)-butenyl 4-diphosphate) and the enzyme IspH is responsible for the conversion of HMBPP into IPP and DMAPP (Kuzuyama 2002; Eoh, 2009; Odom, 2011; Xue et al., 2015).

In the chloroplasts of higher plants, eubacteria and green algae, the non-mevalonate (MEP) pathway drives isoprenoid synthesis (Kuzuyama, 2002). Bacteria harbouring both pathways still use the MEP pathway to produce primary metabolites while the MVA pathway is used for the production of secondary metabolites (Eoh and Crick, 2010). All *Streptomyces* strains use the MEP pathway to produce their essential isoprenoids, but some strains can additionally use the MVA pathway for the biosynthesis of antibiotics and other secondary metabolites (Perez-Gil and Rodriguez-Concepcion, 2013). In most bacteria, the common precursors of all isoprenoids are produced by the MEP pathway. These statements suggest that bacteria show a remarkable flexibility for isoprenoid biosynthesis since some bacteria use the MVA pathway instead of the MEP pathway, others possess both pathways, while some parasitic strains lack both and acquire isoprenoids from their hosts. Additionally, alternative enzymes and intermediates could be used for isoprenoid synthesis and several enzymes unrelated to isoprenoid synthesis could undergo spontaneous mutations and produce intermediates used in the synthesis of isoprenoids (Perez-Gil and Rodriguez-Concepcion, 2013).

Following production of isoprenoid precursors IPP and DMAPP, FPP is produced in the same way as in eukaryotes. Squalene is then synthesized through the head-to-head condensation of two molecules of FPP using a different pathway compared to that found in eukaryotes.

4.5.1 Squalene synthesis in prokaryotes

In a paper by Pan et al. (2015) the authors have identified an alternative route for the production of squalene in bacteria (Figure 4.31) involving 3 enzymes HpnD, HpnC and HpnE in contrast to squalene synthesis in eukaryotes, which requires only a single bifunctional squalene synthase.

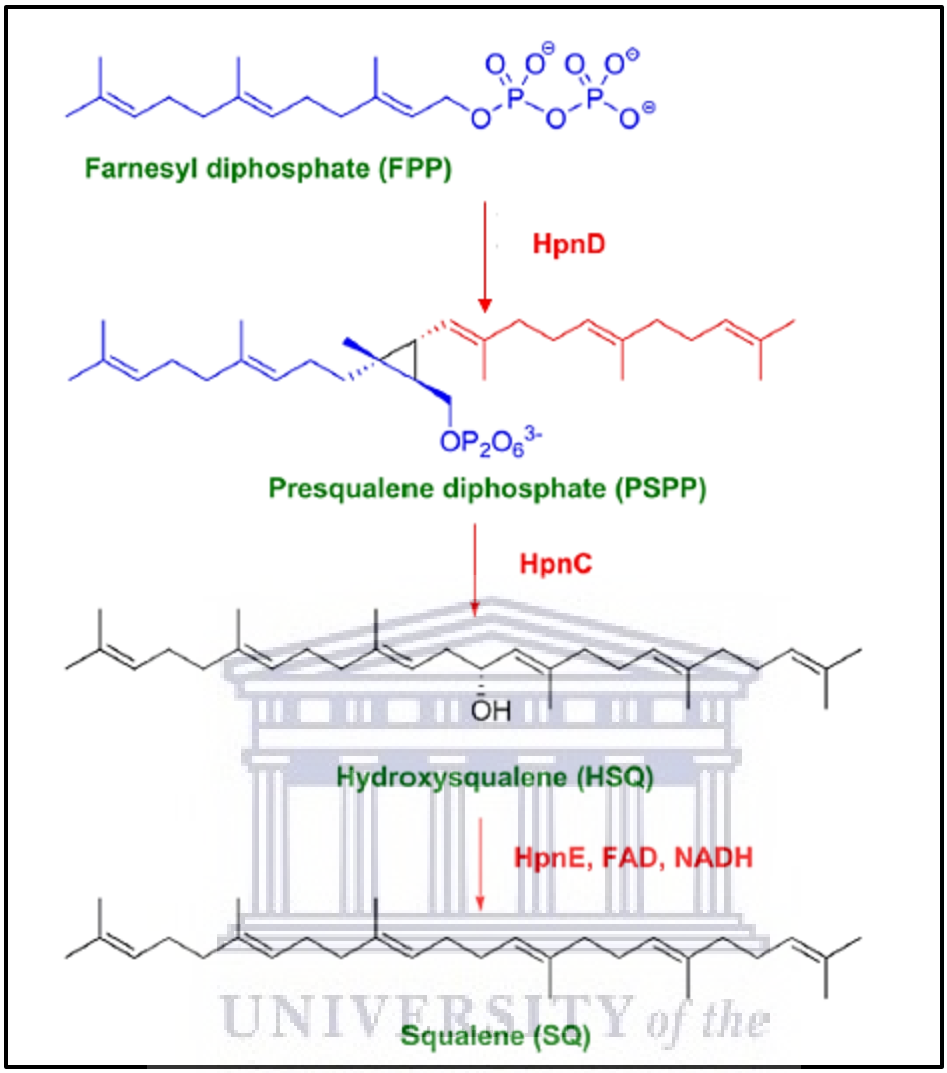

Figure 4.31: Biosynthetic pathway of squalene from FPP in bacteria, taken from van der Donk, 2015

In bacteria, the squalene synthase homolog HpnD catalyzes the head-to-head condensation of two FPP molecules to form PSPP. The enzyme HpnC (another squalene synthase-like enzyme) then converts PSPP to hydroxysqualene through a hydrolytic rearrangement of PSPP. Hydroxysqualene is then converted to squalene through the reductive displacement of the hydroxyl group and this reaction is catalyzed by the enzyme HpnE. Bacteria, who do not produce cholesterol, use squalene as an important precursor for the production of hopanoids (Pan et al., 2015).

4.5.2 Hopanoid synthesis in prokaryotes

Hopanoids are triterpenoid structures and are considered the cholesterol analogues in bacterial membranes (Figure 4.32). The function of hopanoids is not yet fully understood but studies have shown that the deletion of hopanoid expression genes was not lethal to bacteria, but an increase in the sensitivity of the membrane to osmotic pressure, pH, temperature and antibiotics was observed (Pan et al., 2015; Welander et al., 2009; Schmerk et al., 2011). This suggests that they have an important role in protecting the cell from environmental factors that may affect membrane stability (Sáenz et al., 2015).

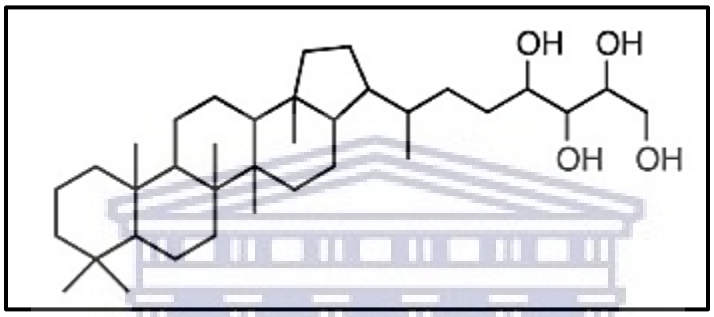

Figure 4.32: Structure of the hopanoid bacteriohopanetetrol taken from Doughty et al., 2014

Hopanoids have been identified in many bacteria from a variety of taxonomic groups including the cyanobacterium *Anabaena variabilis*, *Rhodomicrobium vanielii*, *Rhodopseudomonas palustris* TIE-1 (Rohmer et al., 1984), *Acetobacter pasteurianus* (Kuchta et al., 1998), *Streptomyces scabies* (Seipke and Loria, 2009), *Methylococcus capsulatus* (Neunlist and Rohmer, 1985), , *Burkholderia cenocepacia* K56-2 (Schmerk et al., 2011), *Geobacter metallireducens* and *Geobacter sulphureducens* (Härtner et al, 2005) while the best characterized hopanoid producer is *Zymomonas mobilis* (He et al., 2014).

On the genome of *Z. mobilis*, a biosynthetic gene cluster containing 14 putative hopanoid biosynthetic genes (HpnA – HpnM) have been identified (Figure 4.33). Among these IspH, not directly involved in hopanoid synthesis but involved in isoprenoid synthesis *via* the MEP pathway (used by *Z. mobilis*) was identified (Pan et al., 2015; He et al., 2014). The genes HpnC, HpnD, HpnE are highly conserved and the function of these genes have been established through heterologous expression and characterization of the genes from *Z. mobilis* and *Rhodopseudomonas palustris* in *E. coli*. It was determined that only HpnC, HpnD and HpnE are required for squalene

synthesis, highlighted in blue in Table 4.23 and depicted in Figure 4.33. Furthermore, squalene-hopane cyclase (HpnF), highlighted in red in Table 4.23 is responsible for the cyclization of squalene to hopanoids and other metabolites with a pentacyclic structure. It has been shown that HpnF is essential in hopanoid formation as deletions of this gene in *B. cenocepacia* K56-2 and *R. palustris* TIE-1 resulted in failure to produce hopanoids (Schmerk et al., 2015).

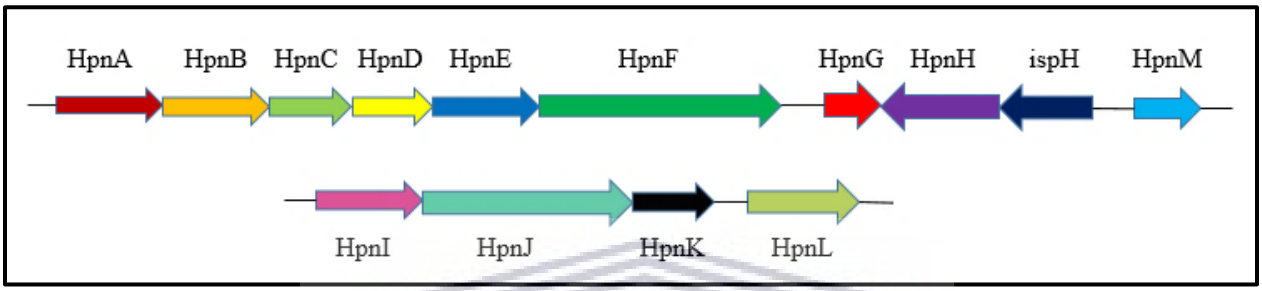

Figure 4.33: Hopanoid biosynthesis operon in *Zymomonas mobilis*, adapted from Pan et al., 2015.

Table 4.23: Hopanoid synthesis genes in *Z. mobilis*, taken from Pan et al., 2015.

Gene	Description
HpnA	Sugar epimerase
HpnB	Glycosyl transferase
HpnC	Squalene synthase-like protein
HpnD	Squalene synthase like protein
HpnE	FAD-dependent amino oxidase, phytoene desaturase
HpnF	Squalene-hopane cyclase
HpnG	phosphatase
HpnH	Radical SAM
HpnI	glycosylase
HpnJ	Radical SAM
HpnK	Polysaccharide hydrolase
HpnL	Membrane spanning protein
HpnM	Membrane associated ABC transporter
ispH	Hydroxymethylallyl diphosphate reductase

To the best of our knowledge, a biosynthetic pathway for bile acid production from the catabolism of hopanoids in bacteria has not been established. Hopanoids have diverse structures and can be methylated, unsaturated and have different side chain functionalities (Welander et al., 2009). Unsaturated hopanoids (containing a double bond) are rare and it has been hypothesized that this modification may be an indication of the first step in hopanoid catabolism as seen in the catabolism of cholesterol in eukaryotes, where the saturated cholesterol molecule is unsaturated during its breakdown to bile acids. Little attention has been paid to hopanoid catabolism and therefore no evidence of the process involving hopanoid catabolism has been reported (Tritz et al., 1999; Cvejic et al., 2000; Belin et al., 2018). Additionally, cholesterol synthesis by bacteria has not been established although some are capable of using cholesterol as a carbon source. Future studies investigating hopanoid catabolism may provide clues as to the synthesis of bile acids from hopanoids. Additionally, cholesterol synthesis in bile acid producing bacteria could also be explored.

4.6 Bile acid production by *T. actiniarum*

In summary, in eukaryotes bile acid production is accomplished through the catabolism of cholesterol which is synthesized through DMAPP and IPP. In prokaryotes, the pathway for bile acid synthesis has not been established but the intermediate steps for the production of IPP and DMAPP, FPP, squalene and hopanoids have been characterized. Using the Prokka annotated genome we established that *T. actiniarum* has the genetic capacity to produce the isoprenoid precursors IPP and DMAPP using the MEP pathway (Table 4.24). Key enzymes involved in the MVA pathway for production of DMAPP and IPP such as HMG-CoA synthase, HMG-CoA reductase were not identified, suggesting that the strain does not have both pathways and that the isoprenoid precursors if produced, are produced through the MEP pathway. This supports the notion that the most common pathway used by bacteria for the production of isoprenoid precursors is the MEP pathway.

Table 4.24: Enzymes involved in the MEP pathway that are present on the genome of *T. actiniarum* based on Prokka annotation.

	MEP pathway	Encoded on *T. actiniarum* genome
Enzymes	*dxs*	✓
	dxr/IspC	✓
	IspD	✓
	IspE	✓
	IspF	✓
	IspG	✓
	IspH	✓

If synthesized, the enzyme farnesyl diphosphate catalyzes the formation of FPP, the precursor of squalene, through the condensation of IPP and DMAPP. A gene encoding a putative farnesyl diphosphate synthase was identified, indicating that the strain is genetically capable of producing the FPPS required to synthesize FPP from IPP and DMAPP. As mentioned in section 4.5.1, in bacteria, the genes HpnC, HpnD and HpnE are involved in squalene synthesis from FPP. No squalene synthase or squalene-hopane cyclase genes were identified based on Prokka annotation, which calls out genes based on a threshold of 1e-06 under default parameters (Seemann, 2014). This would also suggest that neither hopanoids nor cholesterol can be synthesized by this strain given that squalene is a precursor for the production of both these sterols. Notably, these results are only proposed based on bioinformatics analysis and experimental validation is required to determine whether any of the gene products are produced.

Bifunctional squalene synthases have only been characterized from two bacterial strains, *Thermosynechococcus elongatus* and *Methylococcus capsulatus* (Pan et al., 2015). A protein sequence alignment of these characterized bacterial squalene synthases from both species (*T. elongatus* Accession: BAC08649.1; *M. capsulatus* Accession: CAA71097.1 was conducted using NCBI BLASTp and revealed that the similarity between these two sequences was only 31% at an amino acid sequence level, suggesting that *T. actiniarum* may be producing a highly novel squalene synthase given that these sequences are not highly conserved.

Based on genomic analysis, no squalene synthase genes have been identified on the genome of *T. actiniarum* and neither have any squalene-hopane cyclases. These enzymes are essential in cholesterol and hopanoid synthesis. This initial genomic analysis would imply that *T. actiniarum*

does not have the genetic capacity to produce bile acids. However since the bile acids isolated from the fermentation broth were most probably synthesized *de novo* (given that marine broth does not contain bile acids), and based on the overall low sequence homology of a large portion of the genome it is highly probable that *T. actiniarum* produces squalene, cholesterol and/or hopanoids and bile acids with the aid of novel enzymes and perhaps pathways that have yet to be characterized. Furthermore, Prokka uses reference proteins for which experimental data is available which can be disadvantageous since proteins for which no experimental data is available may go undetected.

4.6 Conclusion

Genome mining of *T. actiniarum* for its biosynthetic potential has shown that this strain is capable of producing a variety of potentially novel bioactive compounds belonging to diverse classes, showing low or no homology to known compounds. Here we present the first study investigating the bioactive potential of small molecules produced by *T. actiniarum* and show that these compounds exhibit antibacterial and anticancer activity.

Two bile acids, cholic acid and 3-oxo cholic acid were isolated from the fermentation broth of *T. actiniarum* and although not active or novel compounds, are the first bile acids reported from this genus and species. Future studies could also target select biosynthetic gene clusters for heterologous expression and characterization. Additionally, all HPLC fractions generated during the purification process should be screened for activity. With such a large portion of the genome of *T. actiniarum* unannotated, it is difficult to draw conclusions about the presence or absence of genes and pathways since novel genes that have yet to be characterized may go undetected using homology-based prediction tools. These pathways can only be elucidated using gene discovery approaches such as gene knockouts. A software tool (gutSMASH) designed to predict the biosynthetic pathways for primary metabolites such as bile acids in anaerobic bacteria will soon be available and may provide insight into the bile acid synthesis pathway in *T. actiniarum* (Andreu et al., 2019).

Chapter 5: General Conclusion

The emergence of drug resistant pathogens has been and remains a global health threat, contributing immensely to hospital acquired infections (Wang et al., 2018). Studies have shown that 1 in 7 people infected with SARS-CoV-2 have acquired secondary bacterial infections and 50% of those who have died had acquired secondary infections (Gerberding, 2020). According to the World Health Organization, by the year 2050, 10 million people could die per year as a result of infections caused by multidrug resistant bacteria and individuals with compromised immune systems or underlying disease, such as those infected with HIV, MTB and COVID-19 are at a greater risk of becoming infected. In 2009, nearly 300 000 people died worldwide as a result of the H1N1 influenza virus, with approximately 29%-55% of the deaths related to secondary infections caused by opportunistic multidrug resistant bacterial strains (Gerberding, 2020). It is evident that there is a need for the discovery and development of novel antibiotics to combat the threat of multidrug resistance.

Natural products have been used to treat disease since the earliest times and has proven to be a successful source of new drug candidates (Dias et al., 2012). With the constant rediscovery of known compounds from terrestrial environments, natural product discovery has shifted to the marine environment in which the conditions force the evolution of novel biochemical pathways and products (Felczykowska et al., 2012; Banik & Brady, 2010; Gerwick & Fenner, 2013; Gulder & Moore, 2009). Marine invertebrates are a rich source of bioactive natural products and the majority of marine natural products in clinical trial have been isolated from marine invertebrates (Proksch, et al., 2003). However, structural elucidation revealed that there was a striking similarity between compounds produced by microorganisms and those isolated from the sponges (Li, 2009). Studies later showed that the microbial symbionts of marine sponges are the true producers of many of the bioactive compounds once thought to be produced by these invertebrates. Furthermore, obtaining a renewable supply of biologically active molecules from natural sources like invertebrates can be problematic and is considered one of the bottlenecks in drug discovery (Proksch et al., 2003). Using the marine bacterial symbionts, this bottleneck can be overcome since bacteria are considered a sustainable source of natural products. Additionally, marine

microorganisms show immense genetic and biochemical diversity and the competition between microorganisms for space and nutrients is the driving force behind the production of structurally unique pharmaceutically relevant natural products (Gerwick & Fenner, 2013).

Thalassomonas actiniarum was isolated from a sea anemone that was harvested off the coast of Japan (Hosoya et al., 2009). The aim of this research was to investigate the bioactive potential of the strain using a culture independent and culture dependent approach. It is obvious that this strain has the potential to be a significant source of novel pharmaceutically relevant compounds.

To investigate the antimicrobial potential of *T. actiniarum*, antibacterial screening of 4 size fractions (<3kDa, 3kDa-50kDa, 50kDa-100kDa and >100kDa) for antibacterial activity showed that the strain produces an antibacterial compound with an average size between 50kDa-100kDa. Investigations later revealed that the active compound may be a putative phage encoded lytic protein (TAP1) similar to the TVP1 identified in *T. viridans*, the closest relative of *T. actiniarum*. Heterologous expression revealed that neither TAP1 nor TVP1 showed antibacterial activity suggesting that, if properly expressed, TVP1 was incorrectly identified as being responsible for the observed antibacterial activity in *T. viridans* leading to the incorrect identification of TAP1 as the active protein in *T. actiniarum*. Future studies aiming to establish the function of these proteins could employ gene knockout studies and may lead to the identification of a novel phage encoded protein.

In an attempt to isolate and characterize the high molecular weight active compound, initially thought to be TAP1, from *T. actiniarum*, a bioassay-guided approach was applied. We quickly observed that the standard methods used to isolate, purify and resolve proteins was not providing any clues as to the nature of this compound. This led us to question whether the active compound was a protein and to consider the possibility that it belongs to another class of high molecular weight, negatively charged, extracellular compounds such as exopolysaccharides (EPSs). As discussed in Chapter 3, the 50kDa-100kDa EPS fraction showed antibacterial activity against *P. putida*. The Sevag deproteinization step however proved to be ineffective in removing contaminating proteins from the EPS fraction and future studies could instead use enzymatic deproteinization which is more specific compared to solvent separation. The use of Stains-All to detect polysaccharides in gels was unsuccessful in this study as it became clear that when working

with mixed samples, this dye is not ideal due to the interference of other compounds present. It is also possible that the HMW compound itself may have more than 1 chemical feature such as GAGs, glycoproteins and proteoglycans, further complicating the staining process. The EPS fraction also showed lytic activity in a zymography assay in which whole bacterial cells were used as a substrate. The zones of clearing representative of lytic activity, did not stain with either Coomassie or silver stain, suggesting that the active compound present in these spots is likely not proteinaceous in nature and could be a polysaccharide. To the best of our knowledge this is the first study investigating the lytic activity of an EPS using zymography. We recommend a continued investigation of this EPS fraction, determining both structure and function of the EPS. EPSs produced by microorganisms are known to be unique and therefore have wide application not only in the pharmaceutical industry but also in the food and cosmetics industries.

Antibacterial activity was also observed in the fraction >100kDa. Although not focused on in this study, tailocins were observed in this fraction. Given that some tailocins are antibacterial nanomachines (Duarte, 2012; Ge et al., 2020; Patz et al., 2019; Ghequire and De Mot, 2015) it would be worth investigating whether these particles are responsible for the observed antibacterial activity in the fraction >100kDa which would further expand our knowledge on the bioactive potential of this strain. Additionally, tailocins are known to induce larval metamorphosis of the tube worm *H. elegans*, corals and sea urchins (Shikuma et al., 2014) and future studies could investigate the significance of these particles in aquaculture and give insight into the ecological and symbiotic significance of the producer, *T. actiniarum*.

Antibacterial screening of the fraction <3kDa initially showed no antibacterial activity. However, Chapter 4 shows that by using an alternative method of extraction, prefractionation and screening compared to that used in Chapter 2, previously undetected bioactivity was discovered. A bioassay guided approach to isolate and characterize antibacterial, anticancer and biofilm inhibitory compounds of low molecular weight, i.e., secondary metabolites was employed. Antibacterial and anticancer activity was observed from the secondary metabolite fraction. After bioactivity screening of the characterized compounds cholic acid and 3-oxo cholic acid we observed that these compounds were not responsible for any of the bioactivities. In this study, a bioassay guided approach did not contribute to the isolation of bioactive compounds. However, a few notable errors were made. For one, after screening of the active fraction, target compounds in this fraction were

isolated based on the predicted mass and compound identification generated through HR-MS while other HPLC fractions generated during the purification process were not screened for activity. This suggests that the active compound could possibly be present in another fraction. This study also demonstrated the importance of understanding the limitations associated with MS (Chapter 2) and how isotope pattern and predicted elemental composition cannot be used alone to determine the identity of a compound. Although the isolated compounds cholic acid and 3-oxo cholic were not active, these steroids do play a significant ecological role.

Sea anemones, belonging to the phylum Cnidaria, are sessile animals that attach themselves to rocks and other hard surfaces. Sea anemones have a flat upper surface, with a central mouth surrounded by tentacles, a tubular body, and a flat base that attaches to the substrate. Their tentacles, covered in tiny stinging capsules called nematocysts, are used to catch prey and defend themselves against predators (Green, 2020). Nematocysts are a common feature of all cnidarians and are made up of a cylindrical capsule to which a long hollow thread is attached. The thread is inverted and coiled within the capsule and may be armed with spines depending on the type of nematocyst. During the discharge of nematocysts following chemical or mechanical stimuli, the thread is expelled from within the capsule in a harpoon-like fashion, one of the fastest processes recorded in biology. This thread is accompanied by the release of toxins that kill their prey or predators (Beckman and Ozbek 2012).

In 1942, Pantin investigated the chemical and mechanical stimuli required for nematocyst excitation. Nematocysts respond to physical contact and this contact stimuli is very selective. Studies have shown that *Trichodina pediculus* and *Kerona pediculus* wander freely on the surface of the *Hydra*, a cnidarian and model organism for the study of body part regeneration, without inducing nematocyst excitation. Because of this observation, mechanical stimulus cannot be the deciding factor in nematocyst excitation. Due to the selectivity of the excitation response, it was suggested that it may be due to a 'contact-chemical' stimulus. Nematocyst discharge is easily effected by solid food. Solutions of food derivatives (amino acids and sugars) do not cause nematocyst discharge, but, nematocysts are easily discharged on contact with solid food when food derived solutions are present. This led to the conclusion that food solutions sensitize nematocysts to mechanical stimuli and that nematocyst excitation is indeed a contact-chemical stimulus. Immersion of the tentacles in surface active substances like bile acids, fatty acids and saponin

(toxic, steroidal glycoside) do however cause discharge of all nematocysts and interestingly these are all cytolytic agents. The surface-active molecules such as bile acids and fatty acids present in food (like fish), may sensitize nematocysts to mechanical stimuli.

Marine invertebrates are capable of producing structurally diverse steroids, however, few reports on the isolation of bile acids from invertebrates such as sponges, corals and starfish exist (Lu et al., 2010; Lievens et al., 2004; Malyarenko et al., 2016, Cano et al., 2013) while many more reports on the isolation of bile acids and derivatives from marine bacterial symbionts have been reported (Li et al., 2009; Kim et al., 2012; Kim et al., 2010; Dockyu et al., 2007, Maneerat et al., 2005; Sanchez et al., 2016). Notably, the isolation and extraction methods used for the isolation of these bile acids and derivatives from invertebrates involved maceration of the invertebrate material followed by solvent extraction. Given that bacterial symbionts are present in the tissues of invertebrates, it is possible that the bile acids and derivatives isolated are microbially derived. This would support the hypothesis that the microbial symbionts of invertebrates are producing these bile acids to assist in host survival. Furthermore, in a study conducted by Sanchez and co-workers (2016), taurocholic acid was isolated from a *Rhodococcus erythropolis* strain that formed part of a fish microbiome. This bile acid showed biofilm inhibitory activity against *Vibrio cholera*, known to infect marine and freshwater fish. These studies showcase the bioactivity of bile acids and the diverse chemical defense mechanisms provided by microbial symbionts in order to protect their host and themselves against potential predators. In addition, it suggests that bacterial symbionts of sea anemones may produce bile acids to protect the sea anemone in this mutually beneficial symbiotic relationship.

Given that the biosynthetic pathway for cholic acid production in bacteria has not been elucidated, this study, and the proposed pathway, also serves as a foundation for the elucidation of the pathway. This can be experimentally validated through gene knockouts as well as mutagenesis of the genes involved in cholic acid synthesis. Once the pathway has been identified, pathway engineering could assist in overproducing these cholic acids, or modifying them to produce new cholic-acid-like compounds with new activities.

A culture independent approach was used to investigate the antimicrobial potential of *T. actiniarum*. We observed through genome mining tools like Prokka, antiSMASH and PRISM that *T. actiniarum* is capable of producing a variety of natural products belonging to different

classes. These include nonribosomal peptides, bacteriocins, nonribosomal peptide/polyketide hybrid compounds, exopolysaccharides and GAGs, among others.

Furthermore, genome mining revealed that the strain has the capacity to produce PNAG, an exopolysaccharide consisting of repeating units of N-acetylglucosamine involved in biofilm formation as well as chondroitin, a known antibacterial and anti-inflammatory glycosaminoglycan made up of repeating disaccharide units of N-acetylgalactosamine and glucuronic acid. PNAG has not been recorded to have antibacterial activity but N-acetylglucosamine, the building block of PNAG has shown antibacterial activity and we thus cannot exclude PNAG or its building block as the potential antibacterial polysaccharide identified in this study. Chondroitin sulfate is a known antibacterial agent (Gomez et al., 2018; Karakurt et al., 2019) and it is thus reasonable to consider that this too could be the antibacterial polysaccharide identified in this study. Given that both of these polysaccharides are known, if produced by *T. actiniarum*, these polysaccharides could easily be isolated and screened for bioactivity to determine if these were in fact responsible for the observed activity.

These predicted natural products and biosynthetic pathways showed low or no homology to known biosynthetic gene clusters, showcasing the potential for novel discoveries. One of the major drawbacks of using a culture independent approach in this study is that a large portion of the genome of *T. actiniarum* remains unannotated (47%) and given that predictive bioinformatics tools deduce gene functions through homology based methods, novel discoveries go undetected and complete pathways could not be deciphered. Using a comparative genomics and molecular genetics approach, the genes and their respective functions could be established in future (Lidbury et al., 2015).

Furthermore, the identification of a biosynthetic gene cluster does not indicate that it is expressed or that the end product is bioactive. Many BGCs are often silent under standard lab conditions and the expression of these clusters require an OSMAC approach, involving altering the culturing conditions like carbon source, temperature or using co-culturing to induce expression of silent pathways (Romano et al., 2018). Furthermore, the biosynthetic gene cluster may be producing compounds with activities other than antibacterial activity or the end product may be produced in such low concentrations that the activity is not detectable (Chen et al., 2019). Future studies aiming to fully exploit the biosynthetic potential of this strain could employ OSMAC to induce silent pathways and use alternative isolation, purification and screening methods and platforms.

Additionally, novel biosynthetic pathways can be targeted for heterologous expression and the screening platform expanded to target compounds with neuroprotective properties, anti-inflammatory activity and others.

This study once again highlights the importance of the marine environment and the marine invertebrate bacterial symbionts as sources of novel natural products. It is also the first study to show that this strain produces tailocins, bile acids, and a putative antibacterial exopolysaccharide. Although not responsible for the bioactivity, this is the first study reporting the production of bile acids for this genus and species. This study also emphasizes the importance of using an integrated approach, drawing from both culture dependent and culture independent strategies, toward identification of bioactive compounds and their biosynthetic pathways. Although the bioactive compounds responsible for the observed activity in this study were not isolated and characterized, with so little known about the bioactive potential of this organism and this genus, this study serves as the foundation for future studies investigating its bioactive potential.

Appendices

Appendix 2A

1X TE buffer, pH 8

10mM Tris-HCl, 1mM EDTA

6X DNA sample buffer

20% v/v glycerol, 0.1M EDTA, 1% w/v SDS, 0.25% bromophenol blue

50X TAE buffer (stock solution)

242 g Tris base, 18.6 g EDTA, 57.1ml glacial acetic acid, dH_2O up to 1L

0.1M Tris-HCl pH 8

12.11 g of Tris in 1L of distilled water and the pH adjusted to 8 with HCl

0.5M Tris-HCl, pH 6.8

60.57 g of Tris base in 1L of distilled water, pH adjusted with concentrated HCl

1.5M Tris-HCl, pH 8.8

181.71g of Tris base in 1l of distilled water, pH adjusted with concentrated HCl

1X SDS-PAGE Running Buffer, pH 8.3

25mM Tris base, 192mM glycine, 0.1% (wt/vol) SDS

4X sample buffer

277.8mM Tris-HCl pH 6.8, 4.4% (wt/vol) SDS, 44.4% (v/v) glycerol, 0.02% bromophenol blue and 100µl of B-mercaptoethanol per 900µl

Coomassie staining solution (100ml)

0.25g of Coomassie Brilliant Blue R250 in 10ml glacial acetic acid and 90ml methanol:H_20 (1:1)

Destain solution (100ml)

10ml glacial acetic acid and 90ml methanol: H_20 (1:1)

Luria Broth (LB)

Tryptone (10g/L), Yeast extract (5g/L), NaCl (10g/L), add 15g/L of bacteriological agar for solid media and add no agar for liquid media

Appendix 2B

List of antibiotic against which *E. coli* 1699 is resistant

Compound	**MIC (µg/ml)**	**Target/MOA**	**Antibiotic classification**
A54145CB-181234	> 512	membrane	
Calcimycin (A23187)	64	membrane	ionophore
Daptomycin	> 512	membrane	lipopeptide
Gramicidin	128	membrane	polypeptide
Polymyxin B	1	membrane	polypeptide (cationic)
Ampicillin	> 256	cell wall	aminopenicillin
Aztreonam	≤ 0.03	cell wall	monocyclic beta-lactam
Cephalosporin C	64	cell wall	cephalosporin
Penicillin G	> 256	cell wall	beta-lactam
Ristocetin	> 512	cell wall	aminoglycoside
Teicoplanin	> 512	cell wall	glycopeptide
Vancomycin	512	cell wall	glycopeptide
Aclacinomycin A	> 512	DNA interaction	anthracycline
Actinomycin A	> 256	DNA interaction	polypeptide (toxic)
Actinomycin D	256	DNA interaction	polypeptide (toxic)
Bleomycin A2	> 64	DNA interaction	glycopeptide
Coumermycin A1	64	DNA interaction	aminocoumarin
Daunorubicin	> 256	DNA interaction	anthracycline
Gliotoxin	32	DNA interaction	mycotoxin
Mitomycin C	1	DNA interaction	aziridine-containing

Streptonigrin	2	DNA interaction	quinone-containing
Streptozotocin	> 64	DNA interaction	glucosamine
Chromomycin A3	> 512	gyrase	glycoside
Nalidixic Acid	> 256	gyrase	naphthyridone
Novobicin	> 256	gyrase	aminocoumarin
Apramycin	64	protein synthesis	aminoglycoside
Dibekacin	>256	protein synthesis	aminoglycoside
Gentamycin	128	protein synthesis	aminoglycoside
Kanamycin	>256	protein synthesis	aminoglycoside
Kasugamycin	>64	protein synthesis	aminoglycoside
Neomycin	16	protein synthesis	aminoglycoside
Netilmycin	128	protein synthesis	aminoglycoside
Streptomycin	>256	protein synthesis	aminoglycoside
Streptothricin	256	protein synthesis	aminoglycoside
Tobramycin	>256	protein synthesis	aminoglycoside
Puromycin	>64	protein synthesis	aminonucleoside
Spectinomycin	>256	protein synthesis	aminocyclitol
Chloramphenicol		protein synthesis	acetamide
Chlortetracycline		protein synthesis	tetracyclide
Erythromycin	64	protein synthesis	macrolide
Lincomycin	512	protein synthesis	lincosamide
Spiramycin	256	protein synthesis	macrolide
Tetracycline	>256	protein synthesis	tetracycline
Thiostrepton		protein synthesis	oligopetide
Tylosin	512	protein synthesis	macrolide
Virginamycin	64	protein synthesis	streptogramin
Rifampin	>256	RNA polymerase	rifamycin
Rifamycin SV	>64	RNA polymerase	rifamycin
Albomycin	high	iron metabolism	cyclic polypeptide
Trimethoprim	>400	DHFR	diaminopyrimidine

Appendix 2C

Nucleotide sequence of TAP1 with restriction sites highlighted in yellow and histidine tag highlighted in blue

CCTCTAGAAATAATTTTGTTTAACTTTAAGAAGGAGATAACCATGGCTATGTCAACAATATC
CAATGCTGCACAAATCATGGTTGACAAGCTGGTCGCCGATTTAAACAGCGAAACGCCGCTCA
GCGCCGAAGACCAGTTACTGGTGGCAAAAGCGCTGGACACCATGAAAAACAGCACCACTTT
TGAAACCGCATTGATTGCGGTTGTCGAAGAGCACTTTAATACCGCTGATGCCGCGTTAACCG
CAGCGAAAAATGATATTAATGCTGCGAAAACCTCGATAGAGACCCAGTCGACTAACCTGGA
TTTAATCCCCGGAATACAAACCAGTATAGATACTAGTTTATCGGACATGAATACGAGTTTAG
ATACTTCCCTGGCAACCATAGCACCATCAGTACGTGACAATGTCAGGGGGGTCTTTAATAAA
CATCAAATTGGCTATTATCAAGTTGACCATAGCTTAACCGCATATGTAGGTCAGAACGGTTA
TCAATATGCGCCAGCTAACGTTGCTTCACTCGATAATTATGCGACAGGGGAGTTTTACACTTT
TGTTGATTTTGGTAACCAGACCACAAGTGTCAGACGTGCACTGATTATTCGAGTCAAGTCTG
ATGGTTCGGTGAGTACTGCCAGCCATGCTGCGCAATTTTTTACTAGTGGAATTTATGGTTTTG
TCCTTTCGCTGACGGCAGCAGCCGATTGTGTCGCTATGATGCCGGCACCTTATCGATACAAA
AATTAGGGGCCTTTAGCTGGGAGTTCAGTAAGGCGGTAGATTATCAGAATATCTATTACGAC
AAAGCCAGTAAAGATCTGTACTGTGTCAGCGGTGGTTTTTTACATACCATAGACGCAACCGA
TGGTTTTACCACTATTGGTGATGTTACTTTTATTAATGTTGAGGCTTTTGAAGCTTGGGCGTT
AGAAAATGGCCACCTACGTGCGGACTCTTTTGTTAATTACTTTAATGGTTCCCGCGGTAAAA
ACCAGGTATCTAACCAGGGAAACCGTTTCGATGCGCCAATGATAGTCTCTATAATGGGCGGC
TTTAGCAACACATATACTAAGCGGGCTGGGTTTGACCTGACCAGCGGCATTATGACCGCAGA
CTACCCGTTAACCAATTACTTTTCTGTTTACAATACCGCGATTACGGCATATGACACCACAAC
CTCCCGAGCTGTTTGGTTATCTTGGAAAGGTCAGGCAATGTTTAGGGATGTTTATGGTGTGAT
GGAGCGCCAAAGCGTAGAGCTATTTTCATTGGCGAACACGCATAGAGATGATAATCAACGC
ATGTACACTCCTGTGATGGTTGCTTTTTCTCATATTCATAAATGCCTCATATCTGATGTGTCG
GGATATGACTATTACACTAGCACGTCAGCAGCTTATTGGCAGGCTTGCGGTTTATCATTCGG
GAGACTCGAGCACCACCACCACCACCACTGAGATCCGGCTGCTAACAAAGCCCGAAAGGAA
GCTGAGTT

Nucleotide sequence of TAP1 with restriction sites highlighted in yellow and histidine tag highlighted in blue

CCTCTAGAAATAATTTTGTTTAACTTTAAGAAGGAGATATACATATGTCAACAATATCCAAT
GCTGCACAAATCATGGTTGACAAGCTGGTTGCTGATTTAAACAGCGATACGCCGCTTAGTGC
AGAAGACCAGTTGCTGGTGGCAAAACGCTGGACACCATGAAAAACAGCACTACCTTTGAAA
CCGCCTTGATTGCGGTAGTAGAAGAGCACTTTAATACTGCCGATGCTGCCTTAACCGCAGCA
AAAGATGATATTAATGCCGCGAAGAATTCAATTGAAACCCAGGCGACTAATCTGGATTTGAT
CCCTGGATTACAAACCAGCATAGATACCAGTCTCTCGGGCATGACCAGCAGTTTAGATACTT
CGCTGGCTACTATCGCACCTACGGTGCGTAATAACATTAGCGGTGTCTTTAACAAGCATCAG
ATAGGTTTTTACCAAACTGATCACACTTTGACTGGCGCAGTAGGTCAGAACGGTTATCAGTA
TGCGCCAGCTAACGTAACTTCACTTGATAATTATGCGACGAAAGAGTTTTATTGCTTTCTGGA
TTTTGGCAATCAAACAACGACTTATCGCCGTAGTTGTATCGTTCGGGTTAAAGCTGACGGTT
CGGTGAGTACGGCCACAGGAACGGGACAATTTTTTGCCTCGGGTAGTTACGGTTTTTGTCCT
TTTAGCGATGATAGCTGTCGCCTGCTTCGCTACGATAGCGGAACCTTATATGTGCAAAAATT
GGGTGCTCTTAGCTGGGAGTTCAATAAATCGGTTGATTACCTGAGTATTTATTACGATAAAA
GCAGTAAAGATCTGTACTGTGTCAGCGGTGGCTTTTTGCATACCATCGATGCAACCGATGGC
TTCACTACTATAGGTGATACTACTTTTATCGATGCCGATGCATTCGCTGCCTGGGCAGAAGG
AGAAGGCCACTTACGGGCAGACTCCTTTATCGGTTATTTCAATGGCCAGCGTGGTAAATCTG
ATGTGGAAAACCAGGGATCATATTTCGAAAAGTCCTGGACCGCGCCTTATATGGGAGGGTAT
GCAGCAGCTAGCACAAAACGGACGGGGTTCGATTTGGACAACGGCATTATGGTTGCTGACTT
TCCGCAGGCAAATAATTTCGCCGTTTACAATACTGCCGTGACTCCCATTAATACAACCACCA
CAAGGCCGGTATGGATTTCATGGAAAGGACAAGCCATGTTCCGTGATGTCTATGGCGTGATG
GAACGGCAAAGTATTGACTTATTCTCACTGGCAAATACATATCATTACACTAACCAGCGCAT
GTATACGCCGGTTATGGTGGCTTTTTCGCACATCCATAAATGCCTGATCTCGGATGTGTCGGG
TTACGACTATTACAGTAGTAGCAGTGCTGCGTTCTGGCAGATCTGCGGTTTATCATTCGGGA
GACTCGAGCACCACCACCACCACCACTGAGATCCGGCTGCTAACAAAGCCCGAAAGGAAGC
TGAGTTGGCTG

Appendix 2D

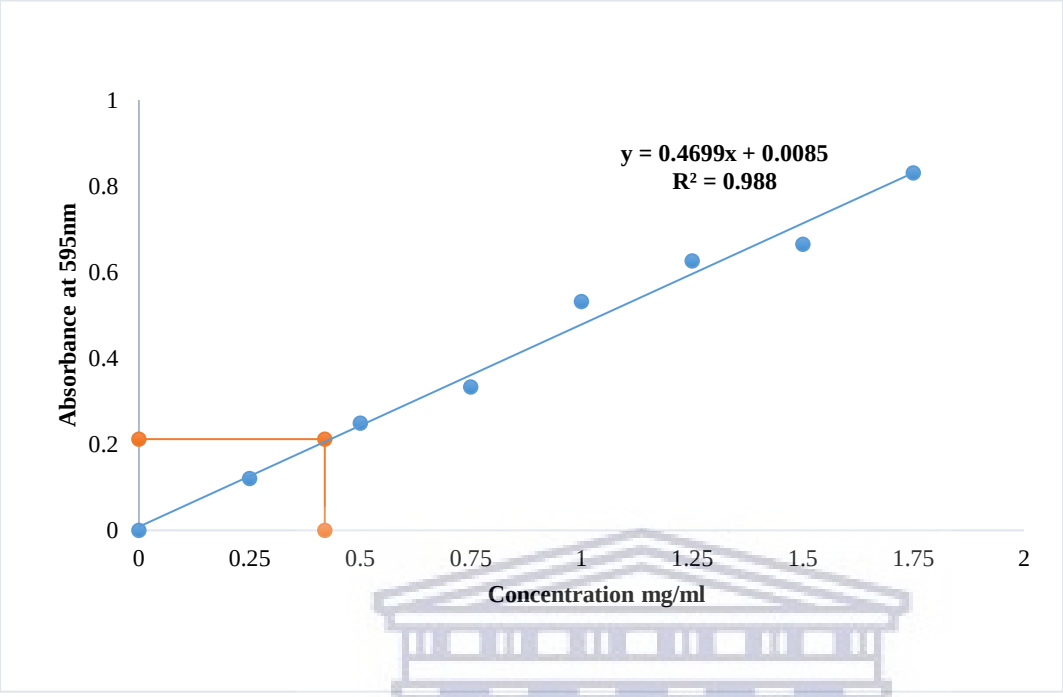

BSA standard curve for determination of TVP1 concentration after semi-purification

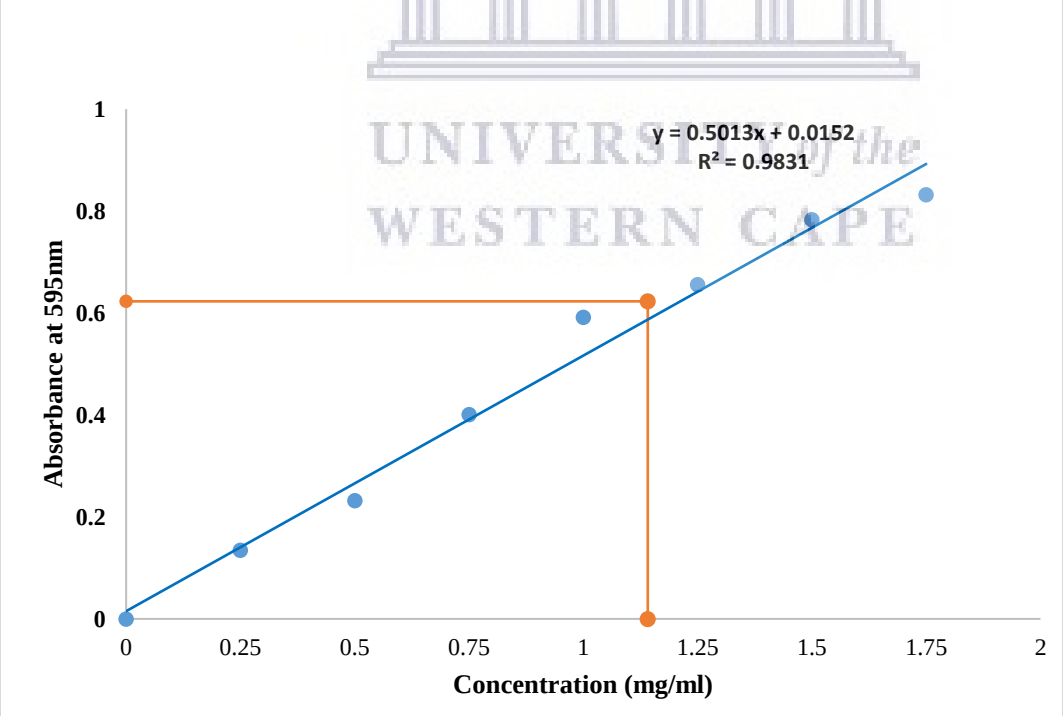

BSA standard curve for determination of TAP1 concentration after semi-purification

Appendix 3A

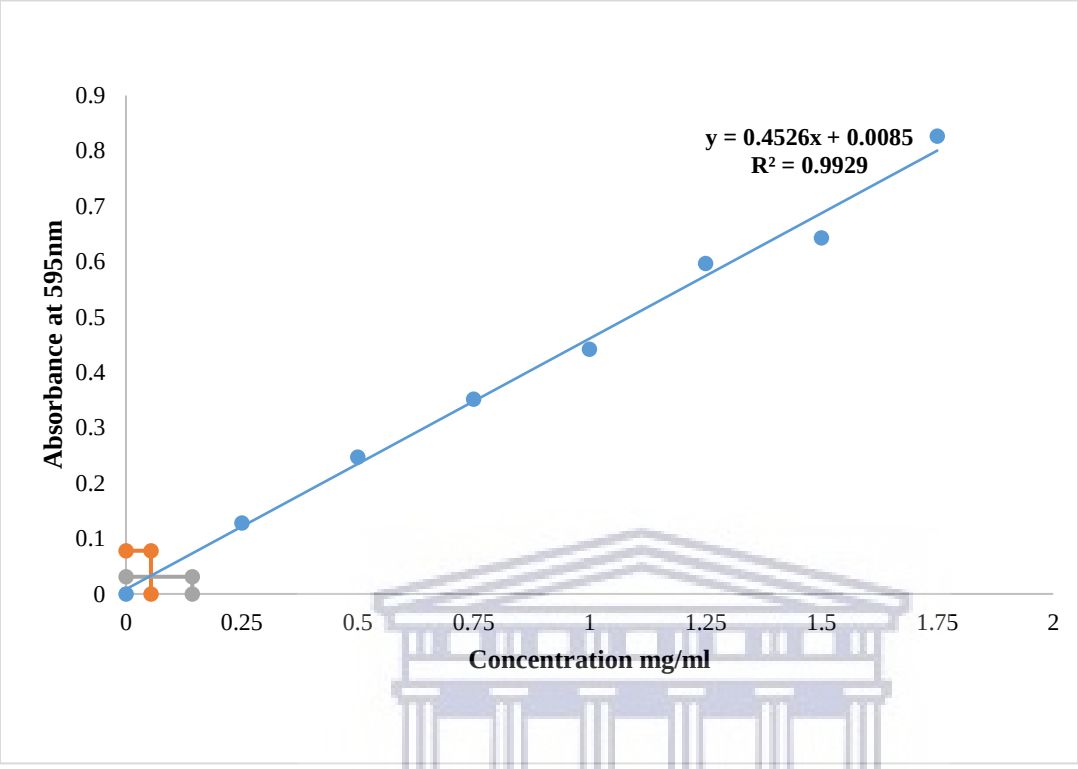

BSA standard curve and concentration of Fraction 1(orange) and Fraction 2 (grey) after semi-purification

Appendix 3B

1M Tris-HCl pH 6.8

121.14 g of Tris in 1L of distilled water and the pH adjusted to 6.8 with HCl

1M NaCl

58.44 g of NaCl in 1L of distilled water

Wash buffer

0.15M PBS pH 7.2 containing 0.15mM $CaCl_2$ and 0.5mM $MgCl_2$

1X native PAGE Running Buffer

25mM Tris, 192mM glycine, pH 8.3

2X native PAGE sample buffer

62.5mM Tris-HCl pH 6.8, 25% glycerol, 1% bromophenol blue

Fixing solution

40% ethanol: 10% acetic acid: 50% H_2O

Sensitizing solution

0.02% sodium thiosulfate (0.04g in 200ml dH_2O)

Silver nitrate solution

0.1% silver nitrate (0.2g in 200ml dH_2O + 40µl of 35% formaldehyde added just before use)

Developer

3% sodium carbonate (7.5g in 250ml dH_2O + 125µl of 35% formaldehyde added just before use)

Appendix 4A

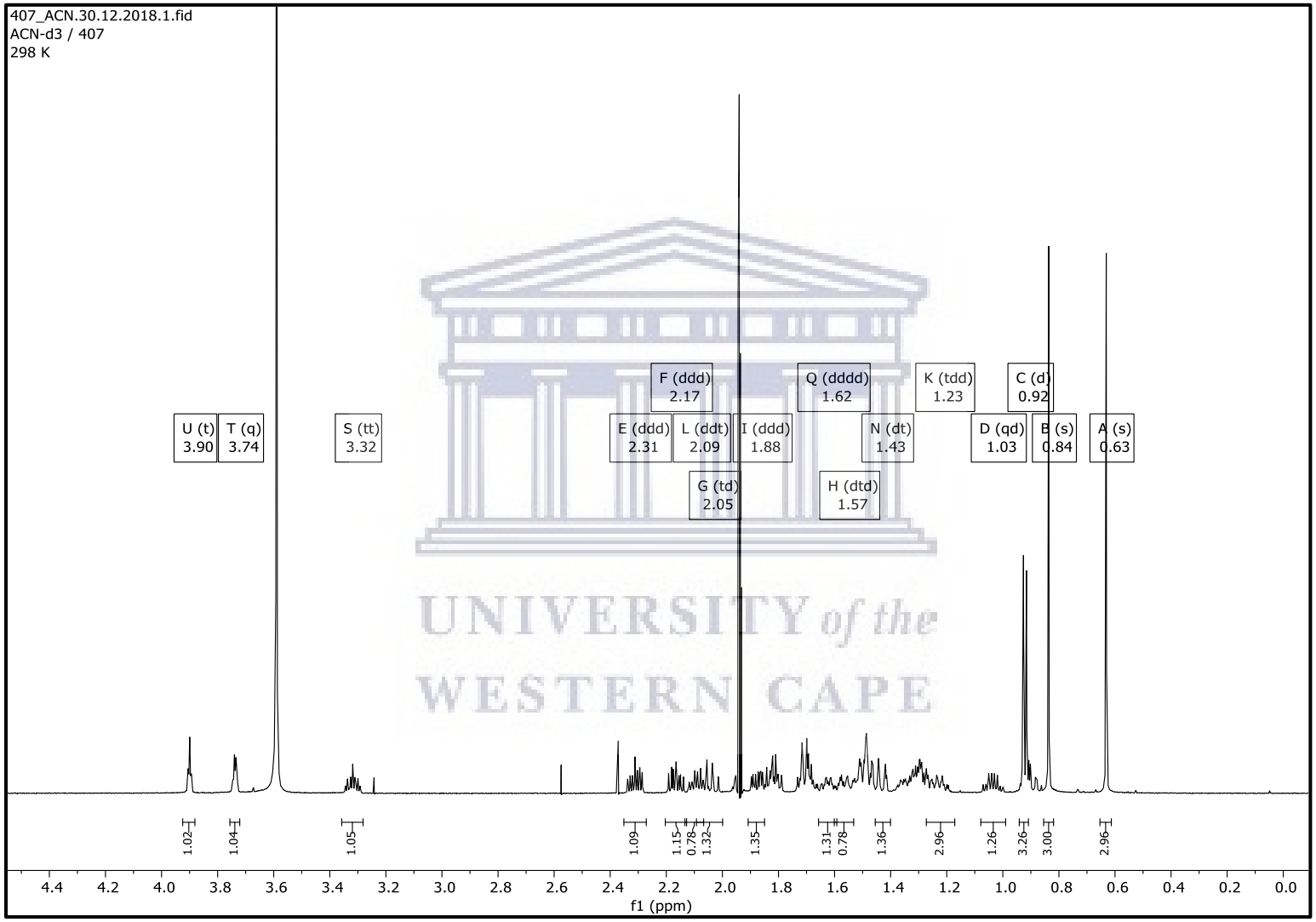

1D Proton NMR spectrum for compound 407 (cholic acid).

Appendix 4B

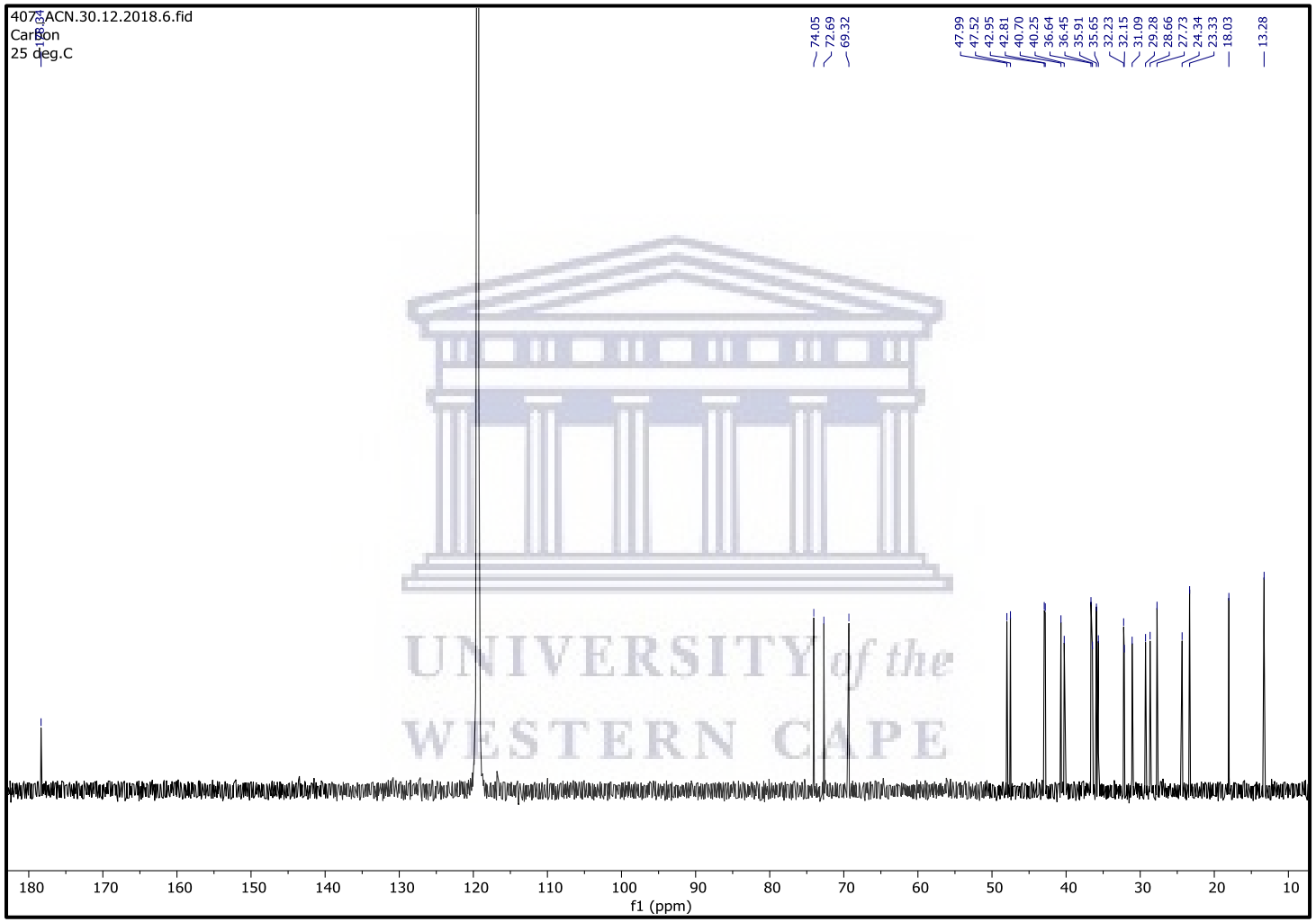

1D Carbon NMR spectrum for compound 407 (cholic acid).

Appendix 4C

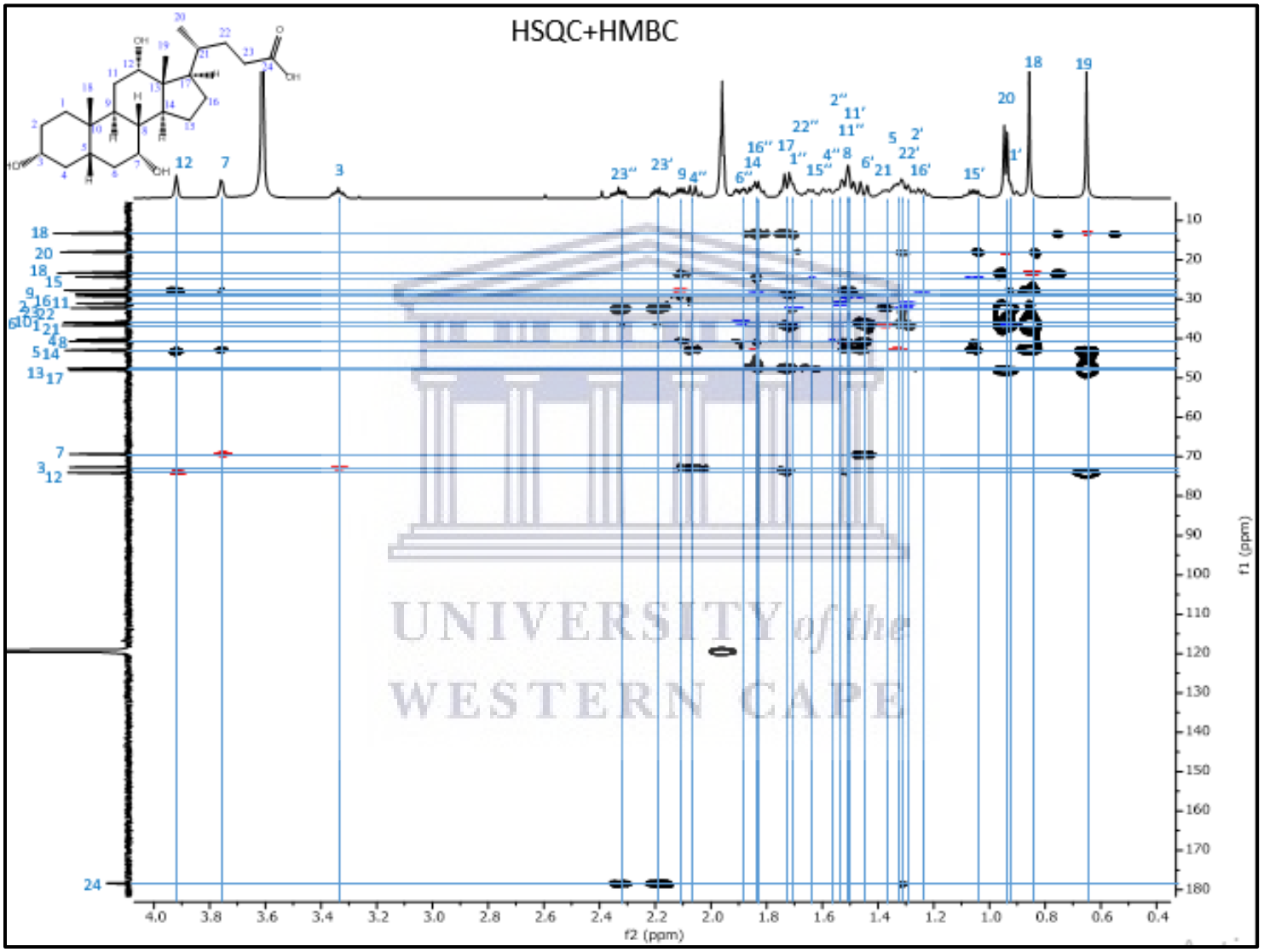

HSQC-HMBC spectrum of compound 407 (cholic acid).

Appendix 4D

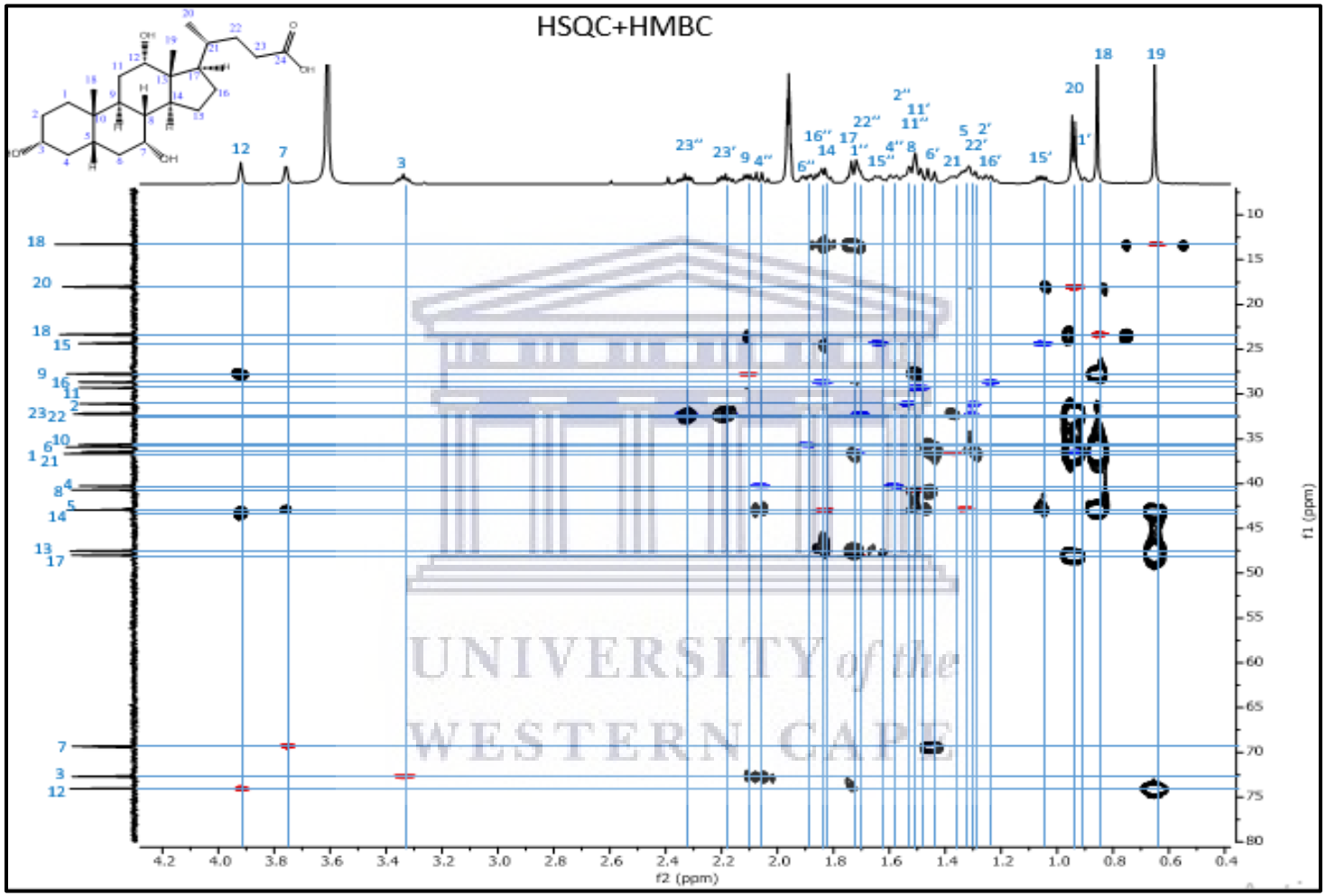

HSQC-HMBC spectrum of compound 405 (3-oxo cholic acid).

Appendix 4E

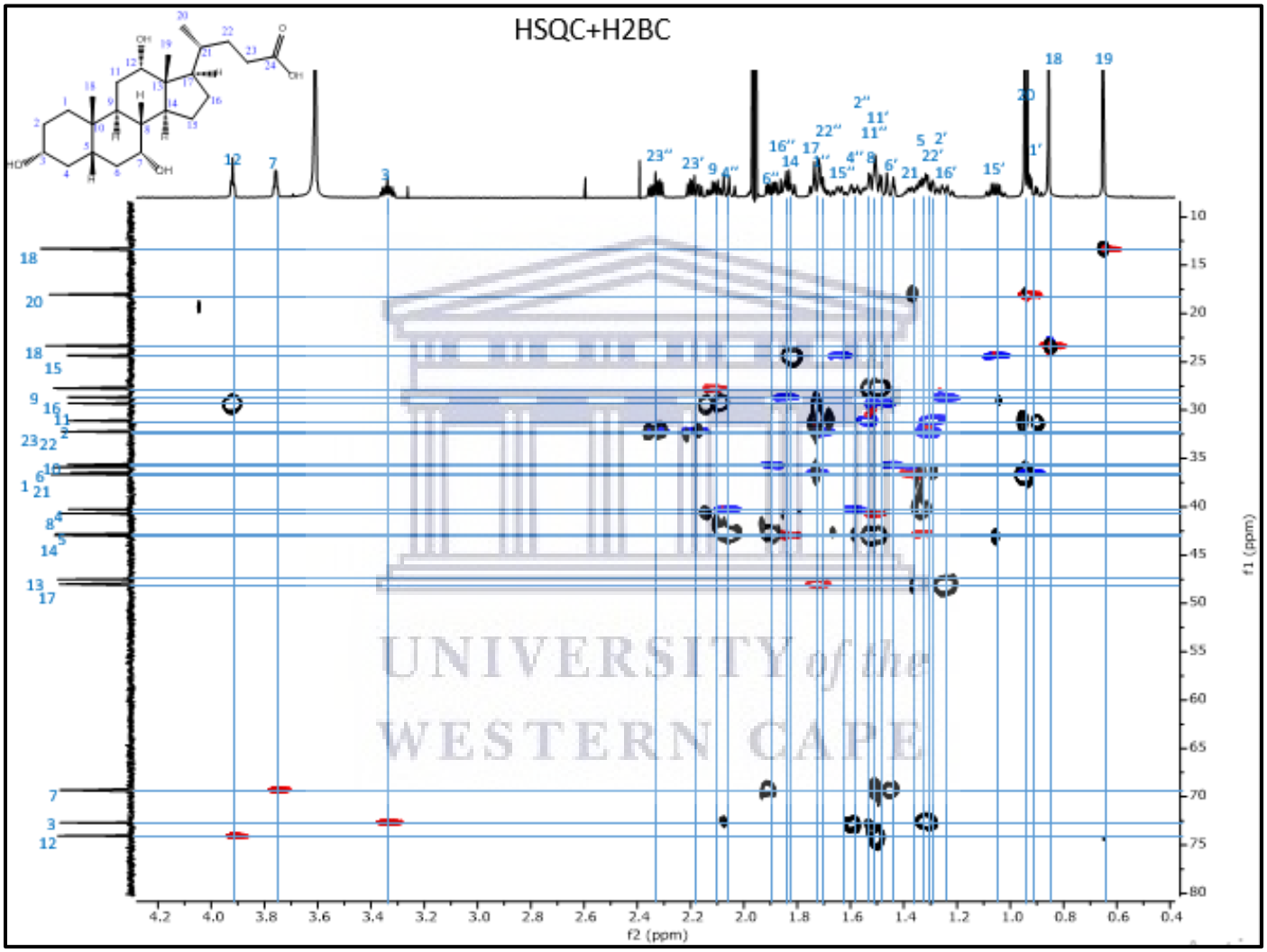

HSQC-H2BC spectrum of compound 407 (cholic acid).

Appendix 4F

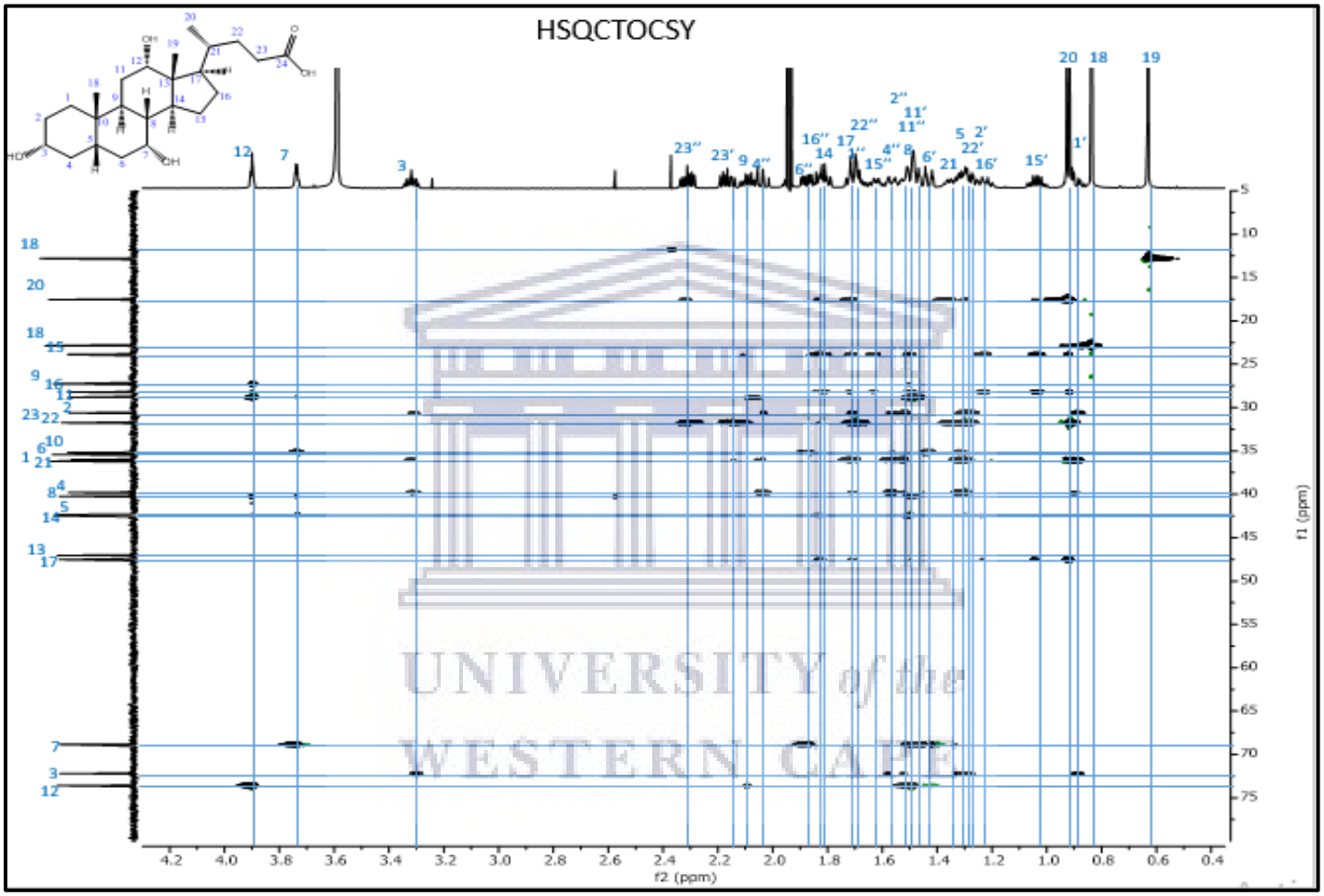

HSQCTOCSY spectrum of compound 407 (cholic acid).

Appendix 4G

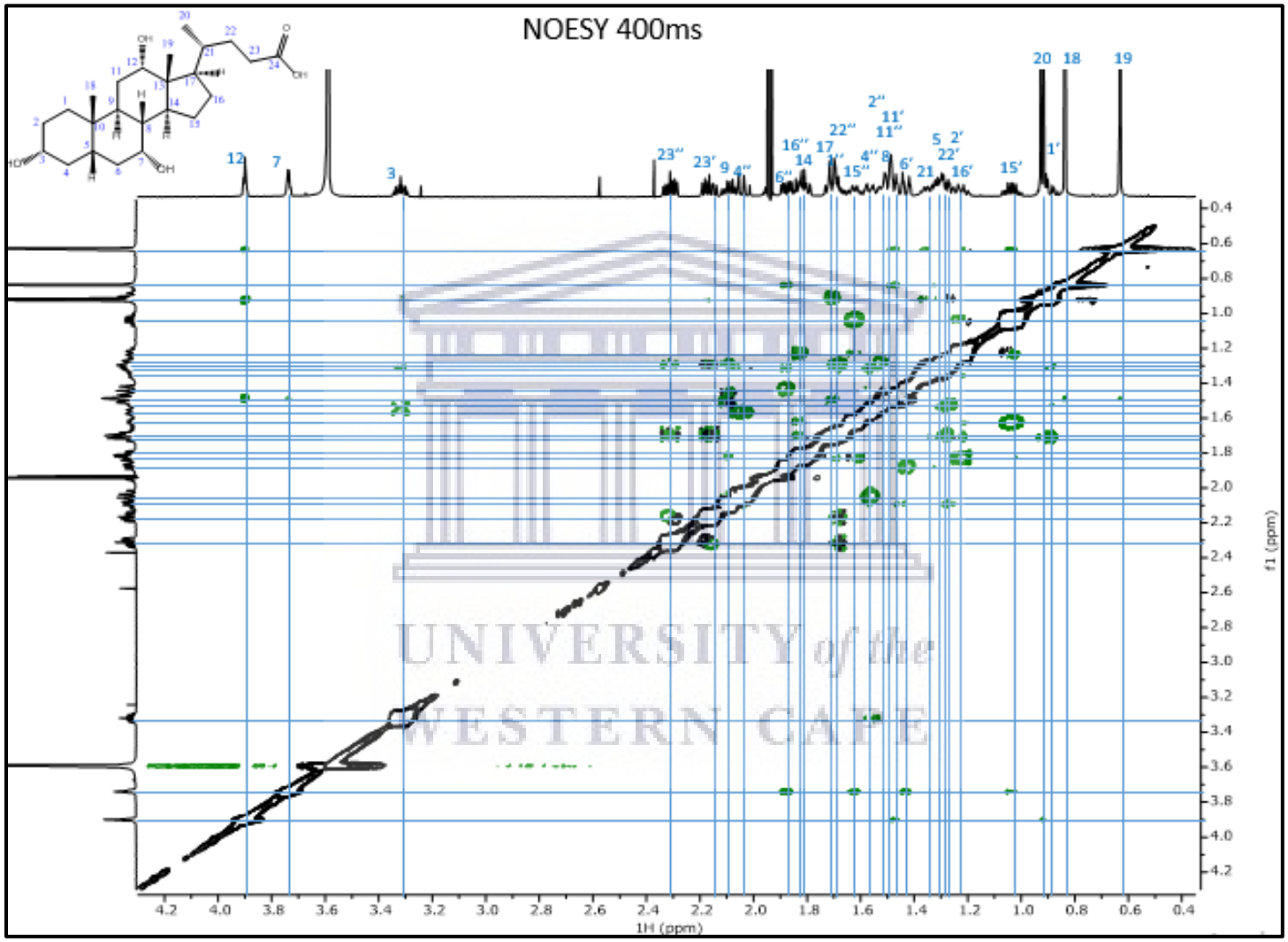

NOESY spectrum of compound 407 (cholic acid).

Appendix 4H

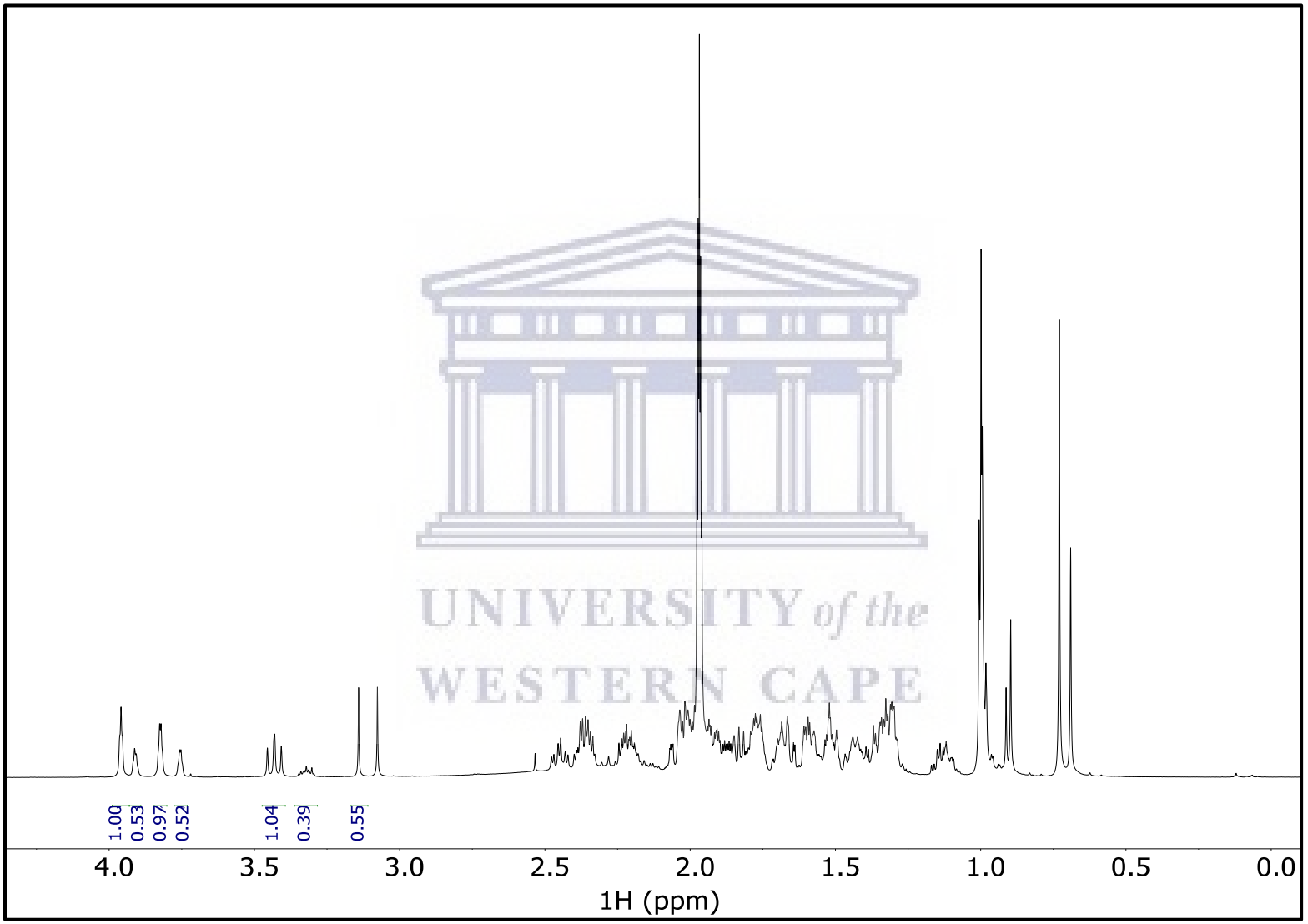

1D Proton NMR spectrum for compound 405 (3-oxo cholic acid).

Appendix 4I

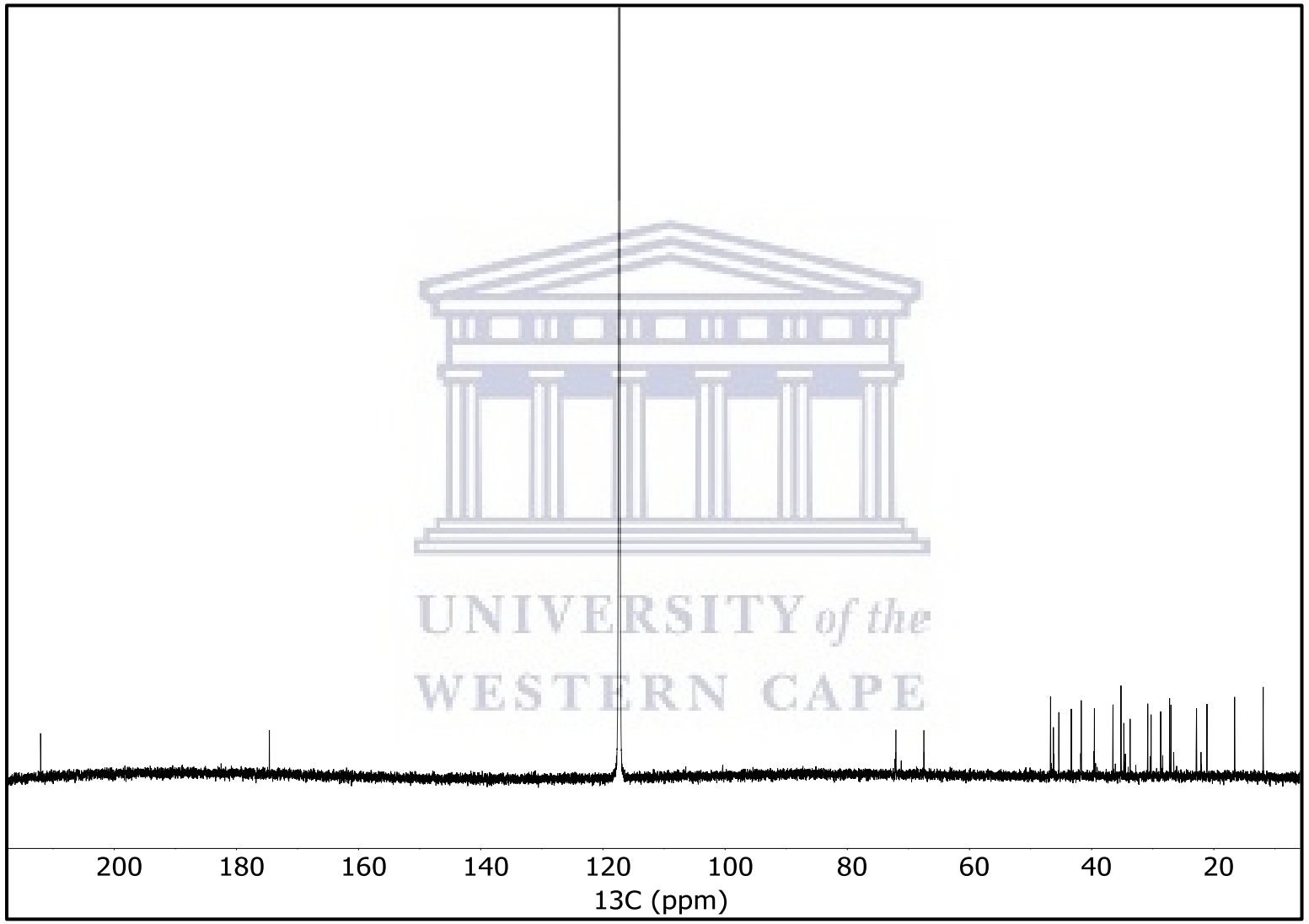

1D Carbon NMR spectrum of compound 405 (3-oxo cholic acid).

Appendix 4J

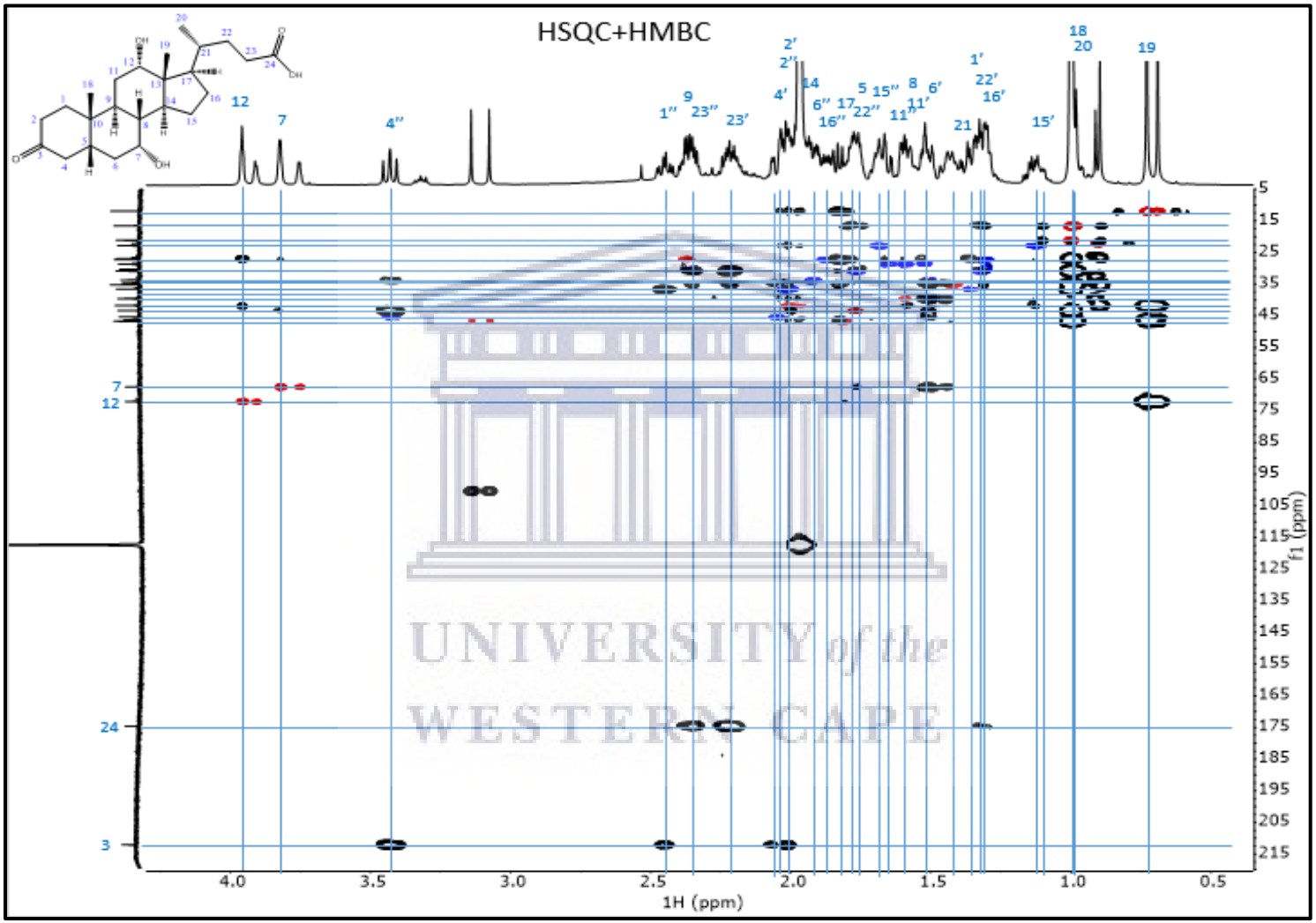

HSQC-HMBC spectrum of compound 405 (3-oxo cholic acid).

Appendix 4K

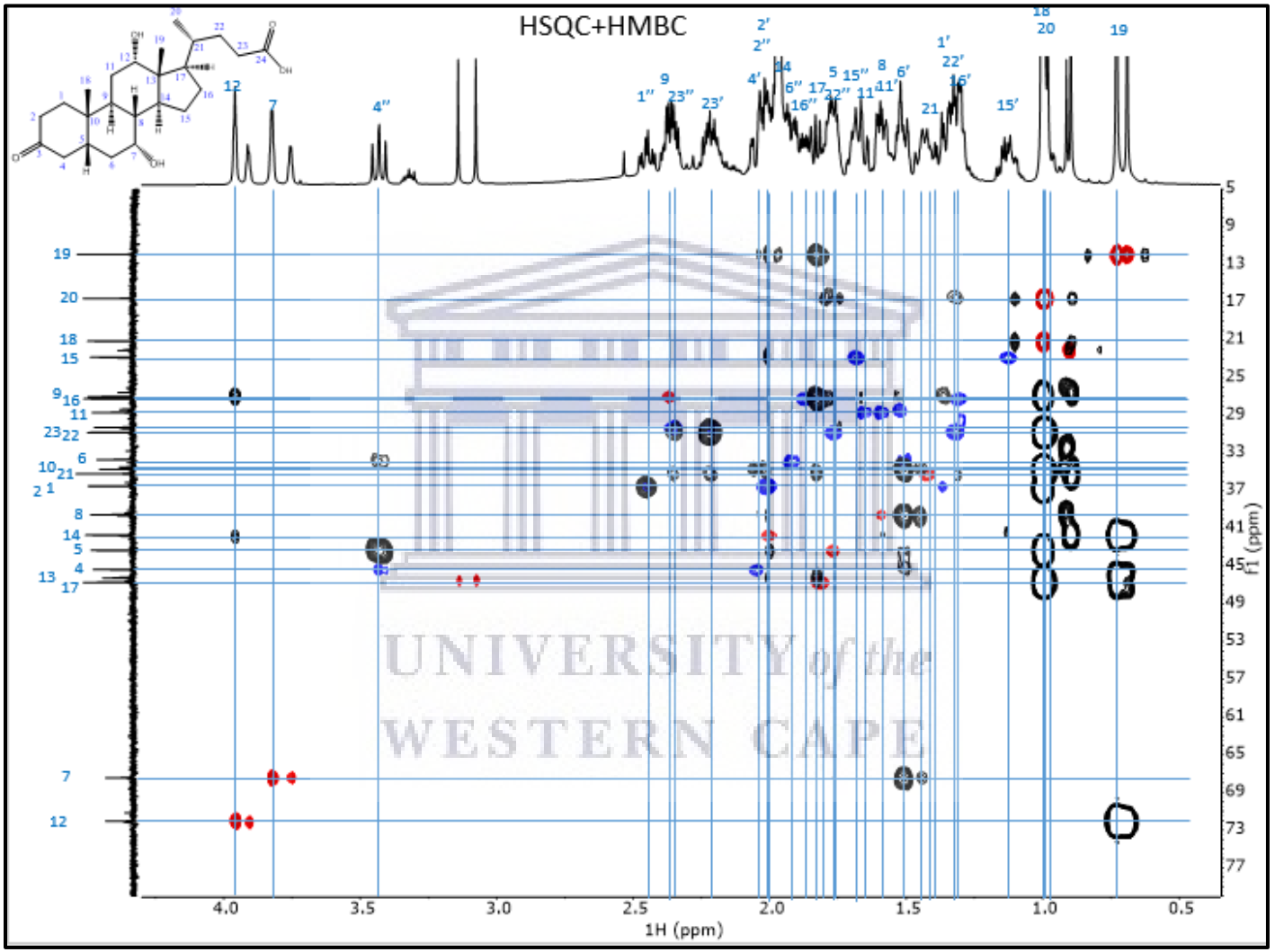

HSQC-HMBC spectrum of compound 405 (3-oxo cholic acid).

Appendix 4L

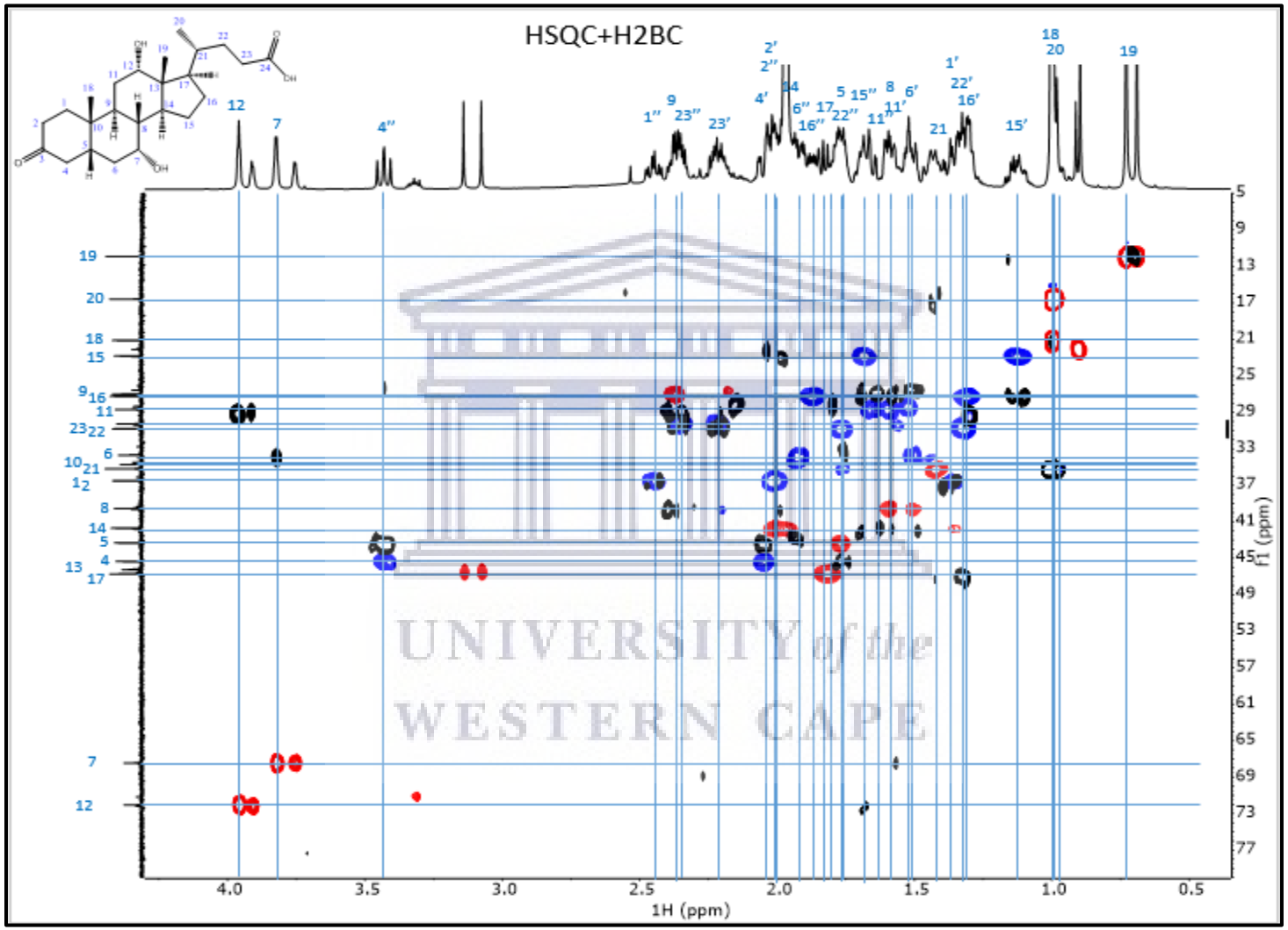

HSQC-H2BC spectrum of compound 405 (3-oxo cholic acid).

References

Adams, S.R. (2019) *Bioactivity-and-genome guided isolation of a novel antimicrobial protein from Thalassomonas viridans*. M.Sc. Thesis. University of the Western Cape. Available at: http://hdl.handle.net/11394/7003 [Accessed 18 February 2020].

Alberti, F., Leng, D.J., Wilkening, I., Song, L., Tosin, M., Corre, C. (2019) Triggering the expression of a silent gene cluster from genetically intractable bacteria results in scleric acid discovery. *Chemical Science*, 10, pp. 453-463.

Allen, H.K., Trachsel, J., Looft, T., Casey, T.A. (2014) Finding alternatives to antibiotics. *Annals of the New York Academy of Sciences*, 1323, pp. 91-100.

Almeida, J.R., Correia-da-Silva, M., Sousa, W., Antunes, J., Pinto, M., Vasconcelos, V., Cunha, I. (2017) Antifouling potential of nature-inspired sulfated compounds. *Scientific Reports*, 7. Available at: https://doi.org/10.1038/srep42424 [Accessed 30 March 2020].

Aminabhavi, T.M. (2015) Chitosan-based hydrogels in biomedicine. *Journal of Pharmaceutical Care and Health Systems*, 2(4). Available at: https://www.longdom.org/open-access/chitosanbased-hydrogels-in-biomedicine-2376-0419-1000e133.pdf [Accessed 8 June 2020].

Andreu, V.P., Dodd, D., Fischbach, MA., Medema, M.H. (2019) gutSMASH: a software package that facilitates systematic analysis of the metabolic potential of anaerobic bacteria. In: *Proceedings of the 5th Dutch Bioinformatics and Systems Biology Conference*, 2-3 April, pp. 79. Available at: https://www.biosb.nl/wp-content/uploads/2019/04/Abstract-book-BioSB-2019-sv.pdf [Accessed 9 June 2020].

Appleton, D.R., Buss, A.D., Butler, M.S. (2007) A simple method for high-throughput extract prefractionation for biological screening. *Chimia*, 61(6), pp. 327-331.

Armbruster, C.R. and Parsek, M.R. (2018) New insight into the early stages of biofilm formation. *Proceedings of the National Academy of Sciences of the United States of America*, 15(7), pp. 4317- 4319.

Arndt, D., Marcu, A., Liang, Y., Wishart, D.S. (2019) PHAST, PHASTER and PHASTEST: Tools for finding prophage in bacterial genomes. *Briefings in Bioinformatics*, 20(4), pp. 1560-1567.

Aslantas, Y. and Surmeli, N.B. (2019) Effects of N-terminal and C-terminal polyhistidine tag on the stability and function of the thermophilic p450 CYP119. *Bioinorganic Chemistry and Applications*. Available at: https://doi.org/10.1155/2019/8080697 [Accessed 16 April 2020].

Atkin, K.E., MacDonald, S.J., Brentnall, A.S., Potts, J.R., Thomas, G.H. (2014) A different path: Revealing the function of staphylococcal proteins in biofilm formation. *FEBS Letters*, 588, pp. 1869-1872.

Aullybux, A.A., Puchooa, D., Bahorun, T., Jeewon, R. (2019) Phylogenetics and antibacterial properties of exopolysaccharides from marine bacteria isolated from Mauritius seawater. *Annals of Microbiology*, 69, pp. 95-972.

Avonce, N., Mendoza-Vargas, A., Morett, E., Iturriaga, G. (2006) Insights on the evolution of trehalose biosynthesis. *BMC Evolutionary Biology*, 6(109). Available at: https://doi.org/10.1186/1471-2148-6-109 [Accessed 25 November 2019].

Badri, A., Williams, A., Lindhardt, R.J., Koffas, M.A.G. (2018) The road to animal-free glycosaminoglycan production: current efforts and bottlenecks. *Current Opinion in Biotechnology*, 53, pp. 85-92.

Bajpai, V.K., Rather, I.A., Lim, J., Park, Y. (2014) Diversity of bioactive polysaccharide originated from marine sources: A review. *Indian Journal of Geo-Marine Sciences*, 43(10), pp. 1857-1869.

Bajracharya, R., Song, J.G., Back, S.Y., Han, H. (2019) Recent Advancements in Non-Invasive Formulations for Protein Drug Delivery. *Computational and Structural Biotechnology Journal*, 17, pp. 1290-1308.

Banik, J.J. and Brady, S.F. (2010) Recent application of metagenomic approaches toward the discovery of antimicrobials and other bioactive small molecules. *Current Opinion in Microbiology*, 13, pp. 603-609.

Banik, S.P., Pal, S., Ghorai, S., Chowdhury, S., Khowala, S. (2009) Interference of sugars in the Coomassie Blue G dye binding assay of proteins. *Analytical Biochemistry*, 386, pp. 113-115.

Bao, H., Li, L., Gan, L.H., Zhang, H. (2008) Interactions between ionic surfactants and polysaccharides in aqueous solutions. *Macromolecules*, 41, pp. 9406-9412.

Becker, A. (2015) Challenges and perspectives in combinatorial assembly of novel exopolysaccharide biosynthesis pathways. *Frontiers in Microbiology*, 6. Available at: https://doi.org/10.3389/fmicb.2015.00687 [Accessed 20 April 2020].

Beckmann, A. and Özbek, S. (2012) The nematocyst: a molecular map of the cnidarian stinging organelle. *The International Journal of Development Biology*, 56, pp. 577-582.

Begley, M., Gahan, C.G.M., Hill, C. (2005) The interaction between bacteria and bile. *FEMS Biotechnology Reviews*, 29, pp. 625-651.

Behrens, H.M., Six, A., Walker, D., Kleanthous, C. (2017) The therapeutic potential of bacteriocins as protein antibiotics. *Emerging Topics in Life Sciences*, 1, pp. 65-74.

Belin, B.J., Busset, N., Giraud, E., Molinaro, A., Silipo, A., Newman, D.K. (2018) Hopanoid lipids: from membranes to plant-bacteria interactions. *Nature Reviews Microbiology*, 16(5), pp. 304-315.

Belter, A., Skupinska, M., Giel-Pietraszuk, M., Grabarkiewicz, T., Rychlewski, L., Barciszewski, J. (2011) Squalene monooxygenase-a target for hypercholesterolemic therapy. *Biological Chemistry*, 392, pp. 1053-1075.

BeMiller, J.N. (2019) Carbohydrate chemistry for food scientists. [e-book] 3rd edition. *ACCC International Press*. Available at: https://doi.org/10.1016/B978-0-12-812069-9.00005-4 [Accessed 16 October 2019].

Benhabiles, M.S., Salah, R., Lounici, H., Drouiche, N., Goosen, M.F.A., Mameri, N. (2012) Antibacterial activity of chitin, chitosan and its oligomers prepared from shrimp shell waste. *Food Hydrocolloids*, 29, pp. 48-56.

Bertrand S, Bohni N, Schnee S, Schump O, Gindro K, Wolfender JL (2014) Metabolite induction via microorganism co-culture: A potential way to enhance chemical diversity for drug discovery. *Biotechnology advances* 32, pp. 1180-1204.

Bhaskar, P.V. and Bhosle, N.B. (2005) Microbial extracellular polymeric substances in marine biogeochemical processes. *Current Science*, 88(1), pp. 45-53.

Birkholtz, L., Blatch, G., Coetzer, T.L., Hoppe, H.C., Human, E., Morris, E.J., Ngcete, Z., Oldfield, L., Roth, R., Shonhai, A., Stephens, L., Louw, A.I. (2008) Heterologous expression of plasmodial proteins for structural studies and functional annotation. *Malaria Journal*, 7(197). Available at: https://doi.org/10.1186/1475-2875-7-197 [Accessed 21 May 2020].

Birri, D.J., Brede, D.A., Forberg, T., Holo, H., Nes, I.F. (2010) Molecular and Genetic Characterization of a Novel Bacteriocin Locus in *Enterococcus avium* Isolates from Infants. *Applied and Environmental Microbiology*, 76(2), pp. 483-492.

Blaszczyk, U. and Moczarny, J. (2016) Bacteriocins of Gram-negative bacteria – structure, mode of action and potential application. *Advancements of Microbiology*, 55(2), pp. 157-171.

Blockley, A., Elliott, D.R., Roberts, A.P., Sweet, M. (2017) Symbiotic Microbes from Marine Invertebrates: Driving a New Era of Natural Product Drug Discovery. *Diversity*, 9(4). Available at: https://doi.org/10.3390/d9040049 [Accessed 8 January 2020].

Bobzin, S.C., Yang, S., Kasten, T.P. (2000) LC-NMR: a new tool to expedite the dereplication and identification of natural products. *Journal of Industrial Microbiology and Biotechnology*, 25, pp. 342-345.

Bolanos-Garcia, V.M. and Davies, O.R. (2006) Structural analysis and classification of native proteins from E. coli commonly co-purified by immobilized metal affinity chromatography. *Biochimica et Biophysica Acta*, 1760, pp. 1304-1313.

Boleij, M., Pabst, M., Neu, T.R., van Loosdrecht, M.C.M., Lin, Y. (2018) Identification of glycoproteins isolated from extracellular polymeric substances of full-scale anammox granular sludge. *Environmental Science and Technology*, 52, pp. 13127-13135.

Borbón, H., Váldes, S., Alvarado-Mesén, J., Soto, R., Vega, I. (2016) Antimicrobial properties of sea anemone *Anthopleura nigrescens* from Pacific coast of Costa Rica. *Asian Pacific Journal of Tropical Biomedicine*, 6(5), pp. 418-421.

Bosch, T.C.G. (2013) Cnidarian-Microbe Interactions and the Origin of Innate Immunity in Metazoans. *Annual Review of Microbiology*, 67, pp. 499-518.

Broach, B., Gu, X., Bar-Peled, M. (2012) Biosynthesis of UDP-glucuronic acid and UDP-galacturonic acid in *Bacillus cereus* subsp. cytotoxis NVH 391-98. *FEBS Journal*, 279(1). Available at: https://doi.org/10.1111/j.1742-4658.2011.08402.x [Accessed 6 December 2019].

BundaloviC-Torma, C., Whitfield, G.B., Marmont, L.S., Howell, P.L., Parkinson, J. (2020) A systematic pipeline for classifying bacterial operons reveals the evolutionary landscape of biofilm machinery. *PLoS Computational Biology*, 16(4). Available at: https://doi.org/10.1371/journal.pcbi.1007721 [Accessed 22 April 2020].

Burg, A. and Oshrat, L. (2015) Salt effect on the antioxidant activity of red microalgal sulfated polysaccharides in soy-bean formula. *Marine Drugs*, 13, 6425-6439.

Callister, S.J., Barry, R.C., Adkins, J.N., Johnson, E.T., Qian, W., Webb-Robertson, B.M., Smith, R.D., Lipton, M.S. (2006) Normalization approaches for removing systematic biases associated with mass spectrometry and label-free proteomics. *Journal of Proteome Research*, 5(2), pp. 277-286.

Campbell, K.P., MacLennan, D.H., Jorgensen, A.O. (1983) Staining of the Ca^{2+} -binding proteins, calsequestrin, calmodulin, troponin C, and S-100, with cationic carbocyanine dye "Stains-All". *The Journal of Biological Chemistry*, 258(18), pp. 11267-11273.

Cane, D.E., Walsh, C.T. (1999) The parallel and convergent universes of polyketide synthases and nonribosomal peptide synthetases. *Chemistry and Biology*, 6(12), pp. 319-325.

Cano, L.P.P., Bartolotta, S.A., Casanova, N.A., Siless, G.E., Portmann, E., Schejter, L., Palermo, J.A., Carballo, M.A. (2013) Isolation of acetylated bile acids from the sponge Siphonochalina fortis and DNA damage evaluation by comet assay. *Steroids*, 78, pp. 982-986.

Cao, S., Xu, S., Wang, H., Ling, Y., Dong, J., Xia, R., Sun, X. (2019) Nanoparticles: Oral delivery for protein and peptide drugs. *AAPS PharmSciTech*, 20(190). Available at: https://doi.org/10.1208/s12249-019-1325-z [Accessed 28 April 2020].

Carvalhal, F., Correira-da-Silva, M., Sousa, E., Pinto, M., Kijjoa, A. (2018) Sources and biological activities of marine sulfated steroids. *Journal of Molecular Endocrinology*, 61(2), pp. 211-231.

Casertano, M., Avunduk, S., Kacar, A., Omuzbuken, B., Menna, M., Luciano, P., Aiello, A., Imperatore, C. (2019) Analysis of Anti-Biofilm Activities of Extracts from Marine Invertebrate Collected from Izmir Bay (Eastern Aegean Sea). *Biomedical Journal of Scientific and Technical Research*, 20(3), pp. 15023-15028.

Casillo, A., Lanzetta, R., Parrilli, M., Corsaro, M.M. (2018) Exopolysaccharides from Marine and Marine Extremophilic Bacteria: Structures, Properties, Ecological Roles and Applications. *Marine Drugs*, 16(2). Available at: https://doi.org/10.3390/md16020069 [Accessed 9 April 2019].

Castellane, T.C.L., Otoboni, A.M.M.B., Lemos, E.G.M. (2015) Characterization of exopolysaccharides produced by *Rhizobia* species. *Brazilian Journal of Soil Science*, 39, pp. 1566-1575.

Catanzaro, K.C.F., Champion, A.E., Mohaptra, N., Cecere, T., Inzana, T.J. (2017) Glycosylation of a capsule-like complex (CLC) by *Francisella novicida* is required for virulence and partial protective immunity in mice. *Frontiers in Microbiology*, 8(935). Available at: https://doi.org/10.3389/fmicb.2017.00935 [Accessed 8 May 2020].

Cerqueira, N.M.F.S.A., Oliveira, E.F., Gesto, D.S., Santos-Martins, D., Moreira, C., Moorthy, H.N., Ramos, M.J., Fernandes, P.A. (2016) Cholesterol biosynthesis: A mechanistic overview. *Biochemistry*, 55, pp. 5483-5506.

Cescutti, P. (2009) Bacterial capsular polysaccharides and exopolysaccharides. In: O. Holst, P.J. Brennan, M. von Itzstein, eds. *Microbial glycobiology*. 1st ed. Elsevier Inc., pp. 93-108.

Chater, K.F. (2016) Recent advances in understanding Streptomyces. *F1000 Research*, 5:2795. Available at: https://doi.org/10.12688/f1000research.9534.1 [Accessed 23 January 2020].

Chen, H., O'Connor, S., Cane, D.E., Walsh, C.T. (2001) Epothilone biosynthesis: assembly of the methylthiazolylcarboxy starter unit on the EpoB subunit. *Chemistry and biology*, 8, pp. 899-912.

Chen, R., Wong, H.L., Burns, B.P. (2019) New approaches to detect biosynthetic gene clusters in the environment. *Medicines*, 6(1). Available at: https://doi.org/10.3390/medicines6010032 [Accessed 2 April 2020].

Chen, Y., Yuan, Q., Shan, L., Lin, M., Cheng, D., Li, C. (2013) Antitumor activity of bacterial exopolysaccharides from the endophyte *Bacillus amyloliquefaciens* sp. isolated from *Ophiopogon japonicus. Oncology Letters*, 5, pp. 1787-1792.

Cheng, J., Sibley, C.D., Zaheer, R., Finan, T.M. (2007) A *Sinorhizobium meliloti minE* mutant has an altered morphology and exhibits defects in legume symbiosis. *Microbiology*, 153, pp. 375-387.

Chhonker, Y.S., Haney, S.L., Bala, V., Holstein, S.A., Murry, D.J. (2018) Simultaneous quantitation of isoprenoid pyrophosphates in plasma and cancer cells using L-MS/MS.

Molecules, 23(12). Available at: https://doi.org/10.3390/molecules23123275 [Accessed 20 February 2020].

Chiang Y, Chang S, Oakley BR, Wang CCC (2011) Recent advances in awakening silent biosynthetic gene clusters and linking orphan clusters to natural products in microorganisms. *Current Opinion in Chemical Biology* 15, 137-143.

Chow, P.S. and Landhäusser, S.M. (2004) A method for routine measurement of total sugar and starch content in woody plant tissue. *Tree Physiology*, 24, pp. 1129-1136.

Chludil, H.D. and Maier, M.S. (2005) Minutosides A and B, antifungal sulfated steroid xylosides from the Patagonian starfish *Anasterias minuta*. *Journal of Natural Products*, 68(8). Available from: https://doi.org/10.1021/np050086f [Accessed 24 April 2020].

Choi, A.H.K., Slamti, L., Avci, F.Y., Pier, G.B., Maira-Litrán, T. (2009) The *pgaABCD* locus of Acinetobacter baumannii encodes the production of poly-β-1-6-*N*-acetylglucosamine, which is critical for biofilm formation. *Journal of Bacteriology*, 191(19), pp. 5953-5963.

Chong, B.F., Blank, L.M., Mclaughlin, R., Nielsen, L.K. (2005) Microbial hyaluronic acid production. *Applied Microbiology and Biotechnology*, 66, pp. 341-351.

Christianson, D.A. (2017) Structural and chemical biology of terpenoid cyclases. Chemical Reviews, 117, pp. 11570-11648.

Christie, W.W. (2019) Sterols: Bile acid and alcohols. *The Lipid Web*, 23 December. Available at: https://www.lipidhome.co.uk/lipids/simple/bileacids/index.htm [Accessed 12 February 2020].

Chung, P.Y. and Toh, Y.S. (2014) Anti-biofilm agents: recent breakthrough against multidrug resistant *Staphylococcus aureus*. *Pathogen and Disease*, 70, pp. 231-239.

Cifuente, J.O., Comino, N., Trastoy, B., D'Angelo, C., Guerin, M.E. (2019) Structural basis of glycogen metabolism in bacteria. *Biochemical Journal*, 476, pp. 2059-2092.

Cimini, D., Restaino, O.F., Schiraldi, C. (2018) Microbial production and metabolic engineering of chondroitin and chondroitin sulfate. *Emerging Topics in Life Science*, 2(3), pp. 349-361.

Clardy, J. and Walsh, C. (2004) Lessons from natural molecules. *Nature*, 432, pp. 829-837

Cortazzo, P., Cerveñansky, Marín, M., Reiss, C., Ehrlich, R., Deana, A. (2002) Silent mutations affect in vivo protein folding in *Escherichia coli*. *Biochemical and Biophysical Research Communications*, 293, pp. 537-541.

Corzo, J., Pérez-Galdona, R., León-Barrios, M., Gutiérrez-Navarro, A.M. (1991) Alcian blue fixation allows silver staining of the isolated polysaccharide component of bacterial lipopolysaccharides in polyacrylamide gels. *Electrophoresis*, 12, pp. 439-441.

Cue, D., Lei, M.G., Lee, C.Y. (2012) Genetic regulation of the intracellular adhesion locus in staphylococci. *Frontiers in Cellular and Infection Microbiology*, 2(38). Available at: https://doi.org/10.3389/fcimb.2012.00038 [Accessed 21 April 2020].

Cuevas, D.A., Garza, D., Sanchez, S.E., Rostron, J., Henry, C.S., Vonstein, V., Overbeek, R.A., Segall, A., Rohwer, F., Dinsdale, E.A., Edwards, R.A. (2016) Elucidating genomic gaps using phylogenetic profiles. *F1000 Research*, 3:210. Available at https://doi.org/10.12688/f1000research.5140.2 [Accessed 30 May 2020].

Cvejic, J.H., Putra, S.R., El-Beltagy, A., Hattori, R., Hattori, T., Rohmer, M. (2000) Bacterial triterpenoids of the hopane series as biomarkers for the chemotaxonomy of *Burkholderia*, *Pseudomonas* and *Ralstonia* sp. *FEMS Microbiology Letters*, 183, pp. 295-299.

Cywes-Bentley, C., Skurnik, D., Zaidi, T., Roux. D., DeOliviera, R.B., Garrett, W.S., Lu, X., O'Malley, J., Kinzel, K., Zaidi, T., Rey, A., Perrin, C., Fichorova, R.N., Kayatani, A.K.K., Maira-Litràn, T., Gening, M.L., Tsvetkov, Y.E., Nifantiev, N.E., Bakaletz, L.O., Pelton, S.I., Golenbock, D.T., Pier, G.B. (2013) Antibody to a conserved antigenic target is protective against diverse prokaryotic and eukaryotic pathogens. *PNAS*, 110(24). Available at: https://doi.org/10.1073/pnas.1303573110 [Accessed 14 September 2020].

Czarnik, A.W. and Mei, H.Y. (2007) How and why to apply the latest technology. In: Taylor, J.B. and Triggles, D.J, eds. *Comprehensive Medicinal Chemistry II*. Elsevier Inc., USA.

Available at: https://doi.org/10.1016/B0-08-045044-X/00048-1 [Accessed 23 November 2019].

Da Silva Antonio, A., Wiedemann, L.S.M., Veiga-Junior, V.F. (2020) Natural Products' role against COVID-19. *The Royal Society of Chemistry*, 10, pp. 23379-23393.

Da Silva, L.C.A., Honorato, T.L., Cavalcante, R.S., Franco, T.T., Rodrigues, S. (2012) Effect of pH and temperature on enzyme activity of chitosanase produced under solid state fermentation by *Trichoderma* spp. *Indian Journal of Microbiology*, 52(1), pp. 60-65.

Darkoh, C., Lichtenberg, L.M., Ajami, N., Dial, E.J., Jiang, Z., DuPont, H.L. (2010) Bile acids improve the antimicrobial effect of rifamixin. *Antimicrobial Agents and Chemotherapy*, 54(9), pp. 3618-3624.

Dave, S.R., Upadhyay, K.H., Vaishnav, A.M., Tipre, D.R. (2020) Exopolysaccharides from marine bacteria: production, recovery and applications. *Environmental Sustainability*, 3. Available at: https://doi.org/10.1007/s42398-020-00101-5 [Accessed 2 June 2020].

Davidson, E.A. (2020) *Carbohydrate.* Available at: https://www.britannica.com/science/carbohydrate/Sucrose-and-trehalose [Accessed 8 June 2020].

De Carvalho, C.C.C.R. and Fernandes, P. (2010) Production of Metabolites as Bacterial Responses to the Marine Environment. *Marine Drugs*, 8(3), pp. 705-727.

De Vijlder, T., Valkenborg, D., Lemiére, F., Romjin, E.P., Laukens, K., Cuyckens, F. (2017) A tutorial in small molecule identification via electrospray ionization-mass spectrometry: The practical art of structural elucidation. *Mass Spectrometry Reviews*, 37, pp. 607-629.

Debbab, A., Aly, A.H., Lin, W.H., Proksch, P. (2010) Bioactive compounds from marine bacteria and fungi. *Microbial Biotechnology*, 3(5), pp. 544-563.

Delbarre-Ladrat, C., Sinquin, C., Lebellenger, L., Zykwinska, A., Colliec-Jouault, S. (2014) Exopolysaccharides produced by marine bacteria and their applications as

glycosaminoglycan-like molecules. *Frontiers in Chemistry*, 2(85). Available at https://doi.org/10.3389/fchem.2014.00085 [Accessed 17 April 2020].

Demain, AL (1998) Induction of microbial secondary metabolism. *International Microbiology*,1, pp. 259-264.

Dhar, M.K., Koul, A., Kaul, S. (2013) Farnesyl pyrophosphate synthase: a key enzyme in isoprenoid biosynthetic pathway and potential molecular target for drug development. *New Biotechnology*, 30(2), pp. 114-123.

Dias, D.A., Urban, S., Roessner, U. (2012) A Historical Overview of Natural Products in Drug Discovery. *Metabolites*, 2, pp. 303-336.

Dockyu, K., Lee, J.S., Kim, J., Kang, S., Yoon, J., Kim, W.G., Lee, C.H. (2007) Biosynthesis of bile acids in a variety of marine bacterial taxa. *Journal of Microbiology and Biotechnology*, 17(3), pp. 403-407.

Dong, S., Chesnokova, O.N., Turnbough, C. L. Jnr., Pritchard, D.G. (2009) Identification of the UDP-N-acetylglucosamine 4-epimerase involved in exosporium protein glycosylation in *Bacillus anthracis*. *Journal of Bacteriology*, 191(22), pp. 7094-7101.

Donlan, R.M. (2011) Biofilm Elimination on Intravascular Catheters: Important Considerations for the Infectious Disease Practitioner. *Clinical Infectious Disease*, 52(8), pp. 1038-1045.

Doughty, D.M., Dieterle, M., Sessions, A.L., Fischer, W.W., Newman, D.K. (2014) Probing the subcellular localization of hopanoid lipids in bacteria using NanoSIMS. *PLoS ONE*, 9(1). Available at: https://doi.org/10.1371/journal.pone.0084455 [Accessed 21 February 2020].

Duarte, I. (2012) *Characterization of a broad host range tailocin from Burkholderia*. Ph.D. Thesis. Texas A & M University. Available at: http://hdl.handle.net/1969.1/ETD-TAMU-2012-08-11636 [Accessed 19 September 2019].

Duncan, M.W., Aebersold, R., Caprioli, R.M. (2010) The pros and cons of peptide-centric proteomics. *Nature Biotechnology*, 28(7), pp. 659-664.

Efthimiadou, E.K., Metaxa, A., Kordas, G. (2014) Modified polysaccharides as drug delivery. In: Ramawat, K.G. and Mérillon, J, eds. *Polysaccharides*. Springer International Publishing, pp. 1-26.

Egieyeh, S., Syce, J., Malan, S.F., Christoffels, A. (2018) Predictive classifier model built from natural products with antimalarial bioactivity using machine learning approach. *PLoS One*, 13(9). Available at: https://journals.plos.org/plosone/article?id=10.1371/journal.pone.0204644 [Accessed 2 January 2020].

Elsakhawy, T.A., Sherief, F.A., Abd-EL-Kodoos, R.Y. (2017) Marine Microbial Polysaccharides: Environmental Role and Applications (An Overview). *The Environment, Biodiversity and Soil Security*, 1, pp. 61-70.

Eoh, H., Narayanasamy, P., Brown, A.C., Parish, T., Brennan, P.J., Crick, D.C. (2009) Expression and characterization of soluble 4-diphosphocytidyl-2-C-methyl-D-erythritol kinase from bacterial pathogens. *Chemistry and Biology*, 16(12), pp. 1230-1239.

Eteshola, E., Gottlieb, M., Arad, S.M. (1996) Dilute solution viscosity of red microalga exopolysaccharide. *Chemical Engineering Science*, 51(9), pp. 1487-1494.

Evidente, A., Kornienko, A., Lefranc, F., Cimmino, A., Dasari, R., Evidente, M., Mathieu, V., Kiss, R. (2015) Sesterpenoids with anticancer activity. *Current Medicinal Chemistry*, 22(30), pp. 3502-3522.

Farrel, R.E. (2010) Electrophoresis of RNA. In: *RNA methodologies*. 4th edition. Elsevier Inc., pp. 79-219. Available at: https://doi.org/10.1016/B978-0-12-374727-3.00009-7 [Accessed 17 July 2019].

Felczykowska A, Bloch SK, Nejman-Falenczyk, Baranska S (2012) Metagenomic approach in the investigation of new bioactive compounds in the marine environment. *Acta Biochimica Polonica* 59, 501-505.

Field, D., Cotter, P., Hill, C., Ross, R.P. (2007) Bacteriocin biosynthesis, structure and function. In: O. Gillor and M.A. Riley, eds. *Research and Applications in Bacteriocins*. Horison Bioscience, pp. 6-40.

Fisch, K.M. (2013) Biosynthesis of natural products by microbial iterative hybrid PKS-NRPS. The *Royal Society of Chemistry*, 3, pp. 18228-18247.

Fischer, E. and Braun, V. (1981) Permeability barrier of bacterial cell envelopes as cause of resistance to antibiotics. *Immune Infection*, 9(3), pp. 78-87.

Fournes, F., Val, M., Skovgaard, O., Mazel, D. (2018) Replicate once per cell cycle: Replication control of secondary chromosomes. *Frontiers in Microbiology*, 9. Available at: https://doi.org/10.3389/fmicb.2018.01833 [Accessed 11 March 2020].

François, J. and Parrou, J.L. (2001) Reserve carbohydrates metabolism in the yeast *Saccharomyces cerevisiae*. *FEMS Microbiology Reviews*, 25, pp. 125-145.

Freckelton, M.L., Nedved, B.T., Hadfield, M.G. (2017) Induction of Invertebrate Larval Settlement; Different Bacteria, Different Mechanisms? *Scientific Reports*, 7:42557. Available at https://doi.org/10.1038/srep42557 [Accessed 19 September 2019].

Furuno, J.P., Comer, A.C., Johnson, K., Rosenberg, J.H., Moore, S.L., MacKenzie, T.D., Hall, K.K., Hirshon, J.M. (2014) Using antibiograms to improve antibiotic prescribing in skilled nursing facilities. *Infection Control and Hospital Epidemiology*, 35(3), pp. 56-61.

Gaudelli, N.M., Long, D.H., Townsend, C.A. (2015) β-lactam formation by a non-ribosomal peptide synthetase during antibiotic biosynthesis. Nature, 520(7547), pp. 383-387.

Gaudêncio, S.P., Pereira, F. (2015) Dereplication: racing to speed up the natural products discovery process. *Natural Product Reports*, 32(6), pp. 779-810.

Gaudet, R.G. and Gray-Owen, S.D. (2016) Heptose sounds the alarm: Innate sensing of a bacterial sugar stimulates immunity. *PLoS Pathogens*, 12(9). Available at: https://doi.org/10.1371/journal.ppat.1005807 [Accessed 18 November 2019].

Ge, P., Scholl, D., Prokhorov, N.S., Avaylon, J., Shneider, M.M., Browning, C., Buth, S.A., Plattner, M., Chakraborty, U., Ding, K., Leiman, P.G., Miller, J.F., Zhou, Z.H. (2020) Action of a minimal contractile bactericidal nanomachine. Nature, 580, pp. 658-662.

Gerberding, J.L. (2020) Antibiotic resistance: The hidden threat lurking behind COVID-19. *STAT*, 23 March. Available at: https://www.statnews.com/2020/03/23/antibiotic-resistance-hidden-threat-lurking-behind-covid-19/ [Accessed 1 April 2020].

Gerwick, W.H. and Fenner, A. (2013) Drug discovery from marine microbes. *Microbial ecology* 65(4), pp. 800-806

Ghequire, M.G.K. and De Mot, R. (2015) The tailocin tail: Peeling off phage tails. *Trends in Microbiology*, 23(10), pp. 587-590.

Girri, S. and Singh, J. (2013) New Face in the Row of Human Therapeutics: Bacteriocins. *Journal of Microbiology Research*, 3(2), pp. 71-78.

Goldberg, H.A. and Warner, K.J. (1997) The staining of acidic proteins on polyacrylamide gels: Enhanced sensitivity and stability of "Stains-All" staining in combination with silver nitrate. *Analytical Biochemistry*, 251(2), pp. 227-233.

Gomes, A.R., Byregowda, S.M., Veeregowda, B.M., Balamurugan, V. (2016) An overview of heterologous expression host systems for the production of recombinant proteins. *Advances in Animal and Veterinary Sciences*, 4(7), pp. 346-356.

Gómez, M.A., Bonilla, J.M., Coronel, M.A., Martínez, J., Morán-Trujillo, L., Orellana, S.L., Vidal, A., Giacaman, A., Morales, C., Torres-Gallegos, C., Concha, M., Oyarzun-Ampuero, F., Godoy, P., Lisoni, J.G., Henríquez-Báez, C., Bustos, C., Moreno-Villoslada, I. (2018) Antibacterial activity against *Staphylococcus aureus* of chitosan/chondroitin sulfate nanocomplex aerogels alone and enriched with erythromycin and elephant garlic (*Allium ampeloprasum L. var. ampeloprasum*) extract. In: *Proceedings of the 12th*

European Chitin Society (EUCHIS)/13th International Conference on Chitin and Chitosan (ICCC). Volume 90. Germany, 30 August-2 September, pp. 885-900. Available at: https://doi.org/10.1515/pac-2016-1112 [Accessed 2 April 2020].

Gomez-Orellana, I. (2005) Strategies to improve oral drug bioavailability. *Expert Opinion on Drug Delivery*, 2(3), pp. 419-433.

González, M.A. (2010) Scalarane sesterpenoids. *Current Bioactive Compounds*, 6. Available at: https://www.uv.es/gonzalma/articles/Gonzalez-MS.pdf. [Accessed 14 Sepetember 2019].

Green, D.E. and DeAngelis, P.L. (2017) Identification of a chondroitin synthase from an unexpected source, the green sulphur bacterium *Chlorobium phaeobacteriodes*. *Glycobiology*, 27(5), pp. 469-476.

Green, G. (2020) Introduction to sea anemone. In: Klinkenberg, B, ed. *Electronic Atlas of the Fauna of British Columbia*. Available at: https://ibis.geog.ubc.ca/biodiversity/efauna/IntroductiontoSeaAnemones.html [Accessed Aril 2020].

Griffiths, A.J.F., Gelbart, W.M., Miller, J.H., Lewontin, R.C. (1999) Bacteriophage genetics. In: *Modern Genetic Analysis*. New York. W.H. Freeman and Company. Available at: https://www.ncbi.nlm.nih.gov/books/NBK21417/.

Gulder T.A.M. and Moore, B.S. (2009) Chasing the treasures of the sea- bacterial marine natural products. *Current opinions in microbiology*, 12(3), pp. 252-260.

Guo, X., Bruins, A.P., Covey, T.R. (2006) Characterization of typical chemical background interferences in atmospheric pressure ionization liquid chromatography-mass spectrometry. *Rapid Communications in Mass Spectometry*, 20, pp. 3145-3150.

Hadacek, F. and Bachmann, G. (2015) Low-molecular-weight metabolite systems chemistry. *Frontiers in Environmental Science*, 3(12) Available at: https://doi.org/10.3389/fenvs.2015.00012 [Accessed 9 June 2020].

Hall, M.B. (2013) Efficacy of reducing sugar and phenol-sulphuric acid assays for analysis of soluble carbohydrates in feedstuffs. *Animal Feed Science and Technology*, 185, pp. 94-100.

Hamayeli, H., Hassanshahian, M., Hesni, M.A. (2019) The antibacterial and antibiofilm activity of sea anemone (*Stichodactyla haddoni*) against antibiotic-resistant bacteria and characterization of bioactive metabolites. *International Aquatic Research*, 11, pp. 85-97.

Handford, M., Rodriguez-Furlán, C., Orellana, A. (2006) Nucleotide-sugar transporters: structure, function and roles *in vivo*. *Brazilian Journal of Medical and Biological Research*, 39, pp. 1149-1158.

Hanson, J.R. (2003) Natural Products: The secondary metabolites. In: Abel, E.W, ed. *The classes of natural products and their isolation*. Cambridge, UK. Royal Society of Chemistry, pp. 1-34.

Hanssen, K.O. (2014) *Isolation and Characterization of Bioactive Secondray Metabolites from Arctic, Marine Organisms*. Ph.D. Thesis. The Arctic University of Norway. Available at: https://hdl.handle.net/10037/7017 [Accessed 30 October 2018].

Härtner, T., Straub, K.L., Kannenberg, E. (2005) Occurrence of hopanoid lipids in anaerobic *Geobacter* species. *FEMS Microbiology Letters*, 243, pp. 59-64.

Hassan, S.W.M. and Ibrahim, H.A.H. (2017) Production, Characterization and Valuable Applications of Exopolysaccharides from Marine *Bacillus subtilis* SH1. *Polish Journal of Microbiology*, 66(2), pp. 449-461.

He, F., Yang, Y., Yang, G., Yu, L. (2010) Studies on antibacterial activity and antibacterial mechanism of a novel polysaccharide from *Streptomyces virginia* H03. *Food Control*, 21, pp. 1257-1262.

He, M.X., Wu, B., Qin, H., Ruan, Z.Y., Tan, F.R., Wang, J.L., Shui, Z.X., Dai, L.C., Zhu, Q.L., Pan, K., Tang, X.Y., Wang, W.G., Hu, Q.C. (2014) *Zymomonas mobilis*: a novel platform for future biorefineries. *Biotechnology for Biofuels*, 7. Available at: https://doi.org/10.1186/1754-6834-7-101 [Accessed 9 June 2002].

He, Y., Hu, Z., Li, Q., Haung, J., Li, X., Zhu, H., Liu, J., Wang, J., Xue, Y., Zhang,Y. (2017) Bioassay-Guided Isolation of Antibacterial Metabolites from *Emericella* sp. TJ29. *Journal of Natural Products*, 80, pp. 2399-2405.

Heilmann, C., Gerke, C., Perdreau-Remington, F., Gotz, F. (1996) Characterization of Tn917 insertion mutants of Staphylococcus epidermidis affected in biofilm formation. *Infection and Immunity*, 64, pp. 277-282.

Helfrich EJN, Reiter S, Piel J (2014) Recent advances in genome-based polyketide discovery. *Current opinion in biotechnology* 29, 107-115.

Heuston, S., Begley, M., Gahan, C.G.M., Hill, C. (2012) Isoprenoid biosynthesis in bacterial pathogens. Microbiology, 158, pp. 1389-1401.

Hird, S.J., Lau, B.P.Y., Shuhmacher, R., Krska, R. (2014) Liquid chromatography-mass spectrometry for the determination of chemical contaminants in food. *Trends in Analytical Chemistry*, 59, pp. 59-72.

Hosoya, S., Adachi, K., Kasai, H. (2009) *Thalassomonas actiniarum* sp. nov. and *Thalassomonas haliotis* sp. nov., isolated from marine animals. *International Journal of Systematic and Evolutionary Microbiology*, 59, pp. 686-690.

Hosseini, E., Mozafari, H.R., Hojjatoleslamy, M., Rousta, E. (2017) Influence of temperature, pH and salts on rheological properties of bitter almond gum. *Food Science and Technology*, 37(3), pp. 437-443.

Howard, J. (2019) Cancer now tops heart disease as the No.1 cause of death in these countries. CNN Health, 3 September. Available at: https://edition.cnn.com/2019/09/03/health/leading-cause-of-death-cancer-heart-disease-study/index.html [Accessed 4 April 2020].

Hubert, J., Nuzillard, J., Renault, J. (2017) Dereplication strategies in natural product research: How many tools and methodologies behind the same concept? *Phytochemical Reviews*, 16, 55-59.

Hummel, K.M., Penheiter, A.R., Gathman, A.C., Lilly, W.W. (1996) Anomalous estimation of protease molecular weights using gelatin containing SDS-PAGE. *Analytical Biochemistry*, 233, pp. 140-142.

Isobe, Y., Endo, K., Kawai, H. (1992) Properties of a highly viscous polysaccharide produced by a *Bacillus* strain isolated from soil. *Bioscience, Biotechnology, and Biochemistry*, 56(4), pp. 636-639.

Ivanenkov, Y.A., Zhavoronkov, A., Yamidanov, R.S., Osterman, I.A., Sergiev, P.V., Aladinskiy, V.A., Aladinskaya, A.V., Terentiev, V.A., Veselov, M.S., Ayginin, A.A. et al. (2019) Identification of Novel Antibacterials Using Machine Learning Techniques. *Frontiers in Pharmacology*, 10(13). Available at: https://doi.org/10.3389/fphar.2019.00913 [Accessed 7 January 2020].

Jafari, N. and Abediankenari, S. (2015) Phage Particles as Vaccine Delivery Vehicles: Concepts, Applications and Prospects. *Asian Pacific Journal of Cancer Prevention*, 16(18), pp. 8019-8029.

Jain, V.M., Karibasappa, G.N., Dodamani, A.S., Mali, G.v. (2017) Estimating the carbohydrate content of various forms of tobacco by phenol-sulphuric acid method. *Journal of Education and Health Promotion*, 6(90). Available at: https://doi.org/10.4103/jehp.jehp_41_17 [Accessed 26 November 2019].

January, G.G. (2020) *Exploration of new microbial strains for drug discovery from Antarctic marine sediments*. Ph.D. Thesis (unpublished). University of Compania "Luigi Vanvitelli".

Jaspars, M., De Pascale, D., Andersen, J.H., Reyes, F., Crawford, A.D., Ianora, A. (2016) The marine Biodiscovery pipeline and ocean medicines of tomorrow. *Journal of the Marine Biological Association of the United Kingdom,* 96(1), pp. 151-158.

Jassbi, A.R., Mirzaei, Y., Firuzi, O., Chandran, J.N., Schneider, B. (2016) Bioassay guided purification of cytotoxic natural products from a red alga *Dichotomaria obtusata*. *Brazilian Journal of Pharmacognosy*, 26, 705-709.

Jensen PR, Chavarria KL, Fenical W, Moore BS, Ziemert N (2014) Challenges and triumphs to genomics-based natural product discovery. *Journal of industrial microbial biotechnology* 41(2), 203-209.

Jiang, P., Li, J., Han, F., Duan, G., Lu, X., Gu, Y., Yu, W. (2011) Antibiofilm activity of an Exopolysaccharide from Marine Bacterium *Vibrio* sp. QY101. *PLoS ONE*, 6(4). Available at: https://doi.org/10.1371/journal.pone.0018514 [Accessed 27 January 2020].

Jiao, Y., Cody, G.D., Harding, A.K., Wilmes, P., Schrenk, M., Wheeler, K.E., Banfield, J.F., Thelen, M.P. (2010) Characterization of extracellular polymeric substances from acidophilic microbial biofilms. *Applied and Environmental Microbiology*, 76(9), pp. 2916-2922.

Johnston, C.W., Plumb, J., Li, X., Grinstein, S., Magarvey, N.A. (2016) Informatic analysis reveals *Legionella* as a source of novel natural products. *Synthetic and Systems Biotechnology*, 1, pp. 130-136.

Jun, S.Y., Jang, I.J., Yoon, S., Jang, K., Yu, K., Cho, J.Y., Seong, M., Jung, G.M., Yoon, S.J., Kanga, S.H. (2017) Pharmacokinetics and tolerance of the phage endolysin-based candidate drug SAL200 after a single intravenous administration among healthy volunteers.

Antimicrobial Agents and Chemotherapy, 61(6). Available at: https://doi.org/10.1128/AAC.02629-16 [Accessed 15 May 2019].

Kachlany, S.C., Levery, S.B., Kim, J.S., Reuhs, B.L., Lion, L.W., Ghiorse, W.C. (2001) Structure and carbohydrate analysis of the exopolysaccharide capsule of *Pseudomonas putida* G7. *Environmental Microbiology*, 3(12), pp. 774-784.

Karakurt, I., Ozaltin, K., Vesela, D., Lehocky, M., Humpolíček, P., Mozetič, M. (2019) Antibacterial Activity and Cytotoxicity of Immobilized Glucosamine / Chondroitin Sulfate on Polylactic Acid Films. *Polymers*, 11(7). Available at: https://doi.org/10.3390/polym11071186 [Accessed 8 April 2020].

Karpievitch, Y.V., Polpitiya, A.D., Anderson, G.A., Smith, R.D., Dabney, A.R. (2010) Liquid-chromatography mass spectrometry-based proteomics: Biological and Technological Aspects. *Annals of Applied Statistics*, 4(4), pp. 1797-1823.

Kashani, H.H., Schmelcher, M., Sabzalipoor, H., Hosseini, E.S., Moniri, R. (2018) Recombinant Endolysins as Potential Therapeutics against Antibiotic-Resistant Staphylococcus aureus: Current Status of Research and Novel Delivery Strategies. *Clinical Microbiology Reviews*, 31(1). Available at: https://cmr.asm.org/content/31/1/e00071-17 [29 May 2020].

Katz, L. and Baltz, R.H. (2016) Natural product discovery: past, present, and future. *The Journal of Industrial Microbiology and Biotechnology*, 43, pp. 155-176.

Kawashima, A., Osman, B.A.H., Takashima, M., Kikuchi, A., Kohchi, S., Satoh, E., Tamba, M., Matsuda, M., Okamura, N. (2009) CABS1 is a novel calcium-binding protein specifically expressed in elongate spermatids of mice. *Biology of Reproduction*, 80, pp. 1293-1304.

Keating TA, Walsh C (1999) Initiation, elongation and termination strategies in polyketide and polypeptide antibiotic biosynthesis. *Current Opinion in Chemical Biology*, 598-605.

Kim, S.H., Shin, Y.K., Sohn, Y., Kwon, H.C. (2012) Two new cholic acid derivatives from the marine ascidian-associated bacterium *Hasllibacter halocynthiae*. *Molecules*, 17, pp. 12357-12364.

Kim, S.H., Yang, H.O., Sohn, Y.C., Kwon, H.C. (2010) *Aeromicrobium halocynthiae* sp. nov., a taurocholic acid-producing bacterium isolated from the marine ascidian *Halocynthia roretzi*. *International Journal of Systematic and Evolutionary Microbiology*, 60, pp. 2793-2798.

King, L. E. Jnr. and Morrison, M. (1976) The visualization of human erythrocyte membrane proteins and glycoproteins in SDS polyacrylamide gels employing a single staining procedure. *Analytical Biochemistry*, 71, pp. 223-230.

Kirchweyer, B., Rollinger, J.M. (2018) Virtual Screening for the Discovery of Active Principles from Natural Products. In: Filho, V.C, ed. *Natural Products as source of Molecules with Therapeutic Potential - Research and Development, Challenges and Perspectives.* Switzerland: Springer Nature Switzerland, pp. 333-364.

Kneidinger, B., Marolda, C., Graninger, M., Zamyatina, A., McArthur, F., Kosma, P., Valvano, M.A., Messner, P. (2002) *Journal of Bacteriology,* 184(2), pp. 363-369.

Komaki, H., Sakurai, K., Hosoyama, A., Kimura, A., Igarashi, Y., Tamura, T. (2018) Diversity of nonribosomal peptide synthetase and polyketide synthase gene clusters among taxonomically close *Streptomyces* strains. *Scientific Reports*, 8(1). Available at: https://www.nature.com/articles/s41598-018-24921-y [6 January 2020].

Konisky, J. (1982) Colicins and other bacteriocins with established modes of action. *Annual Review of Microbiology*, 36, pp. 125-144.

Kovaleinen, M. (2018) Biologics vs small molecule drugs-what's the difference? Admescope. 19 November. Available at: https://www.admescope.com/whats-new/blog/2018/biologics-vs-small-molecule-drugs-whats-the-difference.html [Accessed 26 February 2020].

Kropinski, A.M., Berry, D., Greenberg, E.P. (1986) The basis of silver staining of bacterial lipopolysaccharides in polyacrylamide gels. *Current Microbiology*, 13, pp. 29-31.

Kruve, A. and Kaupmees, K. (2017) Adduct formation in ESI/MS by mobile phase additives. *Journal of the American Society for Mass Spectrometry*, 28, pp. 887-894.

Kuchta, T., Kubinec, R., Farkaš, P. (1998) Analysis of hopanoids in bacteria involved in food technology and food contamination. *FEMS Microbiology Letters*, 159, pp. 221-225.

Kumari, A. (2018) Cholesterol synthesis. In: *Sweet Biochemistry*. Elsevier, pp. 27-31. Available at: https://doi.org/10.1016/B978-0-12-814453-4.00007-8 [Accessed 14 March 2020].

Kus, J.V., Gebremedhin, A., Dang, V., Tran, S., Serbanescu, A., Foster, D.B. (2011) Bile salts induce resistance to Polymyxin in enterohemorrhagic Escherichia coli O157:H7. *Journal of Bacteriology*, 193(17), pp. 4509-4515.

Kuzuyama, T. (2002) Mevalonate and nonmevalonate pathways for the biosynthesis of isoprene units. *Bioscience, Biotechnology and Biochemistry*, 66, pp. 1619-1627.

Kuzuyama, T. and Seto, H. (2012) Two distinct pathways for essential metabolic precursors for isoprenoid biosynthesis. *Proceedings of the Japan Academy*, Series B, 88(3), pp. 41-51.

Kwan, D.H. and Whithers, S.G. (2014) Periplasmic de-acylase helps bacteria don their biofilm coat. *PNAS*, 111(30), pp. 10904-10905.

Lagunin, A., Filimonov, D., Poroikov, V. (2010) Multi-Targeted Natural Products Evaluation Based on Biological Activity Prediction with PASS. *Current Pharmaceutical Design*, 16, pp. 1703-1717.

Lahlou, M. (2013) The success of natural products in drug discovery. *Pharmacology and Pharmacy*, 4, pp. 17-31.

Larpin, Y., Oechslin, F., Moreillon, P., Resch, G., Entenza, J.M., Mancini, S. (2018) In vitro characterization of PlyE146, a novel phage lysin that targets Gram-negative bacteria. *PLoS ONE*, 13(2). Available at: https://doi.org/10.1371/journal.pone.0192507 [Accessed 6 January 2020].

Larson, C.B., Crüsemann, M., Moore, B.S. (2017) A PCR-independent method of transformation associated recombination reveals the cosmomycin biosynthetic gene cluster in an ocean streptomycete. *Journal of Natural Products*, 80(4), pp. 1200-1204.

Leber, T.M. and Balkwill, F.R. (1997) Zymography: A single-step staining method for quantitation of proteolytic activity on substrate gels. *Analytical Biochemistry*, 249, pp. 24-28.

Li Z (2009) Advances in marine microbial symbionts in the China Sea and related pharmaceutical metabolites. *Marine drugs* 7, 113-129.

Li, C. and Arakawa, T. (2019) Application of native polyacrylamide gel electrophoresis for protein analysis: Bovine serum albumin as a model protein. *International Journal of Biological Macromolecules*, 125, pp. 566-571.

Li, G. and Lou, H. (2017) Strategies to diversify natural products for drug discovery. *Medicinal Research Reviews*, 38(4), pp. 1255-1294.

Li, H., Shinde, P.B., Lee, H.J., Yoo, E.S., Lee, C., Hong, J., Choi, S.H., Jung, J.H. (2009) Bile acid derivatives from a sponge-associated bacterium *Psychrobacter* sp. *Archives of Pharmaceutical Research*, 32(6), pp. 857-862.

Li, Q., Niu, Y., Xing, P., Wang, C. (2018) Bioactive polysaccharides from natural resources including Chinese medicinal herbs on tissue repair. *Chinese Medicine*, 13(7). Available at: https://doi.org/10.1186/s13020-018-0166-0 [Accessed 15 April 2020].

Li, R., Zhou, Y., Wu, Z., Ding, L. (2006) ESI-QqTOF-MS/MS and APCI-IT-MS/MS analysis of steroid saponins from the rhizomes of *Dioscorea panthaica*. *Journal of Mass Spectrometry*, 41. Available at: https://doi.org/10.1002/jms.988 [Accessed 9 June 2020].

Li, S., Kang, J., Yu, W., Zhou, Y., Zhang, W., Xin, Y., Ma, Y. (2012) Identification of *M. tuberculosis* Rv3441c and *M. smegmatis* MSMEG_1556 and essentiality of *M. smegmatis* MSMEG_1556. *PLoS ONE*, 7(8). Available at: https://doi.org/10.1371/journal.pone.0042769 [Accessed 20 November 2019].

Li, S., Xiong, Q., Lai, X., Li, X., Wan, M., Zhang, H., Yan, Y., Cao, M., Lu, L., Guan, J., Zhang, D., Lin, Y. (2015) Molecular modification of polysaccharides and resulting bioactivities. *Comprehensive Reviews in Food Science and Food Safety*, 15, pp. 237-250.

Li, T. and Chiang, J.Y.L. (2009) Regulation of bile acid and cholesterol metabolism by PPARs. *PPAR Research*. Available at: https://doi.org/10.1155/2009/501739 [Accessed 9 June 2020].

Li, X., Zhao, T., Cheng, D., Chu, C., Tong, S., Yan, J., Li, Q. (2014) Synthesis and biological activity of some bile acid-based camptothecin analogues. *Molecules*, 19, pp. 3761-3776.

Li, Z. (2009) Advances in marine microbial symbionts in the China Sea and related pharmaceutical metabolites. *Marine drugs*, 7, pp. 113-129.

Liang, T. and Wang, S. (2015) Recent advances in exopolysaccharides from *Paenibacillus* spp.: Production, isolation, structure, and bioactivities. *Marine Drugs*, 13, pp. 1847-1863.

Lidbury, I., Kimberley, G., Scanlan, D.J., Murrell, J.C., Chen, Y. (2015) Comparative genomics and mutagenesis analyses of choline metabolism in the marine *Roseobacter* clade. *Environmental Microbiology*, 17(12), pp. 5048-5062.

Lievens, S.C., Hope, H., Molinski, T.F. (2004) New 3-oxo-chol-4-en-24-oic acids from the marine soft coral *Eleutherobia* sp. *Journal of Natural Products*, 67, pp. 2130-2132.

Liigand, P., Kaupmees, K., Haav, K., Liigand, J., Leito, I., Girod, M., Antoine, R., Kruve, A. (2017) Think negative: Finding the best electrospray ionization/MS mode for your analyte. *Analytical Chemistry*, 89, pp. 5665-5668.

Lin, D.M., Koskella, B., Lin, H.C. (2017) Phage therapy: An alternative to antibiotics in the age of multi-drug resistance. *World Journal of Gastrointestinal Pharmacology and Therapeutics*, 8(3), pp. 162-173.

Lindner, H.B., Zhang, A., Eldridge, J., Demcheva, M., Tsichilis, P., Seth, A., Vournakis, J., Muise-Helmericks, R.C. (2011) Anti-bacterial effects of poly-N-acetyl-glucosamine nanofibers in

cutaneous wound healing: Requirement for Akt1. *PLoS ONE*, 6(4). Available at: https://doi.org/10.1371/journal.pone.0018996 [Accessed 25 April 2020].

Lipinski, C.A., Lombardo, F., Donimy, B.W., Feeny, F.J. (1997) Experimental and computational approaches to estimate solubility and permeability in drug discovery and development settings. *Advanced Drug Delivery Reviews*, 23, pp. 3-25.

Little, D.J. (2015) *Modification and translation of the biofilm exopolysaccharide poly-β(1,6)-N-acetyl-D-glucosamine*. Ph.D. Thesis. University of Toronto. Available at: https://tspace.library.utoronto.ca/handle/1807/77728 [Accessed 9 April 2020].

Lu, L., Hu. W., Tian, Z., Yuan, D., Yi, G., Zhou, Y., Cheng, Q., Zhu, J.,Li, M. (2019) Developing natural products as potential anti-biofilm agents. *Chinese Medicine*, 14(11). Available at: https://cmjournal.biomedcentral.com/articles/10.1186/s13020-019-0232-2 [Accessed 29 May 2020]

Lu, Z., Van Wagoner, R.M., Harper, M.K., Hooper, J.N.A., Ireland, C.M. (2010) Two ring-A-aromatized bile acids from the marine sponge *Sollasella moretonensis*. *Natural Product Communications*, 5(10), pp. 1571-1574.

Luo, Y., Cobb R.E., Zhao, H. (2014) Recent advances in natural product discovery. *Current Opinion in Biotechnology*, 20, pp. 230-237.

Ma, L., Zhang, Q., Yang, C., Zhu, Y., Zhang, L., Wang, L., Liu, Z., Zhang, G., Zhang, C. (2019) Assembly line and post-PKS modifications in the biosynthesis of marine polyketide natural products In: *Chemistry, Molecular Sciences and Chemical Engineering*. Elsevier. USA. Available at: https://doi.org/10.1016/B978-0-12-409547-2.14711-0 [Accessed 23 February 2020].

Machado H, Sonnenschein EC, Melchiorsen J, Gram L. (2015) Genome mining reveals unlocked bioactive potential of marine Gram-negative bacteria. *BMC Genomics* 16(158), 1-12

Machado, L.R. and Ottolini, B. (2015) An evolutionary history of defensins: a role for copy number variation in maximizing host innate and adaptive immune responses. *Frontiers in Immunology*, 6(115). Available at: https://doi.org/10.3389/fimmu.2015.00115 [Accessed 8 June 2020].

Macián, M.C., Ludwig, W., Schleifer, K.H., Garay, E., Pujalte, M.J. (2001) *Thalassomonas viridans* gen. nov., sp. nov., a novel marine γ-proteobacterium. *International Journal of Systematic and Evolutionary Microbiology*, 51, pp. 1283-1289.

Majorek, K.A., Kuhn, M.L., Chruszcz, M., Anderson, W.F., Minor, W. (2014) Double trouble-buffer selection and His-tag presence may be responsible for nonreproducibility of biomedical experiments. *Protein Science*, 23, pp. 1359-1368.

Mäki, M. and Renkonen, R. (2004) Biosynthesis of 6-deoxyhexose glycans in bacteria. *Glycobiology*, 14(3). Available at: https://doi.org/10.1093/glycob/cwh040 [Accessed 21 November 2019].

Maldonado, R.F., Sá-Correia, I., Valvano, M.A. (2016) Lipopolysaccharide modification in Gram-negative bacteria during chronic infection. *FEMS Microbiology Reviews*, 40, pp. 480-493.

Malyarenko, T.V., Kicha, A.A., Ivanchina, N.V., Kalinovsky, A.I., Dmitrenok, P.S., Stonik, V.A. (2016) Unusual steroid constituents from the tropical starfish *Leiaster* sp. *Natural Product Communications*, 11(9), pp. 1251-1252.

Maneerat, S., Nitoda, T., Kanzaki, H., Kawai, F. (2005) Bile acids are new products of a marine bacterium, *Myroides* sp. strain SM1. *Applied Microbiology and Biotechnology*, 67, pp. 679-683.

Martinez, A., Kolvek, S.J., Yip, C.L.T., Hopke, J., Brown, K.A., MacNeil, I.A., Osburne, M.S. (2004) Genetically modified bacterial strains and novel bacterial artificial chromosome shuttle vectors for constructive environmental libraries and detecting heterologous natural products in multiple expression hosts. *Applied and Environmental Microbiology*, 70(4), pp. 2452, 2463.

Martínez-Alonso, M., García-Fruitós, E., Ferrer-Miralles, N., Rinas, U., Villaverde, A. (2010) Side effects of chaperone gene co-expression in recombinant protein production. *Microbial Cell*

Factories, 9(64), pp. Available at: https://doi.org/10.1186/1475-2859-9-64 [Accessed 8 Otober 2019].

Martins A, Vieira H, Gaspar H, Santos S (2014) Marketed marine natural products in the pharmaceutical and cosmeceutical industries: Tips for success. *Marine drugs* 12, pp. 1066-1101

Masselon, C.D., Kieffer-Jaquinod, S., Brugière, S., Dupierris, V., Garin, J. (2008) Influence of mass resolution on species matching in accurate mass and retention time (AMT) tag proteomics experiments. *Rapid Communications in Mass Spectrometry*, 22, pp. 986-992.

Masuko, T., Minami, A., Iwasaki, N., Majima, T., Nishimura, S., Lee, Y.C. (2005) Carbohydrate analysis by a phenol-sulphuric acid method in microplate format. *Analytical Biochemistry*, 339, pp. 69-72.

Matobole, R.M., Van Zyl, L.J., Parker-Nance, S., Davies-Coleman, M.T., Trindade, M. (2017) Antibacterial activities of bacteria isolated from the marine sponges *Isodictya compressa* and *Higginsia bidentifera* collected from Algoa Bay, South Africa. *Marine Drugs*, 15(2). Available at: https://doi.org/10.3390/md15020047 [28 February 2019].

Medema, M.H., Blin. K., Cimermancic, P., de Jager, V., Zakrewski, P., Fischbach, M.A., Weber, M., Takano, E., Breitling, R. (2011) antiSMASH: rapid identification, annotation and analysis of secondary metabolite biosynthesis gene clusters in bacterial and fungal genome sequences. *Nucleic Acids Research*, 39, pp. 339-346.

Métayer, S., Dacheux, F., Dacheux J., Gatti, J. (2002) Comparison, characterization, and identification of proteases and protease inhibitors in epididymal fluids of domestic mammals. Matrix metalloproteinases are major fluid gelatinases. *Biology of Reproduction*, 66, pp. 1219-1229.

Micenkova, L., Bosák, J., Kucera, J., Hrala, M., Dolejšová, T., Šedo, O., Linke, D., Fišer, R., Šmajs, D. (2019) Colicin Z, a structurally and functionally novel colicin type that selectively

kills enteroinvasive *Escherichia coli* and *Shigella* strains. *Scientific Reports*, 9. Available at: https://doi.org/10.1038/s41598-019-47488-8 [Accessed 7 January 2020].

Mignon, C., Mariano, N., Stadthagen, G., Lugari, A., Lagoutte, P., Donnat, S., Chenavas, S., Perot, C., Sodoyer, R., Werle, B. (2018) Codon harmonization-going beyond the speed limit for protein expression. *FEBS Letters*, 592, pp. 1554-1556.

Mirski, T., Lidia, M., Nakonieczna, A., Gryko, R. (2019) Bacteriophages, phage endolysins and antimicrobial peptides- the possibilities for their common use to combat infections and in the design of new drugs. *Annals of Agricultural and Environmental Medicine*, 26(2), pp. 203-209.

Mirzaei, H. and Regnier, F. (2006) Enhancing electrospray ionization efficiency of peptides by derivitization. *Analytical Chemistry*, 78, pp. 4175-4183.

Mohamed, S.S., Amer, S.K., Selim, M.S., Rifaat, H.M. (2018) Characterization and applications of exopolysaccharide produced by marine *Bacillus altitudinis* MSH2014 from Ras Mohamed, Sinai, Egypt. *Egyptian Journal of Basic and Applied Sciences*, 5, pp. 204-209.

Molinski TF, Dalisay DS, Lievens SL, Saludes JP (2009) Drug development from marine natural products. *Nature reviews* 8, 69-85

Morris, G. and Harding, S. (2009) Polysaccharides, Microbial. In: *Encyclopedia of Microbiology*. Elsevier Inc., pp. 482-494. Available at: https://doi.org/10.1016/B978-012373944-5.00135-8 [Accessed 16 March 2020].

Muheem, A., Shakeel, F., Jahangir, M.A., Anwar, M., Mallick, N., Jain, G.K., Warsi, M.H., Ahmad, F.J. (2016) A review on the strategies for oral delivery of proteins and peptides and their clinical perspectives. *Saudi Pharmaceutical Journal*, 24, pp. 413-428.

Mukhopadhyay, S. and Maitra, U. (2004) Chemistry and biology of bile acids. *Current Science*, 87(12), pp. 1666-1683.

Mulani, M.S., Kamble, E.E., Kumkar, S.N., Tawre, M.S., Pardesi, K.R. (2019) Emerging strategies to combat ESKAPE pathogens in the era of antimicrobial resistance: A review. *Frontiers in Microbiology*, 10. Available at: https://doi.org/10.3389/fmicb.2019.00539 [Accessed 5 April 2020].

Müller, C.A., Oberauner-Wappls, L., Peyman, A., Amos, G.C.A., Wellington, E.M.H., Berg, G. (2015) Mining for nonribosomal peptide synthetase and polyketide synthase genes revealed a high level of diversity in the *Sphagnum* bog metagenome. *Applied and Environmental Microbiology*, 81(15), pp. 5064-5072.

Müller, M.M. (2018) Post-translational modifications of protein backbones: Unique functions, mechanisms, and challenges. *Biochemistry*, 57, pp. 177-185.

Nakayama, K., Takashima, K., Ishihara, H., Shinomiya, T., Kageyama, M., Kanaya, S., Ohnishi, M., Murata, T., Mori, H., Hayashi, T. (2000) The R-type pyocin of *Pseudomonas aeruginosa* is related to P2 phage, and the F-type is related to lambda phage. *Molecular Microbiology*, 38, pp. 213-231.

Nalini,S., Richard, D.S., Riyaz, S.U.M., Kavitha, G., Inbakandan, D. (2018) Antibacterial macro molecules from marine organisms. *International Journal of Biological Macromolecules*, 115, pp. 696-710.

Neves, M.I., Araújo, M., Moroni, L., da Silva, R.M.P., Barrias, C.C. (2020) Glycosaminoglycan-inspired biomaterials for the development of bioactive hydrogels networks. *Molecules*, 25(4). Available at: https://doi.org/10.3390/molecules25040978 [Accessed 26 April 2020].

Newman, D.J. and Cragg, G.M. (2016) Natural products as sources of new drugs from 1981 to 2014. *Journal of Natural Products*, 79, pp. 629-661.

Nichols, C.M., Lardiére, S.G., Bowman, J.P., Nichols, P.D., Gibson, J.A.E., Guézennec, J. (2005) Chemical characterization of exopolysaccharides from Antarctic marine bacteria. *Microbial Ecology*, 49(4), pp. 578-589.

Nilsson, A.S. (2014) Phage therapy-constraints and possibilities. *Upsala Journal of Medical Sciences*, 119, pp. 192-198.

Ninomiya, T., Sugiura, N., Tawadas, A., Sugimoto, K., Watanabe, H., Kimata, K. (2002) Molecular cloning ad characterization of chondroitin polymerase from *Escherichia coli* strain K4. *The Journal of Biological Chemistry*, 277(24), pp. 21567-21575.

Nobrega, F.L., Vlot, M., de Jonge, P.A., Dreesens, L.L., Beaumont, H.J.E., Lavigne, R., Dutilh, B.E., Brouns, S.J.J. (2018) Targeting mechanisms of tailed bacteriophages. *Nature Reviews Microbiology*, 16, 760-773.

Novy, R., Drott, D., Yaeger, K., Mierendorf, R. (2001) Overcoming the codon bias of *E. coli* for enhanced protein expression. *inNovations*, 12. Available at: http://wolfson.huji.ac.il/expression/Rosetta.pdf [Accessed 8 October 2019].

Nowakowski, A.B., Wobig, W.J., Petering, D.H. (2014) Native SDS-PAGE: High resolution electrophoretic separation of proteins with retention of native properties including bound metal ions. *Metallomics*, 6(5), pp. 1068-1078.

Odom, A.R. (2011) Five questions about non-mevalonate isoprenoid biosynthesis. *PLoS ONE*, 7(12). Available at: https://doi.org/10.1371/journal.ppat.1002323 [Accessed 9 June 2020].

Ohnishi, Y., Takade, A., Takeya, K. (1971) Morphological changes in Pseudomonas aeruginosa treated with rod-shaped Pyocin 28. *Japanese Journal of Microbiology*, 15(2), pp. 201-205.

Olczyk, P., Komosínska-Vassev, K., Winsz-Szczotka, K., Kuźnik-Trocha, K. (2008) Hyaluronan: Structure, metabolism, functions, and role in wound healing. *Advances in Hygiene and Experimental Medicine*, 62, pp. 651-659.

Oliveira, J., Castilho, F., Cunha, A., Pereira, M.J. (2012) Bacteriophage therapy as a bacterial control strategy in aquaculture. *Aquaculture International*, 20, pp. 879-910.

Olonade, I., van Zyl, L.J., Trindade, M. (2015) Draft genome sequences of marine isolates *Thalassomonas viridans* and *Thalassomonas actiniarum*. *Genome Announcements*, 3(2). Available at: https://doi.org/10.1128/GENOMEA.00297-15 [Accessed 20 February 2019].

Orsod, M., Joseph, M., Huyop, F. (2012) Characterization of exopolysaccharides produced by *Bacillus cereus* and *Brahybacterium* sp. isolated from Asian sea bass (*Lates calcarifer*). *Malaysian Journal of Microbiology*, 8(3), pp. 170-174.

Paalman, J.W.G., Verwaal, R., Slofstra, S.H., Verkleij, A.J., Boonstra, J., Verrips, C.T. (2003) Trehalose and glycogen accumulation is related to the duration of G1 phase of *Saccharomyces cerevisiae*. *FEMS Yeast Research*, 3, pp. 261-268.

Pan, D., Hill, A.P., Kashou, A., Wilson, K.A., Tan-Wilson, A. (2011) Electrophoretic transfer protein zymography. *Analytical Biochemistry*, 411, pp. 277-283.

Pan, J., Solbiati, J.O., Ramamoorthy, G., Hillerich, B.S., Seidel, R.D., Cronan, J.E., Almo, S.C., Poulter, C.D. (2015) Biosynthesis of squalene from farnesyl diphosphate in bacteria: Three steps catalyzed by three enzymes. *ACS Central Science*, 1, pp. 77-82.

Pang, B., Zhu, Y., Lu, L., Gu, F., Chen, H. (2016) The applications and features of liquid chromatography-mass spectrometry in the analysis of Traditional Chinese medicine. *Evidence-Based Complementary and Alternative Medicine*. Available at: https://doi.org/10.1155/2016/3837270 [Accessed 9 March 2020].

Panter, F., Krug, D., Baumann, S., Müller, R. (2018) Self-resistance guided genome mining uncovers new topoisomerase inhibitors from myxobacteria. *Chemical Science*, 9, pp. 4898-4908.

Pantin, C.F.A. (1942) The excitation of nematocysts. *Journal of Experimental Biology*, 19(3), pp. 294-310.

Park, H.B., Perez, C.E., Barber, K.W., Rinehart, J., Crawford, J.M. (2017) Genome mining unearths a hybrid nonribosomal peptide synthetase-like-pteridine synthase biosynthetic gene cluster. *eLife*. Available at: https://doi.org/10.7554/eLife.25229.001 [Accessed 11 April 2020].

Parkar, D., Jadhav, R., Pimpliskar, M. (2017) Marine bacterial exopolysaccharides: A review. *Journal of Coastal Life Medicine*, 5(1), pp. 29-35.

Patrick, S. (2014) Bacteriodes. In: Tang, Y., Sussman, M., Liu, D., Poxton, I.R., Schwartzman, J, eds. *Molecular Medical Microbiology*. Elsevier Inc., pp. 917-944

Patridge, E., Gareiss, P., Kinch, M.S., Hoyer, D. (2016) An analysis of FDA-approved drugs: natural products and their derivatives. *Drug Discovery Today*, 21(2), pp. 204-207.

Patz, S., Becker, Y., Richert-Pöggeler, K.R., Berger, B., Ruppel, S., Huson, D.H., Becker, M. (2019) *Journal of Advanced Research*, 19, pp. 75-84.

Pérez-Burgos, M., García-Romero, I., Jung, J., Schander, E., Valvano, M.A., Søgaard-Andersen, L. (2020) Characterization of the exopolysaccharide biosynthesis pathway in *Myxococcus xanthus*. *Journal of Bacteriology*, 202(19). Available at: https://doi.org/10.1128/JB.00335-20. [Accessed 14 October 2020].

Pérez-Gil, J. and Rodríguez-Concepción, M. (2013) Metabolic plasticity for isoprenoid biosynthesis in bacteria. *Biochemical Journal*, 452, pp. 19-25.

Pham, J.V., Yilma, M.A., Feliz, A., Majid, M.T., Maffetone, N., Walker, J.R., Kim, E., Cho, H.J., Reynolds, J.M., Song, M.C., et al. (2019) A review of the microbial production of bioactive natural products and biologics. *Frontiers in Microbiology*, 10. Available at: https://doi.org/10.3389/fmicb.2019.01404 [Accessed 7 January 2020].

Pieterse, R. and Todorov, S.D. (2010) Bacteriocins-exploring alternatives to antibiotics in mastitis treatment. *Brazilian Journal of Microbiology*, 41, pp. 542-562.

Plata, M.R., Koch, C., Wechselberger, P., Herwig, C., Lendl, B. (2013) Determination of carbohydrates present in Saccharomyces cerevisiae using mid-infrared spectroscopy and partial least squares regression. *Analytical and Bioanalytical Chemistry*, 405, pp. 8241-8250.

Poli, A., Anzelmo, G., Nicolaus, B. (2010) Bacterial exopolysaccharides from extreme marine habitats: Prodcution, characterization and biological activities. *Marine Drugs*, 8, pp. 1779-1802.

Prasad, P. (2017) *Marine biodiversity: Exploring bioactive chemical space*. Ph.D. Thesis. The University of Queensland. Available at: https://doi.org/10.14264/uql.2017.724 [Accessed 23 February 2020].

Príncipe, A., Fernandez, M., Torasso, M., Godino, A., Fischer, S. (2018) Effectiveness of tailocins produced by *Pseudomonas fluorescens* SF4c in controlling the bacterial-spot disease in tomatoes caused by *Xanthomonas vesicatoria*. *Microbiological Research*, 212-213, pp. 94-102.

Proksch, P., Edrada-Ebel, R., Ebel, R. (2003) Drugs from the sea-opportunities and obstacles. *Marine Drugs*, 1(4), pp. 5-17.

Prouty, A.M., Van Velkinburgh, J.C., Gunn, J.S. (2002) Salmonella enterica Serovar Typhimurium resistance to bile: Identification and characterization of the *tolQRA* cluster. *Journal of Bacteriology*, 184(5), pp. 1270-1276.

Purwanto, M.G.M. (2016) The role and efficiency of ammonium sulfate precipitation in purification process of papain crude extract. *Procedia Chemistry*, 18, pp. 127-131.

Raut, A.V., Satvekar, R.K., Rohiwal, S.S., Tiwari, A.P., Gnanamani, A., Pushpavanam, S., Nanaware, S.G., Pawar, S.H. (2016) *In vitro* biocompatibility and antimicrobial activity of chitin monomer obtained from hollow fiber membrane. *Designed Monomers and Polymers*, 19(5), pp. 445-455.

Rayan, A., Raiyn, J., Falah, M. (2017) Nature is the best source of anticancer drugs: Indexing natural products for their anticancer bioactivity. *PLoS ONE*, 12(11). Available at: https://doi.org/10.1371/journal.pone.0187925 [Accessed 14 January 2020].

Rederstorff, E., Fatima, A., Sinquin, C., Ratiskol, J., Merceron, C., Vinatier, C., Weiss, P., Colliec-Jouault, S. (2011) Sterilization of exopolysaccharides produced by deep-sea bacteria: Impact on their stability and degradation. *Marine Drugs*, 9, pp. 224-241.

Righetti, P.G. and Boschetti, E. (2013) Low-abundance protein access by combinatorial peptide libraries. In: *Low abundance proteome discovery*. Elsevier Inc. Available at: https://doi.org/10.1016/B978-0-12-401734-4.00004-X [Accessed 14 July 2019].

Rizkia, P.R., Silaban, S., Hasan, K., Kamara, D.S., Subroto, T., Soemitro, S., Maksum, I.P. (2015) Effect of isopropyl-β-D-thiogalactopyranoside concentration on prethrombin-2 recombinant gene expression in *Escherichia coli* ER2566. *Procedia Chemistry*, 17, pp. 118-124.

Rocha, J., Peixe, L., Gomes, N.C.M., Calado, R. (2011) Cnidarians as a source of new marine bioactive compounds-An overview of the last decade and future steps for bioprospecting. *Marine Drugs*, 9, pp. 1860-1886.

Rodríguez-Díaz, J., Rubio-del-Campo, A., Yebra, M.J. (2012) Regulatory insights into the production of UDP-N-acetylglucosamine by *Lactobacilli casei*. *Bioengineered*, 3(6), pp. 339-342.

Rodríguez-Rubio, L., Donovan, D.M., Martínez, B., Rodríguez, A., García, P. (2019) Peptidoglycan hydrolytic activity of bacteriophage lytic proteins in zymogram analysis. In: Clokie, M., Kropinski, A., Lavigne, R, eds. *Bacteriophages. Methods in Molecular Biology*. Humana Press. New York, pp. 107-115.

Roger, O., Kervarec, N., Ratiskol, J., Colliec-Jouault, S., Chevolot, L. (2004) Structural studies of the main exopolysaccharide produced by the deep-sea bacterium *Alteromonas infernus*. *Carbohydrate Research*, 339, pp. 2371-2380.

Rohde, S., Nietzer, S., Schupp, P.J. (2015) Prevalence and mechanism of dynamic chemical defense in tropical sponges. *PLoS ONE*, 10(7). Available at: https://doi.org/10.1371/journal.pone.0132236 [Accessed 30 May 2020].

Rohmer, M., Bouvier-Nave, P., Ourisson, G. (1984) Distribution of hopanoid triterpenes in prokaryotes. *Journal of General Microbiology*, 130, pp. 1137-1150.

Romano, S., Jackson, S.A., Patry, S., Dobson, A.D.W. (2018) Extending the "One Strain Many Compounds" (OSMAC) principle to marine microorganisms. *Marine Drugs*, 16(7). Available at: https://doi.org/10.3390/md16070244 [Accessed 3 April 2020].

Rosano, G.L. and Ceccarelli, E.A. (2014) Recombinant protein expression in *Escherichia coli*: advances and challenges. *Frontiers in Microbiology*, 5. Available at: https://doi.org/10.3389/fmicb.2014.00172 [Accessed 28 January 2020].

Rounge, T.B., Rohrlac, T., Tooming-Klunderud, A., Kristensen, T., Jakobsen, K.S. (2007) Comparison of cyanopeptolin genes in *Planktothrix*, *Microcystis*, and *Anabaena* strains: Evidence for independent evolution within each genus. *Applied and Environmental Microbiology*, 73(22), pp. 7322-7330.

Ruocco, N., Costantini, S., Gauriniello, S., Costantini, M. (2016) Polysaccharides from the marine environment with pharmacological, cosmeceutical and nutraceutical potential. *Molecules*, 2(5). Available at: https://doi.org/10.3390/molecules21050551 [Accessed 14 October 2019].

Rupp, M., Bauer, M.R., Wilcken, R., Lange, A., Reutlinger, M., Boeckler, F.M., Schneider, G. (2014) Machine learning estimates of natural product conformational energies. *PLoS Computational Biology*, 10(1). Available at: https://doi.org/10.1371/journal.pcbi.1003400 [Accessed 21 January 2020].

Saba, A., Frascarelli, S., Campi, B. (2018) The role of tandem mass spectrometry in clinical dentistry: Quantification of steroid hormones and Vitamin D. In: Cappiello, A., Palma, P, eds. *Comprehensive Analytical Chemistry: Advances in the use of Liquid Chromatography*

Mass Spectrometry (LC-MS): Instrumentation Developments and Applications. Elsevier Inc., pp. 301-307.

Sáenz, J.P., Grosser, D., Bradley, A.S., Lagny, T.J., Lavrynenko, O., Broda, M., Simons, K. (2015) Hopanoids as functional analogues of cholesterol in bacterial membranes. *PNAS*, 112(38), pp. 11971-11976.

Saha, S. (2016) *A tale of two tails: Characterization of R-type and F-type Pyocins of Pseudomonas aeruginosa.* Ph.D. Thesis. University of Toronto. Available at: https://tspace.library.utoronto.ca/handle/1807/92667 [Accessed: 19 September 2019].

Saïda, F., Uzan, M., Odaert, B., Bontems, F. (2006) Expression of highly toxic genes in E.coli: Special strategies and genetic tools. *Current Protein and Peptide Science*, 7, pp. 47-56.

Samuelsen, J.C. (2016) Purifying recombinant His-tagged proteins. *Genetic Engineering and Biotechnology News*, 36(5). Available at: https://www.genengnews.com/magazine/267/purifying-recombinant-his-tagged-proteins/ [Accessed 15 September 2020].

Sanchez, L.M., Cheng, A.T., Warner, C.J.A., Townsley, L., Peach, K.C., Navarro, G., Shikuma, N.J., Bray, W.M., Riener, R.M., Yildiz, F.H., Linington, R.G. (2016) Biofilm formation and detachment in Gram-negative pathogens is modulated by select bile acids. *PLoS ONE*, 11(3). Available at: https://doi.org/10.1371/journal.pone.0149603 [Accessed 20 February 2020].

Sannasiddappa, T.H., Lund, P.A., Clarke, S.R. (2017) *In vitro* antibacterial activity of unconjugated and conjugated bile salts on *Staphylococcus aureus*. *Frontiers in Microbiology*, 8. Available at: https://doi.org/10.3389/fmicb.2017.01581 [Accessed 4 March 2020].

Santajit, S. and Indrawattana, N. (2016) Mechanisms of antimicrobial resistance in ESKAPE pathogens. BioMed Research International. Available at: https://doi.org/10.1155/2016/2475067 [Accessed 4 April 2020].

Santhi, L.S., Prasad, T.V.S.S.L., Nagendra, S.Y., Radha, K.E. (2017) Bioactive compounds from marine sponge associates: Antibiotics from *Bacillus* sp. *Natural Products Chemistry and Research*, 5(4). Available at: https://www.longdom.org/open-access/bioactive-compounds-from-marine-sponge-associates-antibiotics-frombacillus-sp-2329-6836-1000266.pdf [Accessed 30 May 2020].

Šarenac, T.M. and Mikov, M. (2018) Bile acid synthesis: From nature to the chemical modification and synthesis and their application as drugs and nutrient. *Frontiers in Pharmacology*, 9. Available at: https://doi.org/10.3389/fphar.2018.00939 [Accessed 14 June 2019].

Schinke, C., Martins, T., Queiroz, S.C.N., Melo, I.S., Reyes, F.G.R. (2017) Antibacterial compounds from marine bacteria, 2010-2015. Journal of Natural Products, 80, pp. 1215-1228.

Schiraldi, C., Cimini, D, De Rosa, M. (2010) Production of chondroitin sulfate and chondroitin. Applied Microbiology and Biotechnology, 87, pp. 1209-1220.

Schmerk, C.L., Welander, P.V., Hamad, M.A., Bain, K.L., Bernards, M.A., Summons, R.E., Valvano, M.A. (2015) Elucidation of the *Burkholderia cenocepacia* hopanoid biosynthesis pathway uncovers functions for conserved proteins in hopanoid-producing bacteria. *Environmental Microbiology*, 17(3), pp. 735-750.

Schmid, F. (2001) Biological macromolecules: UV-visible spectrophotometry. In: *Encyclopedia of Life Sciences*. MacMillan Press. London, UK. Available at: https://doi.org/10.1038/npg.els.0003142 [Accessed 16 October 2019].

Schmid, J., Sieber, V., Rehm, B. (2015) Bacterial exopolysaccharides: biosynthesis pathways and engineering strategies. *Frontiers in Microbiology*, 6(496). Available at: https://doi.org/10.3389/fmicb.2015.00496 [Accessed 10 October 2019].

Schmidt, C. (2019) Phage therapy's latest makeover. *Nature Biotechnology*, 37, pp. 581-586.

Seemann, T. (2014) Prokka: rapid prokaryotic genome annotation. *Bioinformatics*, 30(14), pp. 2068-2069.

Seibold, G.M. and Eikmanns, B. (2007) The *glgX* gene product of *Corynebacterium glutamicum* is required for glycogen degradation and for fast adaptation to hyperosmotic stress. *Microbiology*, 153, pp. 2212-2220.

Seipke, R.F. and Loria, R. (2009) Hopanoids are not essential for growth of *Streptomyces scabies* 87-22. *Journal of Bacteriology*, 191(16), pp. 5216-5223.

Sekurova, O.N., Schneider, O., Zotchev, S.B. (2019) Novel bioactive natural products from bacteria via bioprospecting, genome mining and metabolic engineering. *Microbial Biotechnology*, 12(5), pp. 828-844.

Shaji, J. and Patole, V. (2008) Protein and Peptide drug delivery: oral approaches. *Indian journal of pharmaceutical sciences*, 70(3), pp. 269–277.

Shannon, E. and Abu-Ghannam, N. (2016) Antibacterial derivatives of marine algae: An overview of pharmacological mechanism and applications. *Marine Drugs*, 14(4). Available at: https://doi.org/10.3390/md14040081 [Accessed 14 October 2019].

Sharma, D., Misba, L., Khan, A.U. (2019) Antibiotic versus biofilm: an emerging battleground in microbial communities. *Antimicrobial Resistance and Infection Control*, 8(76). Available at: https://doi.org/10.1186/s13756-019-0533-3 [Accessed 5 April 2020].

Shelke, N.B., James, R., Laurencin, C.T., Kumbar, S.G. (2014) Polysaccharide biomaterials for drug delivery and regenerative engineering. *Polymers of Advanced Technologies*, 25, pp. 448-460.

Shikuma, N.J., Pilhofer, M., Weiss, G.L., Hadfield, M.G., Jensen, G.J., Newman, D.K. (2014) Marine tubeworm metamorphosis induced by arrays of bacterial phage tail-like structures. *Science*, 343(6170), pp. 529-533.

Shikuma, N.J., Pilhofer, M., Weiss, G.L., Hadfield, M.G., Jensen, G.J., Newman, D.K. (2014) Marine tubeworm metamorphosis induced by arrays of bacterial phage tail-like structures. *Science*, 343(6170), pp. 529-533.

Shmerk, C.L., Bernards, M.A., Valvano, M.A. (2011) Hopanoid production is required for low-pH tolerance, antimicrobial resistance, and motility in *Burkholderia cenocepacia*. *Journal of Bacteriology*, 193(23), pp. 6712-6723.

Shukla, P.J. and Dave, B.P. (2018) Screening and molecular identification of potential exopolysaccharides (EPSs) producing marine bacteria from the Bhavnagar coast, Gujarat. *International Journal of Pharmaceutical Sciences and Research*, 9(7), pp. 2973-2981.

Singh, R., Singh, S., Lilliard, J.W. (2008) Past, present, and future technologies for oral delivery of therapeutic proteins. Journal of Pharmaceutical Sciences, 97(7), pp. 2497-2523.

Siranjeevi, R.P.M.M. (2019) *Isolation and characterization of new secondary metabolites from the Arctic bryozoanz Securiflustra securifrons and Dendrobeania murrayana*. Ph.D. Thesis. The Arctic University of Norway. Available at: https://hdl.handle.net/10037/15918 [Accessed 6 April 2020].

Skiba, M.A., Sikkema, A.P., Fiers, W.D., Gerwick, W.H., Sherman, D.H., Aldrich, C.C., Smith, J.L. (2016) Domain organization and active site architecture of a polyketide synthase *C*-methyltransferase. ACS Chemical Biology, 11(12), pp. 3319-3327.

Skinnider, M.A., Dejong, C.A., Rees, P.N., Johnston, C.W., Li, H., Webster, A.L.H., Wyatt, M.A., Magarvey, N.A. (2015) Genomes to natural products PRediction Informatics for Secondary Metabolomes (PRISM). *Nucleic Acids Research*, 43(20), pp. 9645-9662.

Somerville, M.J., Hooper, J.N.A., Garson, M.J. (2006) Mooloolabenes A-E, norsesterpenes from the Australian sponge *Hyatella intestinalis*. *Journal of Natural Products*, 69, pp. 1587-1590.

Sørensen, H.P. and Mortensen, K.K. (2005) Soluble expression of recombinant proteins in the cytoplasm of *Escherichia coli*. *Microbial Cell Factories*, 4(1). Available at: https://doi.org/10.1186/1475-2859-4-1 [Accessed 13 April 2020].

Sreekanth, V., Bansal, S., Motiani, R.K., Kundu, S., Muppu, S.K., Majumdar, T.D., Panjamurthy, K., Sengupta, S., Bajaj, A. (2013) Design, synthesis, and mechanistic investigations of bile acid-tamoxifen conjugates for breast cancer therapy. *Bioconjugate Chemistry*, 24(9), pp. 1468-1484.

Stellavato, A., Tirino, V., de Novellis, F., Vecchia, A.D., Cinquegrani, F., De Rosa, M., Papaccio, G., Schiraldi, C. (2016) Biotechnological chondroitin a novel glycosaminoglycan with remarkable biological function on human primary chondrocytes. *Journal of Cellular Biochemistry*, 117, pp. 2158-2169.

Su, C., Xu, X., Liu, D., Wu, M., Zeng, F., Zeng, M., Wei, W., Jiang, N., Luo, X. (2013) Isolation and characterization of exopolysaccharide with immunomodulatory activity from fermentation broth of *Morchella conica*. *DARU Journal of Pharmaceutical Sciences*, 21(5). Available at: https://doi.org/10.1186/2008-2231-21-5 [Accessed 6 August 2019].

Sun, W., Wu, W., Liu, X., Zaleta-Pinet, D.A., Clark, B.R. (2019) Bioactive compounds isolated from marine-derived microbes in China: 2009-2018. Marine Drugs, 17(6). Available at: https://doi.org/10.3390/md17060339 [Accessed 4 April 2020].

Svenson, J. (2013) MabCent: Arctic marine bioprospecting in Norway. *Phytochemistry Reviews*, 12(3), pp. 567-578.

Tachaboonyakiat, W. (2017) Antimicrobial applications of chitosan. *Chitosan Based Biomaterials*, 2, pp. 246-274.

Teasdale, M.E., Liu, J., Wallace, J., Akhlaghi, F., Rowley, D.C. (2009) Secondary metabolites produced by the marine bacterium *Halobacillus salinus* that inhibit quorum sensing-controlled phenotypes in Gram-negative bacteria. Applied and Environmental Microbiology, 75(3), pp. 56-572.

Tewari, A., Jain, B., Dhammanapatil, P.S., Saxena, M.K. (2018) Biofilm resistance to antimicrobial agents and novel approaches to combat biofilm mediated resistance in bacteria. EC Microbiology, 14(3), pp. 71-77.

Thammahong, A., Puttikamonkul, S., Perfect, J.R., Brennan, R.G., Cramer, R.A. (2017) Central role of the trehalose biosynthesis pathway in the pathogenesis of human fungal infections: Opportunities and challenges for therapeutic development. *Microbiology and Molecular Biology Reviews,* 81(2). Available at: https://mmbr.asm.org/content/81/2/e00053-16/article-info [Accessed 26 November 2019].

Tokmakov, A.A., Kurotani, A., Takaji, T., Toyama, M., Shirouza, M., Fukami, Y., Yokoyama, S. (2012) Multiple post-translational modifications affect heterologous protein synthesis. *The Journal of Biological Chemistry*, 287(32), pp. 27106-27116.

Tran, J.C. and Doucette, A.A. (2016) Cyclic polyamide oligomers extracted from nylon 66 membrane filter disks as a source of contamination in liquid chromatography/mass spectrometry. *Journal of the American Society for Mass Spectrometry*, 17, pp. 652-656.

Trindade, M., van Zyl, L.J., Navarro-Fernández, J., Elrazak, A.A. (2015) Targeted metagenomics as a tool to tap into marine natural product diversity for the discovery and production of drug candidates. Frontiers in Microbiology, 6(890). Available at: https://doi.org/10.3389/fmicb.2015.00890 [Accessed 20 February 2020].

Tritz, J.P., Herrmann, D., Bisseret, P., Connan, J., Rohmer, M. (1999) Abiotic and biological hopanoid transformation: towards the formation of molecular fossils of the hopane series. *Organic Geochemistry*, 30, pp. 499-514.

Tyson, J.R., O'Neil, N.J., Jain, M., Olsen, H.E., Hieter, P., Snutch, T.P. (2018) MinION-based long-read sequencing and assembly extends the *Caenorhabditis elegans* reference genome. *Genome Research*, 28, pp. 266-274.

Urban, S., Dias, D.A. (2013) NMR Spectroscopy: Structure Elucidation of Cycloelatanene A: A Natural Product Case Study. In: Roessner, U., Dias D. (eds) Metabolomics Tools for

Natural Product Discovery. *Methods in Molecular Biology (Methods and Protocols)*, 1055, pp. 99-116.

Urbarova, I., Karlsen, B.O., Okkenhaug, S., Seternes, O.M., Johansen, S.D., Emblem, A. (2012) Digital marine bioprospecting: Mining new neurotoxin drug candidates from the transcriptomes of cold-water sea aemones. Marine Drugs, 10, pp. 2265-2279.

Urdaneta, V. and Casadesús, J. (2017) Interactions between bacteria and bile salts in the gastrointestinal and hepatobiliary tracts. *Frontiers in Medicine*, 4. Available at: https://doi.org/10.3389/fmed.2017.00163 [Accessed 17 January 2020].

Valence, F. and Lortal, S. (1995) Zymogram and preliminary characterization of *Lactobacillus helveticus* autolysins. *Applied and Environmental Microbiology*, 61(9), pp. 3391-3399.

Valentini, M. and Filloux, A. (2016) Biofilms and cyclic di-GMP (c-di-GMP) signaling: Lessons from *Pseudomonas aeruginosa* and other bacteria. *The Journal of Biological Chemistry*, 291(24), pp. 12547-12555.

Van der Donk, W.A. (2015) Bacteria do it differently: An alternative path to squalene. *ACS Central Science*, 1, pp. 64-65.

Vandooren, J., Geurts, N., Martens, E., Van den Steen, P.E., Opdenakker, G. (2013) Zymography methods for visualizing hydrolytic enzymes. *Nature Methods*, 10(3), pp. 211-220.

Veber, D.F., Johnson, S.R., Cheng, H., Smith, B.R., Ward, K.W., Kopple, K.D. (2002) Molecular properties that influence the oral bioavailability of drug candidates. Journal of Medicinal Chemistry, 45, pp. 2615-2623.

Viju, N., Ezhilraj, N., Shankar, C.V.S., Punitha, S.M.J., Satheesh, S. (2018) Antifouling activities of extracellular polymeric substances produced by marine bacteria associated with the gastropod (*Babylonia* sp.). *Nova Biotechnologica et Chimica*, 17(2), pp. 115-124.

Villa, F.A. and Gerwick, L. (2010) Marine natural product drug discovery: Leads for treatment of inflammation, cancer, infections, and neurological disorders. *Immunopharmacology and Immunotoxicology*, 32(2), pp. 228-237.

Volpi, N. (2019) Chondroitin sulfate safety and quality. Molecules, 24(8). Available at: https://doi.org/10.3390/molecules24081447 [Accessed 15 April 2020].

Wagenaar, M.M. (2008) Pre-fractionated microbial samples- The second generation natural products library at Wyeth. Molecules, 13, pp. 1406-1426.

Walsh, C.T. (2008) The chemical versatility of natural-product assembly lines. Accounts of Chemical Research, 41(1). Available at: https://doi.org/10.1021/ar7000414 [6 January 2020].

Walsh, C.T. (2008) The chemical versatility of natural-product assembly lines. *Accounts of Chemical Research*, 41(1), pp. 4-10.

Wang, M., Wei, H., Zhao, Y., Shang, L., Di, L., Lyu, D., Liu, J. (2018) Analysis of multidrug-resistant bacteria in 3223 patients with hospital-acquired infections (HAI) from a tertiary general hospital in China. Bosnian Journal of Basic Medical Science, 19(1), pp. 86-93.

Wang, X. and Quinn, P.J. (2010) Endotoxins: Lipopolysaccharides of Gram-negative bacteria. In: Wang, X and Quinn, P.J, eds. *Subcellular Biochemistry*. Springer. Dordrecht, pp. 3-25.

Wang, Y., Pannuri, A.A., Ni, D., Zhou, H., Cao, X., Lu, X., Romeo, T., Huang, Y. (2016) Structural basis for translocation of a biofilm-supporting exopolysaccharide across the nacterial outer membrane. *The Journal of Biological Chemistry*, 291(19), pp. 10046-10057.

Watanabe, M., Fukiya, S., Yokota, A. (2017) Comprehensive evaluation of the bactericidal activities of free bile acids in the large intestine of humans and rodents. *Journal of Lipid Research*, 58, pp. 1143-1152.

Weber T (2014) *In silico* tools for the analysis of antibiotic biosynthetic pathways. *International journal of medical microbiology* 304, 230-235.

Weber, T. and Kim, H.U. (2016) The secondary metabolite bioinformatics portal: Computational tools to facilitate synthetic biology of secondary metabolite production. Synthetic and Systems Biotechnology, 1, pp. 69-79.

Weigel, P.H. and DeAngelis, P.L. (2007) Hyaluronan synthases: A decade-plus novel glycosyltransferases. *The Journal of Biological Chemistry*, 282(51), pp. 36777-36781.

Welander, P.V., Hunter, R.C., Zhang, L., Sessions, A.L., Summons, R.E., Newman, D.K. (2009) Hopanoids play a role in membrane integrity and pH homeostasis in *Rhodopseudomonas palustris* TIE-1. *Journal of Bacteriology*, 191(19), pp. 6145-6156.

White, N.J., Watson, J.A., Hoglund, R.M., Chan, X.H.S., Cheah, P.Y., Tarning, J. (2020) COVID-19 prevention and treatment: A critical analysis of chloroquine and hydroxycholorquine clinical pharmacology. PloS Medicine, 17(9). Available at: https://doi.org/10.1371/journal.pmed.1003252 [Accessed 9 October 2020].

Whitfield, G.B., Marmont, L.S., Bundalovic-Torma, C., Razvi, E., Roach, E.J., Khursigara, C.M., Parkinson, J., Howell, L. (2020) Discovery and characterization of a Gram-positive Pel polysaccharide biosynthetic gene cluster. *PLoS Pathogens*, 16(4). Available at: https://doi.org/10.1371/journal.ppat.1008281 [Accessed 26 April 2020].

Whitman, C.M., Bond, M.R., Kohler, J.J (2010) Chemical glycobiology. In: Liu, H. and Mander, L.L, eds. *Comprehensive natural products II*. Elsevier. USA. Available at: https://doi.org/10.1016/B978-008045382-8.00681-X [Accessed 24 Novemebr 2019].

Whitney, J.C and Howell, P.L. (2013) Synthase-dependent exopolysaccharide secretion in Gram-negative bacteria. *Trends in Microbiology*, 21(2), pp. 63-72.

Whitworth, J.A. (2004) The need for new drugs: a response. Australian Prescriber, 27(6), pp. 137-138.

Who.int. (2019) *No time to wait: Securing the future from drug-resistant infections*. [pdf] Report to the secretary-general of the United Nations. Available at: https://www.who.int/antimicrobial-resistance/interagency-coordination-group/IACG_final_report_EN.pdf?ua=1 [Accessed 14 June 2020].

Williams, S.R., Gebhart, D., Martin, D.W., Scholl, D. (2008) Retargeting the R-type pyocins to generate novel bactericidal protein complexes. Applied and Environmental Microbiology, 74(12), pp. 3868-3876.

Wingfield, P.T. (2001) Protein precipitation using ammonium sulfate. *Current Protocols in Protein Science*, 13(1). Available at: https://doi.org/10.1002/0471140864.psa03fs13 [Accessed 8 June 2020].

Winn, M., Fyans, J.K., Zhuo, Y., Micklefield, J. (2016) Recent advances in engineering nonribosomal peptide assembly lines. *Natural Product Reports*, 33, 317-347.

Wohlleben, W., Mast, Y., Stegmann, E., Ziemert, N. (2016) Antibiotic drug discovery. Microbial Biotechnology, 9(5), 541-548.

Woodhouse JN, Fan L, Brown MV, Thomas T, Neilan BA (2013) Deep sequencing of non-ribosomal peptide synthetases and polyketide synthases from the microbiomes of marine sponges. *The international society for microbial ecology* 7, 1842-1851.

Wu, S., Liu, G., Jin, W., Xiu, P., Sun, C. (2016) Antibiofilm and anti-infection of a marine bacterial exopolysaccharide against *Pseudomonas aeruginosa*. *Frontiers in Microbiology*, 7(102). Available at: https://doi.org/10.3389/fmicb.2016.00102 [Accessed 14 October 2019].

Xian, Y., Zhang, J., Bian, Z., Zhou, H., Zhang, Z., Lin, Z., Xu, H. (2020) Bioactive natural compounds against human coronaviruses: a review and perspective, *Acta Pharmaceutica Sinica B*. Available at: https://doi.org/10.1016/j.apsb.2020.06.002 [Accessed 6 July 2020].

Xie, F., Liu, T., Qian, W., Petyuk, V.A., Smith, R.D. (2011) Liquid chromatography-mass spectrometry-based quantitative proteomics. *The Journal of Biological Chemistry*, 286(29), pp. 25443-25449.

Xing, K., Chen, X.G., Kong, M., Liu, C.S., Cha, D.S., Park, H.J. (2009) Effect of oleoyl-chitosan nanoparticles as a novel antibacterial dispersion system on viability, membrane

permeability and cell morphology of *Escherichia coli* and *Staphylococcus aureus*. *Carbohydrate Polymers*, 76, pp. 17-22.

Xue, D., Abdallah, I.I., de Haan, I.E.M., Sibbald, M.J.J.B., Quax, W.J. (2015) Enhanced C30 carotenoid production in Bacillus subtilis by systematic overexpression of MEP pathway genes. *Applied Genetics and Molecular Biotechnology*, 99, pp. 5907-5915.

Yan, G., Yang, R., Fan, K., Dong, H., Gao, C., Wang, S., Yu, L., Cheng, Z., Lei, L. (2019) External lysis of Escherichia coli by a bacteriophage endolysin modified with hydrophobic amino acids. AMB Express, 9(106). Available at: https://doi.org/10.1186/s13568-019-0838-x [Accessed 30 May 2020].

Yates, L.E., Mills, D.C., DeLisa, M.P. (2017) Bacterial glycoengineering as a biosynthetic route to customized glycomolecules. In: *Advances in Biochemical Engineering/Biotechnology*. Springer. Berlin, Heidelberg. Available at: https://doi.org/10.1007/10_2018_72 [Accessed 20 April 2020].

Zampara, A., Sørensen M.C.H., Grimon, D., Antenucci, F., Briers, Y., Brøndsted, L. (2018) Innolysins: A novel approach to engineer endolysins to kill Gram-negative bacteria. bioRxiv-The Preprint Server for Biology. Available at: https://doi.org/10.1101/408948 [Accessed 30 May 2020].

Zanfardino, A., Restaino, O.F., Notomista, E., Cimini, D., Schiraldi, C., De Rosa, M., De Felice, M., Varcamonti, M. (2010) Isolation of an *Escherichia coli K4 kfoC* mutant over-producing capsular chondroitin. *Microbial Cell Factories*, 9(34). Available at: https://doi.org/10.1186/1475-2859-9-34 [Accessed 4 April 2020].

Zarei, O., Dastmalchi, S., Hamzeh-Mivehroud, M. (2016) A simple and rapid protocol for producing yeast extract from Saccharomyces cerevisiae suitable for preparing bacterial culture media. *Iranian Journal of Pharmaceutical Research*, 15(4), pp. 907-913.

Zerikly M, Challis GL (2009) Strategies for the discovery of new natural products by genome mining. *ChemBioChem*, 625-633.

Zhang, L. (2005) Integrated approaches for discovering novel drugs from microbial natural products. *Natural Products: Drug discovery and therapeutic medicine*, pp. 33-54.

Zhang, L., Liu, C., Li, D., Zhao, Y., Zhang, X., Zeng, X., Yang, Z., Li, S. (2013) Antioxidant activity of an exopolysaccharide isolated from *Lactobacillus plantarum* C88. *International Journal of Biological Macromolecules*, 54, pp. 270–275.

Zhang, Z., Chen, Y., Wang, R., Cai, R., Fu, Y, Jiao, N. (2015) The fate of marine bacterial exopolysaccharide in natural marine microbial communities. *PLoS ONE*, 10(11). Available at: https://doi.org/10.1371/journal.pone.0142690 [Accessed 8 June 2020].

Zhang, Z., Shen, C., Gao, F., Wei, H., Ren D., Lu, J. (2017) Isolation, purification and structural characterization of two novel water-soluble polysaccharides from *Anredera cordifolia*. Molecules, 22(8). Available at: https://doi.org/10.3390/molecules22081276 [Accessed 8 June 2020].

Zhao, D and Huang, Z. (2016) Effect of his-tag on expression, purification, structure or zin finger protein, ZNF191 (243-368). *Bioinorganic Chemistry and Applications*. Available at: https://doi.org/10.1155/2016/8206854 [Accessed 11 September 2019].

Zilli, D.M.W., Lopes, R.G., Alves, S. L. Jnr., Miletti, B.L.C., Stambuk, B.U. (2015) Secretion of the acid trehalase encoded by the *CgATH1* gene allows trehalose fermentation by *Candida glabrata*. *Microbiological Research*, 179, pp. 12-19.

Zwahlen, R.D. (2018) Nonribosomal peptide synthetases: Engneering, characterization and biotechnological application. Ph.D. Thesis. University of Groningen. Available at: http://hdl.handle.net/11370/6ea54e57-d551-4c36-864b-b41ae31faede [Accessed 30 March 2020].